Universidade de Aveiro Departamento de Biologia
2013

Marisa Susete Reverendo Simões

Estudo do stress proteotóxico no peixe zebra

Characterization of proteotoxic stress in zebrafish

Tese apresentada à Universidade de Aveiro para cumprimento dos requisitos necessários à obtenção do grau de Doutor em Biologia, realizada sob a orientação científica do Doutor Manuel Santos, Professor Associado do Departamento de Biologia da Universidade de Aveiro

Apoio financeiro da FCT e do FSE no âmbito do III Quadro Comunitário de Apoio.

Dedico este trabalho ao meu avô, Daniel Augusto Francisco Reverendo.

o júri

Presidente

Doutor Luís António Ferreira Martins Dias Carlos
Professor Catedrático da Universidade de Aveiro

Doutor António Carlos Matias Correia
Professor Catedrático da Universidade de Aveiro

Doutor Vítor Manuel Vieira da Costa
Professor Associado do Instituto de Ciências Biomédicas Abel Salazar da Universidade do Porto

Doutor Manuel António da Silva Santos
Professor Associado da Universidade de Aveiro

Doutora Ana Cristina Carvalho Rego
Professora Auxiliar com Agregação da Faculdade de Medicina da Universidade de Coimbra

Doutor Miguel Jorge Zuzarte de Mendonça Godinho Ferreira
Investigador Principal do instituto Gulbenkian de Ciências - Oeiras

agradecimentos

I would like to thank my supervisor Manuel Santos for this challenge that he offered me. Through the years science has always been in my mind and became a very important part of my life. Thank you for your confidence in me and in my work. Thank you for your teaching and patience.

I would like to thank the people that make the RNA Lab, they made it easier. To Tatiana who welcomed me to the lab. To Ana for being my partner. To João and Rita for being insightful and funny as well. To Patrícia, she brightened our days. To Cristina, Céu, Laura, João Paredes, Denisa, Jörg, Lapo and Tobias for the friendship and the good moments. And Violeta, precious Violeta, the fish couldn't survive without her, neither could we.

I would like to acknowledge Fundação para a Ciência e Tecnologia (FCT) and University of Aveiro for the PhD grant and financial support that were essential for this work.

To all my friends, especially Anabela and Eunice thank you for your friendship and patience.

To my family Mum, Dad and Will, for believing in me. They managed to lead me onward and to deal with stressed me through these years.
Thank you Ricardo, you are the bright to my gloom.

palavras-chave

Erros de tradução, stress proteotóxico, tRNA, agregados proteicos, expressão génica, miRNAs, peixe zebra.

resumo

A fidelidade da síntese proteica é fundamental para a estabilidade do proteoma e para a homeostasia celular. Em condições fisiológicas normais as células têm uma taxa de erro basal associada e esta muitas vezes aumenta com o envelhecimento e doença. Problemas na síntese das proteínas estão associados a várias doenças humanas e aos processos de envelhecimento. De facto, a incorporação de erros nas proteínas devido a tRNAs carregados pelas aminoacil-tRNA sintetases com o amino ácido errado causa doenças neurodegenerativas em humanos e ratos. Ainda não é claro como é que estas doenças se desenvolvem e se são uma consequência directa da disrupção do proteoma ou se são o resultado da toxicidade produzida pela acúmulação de proteínas mal traduzidas ao nível do ribossoma. Para elucidar como é que as células eucarióticas lidam com proteínas aberrantes e agregados proteicos (stress proteotóxico) desenvolvemos uma estratégia para destabilizar o proteoma. Para isso estabelecemos um sistema de erros de tradução em embriões de peixe zebra que assenta em tRNAs mutantes capazes de incorporar erradamente serina nas proteínas. As proteínas produzidas neste sistema despoletam as vias de resposta ao stress, nomeadamente a via da ubiquitina-proteassoma (UPP – “ubiquitin protesome pathway”) e a via do retículo endoplasmático (UPR – “unfolded protein response”). O stress proteotóxico gerado pelos erros de tradução altera a expressão génica e perfis de expressão de miRNAs, o desenvolvimento embrionário e viabilidade, aumenta a produção de espécies reactivas de oxigénio (ROS), leva ainda à acumulação de agregados proteicos e à disfunção mitocondrial. As malformações embrionárias e fenótipos de viabilidade que observámos foram revertidos por antioxidantes, o que sugere que os ROS desempenham papéis importantes nos fenótipos degenerativos celulares induzidos pela produção de proteínas aberrantes e agregação proteica. Estabelecemos ainda uma linha de peixe zebra transgénica para o estudo do stress proteotóxico. Este trabalho mostra que a destabilização do proteoma em embriões de peixe zebra com tRNAs mutantes é uma boa metodologia para estudar a biologia do stress proteotóxico visto que permite a agregação controlada do proteoma, mimetizando os processos de agregação de proteínas que ocorrem naturalmente durante o envelhecimento e em doenças conformacionais humanas.

keywords

Mitranslation, proteotoxic stress, tRNA, protein aggregates, gene expression, miRNAs, zebrafish

abstract

Protein synthesis fidelity is pivotal for proteome stability and cellular homeostasis. Even though normal physiologic conditions have an associated low protein synthesis error rate, this is frequently increased with aging and disease and the resulting protein misfolding is associated with various human diseases and aging processes. Importantly, gene mistranslations produced by tRNA misreading in the ribosome or tRNA mischarging by aminoacyl-tRNA synthetases cause neurodegenerative diseases in humans and mice. It is not yet clear how such diseases develop and whether they are a direct consequence of proteome disruption or a result of the toxicity produced by accumulation of mistranslated proteins. To elucidate how eukaryotic cells cope with protein misfolding and aggregation (proteotoxic stress) we have developed a strategy to destabilize the proteome in a regulated manner. We engineered transfer RNA (tRNAs) to misincorporate serine into proteins in zebrafish embryos. The mutant proteins misfold, trigger the unfolded protein response (UPR), up-regulate the ubiquitin proteasome pathway (UPP) and down-regulate protein synthesis. Proteotoxic stress generated by these gene mistranslations has strong effects on gene expression and miRNA profiles, embryo development and viability, increases the production of reactive oxygen species (ROS), accumulation of protein aggregates and mitochondrial dysfunction. Interestingly, embryo malformations and viability phenotypes could be reversed by ROS scavengers, suggesting that ROS play major roles in the cell degeneration phenotypes induced by protein misfolding and aggregation. We have also established a transgenic zebrafish line for proteotoxic stress studies. Hence, proteome mutagenesis by misreading tRNAs in zebrafish embryos is a powerful methodology to destabilize the proteome to study the biology of proteotoxic stress, it allows for controlled proteome aggregation and mimicking protein aggregation processes that occur naturally during aging and in human conformational diseases.

Contents

List of abbreviations v

List of figures vi

List of tables vii

Thesis outline 1

Chapter 1 - General Introduction 5

1.1. Eukaryotic translational control 7

1.1.1. Translation initiation 7

1.1.2. Translation elongation and termination 10

1.1.3. Translation accuracy 12

1.2. Post translational protein quality control 16

1.2.1. Quality control in the cytosol 16

1.2.2. Protein folding and quality control in the endoplasmic reticulum .. 25

1.2.3. Dealing with protein aggregation 27

1.3. Implications of mistranslation for cellular homeostasis 30

1.4. Diseases associated with altered protein synthesis 33

1.5. Control of cellular homeostasis by non-coding RNAs 35

1.6. Zebrafish as a proteotoxic stress model 38

1.7. Objectives of this thesis 40

1.8. References 41

Chapter 2 - Viable levels of mRNA mistranslation generate proteome aggregation and mitochondrial dysfunction in zebrafish 47

2.1. Abstract 49

2.2. Introduction 51

2.3. Material and methods 54

2.3.1. Maintenance of zebrafish (*Danio rerio*) 54

2.3.2. Mutant tRNA plasmid construction and microinjection 54

2.3.3. Northern blot analysis 54

2.3.4. GFP fluorescence reporter 55

2.3.5. Western immunoblotting **56**
2.3.6. SDS-PAGE of protein aggregates **56**
2.3.7. Measurement of protein carbonyls **57**
2.3.8. HSPB1 mCherry fusion reporter **57**
2.3.9. Immunofluorescence **58**
2.3.10. Protein synthesis rate determination **58**
2.3.11. Proteasome chymotrypsin-like activity assay **59**
2.3.12. Total RNA extraction **59**
2.3.13. Gene expression microarrays **60**
2.3.14. Microarray data extraction and analysis **60**
2.3.15. Real-time quantitative PCR **61**
2.3.16. *xbp1* semi quantitative real-time PCR **62**
2.3.17. Dihydroethidium assay **62**
2.3.18. Hydrogen peroxide detection **63**
2.3.19. Catalase activity detection **64**
2.3.20. Mitochondrial and nuclear DNA damage **64**
2.3.21. Mitochondrial membrane potential **65**
2.3.22. Mitochondria staining **65**
2.3.23. Statistical analysis **66**

2.4. Results 67

2.4.1. Direct proteome mutagenesis using sense codon misreading tRNAs **67**
2.4.2. Protein synthesis errors increase protein ubiquitination and aggregation **69**
2.4.3. Translational errors down regulate protein synthesis **74**
2.4.4. Global transcriptional responses to proteome instability **75**
2.4.5. Stress responses induced by protein biosynthesis errors **79**
2.4.6. Proteome instability leads to the accumulation of reactive oxygen species **82**
2.4.7. Proteome instability impacts mitochondrial organization and function **84**

2.5. Discussion 90

2.5.1. Mistranslation induces proteome aggregation in zebrafish **90**
2.5.2. Proteotoxic stress destabilizes the nuclear and mitochondrial genomes **91**
2.5.3. Protein aggregation during ageing **94**

2.6. Supplementary data 96

2.7. References 102

Chapter 3 - Proteotoxic stress induces developmental malformations and deregulates specific microRNAs in zebrafish mistranslating embryos..... 111

3.1. Abstract 113

3.2. Introduction 115

3.3. Methods 118

3.3.1. Zebrafish husbandry and mutant serine tRNA microinjection..... 118
3.3.2. Alcian blue staining..... 118
3.3.3. ROS scavengers..... 118
3.3.4. Total RNA extraction..... 119
3.3.5. MicroRNA microarrays..... 119
3.3.6. MicroRNA microarray data extraction and analysis..... 120
3.3.7. Real-Time Quantitative PCR..... 120
3.3.7. MiRNA target prediction..... 121
3.3.8. Gene expression microarrays..... 121
3.3.9. Gene expression microarray data extraction and analysis..... 122
3.3.10. Cell death assay..... 122
3.3.11. Caspase activity assays..... 123
3.3.12. Statistical analysis..... 123

3.4. Results 124

3.4.1. Impact of proteome instability on zebrafish embryo development 124
3.4.2. MiRNA expression in response to mRNA mistranslation..... 127
3.4.3. Target Prediction for miRNAs deregulated by proteotoxic stress. 130
3.4.4. Transcriptional profiles of zebrafish embryos..... 135
3.4.5. Deregulation of apoptotic genes by proteotoxic stress..... 141
3.4.6. Apoptotic pathways are activated by proteotoxic stress..... 144
3.4.7. Proteotoxic stress deregulates genes associated with Hedgehog, Wnt and Notch signaling..... 146

3.5. Discussion 150

3.6. Supplementary data 155

3.7. References 175

Chapter 4 - Establishing a zebrafish transgenic line to study proteotoxic stress..... 181

4.1. Abstract 183

4.2. Introduction 185

4.3. Material and methods 188
4.3.1. Zebrafish husbandry and mutant serine tRNA plasmid construct 188
4.3.2. Northern blot analysis ... 189
4.3.3. Southern blot analysis ... 189
4.3.4. Western immunoblotting ... 189
4.3.5. HSPB1 mCherry fusion reporter ... 190
4.3.6. Acridine orange staining ... 190
4.3.7. Mitochondria staining ... 191
4.3.8. Total RNA extraction ... 191
4.3.9. Real-time quantitative PCR ... 191
4.3.11. Statistical analysis ... 192
4.4. Results 193
4.4.1. Transgenesis system ... 193
4.4.2. Transgenics early development ... 195
4.4.3. Transgenics recapitulate several proteotoxic stress features ... 197
4.4.4. MiRNA expression driven by proteotoxic stress ... 201
4.5. Discussion 203
4.6. Supplementary data 206
4.7. References 210
Chapter 5 – General discussion ... 213
5.1. The cellular effects of mistranslation on zebrafish proteostasis 215
5.2. Implication of mRNA mistranslation for ROS production and mitochondrial dysfunction 219
5.3. Gene expression changes in mistranslating zebrafish embryos 222
5.4. MicroRNA misexpression in mistranslating zebrafish embryos 224
5.5. Proteotoxic stress transgenics 226
5.6. Conclusions and future perspectives 228
5.7. References 230

List of abbreviations

mA	Ampère
APS	ammonium persulphate
ATP	adenosine 5'-triphosphate
cDNA	complementary deoxyribonucleic acid
μCi	microcurie
cm	centimeter
Cy3	cyanine 3
DMSO	dimethyl sulfoxide
DNA	deoxyribonucleic acid
DTT	dithiotreitol
EDTA	ethylenediamine tetracetic acid
g (mg, μg, ng)	gram (miligram, microgram, nanogram)
GTP	guanosine 5'-triphosphate
H_2O_2	hydrogen peroxide
kDa	kilodalton
l (ml, μl)	liter (mililiter, microliter)
mRNA	messenger ribonucleic acid
nm	nanometers
PMSF	phenylmethylsulfonyl fluoride
RNA	ribonucleic acid
rpm	revolutions per minute
rRNA	ribosomal ribonucleic acid
SDS	sodium dodecyl sulphate
SDS-PAGE	sodium dodecyl sulphate-polyacrylamide gel electrophoresis
Suc-LLVY-MCA	succinyl-leucyl-leucyl-valyl-tyrosine 4-methylcoumaryl-7-amide
TCA	trichloroacetic acid
TEMED	N,N,N,'N,'-tetramethylethylenediamine
Tris	2-amino-2-hydroxymethyl-1,3-propanodiol
tRNA	transfer ribonucleic acid
U	units
V	Volt
W	Watt

Other abbreviations will be explained when used in the text.

List of figures

Figure 1.1. Canonical eukaryotic translation initiation model. 9
Figure 1.2. Steps of eukaryotic elongation and termination. 11
Figure 1.3. Translational errors. 13
Figure 1.4. AaRS and ribosome quality control. 15
Figure 1.5. Cytosolic proteostais network. 17
Figure 1.6. Proteostasis maintenance by molecular chaperones. 18
Figure 1.7. Chaperones involved in cytosolic aggregates clearance. 21
Figure 1.8. The ubiquitin proteasome system. 22
Figure 1.9. Network of ubiquitin proteasome system interactions. 24
Figure 1.10. ER stress integrated signaling. 26
Figure 1.11. Sequestration of protein aggregates. 29
Figure 1.12. Mechanism of miRNA repression. 37
Figure 2.1. Proteome mutagenesis using misreading tRNAs. 68
Figure 2.2. Mistranslation increases the levels of protein ubiquitination and aggregation. 71
Figure 2.3. Mistranslation induces the formation of protein aggregates. 73
Figure 2.4. Mistranslation decreases the rate of protein synthesis. 75
Figure 2.5. Induction of stress responses by mRNA mistranslation. 81
Figure 2.6. Oxidative stress is one of the endpoints of mistranslation. 83
Figure 2.7. Mistranslation increases damage of mitochondrial and nuclear DNA and alters the mitochondrial morphology. 87
Figure 3.1. Impact of mRNA mistranslation on early zebrafish development. 125
Figure 3.2. ROS scavengers ameliorate mistranslation effects on zebrafish survival and developmental phenotypes. 126
Figure 3.3. MiRNAs deregulated by proteotoxic stress. 129
Figure 3.4. qPCR validation of miRNA microarrays. 129
Figure 3.5. Mistranslation strongly deregulates gene expression. 135
Figure 3.6. Global transcriptional signature of mistranslation in zebrafish embryos. 137
Figure 3.7. Development related BP terms enrichment analysis. 141
Figure 3.8. Mistranslation has a strong impact on gene expression. 143
Figure 3.9. Mistranslation strongly induces apoptosis. 145
Figure 4.1. Mistranslation model and plasmid construct. 194
Figure 4.2. tRNA detection and activity. 195
Figure 4.3. Transgenic embryo suvival. 196
Figure 4.4. Phenotypic analysis of mistranslating transgenic zebrafish. 197
Figure 4.5. Mistranslation up regulates expression of molecular chaperones. 198
Figure 4.6. Protetoxic stress transgenic zebrafish accumulate intracellular protein aggregates. 199
Figure 4.7. Protetoxic stress induced by mistranslations increased apoptosis. 200
Figure 4.8. Mistranslation has a strong impact on the mitochondrial network. 201
Figure 4.9. Mistranslation deregulated miRNA expression. 202
Figure 5.1 General overview of the effects of mistranslation on cellular deregulation. 229

List of tables

Table 2.1 Stress response and ER genes deregulated by mistranslation in zebrafish embryos. 78
Table 2.2. Oxidant defense genes deregulated by mistranslation in zebrafish embryos. 84
Table 2.3. Mitochondrial genes deregulated in mistranslating embryos. 89
Table 3.1. Putative targets of miR-2195. 131
Table 3.2. Putative targets of miR-145. 132
Table 3.3. Putative targets of mir 27c. 134
Table 3.4. General overview of enriched GO terms for mistranslation conditions. 139
Table 3.5. General overview of enriched KEGG pathways for mistranslation conditions. 140
Table 3.6. Putative targets deregulated by proteotoxic stress 149

Thesis outline

Thesis outline

This thesis is organized in five chapters. Chapter 1 is a general introduction focused on eukaryotic translation, translational and post-translational quality control mechanisms and also, on miRNA biogenesis and function. In chapter 2 we describe a mistranslation model of proteotoxic stress in zebrafish embryos and explore the cellular responses to proteotoxic stress. Chapter 3 describes the characterization of miRNA and mRNA profiles of zebrafish embryos subjected to mRNA mistranslation. Chapter 4 describes the establishment of a zebrafish transgenic line to study protetoxic stress. Finally, chapter 5 is a general discussion that addresses the global results presented in this thesis and future work perspectives.

Chapter 1 - General Introduction

1. General introduction

1.1. Eukaryotic translational control

Translation is a complex and highly regulated process that mediates the flow of information from the genome to proteins - the main building blocks of the cell. Information encoded in the genes is copied during transcription to messenger RNA (mRNA), and is then decoded by the ribosome where amino acids are incorporated into proteins. Translation can be divided mechanistically in three major sequential steps, namely initiation, elongation and termination. During the initiation step the eukaryotic initiation factors (eIFs), the initiator $tRNAi^{Met}$ and the ribosomal subunits 40S and 60S assemble with the mRNA. After this, protein synthesis starts and the ribosome moves along the mRNA until in encounters a stop codon. Translation termination releases the newly synthetized protein and the various components of the translational machinery, which are recycled for new rounds of translation.

1.1.1. Translation initiation

Translation initiation can be divided in several steps (Figure 1.1). Firstly, the $tRNAi^{Met}$ binds to the eIF2-GTP to form a ternary complex in a process regulated by eIF2B. This ternary complex then binds the 40S ribosomal subunit and its associated initiation factors (eIF3, eIF1, eIF1A, eIF5) to form the 43S preinitiation complex. The eIF3 factor prevents premature association between the 40S and the 60S subunits and promotes ribosomal mRNA scanning along the mRNA 5'-untranslated region (5'-UTR). The eIF1 and eIF1A factors stimulate the binding of the ternary complex to the 40S

subunit and also promote mRNA scanning. The eIF5 induces hydrolysis of the GTP bound to eIF2 when the initiation codon is recognized by the $tRNA_i^{Met}$.

The eIF4F complex (composed by eIF4E, eIF4A and eIF4G) and eIF4B are responsible for the activation of the mRNA for translation. The eIF4E is responsible for the cap-binding activity, while eIF4A has helicase activity that resolves 5'-UTR secondary structure with the cooperation of the eIF4B factor. The other component, eIF4G, binds eIF4E and the poly(A) binding protein PAB, thus assembling the EIF4 complex and its subsequent binding of the mRNA. The eIF4 complex recognizes the 5'-UTR of polyadenilated and capped mRNA and promote 5'-UTR unwinding, this prepares the mRNA for assembly with the 43S complex.

The activated mRNA and the 43S complex associate forming a stable preinitiation 48S complex that scans the mRNA 5'-UTR until the initiation AUG codon is recognized. The recognition of the initiation codon by the initiator $tRNAi^{Met}$ activates eIF2-GTP hydrolysis with Pi release and promotes the assembly of the 60S subunit. Association of the 60S subunit to the previous 48S complex and posterior eIF dissociation (eIF2-GDP, eIF1, eIF3, eIF4F) is triggered by eIF5B-GTP. Finally, eIF5B-GTP hydrolysis allows for the factor own release alongside with eIF1A, leaving the 80S initiation complex with the initiation codon located at the peptidyl site [1].

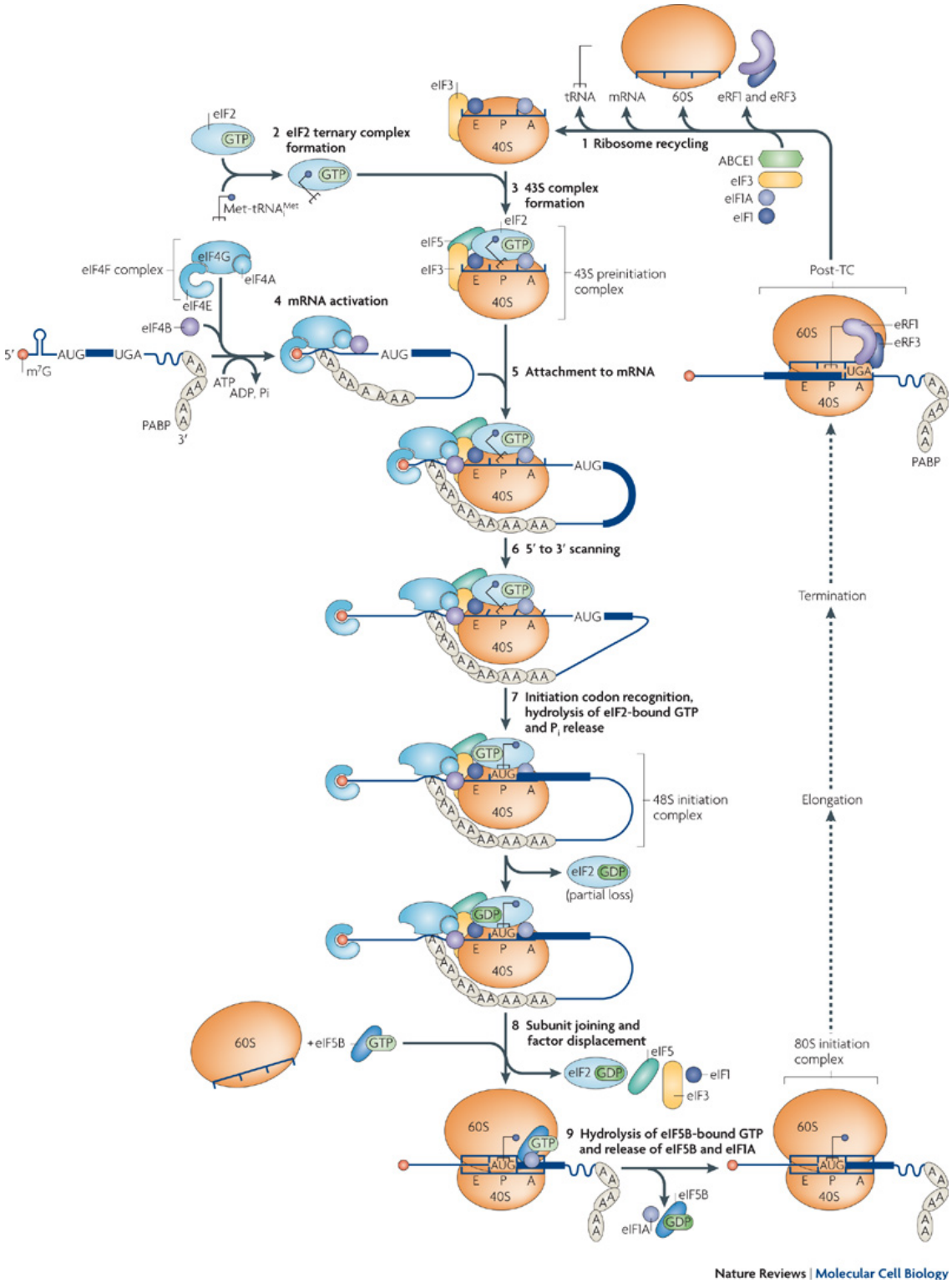

Nature Reviews | Molecular Cell Biology

Figure 1.1. Canonical eukaryotic translation initiation model.
Illustration of the 80S initiation complex (steps 2-9) and ribosomal subunit recycling (1). Early steps of translation initiation begin with the formation of the ternary complex $tRNA_i^{Met}$-eIF2-GTP (2), and posterior association with the 40S and eIFs (3). After this the 43S complex is recruited to the activated mRNA(4), where it scans the 5' untranslated region (5'-UTR) until an initiation codon is recognized (5-7). Finally, joining of the 60S and displacement of the eIFs associated with two stpes of GTP hydrolysis form the 80S complex [1].

1.1.2. Translation elongation and termination

The elongation phase is a cyclic process where a charged tRNA is delivered to the 80S ribosome A-site, the peptidyl bond formation occurs followed by translocation of the peptidyl tRNA from the A-site to the P-site, freeing the ribosomal A-site for a new round of elongation (Figure 1.2 I). The eukaryotic elongation factor 1A-GTP (eEF1A-GTP) binds the aminoacyl-tRNA and delivers it to the ribosomal A-site. After this, GTP hydrolysis allows for tRNA accommodation and elongation factor release from the ribossome. Following the ribosome catalysed peptide bond formation between the growing peptide at the P-site and the new amino acid of the A-site, the polypeptide is bound to tRNA located at the A-site. The eEF2-GTP translocates and pushes the peptidyl-tRNA into the P-site and the deacylated tRNA into the E-site, exposing a free A site for a new cycle of tRNA selection. These reactions shift the ribosome 3 nucleotides along the mRNA to read the next codon. Translation progresses until the ribosomes reach a stop codon and release factors bind to it (Figure 1.2 II). For translation termination to occur the eRF1 and associated eRF3-GTP recognize the stop codon triggering the hydrolysis of the ester bond between the tRNA in the P-site and the polypeptide chain. The translation machinery then dissociates and can be re-used to initiate a new round of translation [2].

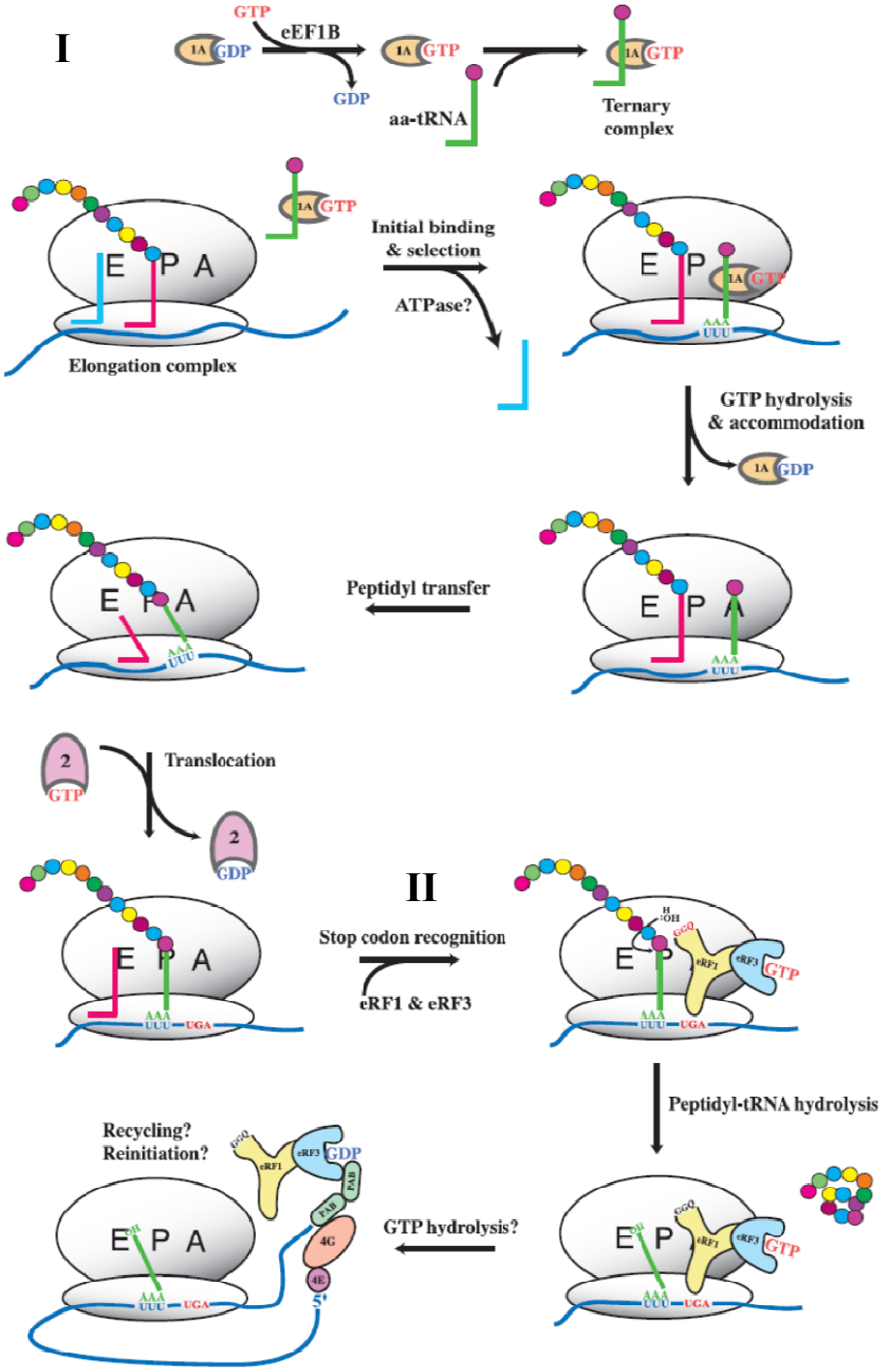

Figure 1.2. Steps of eukaryotic elongation and termination.
I) The elongation phase of protein synthesis is initiated by the delivery of charged tRNA to the ribosome A-site. Followed by peptide bond formation, catalyzed by the ribosome, and transfer of the polypeptide to the tRNA located at the ribosome A-site. Finally, eEF2-GTP translocates the polypeptide-tRNA to the P-site, the ribosome advances in the mRNA, positioning the next codon in the A-site to continue translation. **II)** When the stop codon reaches the ribosomal A-site translation is terminated. The stop codons are recognized by the eRF1-eRF3 complex that binds to the ribosome, promoting polypeptide release and translational complex disassembly [2].

1.1.3. Translation accuracy

Translation is a highly efficient and accurate process, however errors (mistranslation) occur at an estimated rate of 10^{-4} [3-5]. Considering this typical error rate, it is estimated that approximately 15% of polypeptides contain at least one misincorporated amino acid, indicating that translational errors may contribute to protein misfolding and aggregation [3]. Amino acid misincorporation errors can happen as a result of tRNA misacylation or incorrect tRNA selection by the ribossome. Decoding errors at the ribosome occur as well, these are mainly nonsense and missense errors (Figure 1.3). Nonsense or processivity errors are mainly stop codon readthrought, frameshifting, premature termination and ribosome drop off [3]. Readthrough errors occur when translation does not end at stop codons, leading to the production of proteins with extended C-termini [6, 7]. Frameshifting and premature termination are processivity errors that lead to the production of misframed and truncated proteins, respectively. Premature termination is the most frequent of the processivity errors with a frequency of 10^{-3} and is mainly caused by ribosome editing, a process by which non-cognate peptidyl-tRNA dissociates from the ribosomal P site due to the tRNA weak interaction with the mRNA being translated [8, 9]. Frameshifting errors are due to slippage of the tRNA to the -1 or +1 reading frame. These errors occur at a frequency of 10^{-5} in *E. coli* [6, 10]. Such translational errors may be influenced by physiology but they are also influenced by tRNA base modifications and tRNA abundance. Indeed, base modifications help stabilize the tRNA structure and permit codon wobbling during codon recognition, contributing to translational accuracy [5]. On the other hand, tRNA abundance is fundamental to control translational speed and accuracy since tRNA availability is the limiting step in translation [3, 11]. Near cognate tRNAs compete with cognate tRNAs at the ribosomal A-site, and this competition can be shifted to the non-

cognate tRNAs if their expression increases, leading to increased missense error rate [7].

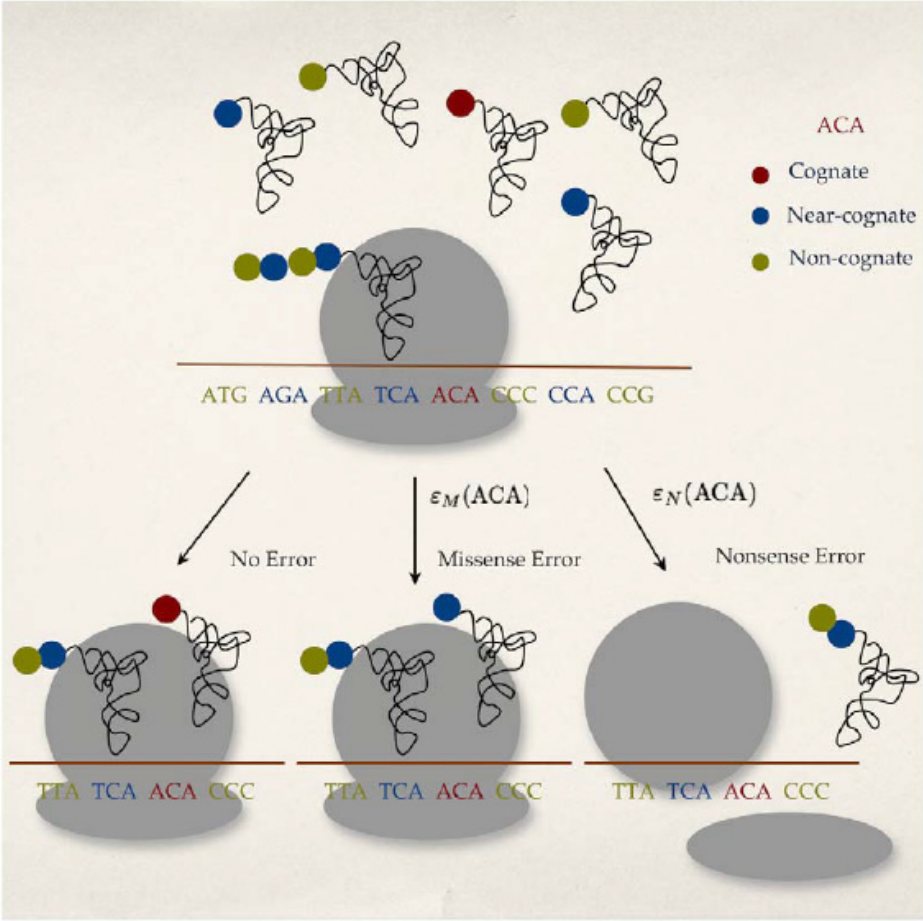

Figure 1.3. Translational errors.
In this example a ribosome pauses at ACA codon and waits for the cognate tRNA. During this waiting period one of three situations can occur. In the first example elongation with the cognate tRNA occurs leading to the production of the correct polypeptide. In the second example elongation proceeds with a near cognate tRNA thus leading to a missense error. In the last example a non-cognate tRNA causes premature termination of translation due to recognition by release factors, spontaneous ribosome dropoff or frameshifting leading to nonsense errors [7].

Missense errors can be introduced by mischarged tRNAs (Figure 1.4). Aminoacyl tRNA-synthethases (AARSs) catalize amino acid activation and charging on the tRNAs in a two-step reaction involving activation of the amino acid by ATP with loss of PPi and transfer of the activated amino acid into the tRNA with loss of AMP [12]. These

enzymes are characterized by complex, multi-domain architectures in which synthetic and editing functions are located into different structural regions. Aminoacylation is a very accurate process with an estimated error rate of 10^{-4} to 10^{-5} [13]. However, correct amino acid recognition can be difficult for chemically and physically similar amino acids and some AARSs are able to correct mischarged tRNAs using an editing mechanism [5]. Non-cognate amino acid editing can occur independently of the tRNA by hydrolysis of the adenylated amino acid (pre-transfer editing). If this fails, the incorrectly aminoacylated tRNA moves its 3'-end to the editing site where the ester link between the tRNA and amino acid is hydrolyzed (post-transfer editing). Post-transfer editing can also be accomplished by trans acting factors such as tRNA deacylases following tRNA charging and release from the aaRS [5]. The editing properties of aaRSs are of major importance to ensure accurate protein synthesis. Indeed, a mouse model harboring a mutation in the editing site of the alanyl-tRNA synthetase (AlaRS) has high level of mistranslation, protein misfolding and neuronal death [14]. Interestingly, the ribosome is unable to discriminate between correctly acylated and misacylated tRNAs, indicating that mischarged and correctly charged tRNAs misincorporate their amino acids into proteins in the same way.

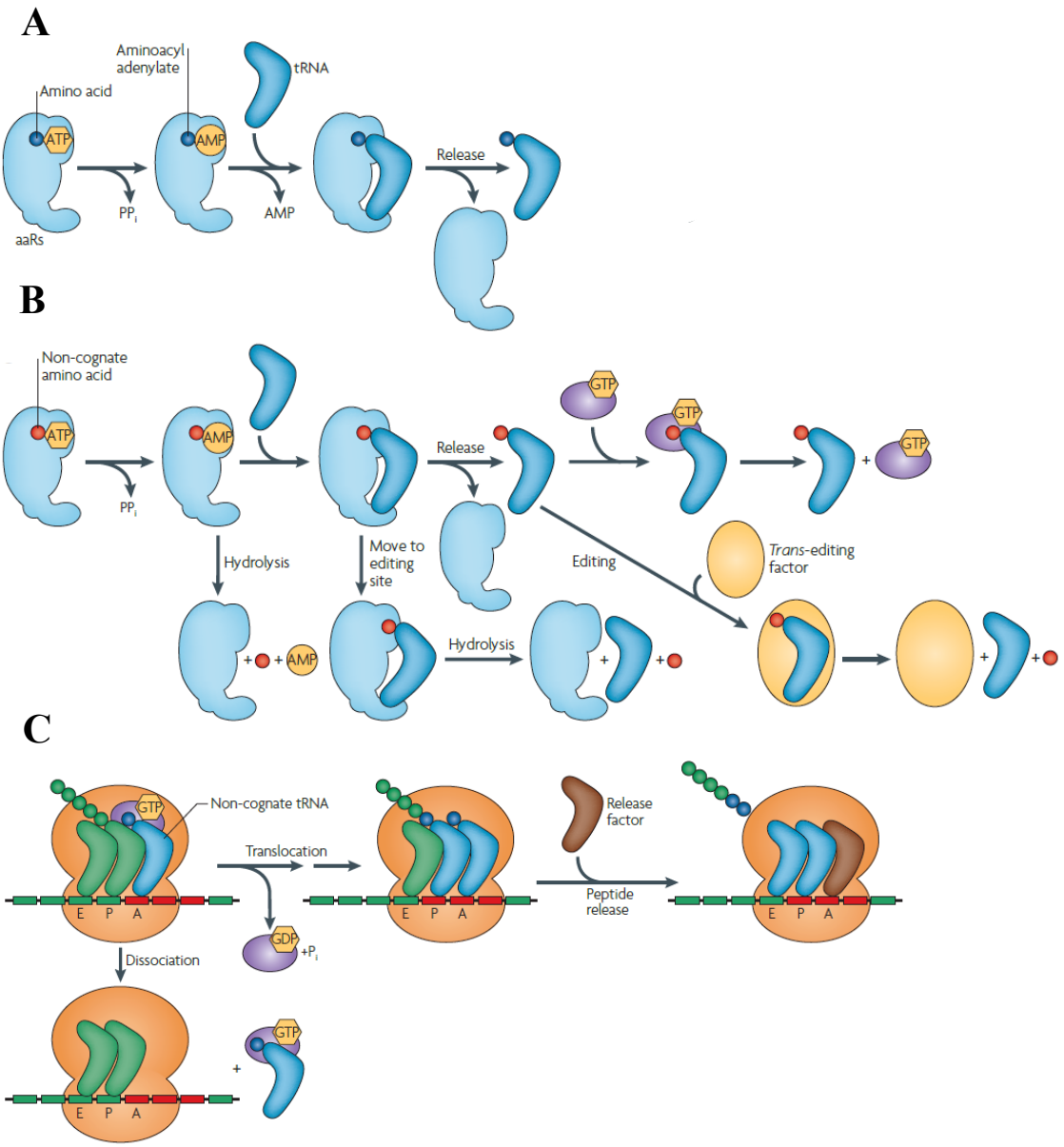

Figure 1.4. AaRS and ribosome quality control.
A) tRNA aminoacylation. The cognate amino acid is recognized and adenylated in the active site of the aaRS. This is followed by the binding of the amino acid to the 3' end of the cognate tRNA. **B)** Pre-transfer and post-transfer editing by the aaRS. When a non-cognate amino acid is adenylated the active site has a mechanism to hydrolyse and release the amino acid. When non-cogante amino acids are incorrectly attached to tRNA the editing site of the aaRS hydrolyses the ester bond and releases the tRNA and non-cognate amino acid. If the mischarged tRNA is released, additional trans factors can hydrolyze it (trans editing). **C)** Polypeptide synthesis. Non cognate tRNAs are screened and release at the ribosomal A-site [5].

1.2. Post translational protein quality control

Even though the translational process has several quality control mechanisms errors still occur in polypeptide synthesis and their removal requires quality control systems to prevent proteotoxic stress. Indeed, proteins often misfold due to amino acid misincorporations, stress conditions or unique metabolic challenges, such as those occurring during amino acid starvation and human diseases [15]. Protein quality control (PQC) mechanisms prevent proteotoxic stress through the destruction or salvage of aberrant proteins, using molecular chaperones, the ubiquitin proteasome pathway, endoplasmic reticulum associated degradation (ERAD) and autophagy [15].

1.2.1. Quality control in the cytosol

Increased protein misfolding affects cellular proteostasis putting the cell on demand for a fast response to control and maintain cellular homeostasis. Cellular responses to protetoxic stress involve up-regulation of molecular chaperones, the ubiquitin proteasome pathway and autophagy which intervene to re-fold or destroy aberrant proteins (Figure 1.5) [15].

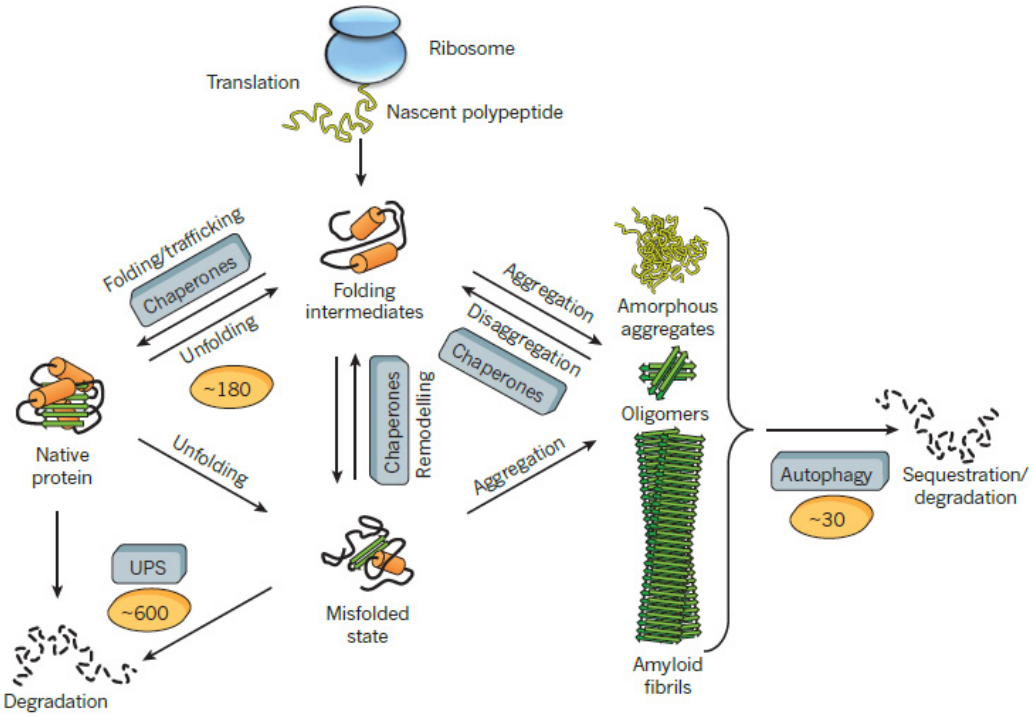

Figure 1.5. Cytosolic proteostais network.
Various quality control mechanisms contribute to cellular proteostasis. Molecular chaperones are responsible for protein *de novo* folding and refolding following stress conditions. When aberrant proteins escape chaperone management they may accumulate in insoluble aggregates that can be subsequently cleared by autophagy. On the other hand chaperones target aberrant proteins to the ubiquitin proteasome system for destruction [16].

Chaperones are mainly involved in folding of newly synthesized polypetides and articulate with other quality control mechanisms to prevent protein aggregation or accumulation of terminally aberrant proteins (Figure 1.5, Figure 1.6). Chaperones recognize exposed polypeptidic hydrophobic stretches that are usually buried in the protein core. When these are exposed the non-native interactions increase alongside with the potential for protein aggregation. To improve protein folding and prevent protein misfolding two chaperone networks assist folding during and post-synthesis [17, 18]. The first chaperone network is associated with the translation machinery. It stabilizes nascent polypeptides and assists *de novo* folding. The second layer of heat shock protein (HSP) chaperones exerts its function on the mature proteome to protect it from stress.

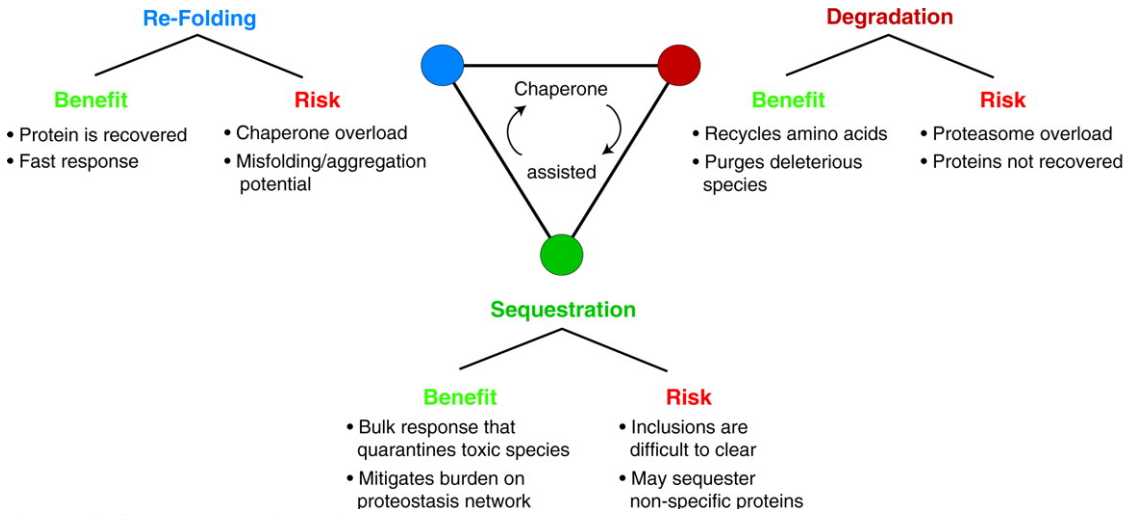

Figure 1.6. Proteostasis maintenance by molecular chaperones.
Protein misfolding situations can be resolved by an interconnected chaperone assisted re-folding, degradation or delivery to quality control compartments. Each strategy has associated benefits and risk and all rely on molecular chaperone intervention. The balanced action of the proteostatis molecular network maintains cellular fitness and is essential to maintain cellular balance [15].

Chaperones are crucial for proper cell functioning and their expression can either be constitutive or induced by stress conditions. They can be classified accordingly to their molecular mass (for example: HSP70) and small HSPs [18]. Each chaperone family has several isoforms and many chaperones, namely HSP90 or HSP70 have co-chaperone factors that regulate their activity. In addition, they can perform their functions at different levels of the proteostasis network. The HSP60 member chaperonin TRiC/CCT and Hsp70s can associate with the ribosome and facilitate folding of complex proteins [15, 16]. Hsp70s, Hsp90s, and the sHSPs are committed to stability, refolding and degradation [15]. One of the most important families of chaperones is HSP70. Members of this chaperone class are involved in co- or post-translational folding and protein trafficking and assist proteolytic degradation of aberrant proteins. Besides this array of functions, these chaperones have a wide cellular distribution and can be found mainly in the cytosol, but are also present in the ER and in the mitochondria [19]. HSP70 chaperones are present in the cytoplasm of higher eukaryotes

in HSC70 constitutively expressed and in HSP70 stress inducible forms. HSP70 has an ATPase domain which is responsible for peptide binding. HSP70 shifts between ATP and ADP bound states and this regulates client protein binding affinity. Protein binding is facilitated by ATP and ATP hydrolysis is necessary to stabilize and maintain protein interaction. But, the ATPase activity of HSP70 is very low and cofactors, such as DNAJ proteins and nucleotide exchange factors are required to enhance HSP70 activity [19]. Binding occurs at polypeptide regions exposed in non-native states and affinity is improved by the co-chaperone HSP40 which accelerates ATP hydrolysis and stabilizes chaperone substrate interaction. HSP40 can also recognize unfolded proteins and subsequently recruit HSP70 to stabilize these misfolded proteins [18-20].

The HSP90 is another important chaperone family. It works downstream of HSP70 chaperones, participates in the late stages of *de novo* folding and also contributes to protein refolding and degradation following stress conditions. Several of the client proteins of HSP90 are transcription factors and protein kinases, suggesting that HSP90 may be an important modulator of processes such as cell cycle, development and stress response [21]. Even though the mechanism has not been elucidated the activity of HSP90 requires ATP and several co-chaperones modulate its activity [21]. In the case of client proteins, such as steroid hormone receptors, HSP90 is recruited to its clients in cooperation with the HSP70/HSP40 system. Binding specificity of this chaperone is also not well known and, in some cases, it can be provided by adaptor proteins as is the case of client protein kinases that are probably recognized not by HSP90 itself [22]. HSP90 and HSP70 chaperones can also promote degradation of client proteins through interaction with the carboxyl terminus of HSC70-interacting protein (CHIP). Even though this regulatory mechanism in not well understood, CHIP, an E3 ubiquitin ligase, is able to ubiquitinate client proteins that are stably bound to HSP70 and HSP90

chaperone complexes and target them for proteasomal degradation [23]. Another relevant class of HSPs is the small HSPs, these chaperones have the capacity to bind and maintain misfolded and unfolded polypeptides in folding competent state. Therefore, they are important during recovery from stress where resolving protein aggregates becomes essential (Figure 1.7). This diverse family of proteins is largely present in the eyes tissue, but they are present in other cell types such as neurons and muscle cells [24]. They are characterized by low molecular mass (15-43 kDa) and a conserved α-crystallin domain. sHSPs are distinct from other disaggregating chaperones such as HSP70 and HSP100 because their activity does not depend on ATP hydrolysis [25-27]. These chaperones form oligomers; small oligomers of HSPB8 and big multimers of HSPB1 and HSPB5 [27] provide additional proteome protection against protein misfolding and aggregation. Several human diseases are associated with defects in these chaperones, and their expression is increased in the context of neurodegenerative diseases such as Alzheimer's and Parkinson's disease [27]. The HSPB1 helps disaggregating intrinsically disordered proteins, such as α-synuclein and tau and also amyloid peptides [27]. These sHSP work in coordination with other molecular chaperones, such as HSP70, and help transfer partially aggregated proteins to refolding chaperones. The latter can target the client proteins of sHSPs to proteasomal degradation in the case the aberrant client proteins cannot be refolded [25, 27].

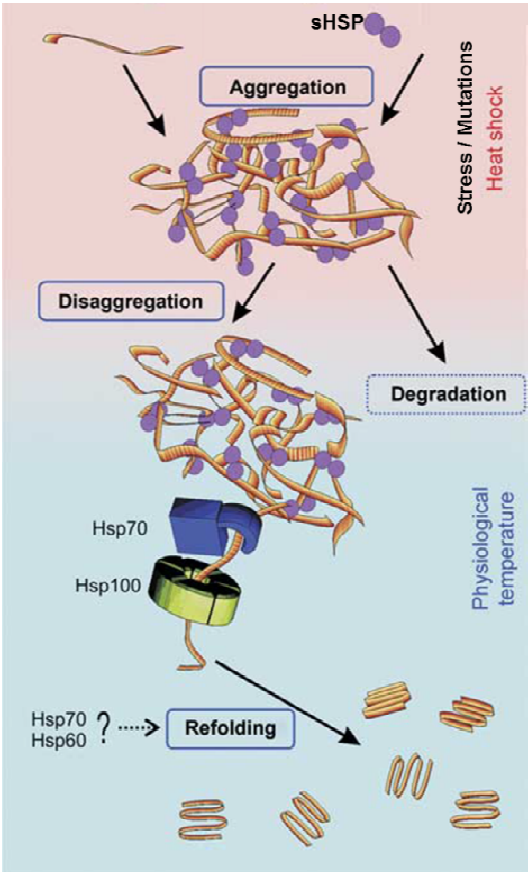

Figure 1.7. Chaperones involved in cytosolic aggregates clearance.
Small heat shock proteins (sHSPs) are oligomeric chaperones that bind destabilized proteins and improve disaggregation efficiency. Misfolded proteins are maintained in a folding competent state by sHSPs and delivered to HSP70 and HSP100 for disaggregation, this bi-chaperone system mediates protein refolding, protein aggregates can also be resolved by subsequent proteolysis [25].

Even though priority is given to chaperone repair of damaged/misfolded proteins, the majority of terminally aberrant proteins are targeted for destruction. The ubiquititn proteasome pathway (UPP) is responsible for the proteolysis of soluble proteins, while autophagy plays a role in the elimination of bulkier, insoluble proteins and organelles [15]. Proteins are tagged with multiple ubiquitin molecules that signal them for degradation by the proteasome (Figure 1.8). Protein tagging for degradation is an ordered enzymatic process of E1/E2/E3 ubiquitination. This process requires that an E1 ubiquitin-activating enzyme recognizes and transfers free ubiquitin molecules to an E2 ubiquitin-conjugating enzyme, which then in cooperation with ubiquitin protein ligases

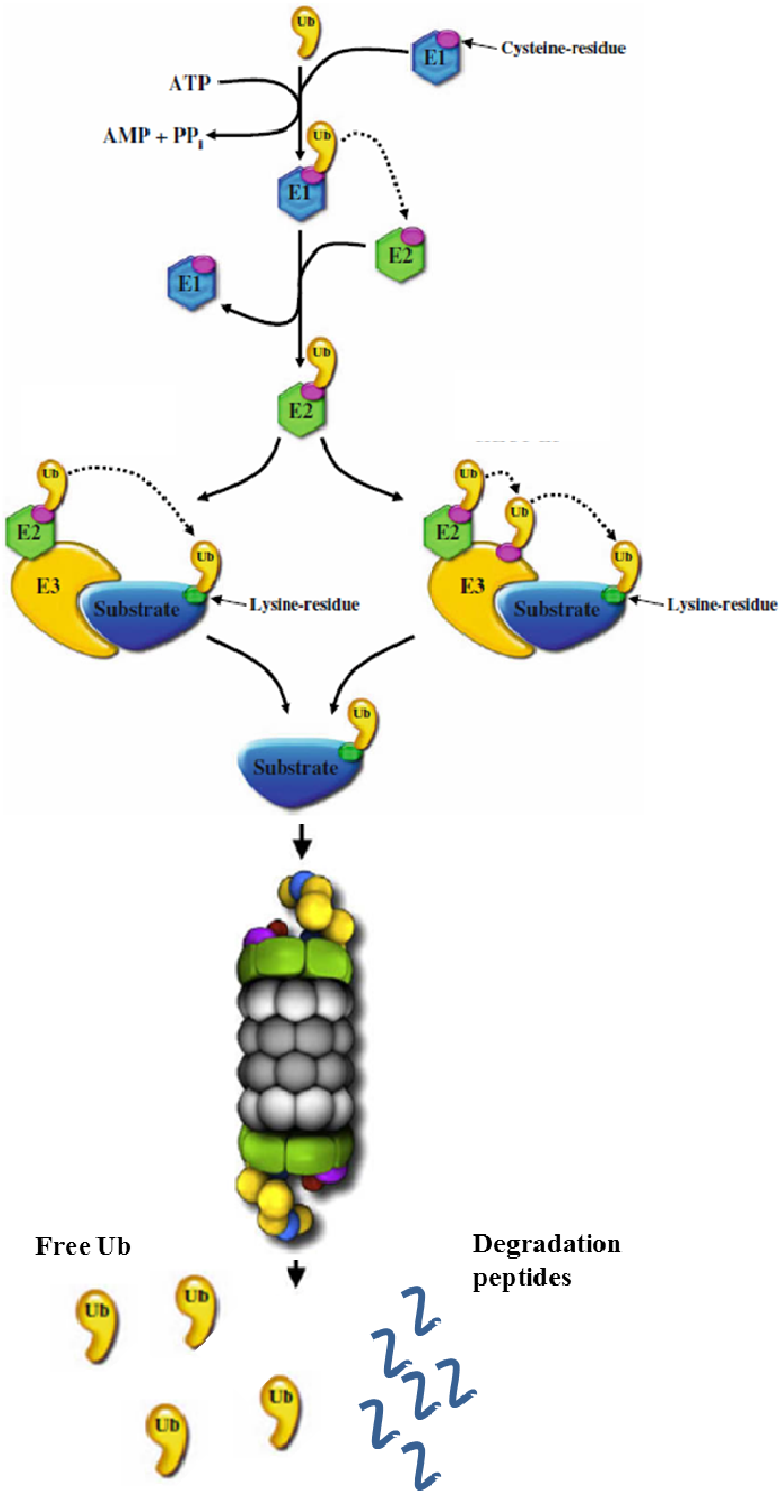

Figure 1.8. The ubiquitin proteasome system.
A sequential enzymatic cascade E1/E2/E3 adds ubiquitn molecules to polypeptidic substrates at lysine residues. A polyubiquitin tag targets polypeptides for degradation by the proteasome. The eukaryotic 26S proteasome recognizes polyubiquitin chain tags on client polypeptides and cleaves them, resulting in free ubiquitin molecules and short degradation peptides [28].

bind ubiquitin to a target protein at lysine residues. In this process several ubiquitin molecules are sequentially added to the initial ubiquitin to form a polyubiquitin chain necessary for proteasomal recognition [28]. The eukaryotic 26S proteasome is composed by a 20S proteolytic core and two 19S ATP-dependent regulatory caps. The 19S cap recruits ubiquitin conjugates and delivers them to the 20S subunit. The 19S cap is responsible for target recognition, ubiquitin cleavage, polypeptide unfolding and delivery to the 20S subunit proteolytic core [28]. Even though the mechanism that articulates the chaperone network and UPS is not fully understood these quality control systems communicate and the chaperone machinery interacts with the UPS to destroy aberrant proteins. Indeed, E3 ubiquitin ligases can ubiquitinate client proteins in a HSP70 dependent fashion [15]. Furthermore, the UPS also degrades misfolded proteins that originate in the ER in a degradation pathway known as endoplasmic reticulum associated degradation (ERAD) [29]. In mammalian cells the ER folds around 7500 different proteins and considering that aproximatly 30% of nascent proteins are aberrantly synthesized at the ribosome the ERAD is essential to maintain ER homeostasis [28, 30]. These misfolded proteins are recognized by ER chaperones, such as BIP, and retrotranslocated to the cytoplasm where degradation occurs by the UPS [28]. The functions of the UPS in eurkaryotic cells extend well beyond aberrant polypeptide destruction. Indeed, this proteolytic system is involved in several aspects of cellular regulation, namely regulation of the transcription factors NFkB, p53, c-jun, β-catenin, E2F-1; therefore regulating expression of their targets (Figure 1.9) [28, 31].

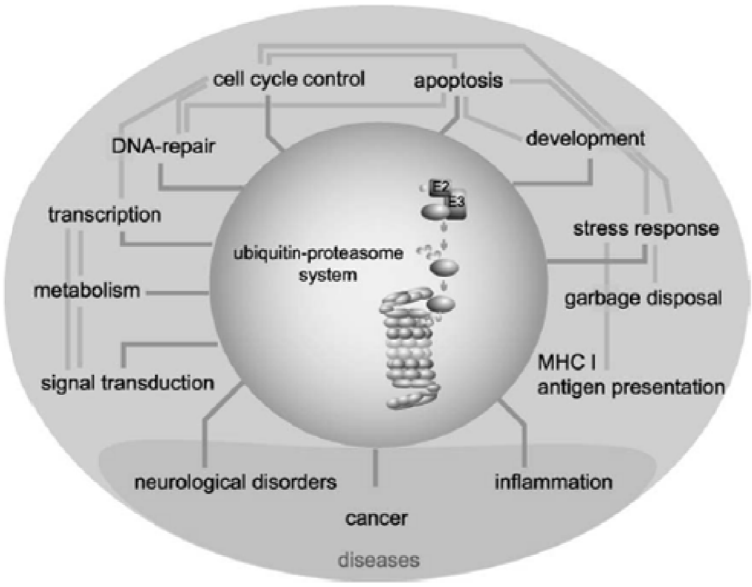

Figure 1.9. Network of ubiquitin proteasome system interactions.
Concerted deregulation of specific targets by the UPS has a regulatory effect on numerous processes relevant for cellular functioning. The UPS pathway degrades several targets in a regulatory fashion, that are involved in central cellular pathways, e.g., such as transcription, metabolism and cell cycle control [31].

As mentioned above the UPS degrades mainly soluble misfolded proteins while the lysosome deals mainly with the turnover of longer lived proteins, organelles, lipid deposits and protein aggregates, and also pathogens. In higher eukaryotes delivery to the lysosome can occur by means of chaperone mediated autophagy (CMA), microautophagy and macroautophagy. CMA degrades soluble proteins that contain the targeting motif KFERQ through chaperone mediated translocation to the lysosome. The other two autophagic pathways have the capacity to engulf large portions of the cytoplasm or even organelles/structures through both selective and non-selective mechanisms and deliver them to the lysosome [32]. Moreover, macroautophagy relies on a double-membrane structure (autophagosome) to deliver cargo to the lysosome while microautophagy relies only on invagination of the lysosomal membrane [32]. Importantly, autophagy is coordinated with the UPS system in a way that upon

proteasomal activity inhibition autophagy is activated in a compensatory fashion. For example, autophagy can relieve the cell from misfolded proteins originated in the ER when the UPS in unable to degrade them [33].

1.2.2. Protein folding and quality control in the endoplasmic reticulum

The endoplasmic reticulum (ER) provides a folding environment for proteins of the secretory pathway which are destined to the Golgi compartment, plasma membrane, lysosomes and the extracellular region. It possesses enzymes that maintain the oxidizing potential, that allows for disulfide bond formation, relative to the cytoplasm, and catalyze post-translational modifications. Protein maturation mechanisms are strictly controlled, insuring that only correctly folded and modified proteins reach the secretory pathway. It has a high concentration of folding chaperones and a sophisticated quality control system, the unfolded protein response (UPR) and a dedicated protein degradation system, the ERAD, which are activated in cases of protein unfolding and misfolding [34]. The UPR senses the status of the folding ability of the ER, and reprograms its activity to improve folding capacity of the organelle [35]. Upon the accumulation of misfolded and/or aggregated proteins in the ER the UPR is activated by means of three different signaling branches (Figure 1.10). These are the splicing of the transcript of *XBP1* by IRE1, phosphorylation of the translation initiation factor eIF2-α by PERK and cleavage of the transcription factor ATF6 [29]. These signaling cascades increase the folding capacity of the ER, and ultimately target misfolded/aggregated proteins to salvage and refolding pathways or to degradation by the 26S proteasome and/or autophagy [29]. The chaperone BIP directly coordinates activation of the UPR signaling by misfolded protein recognition. Under normal conditions this chaperone binds the ER luminal domains of the ER transmembrane proteins IRE1, PERK and

ATF6, but during ER stress unfolded/misfolded proteins accumulate in the ER and BIP binds their hydrophobic exposed regions to maintain them in a folding competent state, releasing its inhibitory effect on the UPR sensors [29]. Upon stress, IRE1 oligomerization and autophosphorylation activates its endoribonucleolytic activity, resulting in the alternative splicing of *XBP1*. The product of the alternative splicing of XBP1 is a potent transcription factor that mediates transcription of UPR targets genes, namely ER chaperones, the ERAD machinery, and secretory proteins [36, 37]. Another regulatory arm of the UPR is controlled by PERK, a transmembranar protein with a cytosolic kinase domain.

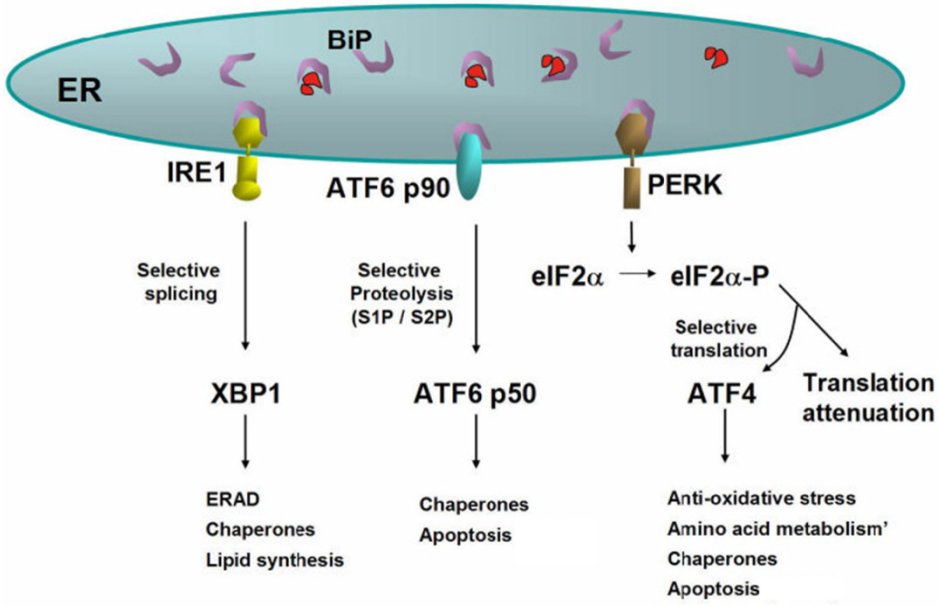

Figure 1.10. ER stress integrated signaling.
The three UPR sensors IRE1, PERK and ATF6 regulate the unfolded protein response (UPR). BIP binds them and maintains them in an inactive state. When proteins fail to reach their native conformation and adopt misfolded/unfolded stastes, they bind BIP relieving inhibition of UPR sensors. Activation of IRE1 leads to alternative splicing of XBP1. The alternative splicing product is a transcription factor that activates ERAD genes, molecular chaperones and lipid synthesis. Activation of ATF6 induces the proteolytic cleave of ATF6 itself, the cleavage product is a transcription factor that activates expression of chaperones and apoptotic genes. Finally, activation of PERK leads to eIF2α phosphorylation with subsequent translational attenuation of genes with cap dependent translation [29].

Upon oligomerization a trans-autophosphorylation reaction phosphorylates PERK itself but also phosphorylates the α-subunit of eukaryotic translation initiation factor-2 (eIF2α). The phosphorylation of eIF2α prevents recycling of the eIF2-GDP/GTP by eIF2B, thereby reducing the availability of this factor necessary for ternary complex assembly and translation initiation [38-40]. Even though the phosphorylation of eIF2α slows down translation rate, the transcription factor ATF4 is activated, leading to transcription of genes related to ER oxidative response, apoptosis and chaperones [37, 41]. The last level of UPR control is executed by ATF6. This transmembranar protein has a stress sensing domain in the ER lumen that binds BIP. When Bip is recruited by misfolded proteins, the free ATF6 is delivered to the Golgi apparatus where its cytosolic domain is cleaved producing yet another transcription factor that controls the expression of chaperones and apoptotic factors [42]. When the UPR is insufficient to sustain the folding load of the ER and terminally misfolded, inefficiently modified proteins and unassembled members of multiprotein complexes accumulate in the ER lumen, the ERAD is activated. This quality control mechanism associates with the cytosolic UPS to degrade aberrant proteins. To do this, ERAD mediates the retrotranslocation of proteins to the cytoplasm with subsequent modification with polyubiquitin chains and degradation by the 26S proteasome [37].

1.2.3. Dealing with protein aggregation

Although the proteostasis network is very dynamic and robust, sustained stress conditions can produce aberrant proteins and ultimately lead to the accumulation of protein inclusion bodies or aggregates. This can happen when the production of aberrant proteins or a combination of stressors overwhelms the folding or degradative capacity of the cell. Even though protein aggregation results from loss of proteostasis new

perspectives have emerged showing that aggregate formation is more than a random cellular process and that misfolded proteins are deposited in specific cellular locations [43]. Indeed, different types of protein deposits have been observed in eukaryotic cells, which can accumulate terminally insoluble aggregated proteins, or even misfolded proteins and the associated refolding chaperones or degradation machinery. Thus, the assembly of protein aggregates is associated with the quality control network [44]. Assembly of protein deposits in the perinuclear region occurs as a result of several stress conditions such as proteasome inactivation [15]. An example of perinuclear protein aggregation is the mammalian aggresome, which co-localizes with the microtubule organizing center in the perinuclear region. These protein deposits are located to indentations of the nuclear envelope and due to their association with the microtubule organizing center are associated with the centrioles [45]. The process of aggresome assembly is initiated by the formation of small polyubiquitinated protein aggregates. These aggregates are scattered throughout the cytoplasm and associate with the cytoskeleton to be transported alongside the microtubules to the microtubule organizing center (MTOC) by HDAC6 associated to dynein where they accumulate (Figure 1.11A) [46].

Recently two compartments involved in the sequestration and degradation of protein aggregates have been described, namely the juxtanuclear quality control (JUNQ) and the insoluble protein deposit (IPOD) (Figure 1.11B) [43]. These structures have distinct functions in protein aggregate handling and are conserved from yeast to mammals. The JUNQ deals with soluble misfolded proteins tagged with polyubiquitin and for this it concentrates disaggregating chaperones and the 26S proteasome. Moreover, it is located close to the perinuclear/endoplasmic reticulum region involved in ERAD. This structure facilitates protein refolding or degradation because it allows

for a close contact between the proteins and quality control components. Saturation of the quality control pathway leads to the accumulation of terminally aggregated proteins with increased toxicity potential. In these cases the protein aggregates are redirected to the IPOD, which accumulates disease-associated proteins such as huntingtin and prions. The IPOD is committed to aggregate degradation but does not associate with the proteasome, instead it co-localizes with autophagy markers [43]. Concentration of insoluble aggregates at the IPOD facilitates delivery of these toxic proteins to the autophagic pathway. Additionally, sequestration of terminally aggregated proteins prevents chaperone retention and also retains toxic aggregates in the mother cell upon cellular division [43].

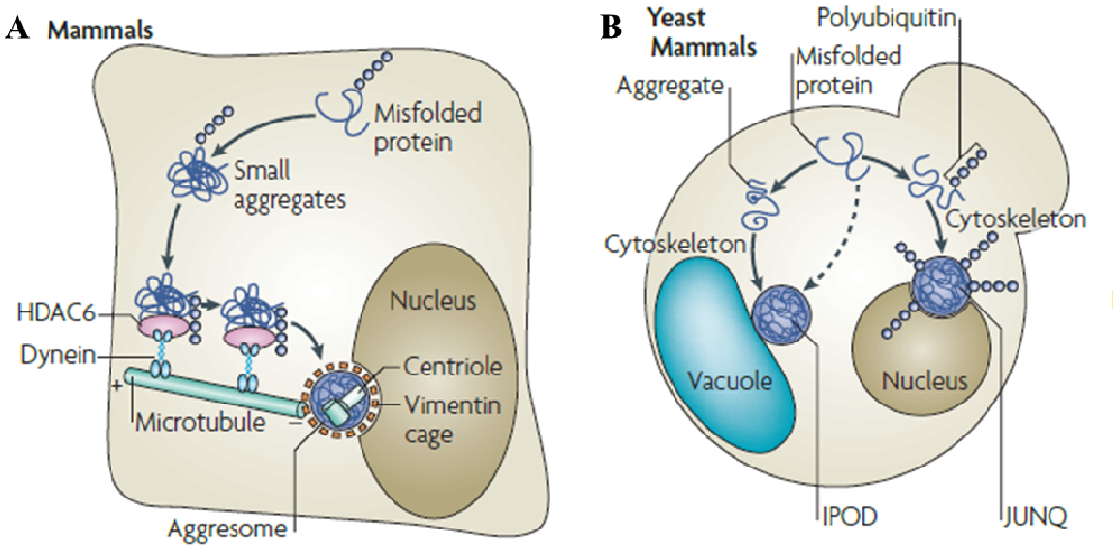

Figure 1.11. Sequestration of protein aggregates.
A) The mammalian aggresome is an example of a protein deposit that is associated with the centriole and localizes to indentations in the nuclear envelope. Small protein aggregates are transported to the aggresome by HDAC6 and dynein. HDAC6 recognizes the polyubiquitination signal and is associated with the cytoskeleton through dynein. **B)** The juxtanuclear quality control (JUNQ) and the insoluble protein deposit (IPOD) are two distinct quality control compartments conserved from yeast to mammalian cells. The JUNQ accumulates soluble misfolded proteins with polyubiquitination signals, molecular chaperones and protein degradation machinery. The IPOD accumulates insoluble protein aggregates at a perivascular location [43].

The mechanism underlying protein aggregate formation and distribution into specific cellular compartments is still not understood. However, polyubiqutin tags separate proteins addressed to the JUNQ and the IPOD [43].

1.3. Implications of mistranslation for cellular homeostasis

The introduction of errors into nascent polypeptides (mistranslation) during translation leads to the production of mutant proteins with increased potential for misfolding, toxicity or aggregation [15]. Therefore, mistranslation is mainly regarded as deleterious since it induces proteotoxic stress. However, mistranslation can be beneficial in mistranslating yeast grown in the stress conditions [47]. Remarkably, in the fungus *Candida albicans*, natural mistranslation of CUG codons generates phenotypic diversity and increases adaption to stress conditions [48, 49]. Moreover, in yeast and mammalian cells, tRNA misacylation with methionine occurs in response to oxidative stress. In this situation there is methionine misincorporation at sites of charged or polar amino acids. As a result, the Met substitutions happen at exposed sites in the proteins structure allowing them to function as scavengers for reactive oxygen species (ROS) [50]. Despite these beneficial aspects, mistranslation and derived proteotoxic stress have a negative impact on proteostasis of higher vertebrates and are involved in several human pathologies and senescence. Studies in the worm *Caenorhabditis elegans* show that during ageing there is extensive proteome aggregation due to loss of proteostasis [51, 52]. Furthermore, loss of proteostasis in specific cellular locations can also occur as a result of mistranslation. For example, loss of proteostasis in the ER with concomitant accumulation of misfolded proteins saturates the organelle's folding capacity and impacts calcium homeostasis, as the ER holds the major intracellular calcium pool.

Importantly, disruption of the normal ER functioning has been implicated in a plethora of human diseases including Alzheimer disease, prion disease, cystic fibrosis and diabetes mellitus [35, 53].

Upon stress conditions the ER activates the UPR and ERAD. The UPR balances the ER folding capacity and enhances secretory capacity, while the ERAD is responsible for protein retro-translocation and destruction of damaged proteins. In a multicellular organism, different cell types have different physiological commitments and adequate chaperone networks to specific proteome maintenance challenges. Likewise, specific cell types are predicted to have different levels of tolerance to ER stress, which is particularly relevant to address the effects of proteotoxic stress in specialized tissues. Although the ER can tolerate stress up to some extent, upon prolonged stress conditions apoptosis is activated. The UPR signaling branches controlled by PERK, ATF6 and IRE1can intervene in the control of pro-survival and pro-apoptotic responses [29, 54]. Activation of PERK promotes expression of the transcription factor ATF4. This transcription factor promotes cell survival by inducing genes involved in amino-acid metabolism, redox reactions, stress response and protein secretion. Furthermore, PERK signaling also induces CHOP a pro-apoptotic factor that inhibits pro-survival factor BCL-2 and induces transcription of GADD34. The phosphatase GADD34 restores translation in order to amplify the apoptotic stimuli and signaling. The ATF6 branch is also a CHOP activator, however the other known targets of this signaling pathway are mainly in pro-survival programs of stress recovery, and these are chaperone proteins such as GRP78, GRP94, protein disulphide isomerase (PDI), and the transcription factor XBP1. The IRE1 can also have a dual role through activation of pro-survival and pro-apoptotic signaling. Pro-survival is mediated by ER chaperones, while the pro-apoptotic response is initiated in late stages of ER stress by

the activation of kinase pathways, in particular the c-Jun N-terminal kinase (JNK) pathway [29, 54]. Additionally, the mitochondrial apoptotic pathway can be activated by the BCL-2 proteins PUMA, BAX and BAK as a result of sustained ER stress. As an example, the BCL-2 proteins BAX and BAK can localize to the ER membrane, oligomerize and allow for calcium leak into the cytosol with subsequent apoptotic signaling by caspases 12 and 4. On the other hand, they can translocate into the mitochondrial outer membrane leading to permeabilization of the mitochondria with concomitant cytochrome c release. Free cytochrome c associates with APAF1 and caspase 9 in the apoptossome with subsequent activation of efector caspases 3 and 7 [29, 54]. The BCL2 protein PUMA/BBC3 is also activated by ER stress, and this can happen in a p53 dependent or independent fashion [55, 56].

Unpublished work form our laboratory shows that mRNA mistranslation is an important source of ROS and oxidative stress. ROS are highly reactive molecules capable of damaging proteins and nucleic acids and have been associated with ageing processes and neurodegeneration [57, 58]. The origin of ROS during mRNA mistranslation remains to be elucidated since ROS can be produced at several cellular locations such as the membrane, cytoplasm, peroxisomes, ER and mitochondria. However, likely origins are the ER and the mitochondria as these have been closely associated with oxidative conditions associated with loss of proteostasis [59-61] The folding environment in the ER is highly oxidizing to promote protein disulfide bond formation, and this oxidative environment also contributes to oxidation of ER chaperones and to accumulation of unfolded client proteins. ROS are produced in the ER lumen during protein folding as a by-product of electron transport from client proteins to molecular oxygen to form the oxidant hydrogen peroxide. Still, the precise mechanism of ROS production in ER stress is not fully understood. However, increased

folding loads trigger Ca^{2+} leakage into the cytoplasm and may induce secondary ROS production in the mitochondria. Finally, increased energetic demands for protein folding stimulate mitochondrial oxidative phosphorylation to increase ATP production, and consequently increase ROS production [29, 61].

1.4. Diseases associated with altered protein synthesis

Several diseases are caused by defects in mRNA translation. A group of diseases including cancer, neuronal pathologies, autoimmune disorders, and disrupted metabolism is connected with mutations in specific AARSs [62]. Mutations in the alanyl, glycyl, tyrosil and lysyl-tRNA synthetases are among the causes of the peripheral neurodegenerative Charcot-Marie-Tooth disease [62-64]. Editing defects in the ValRS that allow for mischarging of valine tRNAs with threonine, and also mutant Ser tRNAs that read non-cognate codons induce apoptosis in mammalian cells [65, 66]. An editing defect in the mouse AlaRS that mischarges alanine tRNAs with glycine and serine causes protein ubiquitination, aggregation and neurodegeneration. In this mouse model tRNA mischarging up-regulates molecular chaperones, but the severe neurodegeneration phenotype shows that constitutive translational errors generate extensive protein misfolding and exhaust the proteostasis network [14]. Mutations in the mitochondrial aspartyl and arginyl tRNA-synthetases cause impaired protein synthesis with associated mitochondrial dysfunction and are among the causes of human leukoencephalopathy, which has brainstem and spinal cord involvement and lactate elevation (LBSL) [67, 68]. In the mitochondrial context, mutations in the tRNA genes are responsible for diseases such as myopathy or hearing loss, or even complex disorders such as encephalopathy and cardiomyophathy [69]. For example the MELAS

syndrome which is characterized by myopathy, encephalopathy, lactic acidosis, stroke-like episodes and other neurological and non-neurological symptoms is associated with several point mutations in mitochondrial tRNA genes [69]. This condition is caused by altered aminoacylation levels of the mt tRNA Leu (UUR) that leads to deficient protein synthesis resulting in mitochondria with respiratory defects [70]. Another example of mitochondrial related diseases is MLASA which is characterized by myopathy, lactic acidosis and sideroblastic anaemia. In this case pseudouridylation of mitochondrial tRNAs is impared due to mutations in the pseudouridine synthase 1 [71]. Ribosomes are vital for cell functioning and mutations that affect the ribosomal machinery and translation factors can promote disease as well. Several mutations in small and large ribosomal proteins especially RSP19 cause Diamond-Blackfan anaemia (DBA) which is an inherited bone marrow failure syndrome characterized by proapoptotic hematopoiesis, bone marrow failure, birth defects and predisposition to cancer [72]. In this condition ribosome biogenesis problems reduce the number of functional ribosomes thus reducing protein synthesis and cellular growth [73]. The 5q− syndrome is a myelodysplastic syndrome with associated acute myeloid leukemia (AML) caused by ribosome biogenesis problems related with deletion of RPS14 [72]. Other examples of ribosomal related diseases are alopecia, neurological defects, and endocrinopathy syndrome (ANE syndrome), Shwachman-Bodian-Diamond syndrome (SDS), Dyskeratosis congenita (DC), skeletal dysplasias and Prader-Willi syndrome (PWS) [72].

1.5. Control of cellular homeostasis by non-coding RNAs

MicroRNAs (miRNAs) are a family of small non coding RNAs (~22 nucleotides) with important roles in the control of gene expression at the translational level, by binding to the 3' untranslated region (UTR) of target mRNAs [74]. Since the first miRNA lin-4 was discovered associated with development in *Caenorhabditis elegans*, the number and diversity of miRNAs has increased dramatically, and they have been described in more than 140 species [75, 76]. MiRNAs are transcribed in the nucleus by Pol II into capped and polyadenylated pri-miRNAs that contain single or multiple encoded miRNAs and are further processed by the RNases Drosha and Dicer to produce the mature miRNA in association with the RNA-induced silencing complex (RISC). Once in the cytoplasm the pre-mIR duplex is cleaved at the hairpin region by Dicer in association with TRBP and Argonaute proteins 1-4, producing the ~22 nucleoide miRNA duplex. The duplex contains the mature miRNA and also its complementary strand (*), but after processing the mature miRNA is preferentially maintained in the RNA-induced silencing complex (RISC) while the miRNA* is released and degraded [74, 77-79]. The RISC identifies target messages based on perfect (or nearly perfect) complementarity between the miRNA seed sequence, which is the region of nucleotides 2-7 or 2-8, and the target mRNA. In metazoans, most of the miRNAs pair imperfectly with their targets and promote translation repression or mRNA degradation (Figure 1.12). Degradation of target mRNA can happen by means of decaping and de-adenylation with subsequent mRNA targeting to the processing body (P-body) where the mRNA can be degraded or stored for later use. The translation process can also be regulated my mIRNA inhibition of translation initiation or miRNA slowing of translation elongation [80].

The mRNA targets of miRNAs in metazoans are mainly located in the 3′ UTR, where multiple miRNAs can bind. Also a single miRNA can target multiple mRNAs. The 5′ UTR and the coding region can also be targeted by miRNAs but few mRNAs are regulated in this manner [74, 80, 81]. In mammals, approximately 50% of protein coding genes are predicted targets of miRNA regulation, highlighting the pivotal relevance of miRNAs in gene expression regulation [82]. Regulation of gene expression by miRNAs is important for processes that control cellular differentiation and also developmental morphogenesis and patterning [74, 83, 84]. Neural differentiation and brain morphogenesis processes have an important component of miRNA regulation in zebrafish [85] and in mammals [86].

Several studies have implicated miRNAs in the regulation of the stress response. DNA damage for example can induce p53, which in turn induces transcription of a group of miRNAs. Namely, miR-34a, miR-34b and miR-34c, also enhance the processing of miR-16, miR-103, miR-143, miR-145, miR-26a and miR-206, thus promoting apoptosis and reducing proliferation [87]. Upon ER stress in human cells, the UPR XBP1 factor is regulated by miRNAs through a process in which PERK activates the transcription factor NF-kB, which in turn activates expression of miR-30c-2-3p that targets the 3’ UTR of XBP1. This mechanism may prevent over-activation of XBP1 [88], but this factor is also capable of inducing miR-346 whose main targets are regulators of the immune response [89]. In mouse fibroblasts the UPR factor IRE1α specifically cleaves several miRNA precursors (miR-17, miR-34a, miR-96, miR-125b) to relieve silencing of caspase-2 and stimulate apoptosis [90].

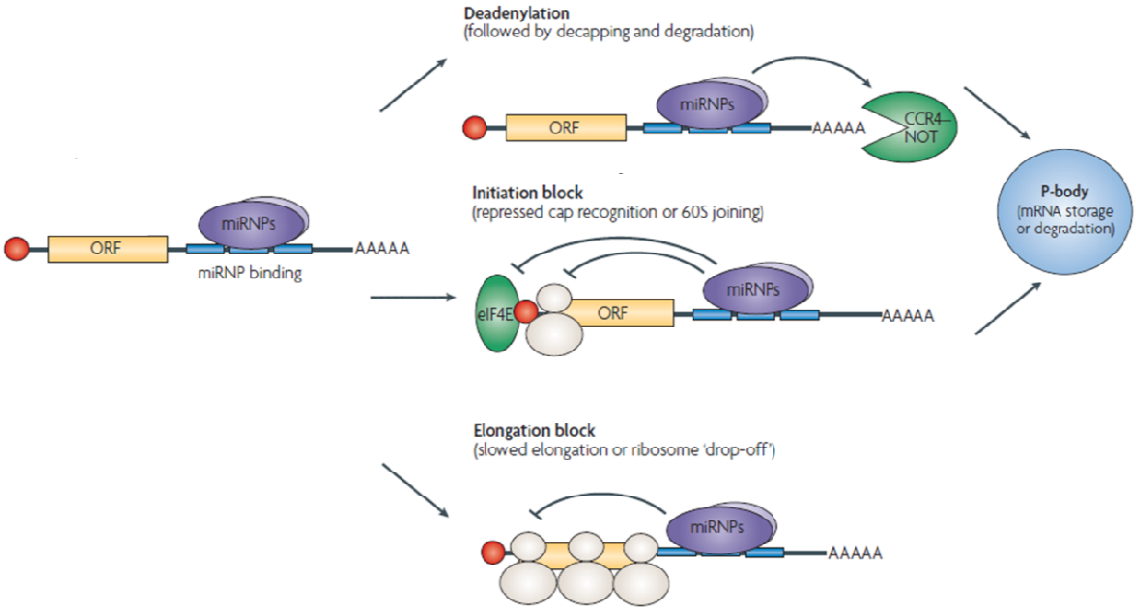

Figure 1.12. Mechanism of miRNA repression.
MiRNAs can induce mRNA decay through deadenylation and decapping. Translation initiation can be repressed at the cap-recognition or 60S assembly stages. These two processes that function at the level of mRNA decay and of translation initiation occur in p-bodies were the mRNAs can either be degraded or stored for latter usage. Translation can additionally be repressed in post initiation stages and this can happen as a result of slow elongation or ribosome drop-off [80].

Furthermore, in mouse heart the UPR factor ATF6 regulates the expression of several miRNAs, under stress situations. In particular, it downregulates mir-455 whose putative targets are involved in cardiac ischemic recovery [91].

Under prolonged ER stress conditions the translational rate is attenuated through eIF2α phosphorylation by PERK. This can lead to the assembly of stress granules which are enriched in RNA regulators that can modulate miRNAs actively. This alteration in cellular localization of miRNAs mRNA targets, Argonaute and miRNA-protein complex components may also contribute to miRNA regulation under stress situations [87]. Various disease states in humans have been described to be regulated by miRNAs. For example, miRNAs can act as oncogenes or tumor suppressor genes and mediate cancer progression of different cellular types [92]. MiRNAs can also be involved in

pathologies such as multiple sclerosis where miR-326 and miR-155 play a pivotal role [93]. Ageing related diseases are also associated with miR-9, miR-29a/b, miR-101, miR-107, miR-125b, miR-146a, miR-153, and miR-195 [94].

1.6. Zebrafish as a proteotoxic stress model

Zebrafish is widely used as a model organism for studying cell development. Zebrafish are small fish that are easily maintained, produce around 200 eggs per week, have ex utero embryo development and the embryos are optically clear, which facilitates organ observation and embryo manipulation and staining. Embryo development is also fast which is ideal to study vertebrate embryonic development. The implementation of genetic techniques in zebrafish, such as cloning, mutagenesis, transgenesis and genetic mapping facilitated the production of fish for studying several human diseases. Since zebrafish is a vertebrate organism it fills the gap between *Drosophila*/*C. elegans* and mouse/human genetics [95, 96]. Genome sequencing also contributes to the use of zebrafish as a vertebrate model and provides additional genome resources to vertebrate research.

Proteotoxic stress affects several domains of cellular homeostasis and has important consequences for ageing processes and neurodegeneration [15]. Therefore, a suitable proteotoxic stress model organism that recapitulates mammalian ageing is needed. Zebrafish has, during development and adulthood, a conserved heat shock response controlled by HSF1 and also a conserved set of the major heat shock chaperones, including HSP90, HSP70, chaperonines and sHSPs that protect cells from various environmental and physiological stresses [97, 98]. The UPP is a conserved quality control mechanism which is involved in protein degradation and in signaling

pathways involved in processes such DNA damage response, embryo and lens development [99-101]. The three UPR factors XBP1, ATF6 and PERK have been identified in zebrafish as being stress responsive [102-104]. This completes the set of the major eukaryotic stress response pathways and shows that zebrafish is a good model system to examine the proteotoxic stress generated by protein biosynthesis errors. Additionally, zebrafish is a powerful model for the study of apoptosis, both at developmental and adult stages, due to high conservation of zebrafish and mammal apoptotic pathways. Indeed, the p53 and Bcl-2 family of apoptotic factors are highly conserved in zebrafish where they play pivotal roles in controlling the intrinsic apoptotic pathway. The extrinsic apoptotic pathway is also conserved between mammals and zebrafish, relying on FADD and caspase 8 activation as well [105, 106]. Furthermore, this model organism is well suited for the study of neurodegeneration and ageing since it displays age related phenotypes such as loss of molecular chaperone activity [107]. The zebrafish central nervous system is organized in a similar fashion, and holds anatomical and chemical similarities with the human central nervous system, which are relevant to the study of neurodegeneration [108]. A zebrafish model of the conformational disease Huntington shows that protein aggregation, chaperone induction and apoptosis are observed as a result of neurodegenative prone conditions [109], confirming that zebrafish is suited to tackle the biology of mRNA mistranslation and proteotoxic stress.

1.7. Objectives of this thesis

Mistranslation of the genetic code leads to proteotoxic stress and causes proteome imbalance and cellular degeneration. However, it is not yet clear how such cellular phenotypes develop and whether they are a consequence of proteome disruption or result from secondary effects associated with accumulation of mistranslated proteins. To understand the biology of proteotoxic stress and how cells respond to accumulation of mistranslated proteins we built a zebrafish model of mRNA mistranslation. The major aims of this work are to address the cellular and developmental responses to proteotoxic stress in a vertebrate model system. The specific objectives of this thesis are:

- Induce mistranslation and protein aggregation in zebrafish embryos;
- Characterize the cellular response of zebrafish to mRNA mistranslation;
- Determine the effect of mistranslation induced proteotoxic stress on zebrafish mRNA and miRNA expression;
- Establish a transgenic zebrafish model of proteotoxic stress.

1.8. References

1. Jackson, R.J., C.U. Hellen, and T.V. Pestova, *The mechanism of eukaryotic translation initiation and principles of its regulation.* Nat Rev Mol Cell Biol, 2010. **11**(2): p. 113-27.
2. Kapp, L.D. and J.R. Lorsch, *The molecular mechanics of eukaryotic translation.* Annu Rev Biochem, 2004. **73**: p. 657-704.
3. Drummond, D.A. and C.O. Wilke, *The evolutionary consequences of erroneous protein synthesis.* Nat Rev Genet, 2009. **10**(10): p. 715-24.
4. Ogle, J.M. and V. Ramakrishnan, *Structural insights into translational fidelity.* Annu Rev Biochem, 2005. **74**: p. 129-77.
5. Reynolds, N.M., B.A. Lazazzera, and M. Ibba, *Cellular mechanisms that control mistranslation.* Nat Rev Microbiol, 2010. **8**(12): p. 849-56.
6. Farabaugh, P.J. and G.R. Bjork, *How translational accuracy influences reading frame maintenance.* EMBO J, 1999. **18**(6): p. 1427-34.
7. Shah, P. and M.A. Gilchrist, *Effect of correlated tRNA abundances on translation errors and evolution of codon usage bias.* PLoS Genet, 2010. **6**(9).
8. Zaher, H.S. and R. Green, *Quality control by the ribosome following peptide bond formation.* Nature, 2009. **457**(7226): p. 161-6.
9. Arava, Y., et al., *Dissecting eukaryotic translation and its control by ribosome density mapping.* Nucleic Acids Res, 2005. **33**(8): p. 2421-32.
10. Curran, J.F. and M. Yarus, *Base substitutions in the tRNA anticodon arm do not degrade the accuracy of reading frame maintenance.* Proc Natl Acad Sci U S A, 1986. **83**(17): p. 6538-42.
11. Rocha, E.P., *Codon usage bias from tRNA's point of view: redundancy, specialization, and efficient decoding for translation optimization.* Genome Res, 2004. **14**(11): p. 2279-86.
12. Ibba, M. and D. Soll, *Aminoacyl-tRNA synthesis.* Annu Rev Biochem, 2000. **69**: p. 617-50.
13. Francklyn, C.S., *DNA polymerases and aminoacyl-tRNA synthetases: shared mechanisms for ensuring the fidelity of gene expression.* Biochemistry, 2008. **47**(45): p. 11695-703.
14. Lee, J.W., et al., *Editing-defective tRNA synthetase causes protein misfolding and neurodegeneration.* Nature, 2006. **443**(7107): p. 50-5.
15. Chen, B., et al., *Cellular strategies of protein quality control.* Cold Spring Harb Perspect Biol, 2011. **3**(8): p. a004374.
16. Hartl, F.U., A. Bracher, and M. Hayer-Hartl, *Molecular chaperones in protein folding and proteostasis.* Nature, 2011. **475**(7356): p. 324-32.
17. Albanese, V., et al., *Systems analyses reveal two chaperone networks with distinct functions in eukaryotic cells.* Cell, 2006. **124**(1): p. 75-88.
18. Vabulas, R.M., et al., *Protein folding in the cytoplasm and the heat shock response.* Cold Spring Harb Perspect Biol, 2010. **2**(12): p. a004390.
19. Hartl, F.U. and M. Hayer-Hartl, *Molecular chaperones in the cytosol: from nascent chain to folded protein.* Science, 2002. **295**(5561): p. 1852-8.
20. Qiu, X.B., et al., *The diversity of the DnaJ/Hsp40 family, the crucial partners for Hsp70 chaperones.* Cell Mol Life Sci, 2006. **63**(22): p. 2560-70.
21. Zhao, R. and W.A. Houry, *Molecular interaction network of the Hsp90 chaperone system.* Adv Exp Med Biol, 2007. **594**: p. 27-36.
22. Pearl, L.H. and C. Prodromou, *Structure and mechanism of the Hsp90 molecular chaperone machinery.* Annu Rev Biochem, 2006. **75**: p. 271-94.
23. Kundrat, L. and L. Regan, *Balance between folding and degradation for Hsp90-dependent client proteins: a key role for CHIP.* Biochemistry, 2010. **49**(35): p. 7428-38.
24. Basha, E., H. O'Neill, and E. Vierling, *Small heat shock proteins and alpha-crystallins: dynamic proteins with flexible functions.* Trends Biochem Sci, 2012. **37**(3): p. 106-17.

25. Liberek, K., A. Lewandowska, and S. Zietkiewicz, *Chaperones in control of protein disaggregation.* EMBO J, 2008. **27**(2): p. 328-35.
26. Frydman, J., *Folding of newly translated proteins in vivo: the role of molecular chaperones.* Annu Rev Biochem, 2001. **70**: p. 603-47.
27. Mymrikov, E.V., A.S. Seit-Nebi, and N.B. Gusev, *Large potentials of small heat shock proteins.* Physiol Rev, 2011. **91**(4): p. 1123-59.
28. Jung, T., B. Catalgol, and T. Grune, *The proteasomal system.* Mol Aspects Med, 2009. **30**(4): p. 191-296.
29. Malhotra, J.D. and R.J. Kaufman, *The endoplasmic reticulum and the unfolded protein response.* Semin Cell Dev Biol, 2007. **18**(6): p. 716-31.
30. Schubert, U., et al., *Rapid degradation of a large fraction of newly synthesized proteins by proteasomes.* Nature, 2000. **404**(6779): p. 770-4.
31. Wolf, D.H. and W. Hilt, *The proteasome: a proteolytic nanomachine of cell regulation and waste disposal.* Biochim Biophys Acta, 2004. **1695**(1-3): p. 19-31.
32. Mizushima, N., et al., *Autophagy fights disease through cellular self-digestion.* Nature, 2008. **451**(7182): p. 1069-75.
33. Ishida, Y., et al., *Autophagic elimination of misfolded procollagen aggregates in the endoplasmic reticulum as a means of cell protection.* Mol Biol Cell, 2009. **20**(11): p. 2744-54.
34. Bukau, B., J. Weissman, and A. Horwich, *Molecular chaperones and protein quality control.* Cell, 2006. **125**(3): p. 443-51.
35. Schroder, M. and R.J. Kaufman, *The mammalian unfolded protein response.* Annu Rev Biochem, 2005. **74**: p. 739-89.
36. Yoshida, H., et al., *XBP1 mRNA is induced by ATF6 and spliced by IRE1 in response to ER stress to produce a highly active transcription factor.* Cell, 2001. **107**(7): p. 881-91.
37. Ron, D. and P. Walter, *Signal integration in the endoplasmic reticulum unfolded protein response.* Nat Rev Mol Cell Biol, 2007. **8**(7): p. 519-29.
38. Proud, C.G., *eIF2 and the control of cell physiology.* Semin Cell Dev Biol, 2005. **16**(1): p. 3-12.
39. Raven, J.F. and A.E. Koromilas, *PERK and PKR: old kinases learn new tricks.* Cell Cycle, 2008. **7**(9): p. 1146-50.
40. Krishnamoorthy, T., et al., *Tight binding of the phosphorylated alpha subunit of initiation factor 2 (eIF2alpha) to the regulatory subunits of guanine nucleotide exchange factor eIF2B is required for inhibition of translation initiation.* Mol Cell Biol, 2001. **21**(15): p. 5018-30.
41. Harding, H.P., et al., *Regulated translation initiation controls stress-induced gene expression in mammalian cells.* Mol Cell, 2000. **6**(5): p. 1099-108.
42. Schindler, A.J. and R. Schekman, *In vitro reconstitution of ER-stress induced ATF6 transport in COPII vesicles.* Proc Natl Acad Sci U S A, 2009. **106**(42): p. 17775-80.
43. Kaganovich, D., R. Kopito, and J. Frydman, *Misfolded proteins partition between two distinct quality control compartments.* Nature, 2008. **454**(7208): p. 1088-95.
44. Tyedmers, J., A. Mogk, and B. Bukau, *Cellular strategies for controlling protein aggregation.* Nat Rev Mol Cell Biol, 2010. **11**(11): p. 777-88.
45. Kopito, R.R., *Aggresomes, inclusion bodies and protein aggregation.* Trends Cell Biol, 2000. **10**(12): p. 524-30.
46. Kawaguchi, Y., et al., *The deacetylase HDAC6 regulates aggresome formation and cell viability in response to misfolded protein stress.* Cell, 2003. **115**(6): p. 727-38.
47. Santos, M.A., et al., *Selective advantages created by codon ambiguity allowed for the evolution of an alternative genetic code in Candida spp.* Mol Microbiol, 1999. **31**(3): p. 937-47.

48. Gomes, A.C., et al., *A genetic code alteration generates a proteome of high diversity in the human pathogen Candida albicans.* Genome Biol, 2007. **8**(10): p. R206.
49. Miranda, I., et al., *A genetic code alteration is a phenotype diversity generator in the human pathogen Candida albicans.* PLoS One, 2007. **2**(10): p. e996.
50. Wiltrout, E., et al., *Misacylation of tRNA with methionine in Saccharomyces cerevisiae.* Nucleic Acids Res, 2012. **40**(20): p. 10494-506.
51. Ben-Zvi, A., E.A. Miller, and R.I. Morimoto, *Collapse of proteostasis represents an early molecular event in Caenorhabditis elegans aging.* Proc Natl Acad Sci U S A, 2009. **106**(35): p. 14914-9.
52. David, D.C., et al., *Widespread protein aggregation as an inherent part of aging in C. elegans.* PLoS Biol, 2010. **8**(8): p. e1000450.
53. Aridor, M., *Visiting the ER: the endoplasmic reticulum as a target for therapeutics in traffic related diseases.* Adv Drug Deliv Rev, 2007. **59**(8): p. 759-81.
54. Szegezdi, E., et al., *Mediators of endoplasmic reticulum stress-induced apoptosis.* EMBO Rep, 2006. **7**(9): p. 880-5.
55. Reimertz, C., et al., *Gene expression during ER stress-induced apoptosis in neurons: induction of the BH3-only protein Bbc3/PUMA and activation of the mitochondrial apoptosis pathway.* J Cell Biol, 2003. **162**(4): p. 587-97.
56. Li, J., B. Lee, and A.S. Lee, *Endoplasmic reticulum stress-induced apoptosis: multiple pathways and activation of p53-up-regulated modulator of apoptosis (PUMA) and NOXA by p53.* J Biol Chem, 2006. **281**(11): p. 7260-70.
57. Winyard, P.G., C.J. Moody, and C. Jacob, *Oxidative activation of antioxidant defence.* Trends Biochem Sci, 2005. **30**(8): p. 453-61.
58. Berlett, B.S. and E.R. Stadtman, *Protein oxidation in aging, disease, and oxidative stress.* J Biol Chem, 1997. **272**(33): p. 20313-6.
59. Brown, G.C. and V. Borutaite, *There is no evidence that mitochondria are the main source of reactive oxygen species in mammalian cells.* Mitochondrion, 2012. **12**(1): p. 1-4.
60. Federico, A., et al., *Mitochondria, oxidative stress and neurodegeneration.* J Neurol Sci, 2012.
61. Malhotra, J.D., et al., *Antioxidants reduce endoplasmic reticulum stress and improve protein secretion.* Proc Natl Acad Sci U S A, 2008. **105**(47): p. 18525-30.
62. Park, S.G., P. Schimmel, and S. Kim, *Aminoacyl tRNA synthetases and their connections to disease.* Proc Natl Acad Sci U S A, 2008. **105**(32): p. 11043-9.
63. Latour, P., et al., *A major determinant for binding and aminoacylation of tRNA(Ala) in cytoplasmic Alanyl-tRNA synthetase is mutated in dominant axonal Charcot-Marie-Tooth disease.* Am J Hum Genet, 2010. **86**(1): p. 77-82.
64. Stum, M., et al., *An assessment of mechanisms underlying peripheral axonal degeneration caused by aminoacyl-tRNA synthetase mutations.* Mol Cell Neurosci, 2011. **46**(2): p. 432-43.
65. Nangle, L.A., C.M. Motta, and P. Schimmel, *Global effects of mistranslation from an editing defect in mammalian cells.* Chem Biol, 2006. **13**(10): p. 1091-100.
66. Geslain, R., et al., *Chimeric tRNAs as tools to induce proteome damage and identify components of stress responses.* Nucleic Acids Res, 2010. **38**(5): p. e30.
67. Edvardson, S., et al., *Deleterious mutation in the mitochondrial arginyl-transfer RNA synthetase gene is associated with pontocerebellar hypoplasia.* Am J Hum Genet, 2007. **81**(4): p. 857-62.
68. Isohanni, P., et al., *DARS2 mutations in mitochondrial leucoencephalopathy and multiple sclerosis.* J Med Genet, 2010. **47**(1): p. 66-70.
69. Yarham, J.W., et al., *Mitochondrial tRNA mutations and disease.* Wiley Interdiscip Rev RNA, 2010. **1**(2): p. 304-24.

70. Yasukawa, T., et al., *Modification defect at anticodon wobble nucleotide of mitochondrial tRNAs(Leu)(UUR) with pathogenic mutations of mitochondrial myopathy, encephalopathy, lactic acidosis, and stroke-like episodes.* J Biol Chem, 2000. **275**(6): p. 4251-7.
71. Bykhovskaya, Y., et al., *Missense mutation in pseudouridine synthase 1 (PUS1) causes mitochondrial myopathy and sideroblastic anemia (MLASA).* Am J Hum Genet, 2004. **74**(6): p. 1303-8.
72. Freed, E.F., et al., *When ribosomes go bad: diseases of ribosome biogenesis.* Mol Biosyst, 2010. **6**(3): p. 481-93.
73. Ellis, S.R. and J.M. Lipton, *Diamond Blackfan anemia: a disorder of red blood cell development.* Curr Top Dev Biol, 2008. **82**: p. 217-41.
74. Bartel, D.P., *MicroRNAs: genomics, biogenesis, mechanism, and function.* Cell, 2004. **116**(2): p. 281-97.
75. Kozomara, A. and S. Griffiths-Jones, *miRBase: integrating microRNA annotation and deep-sequencing data.* Nucleic Acids Res, 2011. **39**(Database issue): p. D152-7.
76. Lee, R.C., R.L. Feinbaum, and V. Ambros, *The C. elegans heterochronic gene lin-4 encodes small RNAs with antisense complementarity to lin-14.* Cell, 1993. **75**(5): p. 843-54.
77. Gregory, R.I., et al., *Human RISC couples microRNA biogenesis and posttranscriptional gene silencing.* Cell, 2005. **123**(4): p. 631-40.
78. Kim, V.N., J. Han, and M.C. Siomi, *Biogenesis of small RNAs in animals.* Nat Rev Mol Cell Biol, 2009. **10**(2): p. 126-39.
79. Lee, Y., et al., *MicroRNA maturation: stepwise processing and subcellular localization.* EMBO J, 2002. **21**(17): p. 4663-70.
80. Filipowicz, W., S.N. Bhattacharyya, and N. Sonenberg, *Mechanisms of post-transcriptional regulation by microRNAs: are the answers in sight?* Nat Rev Genet, 2008. **9**(2): p. 102-14.
81. Pillai, R.S., *MicroRNA function: multiple mechanisms for a tiny RNA?* RNA, 2005. **11**(12): p. 1753-61.
82. Krol, J., I. Loedige, and W. Filipowicz, *The widespread regulation of microRNA biogenesis, function and decay.* Nat Rev Genet, 2010. **11**(9): p. 597-610.
83. Ambros, V., *The functions of animal microRNAs.* Nature, 2004. **431**(7006): p. 350-5.
84. Harfe, B.D., et al., *The RNaseIII enzyme Dicer is required for morphogenesis but not patterning of the vertebrate limb.* Proc Natl Acad Sci U S A, 2005. **102**(31): p. 10898-903.
85. Giraldez, A.J., et al., *MicroRNAs regulate brain morphogenesis in zebrafish.* Science, 2005. **308**(5723): p. 833-8.
86. Krichevsky, A.M., et al., *A microRNA array reveals extensive regulation of microRNAs during brain development.* RNA, 2003. **9**(10): p. 1274-81.
87. Leung, A.K. and P.A. Sharp, *MicroRNA functions in stress responses.* Mol Cell, 2010. **40**(2): p. 205-15.
88. Byrd, A.E., I.V. Aragon, and J.W. Brewer, *MicroRNA-30c-2* limits expression of proadaptive factor XBP1 in the unfolded protein response.* J Cell Biol, 2012. **196**(6): p. 689-98.
89. Bartoszewski, R., et al., *The unfolded protein response (UPR)-activated transcription factor X-box-binding protein 1 (XBP1) induces microRNA-346 expression that targets the human antigen peptide transporter 1 (TAP1) mRNA and governs immune regulatory genes.* J Biol Chem, 2011. **286**(48): p. 41862-70.
90. Upton, J.P., et al., *IRE1alpha cleaves select microRNAs during ER stress to derepress translation of proapoptotic Caspase-2.* Science, 2012. **338**(6108): p. 818-22.
91. Belmont, P.J., et al., *Regulation of microRNA expression in the heart by the ATF6 branch of the ER stress response.* J Mol Cell Cardiol, 2012. **52**(5): p. 1176-82.
92. Kent, O.A. and J.T. Mendell, *A small piece in the cancer puzzle: microRNAs as tumor suppressors and oncogenes.* Oncogene, 2006. **25**(46): p. 6188-96.

93. Jr Ode, F., et al., *MicroRNA dysregulation in multiple sclerosis.* Front Genet, 2012. **3**: p. 311.
94. Holohan, K.N., et al., *Functional microRNAs in Alzheimer's disease and cancer: differential regulation of common mechanisms and pathway.* Front Genet, 2012. **3**: p. 323.
95. Lieschke, G.J. and P.D. Currie, *Animal models of human disease: zebrafish swim into view.* Nat Rev Genet, 2007. **8**(5): p. 353-67.
96. Zon, L.I., *Zebrafish: a new model for human disease.* Genome Res, 1999. **9**(2): p. 99-100.
97. Murtha, J.M. and E.T. Keller, *Characterization of the heat shock response in mature zebrafish (Danio rerio).* Exp Gerontol, 2003. **38**(6): p. 683-91.
98. Rupik, W., et al., *The expression patterns of heat shock genes and proteins and their role during vertebrate's development.* Comp Biochem Physiol A Mol Integr Physiol, 2011. **159**(4): p. 349-66.
99. Imai, F., et al., *The ubiquitin proteasome system is required for cell proliferation of the lens epithelium and for differentiation of lens fiber cells in zebrafish.* Development, 2010. **137**(19): p. 3257-68.
100. Lai, E.C., et al., *The ubiquitin ligase Drosophila Mind bomb promotes Notch signaling by regulating the localization and activity of Serrate and Delta.* Development, 2005. **132**(10): p. 2319-32.
101. Li, J., et al., *Zebrafish Ubc13 is required for Lys63-linked polyubiquitination and DNA damage tolerance.* Mol Cell Biochem, 2010. **343**(1-2): p. 173-82.
102. Garner, J.N., B. Joshi, and R. Jagus, *Characterization of rainbow trout and zebrafish eukaryotic initiation factor 2alpha and its response to endoplasmic reticulum stress and IPNV infection.* Dev Comp Immunol, 2003. **27**(3): p. 217-31.
103. Hu, M.C., et al., *XBP-1, a key regulator of unfolded protein response, activates transcription of IGF1 and Akt phosphorylation in zebrafish embryonic cell line.* Biochem Biophys Res Commun, 2007. **359**(3): p. 778-83.
104. Cinaroglu, A., et al., *Activating transcription factor 6 plays protective and pathological roles in steatosis due to endoplasmic reticulum stress in zebrafish.* Hepatology, 2011. **54**(2): p. 495-508.
105. Eimon, P.M. and A. Ashkenazi, *The zebrafish as a model organism for the study of apoptosis.* Apoptosis, 2010. **15**(3): p. 331-49.
106. Storer, N.Y. and L.I. Zon, *Zebrafish models of p53 functions.* Cold Spring Harb Perspect Biol, 2010. **2**(8): p. a001123.
107. Keller, E.T. and J.M. Murtha, *The use of mature zebrafish (Danio rerio) as a model for human aging and disease.* Comp Biochem Physiol C Toxicol Pharmacol, 2004. **138**(3): p. 335-41.
108. Bai, Q. and E.A. Burton, *Zebrafish models of Tauopathy.* Biochim Biophys Acta, 2011. **1812**(3): p. 353-63.
109. Schiffer, N.W., et al., *Identification of anti-prion compounds as efficient inhibitors of polyglutamine protein aggregation in a zebrafish model.* J Biol Chem, 2007. **282**(12): p. 9195-203.

Chapter 2 - Viable levels of mRNA mistranslation generate proteome aggregation and mitochondrial dysfunction in zebrafish

Marisa Reverendo, Ana R. Soares, Patrícia Pereira, Laura Carreto, Violeta Ferreira, Philippe Pierre, Gabriela R. Moura and Manuel A. S. Santos

Manuscript in preparation

2. Viable levels of mRNA mistranslation accelerate proteome aggregation and mitochondrial dysfunction in zebrafish

2.1. Abstract

Protein misfolding and aggregation deregulate the proteostasis network (PN) and are hallmarks of cell degeneration processes associated with ageing and human diseases. But how proteome aggregation causes cell degeneration remains controversial due to the lack of suitable methods for controlling it at the cellular and organismal levels. We have hypothesized that low level protein mutagenesis by ribosomal amino acid misincorporations would provide a robust model system for controllable proteome aggregation. To test this hypothesis we have engineered transgenic zebrafish embryos to misincorporate Serine (Ser) at various non-cognate protein sites. Chemical differences between Ser and the replaced amino acids produced embryos with variable levels of proteome aggregation. These mistranslating embryos upregulated the unfolded protein response (UPR) and the ubiquitin proteasome pathway (UPP), increased protein ubiquitination and down-regulate protein biosynthesis, whose levels were correlated with the extension of proteome instability. The mitochondrial network was disrupted, mitochondrial and nuclear DNA was damaged and ROS production increased in presence of a fully functional proteostasis network.

Taken together, our data highlight important roles of gene translational accuracy in the maintenance of ER homeostasis, DNA damage, mitochondrial function and oxidative stress. We postulate that protein biosynthesis errors (PBE) contribute to proteome aggregation and are an important cause of mitochondrial disruption and ageing.

2.2. Introduction

Protein homeostasis (proteostasis) is the process by which the cellular proteome is maintained, being crucial for proper development and health [1]. Proteostasis is maintained by multi-layered networks of protein quality control (PQC) systems that act downstream of mRNA translation [2, 3]. These PQC systems involve molecular chaperones and associated factors, the endoplasmic reticulum (ER) associated protein degradation pathway (ERAD), autophagy and the ubiquitin proteasome pathway (UPP) [4, 5]. For example, ER overloading with misfolded proteins triggers the unfolded protein response (UPR) via activation of alternative splicing of the primary transcript of Xbp1, phosphorylation of the translation initiation factor eIF2-α, transient attenuation of protein synthesis rate and cleavage of the transcription factor Atf6. These signaling cascades target misfolded ER proteins to salvage and refolding pathways or to degradation by the 26S proteasome and/or autophagy [2, 6]. Increased protein aggregation during ageing indicates that the capacity to maintain proteostasis becomes compromised or saturated over time. In fact, ageing is associated with progressive proteome aggregation in the worm *Caernobditis elegans* [7, 8], but how and why cells lose their capacity to maintain proteome homeostasis is poorly understood [9-11].

How protein aggregation is initiated in healthy individuals, activate PQC systems and proteostasis networks awaits clarification. A commonly accepted hypothesis posits that reactive oxygen species (ROS) oxidize proteins promoting their aggregation and gradual saturation of PQC systems [12, 13]. This hypothesis is supported by strong association of ROS with protein conformational diseases, such as Parkinson's and Alzheimer's disease, and by increasing ROS levels during ageing [14-16]. Recent studies show that generalized failure of the PN at the onset of adulthood is associated with poor activation of the heat shock and unfolded proteins responses [7]. Therefore,

ROS and proteostasis failure likely act synergistically on protein aggregation complicating the dissection of their individual contributions to ageing processes. Moreover, saturation of the ER protein processing capacity by accumulation of misfolded and aggregated proteins triggers calcium release and activates pro-apoptotic pathways [17, 18] through poorly understood mechanisms [19], suggesting a link between ROS, protein aggregation, ER saturation and cell death. A major unanswered question is whether age related mitochondrial senescence is the main cause of ROS or whether protein aggregation triggers a cascade of degenerative events that ultimately lead to increased ROS production by the mitochondria, ER, peroxisome and cytoplasm, creating a positive feedback loop that potentiates protein oxidation, misfolding and aggregation.

Poly(Q) and other aggregation prone proteins have been extensively used as model systems to study protein conformational diseases, but they have specific functions in the cell and their use to investigate global effects of proteome aggregation and cell degeneration is questionable. Recently, chimeric tRNAs have been validated as tools to induce proteome aggregation in a controlled manner in yeast [20] and mammalian cell lines [18], demonstrating that this methodology activates the stress responses induced by protein misfolding. Here we extended this methodology to the vertebrate model organism zebrafish. This proteome mutagenesis methodology is based on ribosome mediated misincorporation of Ser at non-cognate protein sites and produces variable levels of global proteome aggregation in zebrafish embryos. Our data demonstrate that this model system is suitable for the study of the stress response induced by protein aggregation *in vivo* in a multicellular organism, as embryos exhibit increased protein aggregation accompanied by down regulation of protein synthesis and a sharp increase in oxidative stress, recapitulating the phenotype observed in cells

transiently transfected with chimeric tRNAs [18, 20]. Our model system also recapitulates the protein aggregation phenotype observed in *C. elegans* [7, 8], without loss or decreased activation of stress response pathways. Indeed, in our model system proteins aggregate in presence of up-regulation of the UPR, molecular chaperones and UPS. This uncoupling of protein aggregation from loss of proteostasis shows that proteome aggregation induces disruption of the mitochondrial network and damage of mitochondrial and nuclear DNA in presence of a fully functional PN, establishing a direct link between ribosomal mistranslations, mitochondrial dysfunction and genome damage.

2.3. Material and methods

2.3.1. Maintenance of zebrafish (*Danio rerio*)

The AB zebrafish strain was maintained at 28ºC on a 14 h-light/10 h-dark cycle. Stages of embryonic development were determined based on the number of hours after fertilization and morphological standards [21]. Animal husbandry and experimentation was authorized by the local animal welfare committee and followed the Portuguese law for animal experimentation (Regulatory Guideline nº 1005/92, October 23rd, 1992).

2.3.2. Mutant tRNA plasmid construction and microinjection

Serine tRNA genes and flanking regions were amplified from zebrafish genomic DNA and digested with ApaI and SacII restriction enzymes. The fragments were cloned into the pCS2+EGFP vector [22], producing the plasmid pCS2+EGFPtRNA^{Ser}. Mutant tRNA constructs were produced using the plasmid pCS2+EGFPtRNA^{Ser} by site directed mutagenesis of nucleotide positions corresponding to the anticodon of the mature Ser-tRNA (Supplementary table 1). Mutations were selected according to similarity of amino acid properties, blossom score, codon usage and total codon counts (Supplementary Table 2) [23-27]. Codon analysis was carried out using the Anaconda software package [28]. 65 ng/µL of plasmid in phenol red/KCl were injected in one-cell stage embryos and embryos were observed under a stereo-microscope equipped for fluorescence measurements (Nikon).

2.3.3. Northern blot analysis

Total RNA of 24hpf embryos were resolved on 15% polycralyamide gels for 18 hours at 500V. The section of gel containing the tRNAs was semi-dry transferred to a nitrocellulose membrane (Hybond N, Amershan) and membranes were cross linked

using a UV Stratalinker-1800 from Stratagene. Probes were prepared by 5' phosphorylation of 10pmol of short oligonucleotides with γ-^{32}P-ATP. Membranes were hybridized overnight at the oligos Tm minus 5ºC with rotation, then exposed to a K-screen and scanned using Molecular Imager FX (Bio-Rad).

2.3.4. GFP fluorescence reporter

To check the decoding activity of the mutant tRNAs a green fluorescent protein (GFP) reporter was used. The GFP gene contains a Ser codon at position 65 wich is essential for chromophore formation and mutations at this position result in significant alteration or even loss of GFP fluorescence. Various reporter constructs were built by site directed mutagenesis of codon 65 of the GFP gene cloned into plasmid pCS2+EGFP. The construct with a Ser codon at position 65 (S65) was used as the positive control while the constructs bearing codon (A65 – GCG, G65 – GGA, L65 – CTG, V65 – GTG) were used as gain of function reporters. In these cases wild type levels of GFP fluorescence were dependent on the misincorporation of Ser by the mutant tRNAs at position 65. These reporters were cloned into the pCS2+EGFP plasmid yielding the plasmid pCS2+EGFPtRNA^{Ser} (Supplementary Table 3). Plasmids were prepared and microinjected as described previously. Embryos were observed under an epifluorescence microscope Imager.Z1 (Zeiss), a GFP filter, AxioCam HRm camera (Zeiss) and AxioVision software (Zeiss). The fluorescence levels were determined using ImageJ software; a minimum of 20 embryos were analyzed per assay. 24hpf control and test embryos were collected for western blot analysis.

2.3.5. Western immunoblotting

For western blot analysis 24hpf embryos were dechorionated and deyolked [29]. The whole embryo lysate was extracted using 1x SDS sample buffer at 95ºC for 5 minutes. Approximately 50 µg/lane of protein were loaded on 12% or 15% SDS–PAGE minigels, after electrophoresis proteins were wet transferred to a nitrocellulose membrane. After blocking, membranes were incubated with primary antibodies: anti-GFP (Clontech), anti-β-tubulin (Invitrogen), anti-poliubiquitin (Covance), anti-HSP90 (StressMarq), anti-HSP70 (StressMarq) and anti-HSP27 (Abcam) diluted in TBS-T with 5% LFM. Detection was performed using a secondary antibody labeled with an infrared dye (IRDye 800CW, Li-COR) at room temperature and in the dark. Membranes were scanned and analyzed using the Odyssey® IR scanner and images were analyzed using Odyssey® imageing software 3.0 with default settings. The results obtained are expressed as the relative percentage normalized for control sample values.

2.3.6. SDS-PAGE of protein aggregates

Embryos were collected at 24hpf, dechorionated and deyolked. For rotenone and 3-nitropropionic acid treatments embryos were exposed at 4hpf to a range of 5, 10, 15µg/L and 5, 10, 20mM respectively. Batches of 60 embryos were lysed in 300µL of cold buffer (50mM PBS pH7, 1mM EDTA, 5% Glycerol, 1mM PMSF, 0,5X Protease Inhibitors Roche). To remove embryo debris total extracts were centrifuged at 3000 rpm at 4ºC for 5 minutes. Supernatants were centrifuged again at 13000 rpm at 4ºC for 20 minutes. The resulting pellets were washed with 320 µl of lysis buffer and 80 µl of 10% Triton-X 100 and centrifuged at 13000 rpm at 4ºC for 20 min. Detergent insoluble fractions were fractionated on 15% SDS-PAGE minigels which were stained with Coomasie brilliant blue R, scanned and analyzed using the Odyssey® IR scanner and

imageing software 3.0. Lane signals were normalized to the concentration of the total protein extracts determined by the BCA method. For the experiments using adult tissues, pools of three individuals were used per sample. Briefly, zebrafish were anesthetized, using tricaine, the collected organs were immediately frozen in liquid nitrogen and kept at -80ºC. Samples were lysed and processed as described above for the embryos.

2.3.7. Measurement of protein carbonyls

Protein carbonyls were quantified by spectrophotometry using 2,4-dinitrophenylhydrazine (DNPH). Five hundred microliters of 10 mM DNPH dissolved in 2 M HCl were added to 100 µl of soluble protein fraction. In parallel, a blank reaction was prepared by addition of 500 µl of 2M HCl solution containing no DNPH, both were incubated in the dark for 1 h at 20ºC. After 500µl of 20% trichloroacetic acid were added to the samples and blanks, these were allowed to stand for 15 min at 4°C. Samples were centrifuged at 10,000 *g* for 15 min at 4°C. Pellets were washed three times with 1 ml of a 1:1 (vol/vol) mixture of ethanol and ethyl acetate and centrifuged again for 3 min. Protein samples were dissolved in 1mL of 6 M guanidine hydrochloride and incubated for 30 min at 37°C. The amount of protein dinitrophenylhydrozone derivative was quantified by measuring the absorbance at 370 nm. Carbonyl contents were normalized per amount of protein and expressed as a function of control sample.

2.3.8. HSPB1 mCherry fusion reporter

The mCherry gene was cloned at BamHI and ClaI sites of the pT2AL200R150G vector [30] replacing the GFP gene. HSPB1 promoter [31] and coding region (without stop codon) were amplified from zebrafish genomic DNA and cloned sequentially at

XhoI, SalI and Sal, BamHI sites of the pT2AL200R150G-mCherry vector. A mixture of the mCherry fusion reporter and mutant tRNA plasmids was injected in phenol red/KCl in one-cell stage embryos, and embryos were observed under an epifluorescence microscope Imager.Z1 (Zeiss), a mCherry and a GFP filter, AxioCam HRm camera (Zeiss) and AxioVision software (Zeiss).

2.3.9. Immunofluorescence

Immunofluorescence was carried out on 5-μm sections of paraffin-embedded formaldehyde fixed 5dpf zebrafish embryos. Antigen retrieval was done with Citrate buffer at 98ºC, for 30 minutes. Slides were washed several times with TBS-T and blocked with Ultra V Block (Thermo Scientific). All incubations were performed in a humidified container. Samples were incubated with primary antibody (Mouse anti Ubiquitin, Cell Signaling, 1:500 in Large Volume UltrAb Diluent – Thermo Scientific) for 18 hours at 4°C. An Alexa Fluor® 594 Goat Anti-Mouse (1:500) was used as the secondary antibody. Samples were mounted using DAPI Vectashield, and observed under an epifluorescence microscope Imager.Z1 (Zeiss), a Rhod and DAPI filter, AxioCam HRm camera (Zeiss) and AxioVision software (Zeiss).

2.3.10. Protein synthesis rate determination

Protein synthesis rate was determined using the non-radioactive puromycin based SUnSET method [32]. Puromycin is a tyrosyl tRNA analog which is randomly incorporated by the ribosome into nascent peptides, blocking and labeling newly synthesized polypeptides. Detection of puromycin using an anti-puromycin monoclonal antibody allows for the measurement of protein synthesis rate without the use of radioactivity [32]. For this, 24hpf embryos injected with the mutant tRNAs were

washed, dechorionated and incubated in 10 µg/ml of puromycin for 30 min at 28ºC. After incubation, cycloheximide was added to a final concentration of 100µg/ml. Embryos were then collected for western immunoblotting. Puromycin incorporation into proteins was detected by immunoblotting using the mouse IgG2a monoclonal anti-puromycin antibody (clone 12D10, 1:5000) [32, 33]. Blots were incubated overnight at 4°C in 5% low fat milk TBS-T.

2.3.11. Proteasome chymotrypsin-like activity assay

The proteasome chymotrypsin-like activity was assayed using the fluorogenic substrate peptide succinyl-leucine-leucine-valine-tyrosine-MCA (s-LLVY-MCA). For this, 24 hpf embryos were dechorionated and ressuspendend in lysis buffer. The total protein extracts were centrifuged at 5.000rpm for 5min at 4ºC. Supernatants were transferred to a new tube and centrifuged at 13.000 rpm, 4ºC, for 10 min. 50µg of embryo extracts were incubated at 37ºC in 200 µl of assay buffer (10 mM Tris-Cl, pH 8, 20 mM KCl 1M 5 mM $MgCl_2$), with 50µM of s-LLVY-MCA (diluted in 10 % DMSO). Reactions were started by the addition of s-LLVY-MCA and fluorescence of the proteolytically released MCA was quantified at time 0 and 60 minutes. Fluorescence was recorded using a microplate reader Infinite®200 Tecan at 435 nm emission (excitation at 365 nm). Final activity was calculated as fluorescence emission at time 60 min subtracted from fluorescence emission at time 0 min relative to control [34, 35].

2.3.12. Total RNA extraction

Total RNA was extracted using Trizol® according to the manufacturer instructions. Briefly, 200 24hpf embryos were collected, dechorionated and stored at -80ºC. Frozen embryo pellets were ressuspended in 1ml of TRIZOL and disrupted using

precellys 24 (Bertin technologies). The total extracts were incubated at room temperature for 5 minutes and further extracted with chlorophorm and isopropyl alcohol. Total RNA pellets were washed with 75% ethanol and ressuspended in milliQ water. To remove contaminating DNA, samples were treated with DNAseI (Fermentas) following the manufacturer instructions and stored at -80ºC. RNA was quantified using the Nanodrop 1000 Spectrophotometer (Thermo Scientific) and its quality was verified using the Agilent 2100 Bioanalyzer.

2.3.13. Gene expression microarrays

Gene expression profiling was performed using the Agilent protocol for One-Color Microarray-Based Gene Expression Analysis Quick Amp Labeling v5.7 (Agilent Technologies). Briefly, cDNA was synthesized from 600ng of total RNA using Agilent T7 Promoter Primer and T7 RNA Polymerase Blend and labeled with Cyanine 3-CTP. Labeled cDNA was purified with RNAeasy mini spin columns (QIAGEN) to remove residual Cyanine 3-CTP. Dye incorporation and quantification was monitored using the Nanodrop 1000 Spectrophotometer. Agilent zebrafish (v2) microarrays were hybridized with 1,65 μg of labeled cDNA. Hybridizations were carried out using Agilent gasket slides in a rotating oven for 17hr at 65ºC. After hybridization, microarrays were washed using the wash procedure with stabilization and drying solution following the manufacturer recommendations (Agilent). Slides were immediately scanned using an Agilent G2565AA microarrays scanner (Agilent).

2.3.14. Microarray data extraction and analysis

Probes signal values were extracted from microarray scan data using Agilent Feature Extraction Software (Agilent). The microarray raw data was submitted to the

GEO database and has been given the following accession number: GSE50090. Data were normalized using median centering of signal distribution with Biometric Research Branch BRB-Array tools v3.4.o software. Microarray data analysis was carried out with MEV software (TM4 Microarray Software Suite) [36, 37]. A t test p□0,05 was applied to identify genes that showed statistically significant differences in expression between control and mutant tRNA samples. A general GO term enrichment analysis for total gene lists for all the mutants was carried out using a hypergeometric test in GeneCodis 2.0 [38, 39].

2.3.15. Real-time quantitative PCR

Quantification of gene expression was carried out using Power SYBR® Green PCR Master Mix. Total RNA was extracted using Trizol® and treated with DNAseI. cDNA was prepared from 1µg of total RNA using Superscript II (Invitrogen) following the manufacturer´s instructions. Real-time Quantitative PCR was carried out using the ABI Prism 7500 Sequence Detector System (Applied Biosystems). qPCR reactions were performed with cDNA 1:4 diluted in nuclease-free water in reactions containing 2µL of cDNA template, 0,4µL 10µM forward and reverse primers, 10µL of Power SYBR® Green PCR Master Mix and 7,2µL of nuclease-free water. PCR reactions were carried out at 95ºC for 10min, 95ºC for 15s and 60ºC for 60s with 39 repetitions. All primer sets (Supplementary Table 4) were tested for amplification efficiency using standard dilution curves. The threshold cycle data (CT) and baselines were determined using auto settings. All assays, including no template controls, were performed in triplicate and relative quantification of gene expression was calculated by the $2^{-\Delta\Delta CT}$ method with primer efficiency correction [40, 41] where the control sample was the endogenous serine tRNA. All analysis were carried out using REST-MCS tool [41].

Quantification of mitochondrial DNA was carried out using Power SYBR® Green PCR Master Mix. DNA was extracted using Qiagen Genomic-tip 20/G and Qiagen DNA Buffer Set following the manufacturer´s instructions [42]. The NADH dehydrogenase 1(ND1) gene of the mtDNA and the α-tubulin nDNA gene were amplified by qPCR (ABI 7500 Fast Real-Time PCR System). The ND1 primers were Nd1_Fw 5'-GTAGCTGATGGCGTGAAACT-3' and Nd1_rev 5'-GGTCGAGTACTGGATAGGG-3'. Real-time Quantitative PCR was carried out using the ABI Prism 7500 Sequence Detector System (Applied Biosystems). qPCR was performed with 10ng of DNA diluted in nuclease-free water in reactions containing 2µL of DNA template, 0,4µL 10µM forward and reverse primers, 10µL of Power SYBR® Green PCR Master Mix and 7,2µL of nuclease-free water. PCR reactions and data analysis were carried out as described above.

2.3.16. *xbp1* semi quantitative real-time PCR

RNA extraction and cDNA synthesis were carried out as described above. Primers for the zebrafish *xbp1* that were used in semi-quantitative RT-PCR were XBP1FW 5'-GTTCAGGTACTGGAGTCCGC-3' and XBP1RV: 5'-CTCAGAGTCTGCAGGGC CAG-3' [43]. Tubulin was used as an internal control. PCR products were analysed by electrophoresis on a 3% agarose gel and stained with ethidium bromide.

2.3.17. Dihydroethidium assay

Dihydroethidim detects superoxide production due to its cell permeability and blue-fluorescence in the cytosol. Upon oxidation DHE intercalates within DNA, staining the nucleus as bright fluorescent red. Superoxide levels were determined in dechorionated 24hpf live zebrafish embryos in 96-well black plates. Briefly, embryos

were washed in system water, distributed 20 per well and incubated in 200µL of 10µM dihydroethdium (Sigma- D11347) also in system water. Incubation was carried out in the dark at 28ºC for 30 minutes. The average fluorescence emission at 600 nm following excitation at 530 nm was detected using a microplate reader Infinite®200 Tecan. Distribuition of superoxide in the embryos was documented using an epifluorescence microscope Imager.Z1 (Zeiss), a Rhod 20 filter, AxioCam HRm camera (Zeiss) and AxioVision software (Zeiss). Embryos were prepared following the same workflow used for the fluorimetric mesurements. After DHE incubation embryos were immediately washed and mounted on 3% methylcellulose with a drop of vectashield.

2.3.18. Hydrogen peroxide detection

Detection of hydrogen peroxide on 24hpf zebrafish embryos was carried out with the Amplex® Red Hydrogen Peroxide/Peroxidase Assay kit (Molecular Probes®) following manufacturer's instructions. The Amplex® Red reagent (10-acetyl-3,7-dihydroxyphenoxazine) reacts with hydrogen peroxide in a 1:1 stoichiometry in the presence of horseradish peroxidase (HRP) producing the oxidation product resorufin. Resorufin has excitation and emission maxima of approximately 571 nm and 585 nm and can be detected either fluorometrically or spectrophotometrically. Batches of 30 embryos were dechorionated, deyolked and homogenized in phosphate-buffered saline (PBS; pH 7.4). 50µl of embryo lysates were used and incubated with 50 µl of a working solution of 100 µM Amplex® Red reagent and 0.2 U/mL HRP. Incubations were carried out at room temperature in the dark for 30 mins. Absorbance was measured in a microplate iMark® BioRad reader at 560nm. Samples were normalized with protein concentration determined by the BCA method, and were expressed relative to control sample.

2.3.19. Catalase activity detection

Detection of catalase activity in 24hpf zebrafish embryos was carried out using the Amplex® Red Catalase Assay Kit (Molecular Probes®) following manufacturer's instructions. Briefly, batches of 30 embryos were dechorionated, deyolked and homogenized in 1X Reaction buffer. Catalase hydrolyses hydrogen peroxide to water and oxygen. Amplex® Red detects unreacted hydrogen peroxide in the presence of horseradish peroxidase (HRP) producing resorufin. For this, 50µl of embryo lysates were incubated with 50 µl of a working solution of 100 µM Amplex® Red reagent and 0.4 U/mL HRP. Incubations were carried out at room temperature in the dark for 30 mins. Absorbance was quantified in a microplate iMark® BioRad reader at 560nm. Samples were normalized with protein concentration determined by the BCA method and are expressed relative to control sample.

2.3.20. Mitochondrial and nuclear DNA damage

Quantitative PCR was performed according to [42]. Briefly, 10 ng DNA (quantified with PicoGreen® dye, Invitrogen) was amplified with Gene Amp® XL PCR kit (Applied Biosystems) using the primers and conditions described for zebrafish. Small targets were amplified for normalization/verification of DNA concentration. Final concentrations for all reactions were 1x XL buffer, 100µg/mL of BSA, 200 µM of each dNTP, and 0.4 mM of each primer in 50µL. For short and long mitochondrial targets, 1.2 mM of $Mg(OAc)_2$ was used, in the case of the long nuclear target 1.05mM of $Mg(OAc)_2$ were used in the PCR mix. Cycling conditions for small nuclear and mitochondrial targets were: 75°C 2min; 94°C 1min; 94°C 15s, 60ºC/62°C 45s, and 72°C 30s (24, 21 cycles) and final extension at 72°C for 5min. For long targets nuclear and mitochondrial cycling conditions were: 94°C for 1 min; 94°C for 15 s and

69°C/68ºC for 12 min (24, 19 cycles); and 72°C for 10 min. PCR reactions were hot started at 75ºC for 90s and after this the enzyme *rTth* was added. PCR products were again quantified using PicoGreen® dye, and DNA concentrations were converted to lesion frequencies per 10kB DNA [44].

2.3.21. Mitochondrial membrane potential

Mitochondria of 24hpf zebrafish embryos were isolated following the MITOISO1 isolation kit protocol (MITOISO1; Sigma). All steps were performed on ice or with icecold buffers. Mitochondrial membrane potential was determined with the JC-1 dye according to the manufacturer's instructions (MITOISO1, Sigma). Batches of 60 embryos were dechorionated and homogenized in 1X extraction buffer A, using a Teflon pestle. Embryo lysates were centrifuged at 600xg 5 mins at 4ºC; supernatants were centrifuged again at 11,000× g 10 mins at 4°C. The final pellets were resuspended in extraction buffer centrifuged again as described above. Pellets containing the mitochondrial fraction were resuspended in the supplied 1X storage buffer. For the detection of mitochondrial membrane potential, fractions were incubated with JC-1 dye for 7 mins at room temperature in the dark. Finally, fluorescence was measured at490/590nm with a Perkin Elmer Fluorescence Spectrometer (LS 50B).

2.3.22. Mitochondria staining

Live imaging of mitochondria in zebrafish was carried out using MitoTracker® Red CM-H2XRos (Molecular Probes®). 24hpf embryos were dechorionated and incubated with MitoTracker 500nM for 30 mins in the dark. For imaging, anesthetized zebrafish embryos were embedded in methyl cellulose and overlayed with vectashield. Mito Tracker fluorescence was documented by epifluorescence microscopy.

Fluorescence images were obtained using an Imager.Z1 (Zeiss), a Rhod filter, AxioCam HRm camera (Zeiss) and AxioVision software (Zeiss).

2.3.23. Statistical analysis

Data was analyzed using GraphPad Prism. The differences between control and conditioned embryos were assessed using a Student's t-test or ANOVA with post test Dunnett's Multiple Comparison Test. In all cases, p values < 0.05 were considered statistically significant.

2.4. Results

2.4.1. Direct proteome mutagenesis using sense codon misreading tRNAs

In order to study the cellular consequences of proteome aggregation we have generated mutant zebrafish Ser-tRNAs that misincorporate Ser at non-cognate codons alanine (GCG), glycine (GGA), valine (GTG) and leucine (CTG) (Figure 2.1A). Since the eukaryotic seryl-tRNA synthetase (SerRS) does not interact with the anticodon of Ser-tRNAs [45-47], mutations in the anticodon of the Ser-tRNA did not interfere with serylation by the SerRS, but altered decoding properties of the Ser-tRNAs (Supplementary Table 1). For simplicity, the mutant tRNAs were designated Ser-$tRNA_{CGC}^{Ala}$, Ser-$tRNA_{UCC}^{Gly}$, Ser-$tRNA_{CAC}^{Val}$ and Ser-$tRNA_{CAG}^{Leu}$. The mutant anticodons were chosen on the basis of the chemical differences between Ser and Ala, Gly, Val and Leu, namely polarity and hidropathy. Ser is polar while the replaced amino acids are non polar. Ser is also hydrophilic while the others are hydrophobic and aliphatic, as is the case of Ala and Leu [23, 26, 27]. Importantly, hydrophobic amino acids, such as Ala, Val and Leu are commonly buried in hydrophobic protein cores while, hydrophilic amino acids, such as Gly and Ser, are usually located on protein surfaces [23, 48]. These chemical variables, blossom scores and codon usage patterns were taken into consideration to produce transgenic zebrafish embryos with increasing levels of proteome instability (Supplementary Table 2). For example, the blossom score for Ser-Ala replacements is 1, Ser-Gly is 0 and Ser-Val or Ser-Leu is -2 [24, 25]. Therefore, Ala replacements with Ser were expected to produce minor proteome destabilization, but Leu replacement with Ser expected to produce major proteome instability [23].

The mutant tRNA genes were microinjected into one cell zebrafish embryos after fertilization and their expression was verified by northern blot analysis in 24hpf

embryos (Figure 2.1B). Decoding activity was monitored using a GFP reporter system (Figure 2.1C, D). For this, the non-cognate codon targeted by each mutant tRNA was inserted at codon-65 of the GFP gene, replacing the wild type Ser TCT codon.

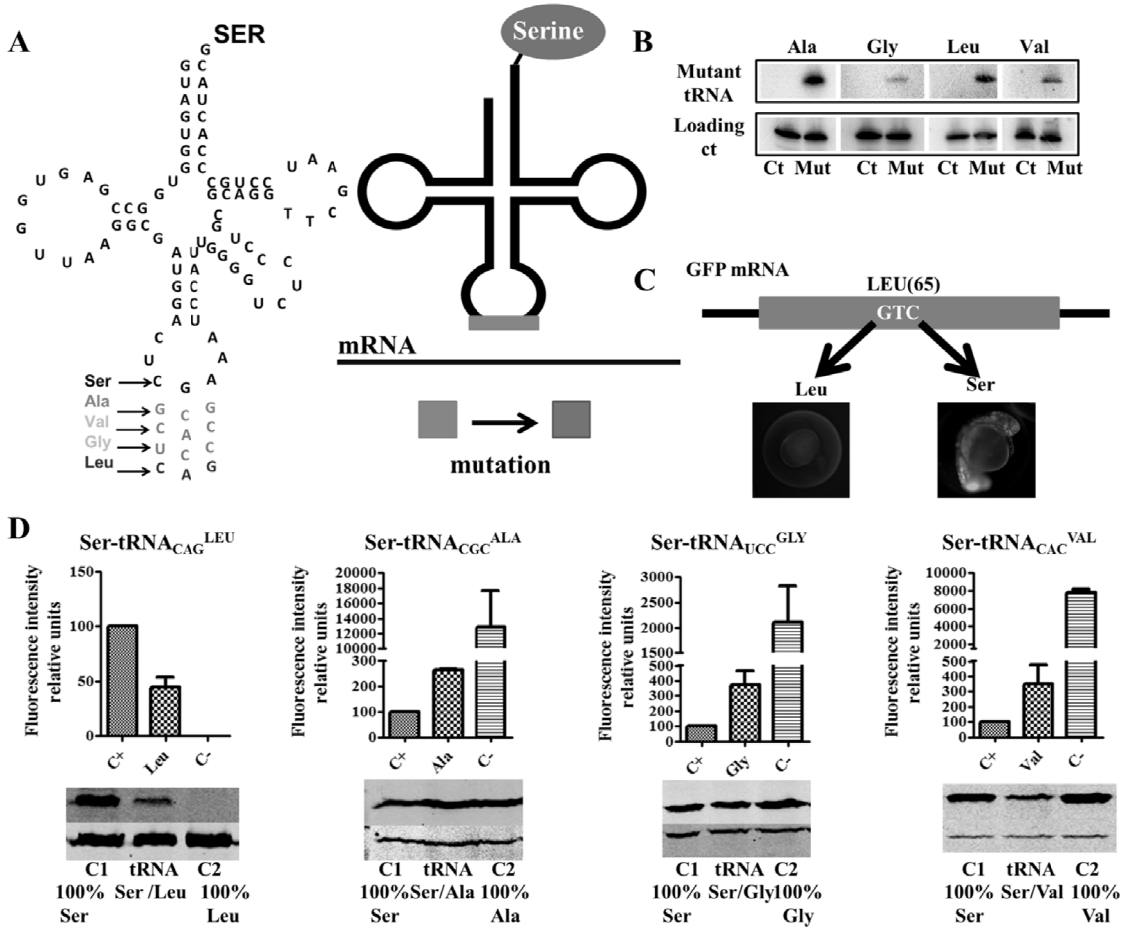

Figure 2.1. Proteome mutagenesis using misreading tRNAs.
A) A Ser-tRNA gene was mutated in the anticodon region by site directed mutagenesis to produce tRNAs that insert Ser at alanine (GCG), valine (GTG), glycine (GGA) and leucine (CTG) codons. Our method takes advantage of the fact that the seryl-tRNA-synthetase (SerRS) does not rely on the anticodon sequence to recognize the Ser tRNAs, thus allowing the mutant tRNA to be charged with Ser. These mutant tRNAs incorporate Ser at non-cognate Ala, Gly, Val and Leu sites producing aberrant proteins. **B)** Northern blot analysis showing that all mutant tRNAs are expressed and processed. **C)** A GFP reporter was used to quantify the level of Ser misincorporation at non-cognate sites. The residue Ser 65 is critical for GFP fluorescence, insertion of another amino acid at this site shifts overall fluorescence. **D)** The mutant tRNAs were able to partially restore wild type GFP fluorescence levels. Western blot analysis showing that Ser insertion at position 65 is able the restore GFP synthesis. Data are presented as the mean ± SD (n =4). Fluorescence units are relative to Control 1. Control 1 refers to 100% insertion of serine at position 65. Control 2 refers to insertion of 100% insertion of the amino acids tested.

Since Ser 65 (S65) is essential for cromophore formation the mutant GFPs had no fluorescence or significantly altered (increased or decreased) fluorescence when expressed in wild type (WT) embryos. However WT fluorescence levels could be partially restored in embryos co-expressing the mutant tRNAs if they inserted Ser at position 65 [49, 50]. Quantification of the relative GFP fluorescence showed that Leu incorporation alone at CTG-65 abolished fluorescence (Figure 2.1C-D), while there was gain of fluorescence in embryos expressing the Ser-$tRNA_{CAG}^{Leu}$ (Figure 2.1C-D). Interestingly, insertion of Ala (GCG), Gly (GGA) and Val (GTG) codons at position 65 of GFP, increased GFP fluorescence sharply producing a hyperfluorescent protein (Figure 2.1D). In these cases, incorporation of Ser at these codons by the mutant heterologous Ser-$tRNA_{CGC}^{Ala}$, Ser-$tRNA_{UCC}^{Gly}$, Ser-$tRNA_{CAC}^{Val}$, reduced fluorescence levels close to wild type GFP fluorescence (Figure 2.1D), indicating that these tRNAs were also active decoders.

2.4.2. Protein synthesis errors increase protein ubiquitination and aggregation

As mentioned above, besides the mutant tRNAs, our transgenic embryos expressed WT $tRNA_{CGC}^{Ala}$, $tRNA_{UCC}^{Gly}$, $tRNA_{CAC}^{Val}$ and $tRNA_{CAG}^{Leu}$, which are encoded by genes whose copy number in the zebrafish genome is 112, 47, 227 and 300, respectively. These WT tRNAs ensure production of wild type polypeptides essential for embryo viability. The mutant Ser-$tRNA_{CGC}^{Ala}$, Ser-$tRNA_{UCC}^{Gly}$, Ser-$tRNA_{CAC}^{Val}$ and Ser-$tRNA_{CAG}^{Leu}$ competed, therefore, with these WT tRNAs for the decoding of the above mentioned codons. In other words, Ser misincoporation at the non-cognate codon positions produced a statistical subpopulation of polypeptides of each protein (statistical proteins), whose abundance should be proportional to the number of non-cognate

codons decoded by the mutant tRNAs. The fate of the mutant polypeptides likely depends on the destabilizing nature of the mutations, i.e., certain mutations may result in protein unfolding, ubiquitination, degradation or aggregation, while others may induce low level protein destabilization and allow for refolding by molecular chaperones. Therefore, we expected that Ser misincorporation would saturate PQC systems, leading to increased protein ubiquitination and aggregation. Indeed, protein ubiquination was increased in all mutants, with the highest levels occurring in the embryos expressing the Ser-$tRNA_{UCC}^{Gly}$ (60%), Ser-$tRNA_{CAC}^{Val}$ (40%) and Ser-$tRNA_{CAG}^{Leu}$ (60%) (Figure 2.2A). Insoluble protein aggregates were also detected and the highest levels were present in the embryos expressing Ser-$tRNA_{CAG}^{Leu}$ (70%) (Figure 2.2B). In line with these data the carbonyl content of proteins, which measures oxidative damages [51], was increased by 370%, 340% and 490% in the embryos expressing the Ser-$tRNA_{UCC}^{Gly}$, Ser-$tRNA_{CAC}^{Val}$ and Ser-$tRNA_{CAG}^{Leu}$, respectively (Figure 2.2C). We used the oxidative stress generators 3-nitropropionic acid (NPA) and rotenone as positive controls for protein aggregation and we observed 120% (20mM NPA) and 90% (15µg/l Rotenone) (Figure 2.2D) increase in protein aggregation, showing that oxidative stress has the potential to increase protein aggregation in WT embryos, showing that oxidative stress has the potential to increase protein aggregation. Taken together these data indicate that mistranslated proteins are more susceptible to oxidative damage and aggregation, that ROS also contributes to protein aggregation and that the chemical differences between Ser and the other amino acids tested determines the intensity of the proteotoxic stress generated by the misreading tRNAs.

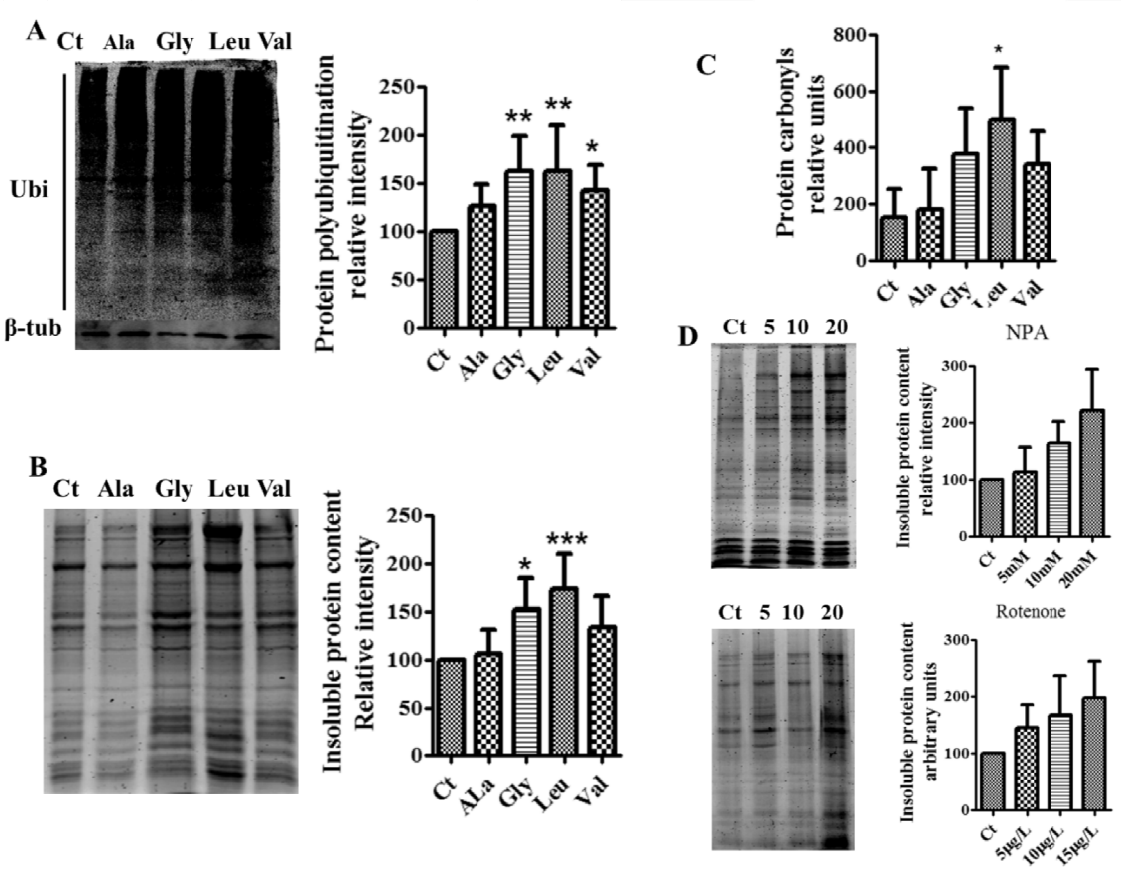

Figure 2.2. Mistranslation increases the levels of protein ubiquitination and aggregation. **A)** Western blot analysis showing that mistranslated proteins are poliubiquitinated. Data showed are the mean ± SD (n =6). (Data analysis was performed using one-way ANOVA followed by a Dunnet test with CI 95% relative to Ct; ***p<0.001, **p<0.01, *p<0.05). **B)** Mutant proteins produced by Ser misincorporation accumulate in insoluble aggregates, especially in embryos expressing the Ser-tRNA$_{UCC}^{Gly}$, Ser-tRNA$_{CAC}^{Val}$ and Ser-tRNA$_{CAG}^{Leu}$. Representative gel showing the insoluble protein fraction of control and mistanslating zebrafish embryos. Data are presented as the mean ± SD (n =5). (Data analysis was performed using one-way ANOVA followed by a Dunnet test with CI 95% relative to Ct; ***p<0.001, **p<0.01, *p<0.05). **C)** Gels showing that mistranslation increases the levels of protein carbonylation. Errors bars represent the standard deviation of four independent experiments (Student's unpaired t-test, *p<0.05). **D)** Gels showing that oxidative stress generates protein aggregation in zebrafish. Embryos incubated with the mitochondrial electron transport chain disruptors 3-Nitropropionic acid (NPA) and Rotenone had high levels of insoluble proteins. Data are presented as the mean ± SD (n =3). Units are relative to control sample in percentage. Western blot and SDS-page samples were normalized for the gel control sample.

The production of protein aggregates in mistranslating embryos was further analyzed using a chimeric HSPB1-mCherry reporter protein (Figure 2.3A). Since HSBP1 is an oligomeric small heat shock protein that binds unfolded proteins and keeps

them in a folding competent state it can be used to monitor protein aggregation *in vivo* if fused to a fluorescent probe [52, 53]. Expression of the Ser-$tRNA_{UCC}^{Gly}$, Ser-$tRNA_{CAC}^{Val}$ and Ser-$tRNA_{CAG}^{Leu}$ produced fluorescent foci localized near the nucleus and also scattered throughout the cytoplasm (Figure 2.3B), confirming the increase in protein aggregation in the mistranslating embryos. Ubiquitin immunofluorescence analysis of 5dpf embryos expressing Ser-$tRNA_{CGC}^{Ala}$ and Ser-$tRNA_{CAG}^{Leu}$ confirmed accumulation of polyubiquitinated proteins in the perinuclear foci in the latter (Figure 2.3C), suggesting that misfolded proteins produced by tRNA misreading are ubiquitinated and aggregate on the perinuclear region.

Previous studies have shown that stress and ageing increase the load of misfolded proteins that saturate the protein quality control machinery located at the juxtanuclear quality control compartment (JUNQ). These JUNQ foci accumulate potentially toxic aggregates that are subsequently directed to the insoluble protein deposits (IPOD) for destruction [15]. Therefore, our results suggest that mistranslation, especially in the case of Leu replacement with Ser targets polypeptides to both the JUNQ and the IPOD.

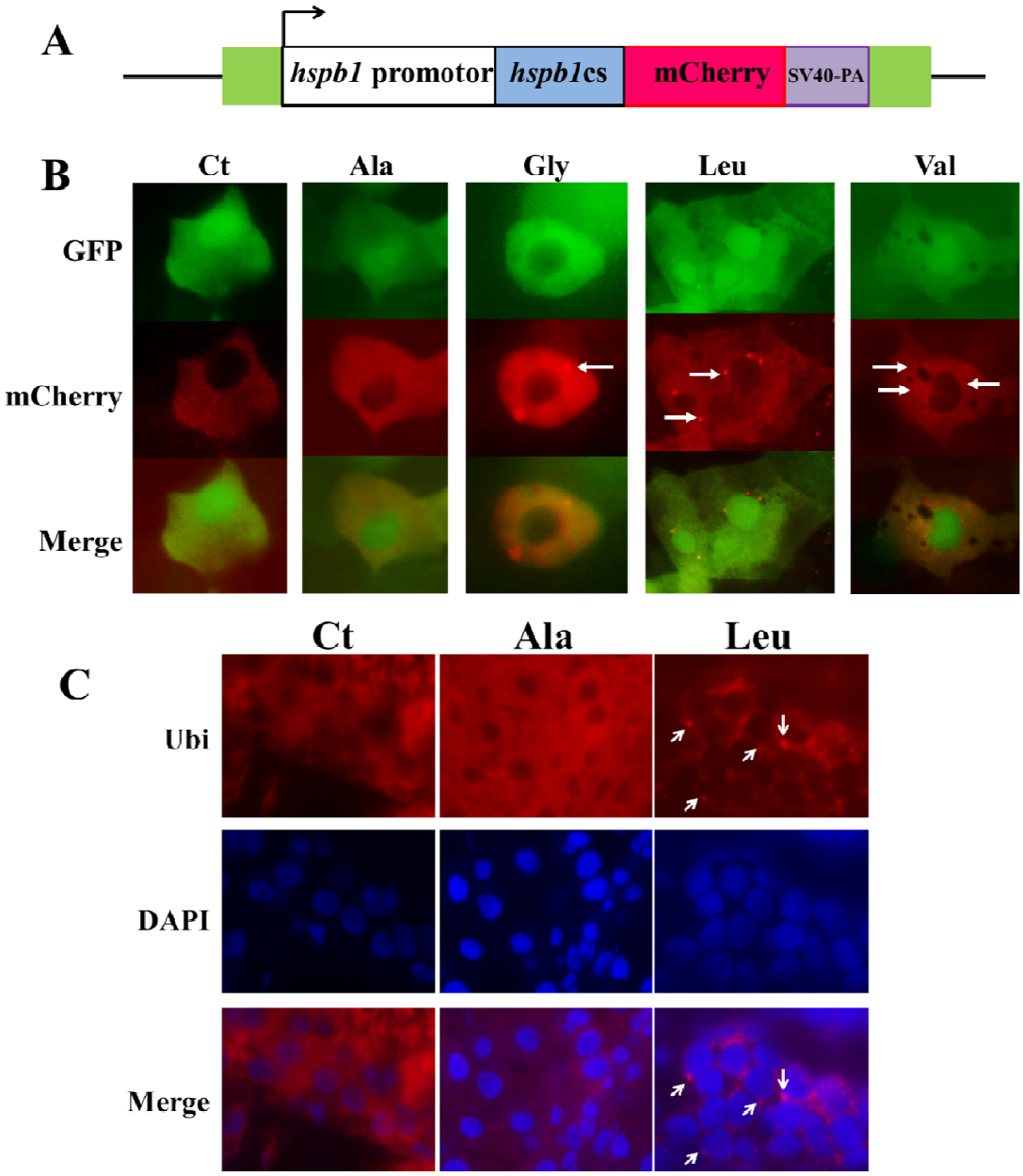

Figure 2.3. Mistranslation induces the formation of protein aggregates.
A) A fluorescence reporter constructed by fusing the zebrafish HSPB1 protein with mCherry was used to monitor the formation of protein aggregates. **B)** Mistranslating embryos expressing the HSPB1-mCherry chimeric protein were observed using fluorescence microscopy. The accumulation of protein aggregates was observed by formation of HSPB1-mCherry fluorescent foci which were more visible in embryos expressing the Ser-tRNA$_{UCC}^{Gly}$, Ser-tRNA$_{CAC}^{Val}$ and Ser-tRNA$_{CAG}^{Leu}$. **C)** Immunofluorescence analysis of 5dpf embryos expressing the Ser-tRNA$_{CGC}^{Ala}$ and the Ser-tRNA$_{CAG}^{Leu}$ show that the ubiquitin foci accumulated in the perinuclear region of the cytoplasm. Nuclei were labeled with DAPI.

To determine whether proteome aggregation is associated with ageing in healthy zebrafish we have analyzed by differential centrifugation and SDS-PAGE the insoluble protein fractions of brain, eyes and heart of 6 months, 1 and 2 years old WT zebrafish (Supplementary Figure 1). There was a gradual increase of insoluble proteins, indicating that ageing zebrafish recapitulates the protein aggregation phenotype observed previously in the worm *C. elegans* [7, 8]. Importantly zerbrafish has also a compromised proteome maintenance and the heat shock response decreases with age [54], and our proteotoxic model stress system mimics this important ageing phenotypes since it stresses the protein quality control systems and produces protein aggregates.

2.4.3. Translational errors down regulate protein synthesis

Our previous studies in yeast showed that mRNA mistranslation has a negative impact on protein synthesis rate [55]. To clarify this issue in zebrafish, protein synthesis was quantified using the SUnSET technology which measures the incorporation of puromycin into nascent polypeptides [32]. Western blot analysis of total protein extracts labeled with puromycin showed 30% and 40% decrease in protein synthesis rate in embryos expressing the Ser-tRNA$_{CAC}^{Val}$ and Ser-tRNA$_{CAG}^{Leu}$ (Figure 2.4A, Supllementary Figure 2). As before, the severity of down regulation was correlated with the differences in the chemical properties between Ser and the other amino acids. This prompted us to monitor the phosphorylation status of the translation initiation factor 2 (eIF2α), which is a major regulator of protein synthesis. Phosphorylation of eIF2α is mediated by PKR, PERK, HRI and GCN2 kinases, increases during UPR and decreases exchange of eIF2-GDP for eIF2-GTP which is required to deliver initiator tRNA$_i^{Met}$ to the ribosome [56-58]. Our data showed increased phosphorylation of eIF2α and stable levels of total eIF2α. And, again, this is in line with the differences in the chemical

properties between Ser and the other amino acids tested; reaching 40% of eIF2α-P in embryos expressing the Ser-tRNA$_{CAG}^{Leu}$. This supports the down regulation of protein synthesis detected by the SUnSET method (Figure 2.4B, Supplementary Figure 2).

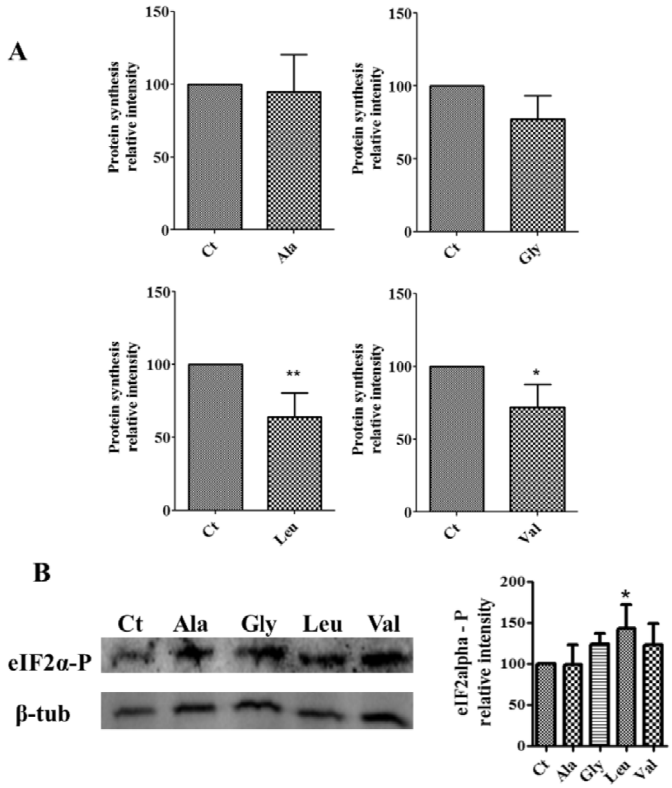

Figure 2.4. Mistranslation decreases the rate of protein synthesis.
A) Protein synthesis was analyzed using the puromycin labelling and western blot detection method. Analysis shows that Ser misincorporation at Gly, Val and Leu codons decreases protein synthesis rate. Data shown are the mean ± SD (n =4). (Student's paired t-test, *p<0.05, **p<0.005). Units are relative to control sample in percentage. Western blot samples were normalized for the gel control sample. **B)** Increased phosphorylation levels of eIF2α are consistent with down regulation of translation in mistranslating embryos. Data shown are the mean ± SD (n =4). (tatistical analysis was carried out using one-way ANOVA followed by a Dunnet test with CI 95% relative to Ct; ***p<0.001, **p<0.01, *p<0.05). Total eIF2α levels (Supplementary Figure 2) are stable in embryos expressing the mutant tRNAs. Units are relative to control sample in percentage. Western blot samples were normalized for the gel control sample.

2.4.4. Global transcriptional responses to proteome instability

To better understand the proteotoxic stress response induced by aggregation of the mistranslated proteins the transcriptomes of the mistranslating embryos were profiled using DNA microarrays. Significant gene expression deregulation was observed in a

mutant dependent manner. The Ser-tRNA$_{CAG}^{Leu}$ showed the highest level of gene deregulation, with a marked trend of gene upregulation (Figure 2.5A). These data (Table 2.1) supported the activation of the stress responses since molecular chaperones, in particular *hsp70l* was 34.2 and 38.3 fold upregulated in embryos expressing the Ser-tRNA$_{CAC}^{Val}$ and Ser-tRNA$_{CAG}^{Leu}$, and *hsp90a.2* was 7.5 fold and 9.4 fold upregulated again in the same embryos. The *hsf4* transcription factor which regulates heat shock protein expression through HSF1 repression was downregulated [59]. The ER resident chaperones *hsp90b1*/*grp94* and *hspa5*/*bip* [60, 61] were also deregulated. The *grp94* was 3.8 and 2.5 fold upregulated in embryos expressing the Ser-tRNA$_{CAC}^{Val}$ and the Ser-tRNA$_{CAG}^{Leu}$, respectively, while *bip* was also upregulated in these embryos by 2.0 fold and 1.7 fold, respectively. Several other genes related to stress response processes were induced (Table 2.1), namely *eif2ak1*, *eif2ak3*/*perk* which are involved in translation attenuation through eIF2α phosphorylation [62, 63]. The major UPR regulator *xbp1* [64] was induced, and overexpression of *hspa5*/*bip*, *hyou1*, *copb*, *zgc:103652*, *sec61a*, *gtpbp1*, *zgc:92245* and *chchd2l* were well correlated with the results obtained for the overexpression of *xbp1-s* [43]. The *sec61a* gene was also upregulated. This gene encodes a membrane ER protein involved in the import of newly synthesized polypeptides that integrates the ERAD machinery providing export capacity to misfolded and non-ubiquitinated proteins for degradation [65]. Sec61a is also a calcium channel that allows Ca^{2+} leakage from the ER under stress conditions. Calcium leakage through Sec61a is mediated by Bip as in normal conditions this chaperone seals Sec61a channels, but it translocates to unfolded/misfolded polypetides leaving the Sec61a channels open during stress conditions [66]. The data suggested therefore that ER stress induced by mistranslation may trigger calcium release to the cytoplasm increasing cytoplasmic calcium levels. Calcium homeostatic control genes, namely

asph, *calr*, *calrl* and *itpr2* and also ER shaping genes were deregulated as well (Table 2.1). Additionally, ERAD mediators were also deregulated, namely *derl3* [67, 68], *herpud1* [69], and *bcap31* [70] (Table 1). The ER co-chaperone *dnajc3* [71] and the co-chaperones *dnajb6* [72] and *dnajc21* [73] were upregulated, while *dnaj5aa* [74] was downregulated (Table 2.1). ER protein transport genes and many ER metabolism related genes, mainly lipid metabolism, were in most cases upregulated (Supplementary Table 6).

DNA repair and DNA-damage response genes were also deregulated by mRNA mistranslation (Table 2.1). The DNA repair genes deregulated were *apex1*, which in zebrafish is a component of the base excision repair mechanism [75], and *xrcc5* which repairs double strand breaks in zebrafish embryos [76]. These genes were upregulated 1.6 and 1.7 fold in embryos expressing the Ser-tRNA$_{CAC}^{Val}$, while the *alkbh2* gene involved in repairing of DNA etheno adducts [77] was upregulated 1.8 and 1.5 in embryos expressing the Ser-tRNA$_{CAC}^{Val}$ and Ser-tRNA$_{CAG}^{Leu}$, respectively. Finally, the nucleotide excision repair *ercc1* gene [78], was upregulated 1.5 fold in embryos expressing the Ser-tRNA$_{CAG}^{Leu}$. The DNA-damage response *gadd45al* gene was upregulated 2.6 and 2.1 fold in embryos expressing the Ser-tRNA$_{CAC}^{Val}$ and Ser-tRNA$_{CAG}^{Leu}$ and *gadd45bl* was upregulated 2.3 and 2.5 fold in embryos expressing the Ser-tRNA$_{CAC}^{Val}$ and Ser-tRNA$_{CAG}^{Leu}$ and finally *gadd45b* was upregulated in the embryos expressing the Ser-tRNA$_{CAC}^{Val}$ and Ser-tRNA$_{CAG}^{Leu}$ 2.6 and 2.4 fold respectively. Gadd45 proteins are involved in cell-cycle regulation and are normally induced by genome damage and stress conditions. They also regulate somite formation in zebrafish [79, 80].

Table 2.1 Stress response and ER genes deregulated by mistranslation in zebrafish embryos.

Microarray data analysis was done with MEV software [36, 37]. Significantly deregulated genes for each mutant tRNA were obtained with a t test analysis (p0.05) and a 1.5 fold change deregulation cut off. Fold change values are displayed.

Gene symbol	Ala	Gly	Val	Leu	Function
hsp70l			34.17	38.32	Heat shock protein
hsp90a.2			7.54	9.40	Heat shock protein
cryaa				3.54	Small heat shock protein [81]
hsp90b1			3.85	2.39	ER chaperone [60]
hspa5			2.02	1.72	ER chaperone [61]
hspb1			3.08	1.99	Small heat shock protein [81]
hspb3				-1.93	Small heat shock protein [81]
hspb8			2.46	2.69	Small heat shock protein [81]
dnajb6				2.08	DNAJ chaperone [72]
dnajc3			3.35	3.33	ER DNAJ chaperone [82] [71]
dnajc5aa				-1.50	DNAJ chaperone [74]
dnajc21			1.68		DNAJ chaperone [73]
ahsa1			2.69		HSP90 ATPase activation [83]
nupr1		2.21			Target of ATF4 [84]
hsf4		-1.70	-2.64	-2.01	Regulator of HSP expression [59, 85, 86]
xbp1			1.70	1.54	Unfolded Protein Response [64]
eif2ak1				2.61	eif2alpha kinase [63]
eif2ak3				1.65	eif2alpha kinase [62]
derl3			3.64	4.90	ER stress response ERAD [67, 68]
Herpud1			2.39	5.13	ER stress response ERAD [69]
bcap31	1.25	1.93	1.82	1.49	ER stress response ERAD [70]
sec61al2			2.34	2.62	ER stress response ERAD [65]
sdf2l1			1.65		ER chaperone [87]
hyou1			2.57		ER chaperone [88]
ergic3			1.91		Response to ER stress [89]
pdia4			2.41		ER chaperone [90]
pdip5			3.50	2.07	ER chaperone [91]
asph	-1.55		2.24	2.43	Calcium homeostasis [92]
calr			1.52		ER calcium binding [93-95]
calrl			1.58		CALR like protein
itpr2			1.76		IP(3)-sensitive Ca(2+) channels [96]
rtn1a		2.12			ER shaping protein[97]
trdn				-1.87	ER calcium release [98]
rtn1b				-1.60	ER shaping protein
rtn2b				-1.64	ER shaping protein [79]
rtn3		1.62			ER shaping protein
rtn4a		1.46			ER shaping protein
ercc1				1.47	DNA repair [78]
alkbh2		1.63	1.87	1.55	DNA repair [77]
xrcc5			1.80		DNA repair [76]
apex1			1.60		DNA repair [75]
gadd45aa			2.60	2.14	DNA-damage response
gadd45bb			2.35	2.50	DNA-damage response [79]
gadd45b			2.67	2.41	DNA-damage response [79]

2.4.5. Stress responses induced by protein biosynthesis errors

The effect of proteome instability and aggregation on stress response pathways was also analyzed, in particular the effect on the heat-shock response and ubiquitin proteasome pathway. For this, we have monitored the levels of the chaperones HSP70 and HSP90 and quantified proteasome activity. Expression of both chaperones was upregulated at both the mRNA and protein levels, especially in the embryos expressing the Ser-tRNA$_{UCC}^{Gly}$, Ser-tRNA$_{CAC}^{Val}$ and Ser-tRNA$_{CAG}^{Leu}$ (Figure 2.5B, C, Supplementary Table 5). In the case of the embryos expressing the Ser-tRNA$_{UCC}^{Gly}$ Hsp70 was induced 3.2 fold at the mRNA level and 1.4 fold at the protein level, Hsp90 was 2.8 fold induced at the mRNA level and 1.7 fold at the protein level. Embryos expressing the Ser-tRNA$_{CAC}^{Val}$ upregulated Hsp70 11.2 fold at the mRNA level and 1.4 fold at the protein level, Hsp90 was 8.8 fold induced at the mRNA level and 1.9 fold at the protein level. Finally, in the case of the Ser-tRNA$_{CAG}^{Leu}$, Hsp70 was upregulated 44.8 fold at the mRNA level and 1.7 fold at the protein level and Hsp90 was upregulated 18.2 fold at the mRNA level and 2 fold at the protein level. The UPP was strongly induced (Figure 2.2A, Figure 2.5D) in particular in the embryos expressing the most destabilizing Ser-tRNA$_{CAG}^{Leu}$. The other mutant tRNAs upregulated the UPP in the following order Gly > Val > Ala. In other words, increased chemical differences between misincorporated and WT amino acids resulted in stronger UPP activation, in line with the results described above. The small heat shock protein HSPB1 was also induced at the mRNA and protein levels (Figure 2.5E) and was accumulated in the insoluble fraction (Figure 2.5E), which is in line with its binding affinity for misfolded and aggregated proteins. These data are in line with the strong up-regulation of the UPP observed above (Figure 2.2A, Figure 2.5D).

We further determined if tRNA mediated proteome instability elicited the ER unfolded protein response (UPR), by analyzing the expression levels of the UPR adaptor *hspa5/bip* and UPR component *xbp1* and up regulation of 2.5 and 1.8 fold respectively, was observed in the embryos expressing the Ser-$tRNA_{CAG}^{Leu}$ (Figure 2.5F, Supplementary Table 5). We have also detected splicing of the transcription factor Xbp1 in all four mutants, with the highest level in the embryos expressing the Ser-$tRNA_{CAG}^{Leu}$ (Figure 2.5G). Since activation of the UPR correlated with the translation attenuation discussed above, which is in line with previous data [19], the response generated by our proteome instability model confirmed that the misreading Ser-tRNAs activated the major cellular stress responses. The tRNAs also produced a scale of increasing toxicity which was dependent upon differences in the amino acid chemical properties.

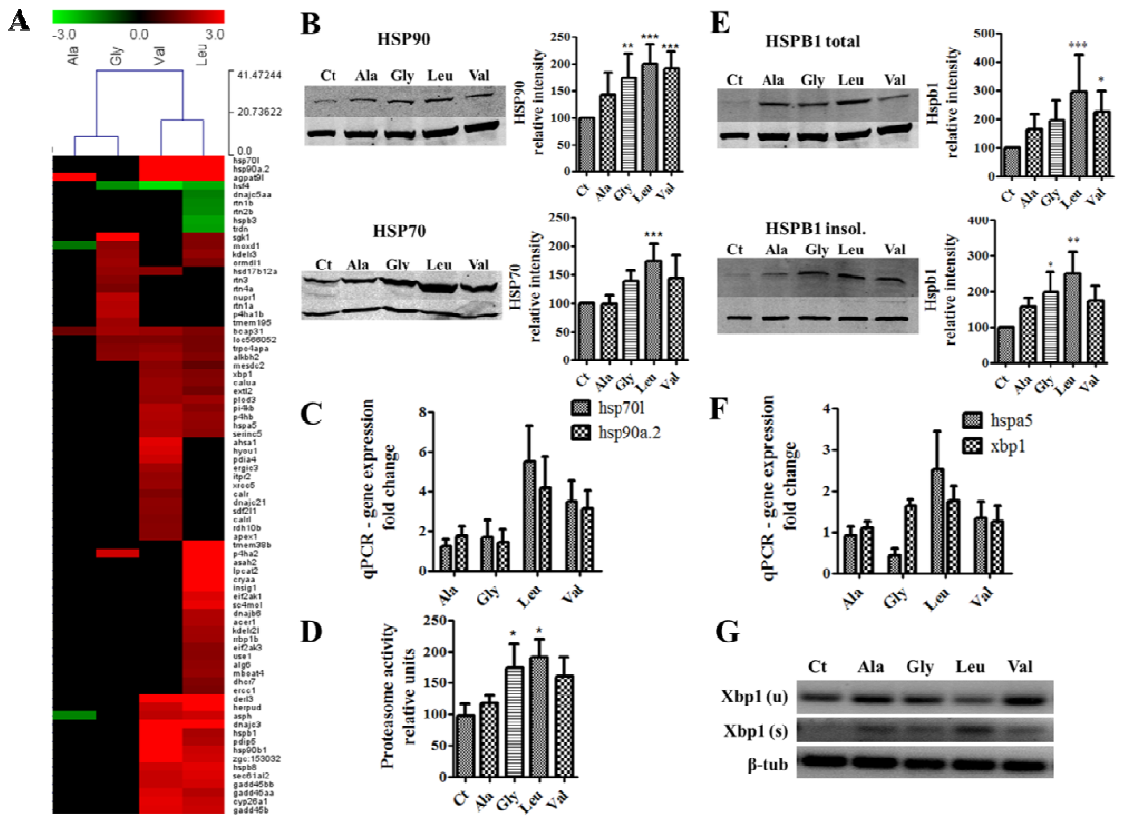

Figure 2.5. Induction of stress responses by mRNA mistranslation.
A) Cluster representation of stress response and Endoplasmic Reticulum (ER) genes that were deregulated in mistranslation embryos. These genes are mainly upregulated, in particular in embryos misincorporating Ser at Leu and Val codons. **B)** Western blot analysis of HSP90 and HSP70 show that these chaperones are induced by mRNA mistranslation. Data shown are the mean ± SD (n =4). (Data statistical analysis was carried out using one-way ANOVA followed by a Dunnet test with CI 95% relative to Ct; ***p<0.001, **p<0.01, *p<0.05). Intensity units are relative to control in percentage. Western blot samples were normalized for the gel control sample. **C)** qRT-PCR was performed to check the levels of *HSP70L* and *HSP90A.2* mRNAs in mistranslating embryos. **D)** Proteasome activity was quantified using the fluorogenic chymotrypsin-like substrate s-LLVY-MCA. Data shown are the mean ± SD (n =4). (Student's unpaired t-test, *p<0.05 was used) Activity units are relative to control. Units are relative to control sample in percentage. **E)** Western blot analysis of HSPB1 in total and insoluble fractions show that this small heat shock protein is induced by mRNA mistranslation and that it accumulates in the insoluble fraction. Data are presented as the mean ± SD (n =3). (Data statistical analysis was carried out using one-way ANOVA followed by a Dunnet test with CI 95% relative to Ct; ***p<0.001, **p<0.01, *p<0.05). Units are relative to control sample in percentage. Western blot samples were normalized for the gel control sample. **F) Induction of the ER stress response by mRNA mistranslation.** qRT-PCR was performed to quantify the levels of HSPA5/BIP mRNA in mistranslating embryos. BIP acts as an early ER stress sensor. It recognizes and links protein hydrophobic exposed regions, thus signaling misfolded/unfolded polypeptides. **G)** Alternative splicing of XBP1 mRNA was monitored by RT-PCR in zebrafish embryos during ER stress induced by mRNA mistranslation. β-tubulin was used as internal control for RT-PCR.

2.4.6. Proteome instability leads to the accumulation of reactive oxygen species

Stress induced production of ROS in the ER and subsequent Ca^{2+} release from the ER increases mitochondrial ROS production in several model systems [6, 99-101]. ER oxidative disulfide folding is the main source of ER ROS as molecular oxygen is the terminal electron acceptor, producing reactive oxygen species and oxidized glutathione [101, 102]. Such ROS accumulation likely expands the proteome damage leading to the accumulation of protein aggregates. In order to clarify whether our misreading tRNAs would impact on oxidative stress we have quantified ROS using DHE and Amplex® Red Hydrogen Peroxide kit (Molecular Probes®) [103]. DHE analysis showed increased production of the superoxide anion in embryos expressing Ser-$tRNA_{UCC}^{Gly}$, Ser-$tRNA_{CAC}^{Val}$ and Ser-$tRNA_{CAG}^{Leu}$ (Figure 2.6A). Production of hydrogen peroxide (H_2O_2), especially in the embryos expressing the Ser-$tRNA_{CAC}^{Val}$ and Ser-$tRNA_{CAG}^{Leu}$ (Figure 2.6B), was increased by 200 and 270%, respectively, and was in line with increased activity of catalase (50% for Ser-$tRNA_{CAC}^{Val}$ and 180% for Ser-$tRNA_{CAG}^{Leu}$) which converts H_2O_2 to H_2O and O_2 (Figure 2.6C, D). The gene expression profiling also showed deregulation of several redox maintenance and antioxidant defence genes (Figure 2.6D, Table 2.2), namely the antioxidant *cat* gene [104] whose expression was upregulated 1.9 fold in Ser-$tRNA_{CAG}^{Leu}$ expressing embryos. Several selenoproteins and other antioxidant defence related genes, such as *glrx*, *mgst1* and *gstp1* were also induced (Table 2.2). Similar results were obtained for the peroxissomal *pex13*, *lonp2*, *zgc:114079* and *pmp34* genes (Table 2.2), indicating that our proteome instability model recapitulated the oxidative stress phenotype observed in protein conformational diseases [12, 105, 106].

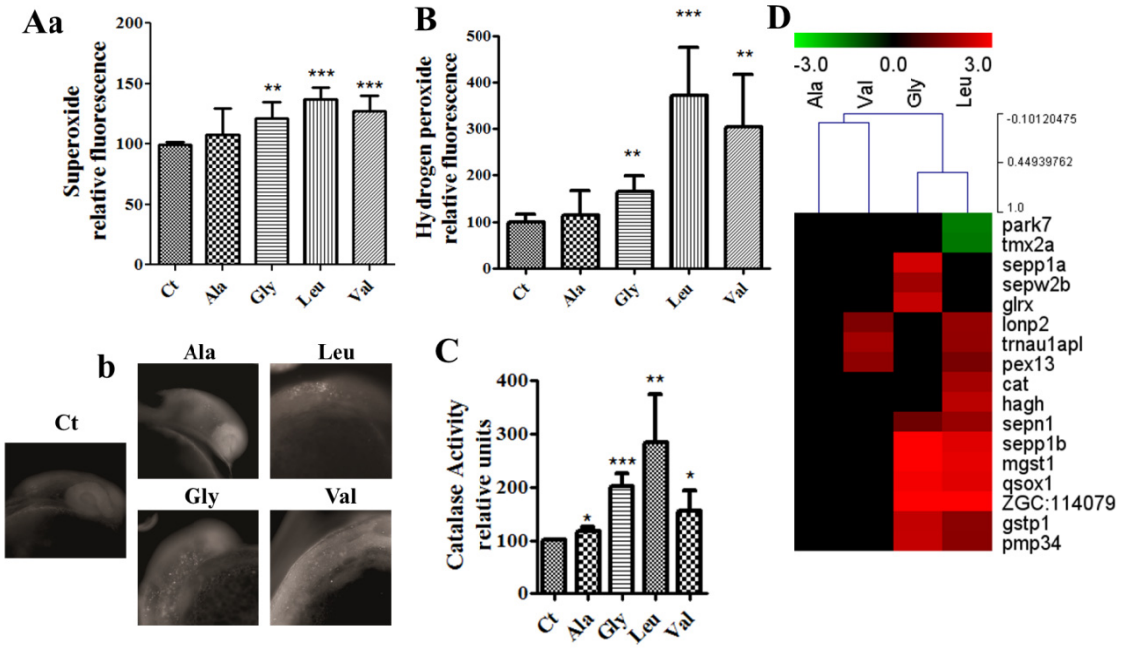

Figure 2.6. Oxidative stress is one of the endpoints of mistranslation.
A) The detection of the superoxide anion with dihydroethidium by fluorimetry (a) and microscopy (b) showed a discrete increase in its levels in the mutant embryos expressing the mutant tRNAs. Data are presented as the mean ± SD (n =5) (Student's unpaired t-test, **p<0.005, ***p<0.0001 was used for data statistical analysis). Units are relative to control sample in percentage. **B)** Hydrogen peroxide levels were highly increased in the mistranslating embryos. Data are presented as the mean ± SD (n =4) (Student's unpaired t-test, **p<0.01, ***p<0.001). Units are relative to control sample in percentage. **C)** Catalase activity was also induced by mistranslation, balancing the increase in the production of hydrogen peroxide. Data are presented as the mean ± SD (n =4) (Student's unpaired t-test, *p<0.05, **p<0.0005, ***p<0.05). Units are relative to control sample in percentage. **D)** Cluster representation of redox maintenance and antioxidant defense genes deregulated in mistranslating embryos, showing that these genes are mainly upregulated, with the strongest upregulation in embryos expressing the Ser-tRNA$_{UCC}^{Gly}$ and the Ser-tRNA$_{CAG}^{Leu}$.

Table 2.2. Oxidant defense genes deregulated by mistranslation in zebrafish embryos. Microarray data analysis was done with MEV software [36, 37]. Significantly deregulated genes for each mutant tRNA were obtained with a t test analysis (p0.05) and a 1.5 fold change deregulation cut off. Fold change values are displayed.

Gene symbol	Ala	Gly	Val	Leu	Function
park7				-1.48	Oxidative stress response, apoptosis activator[107, 108]
sepp1a		2.49			Selenoprotein [109]
sepp1b		3.26		2.66	Selenoprotein
sepn1		1.32		1.81	Selenoprotein
sepw2b		1.90			Selenoprotein
trnau1apl			1.93	1.75	Protein associated with selenocysteine tRNA [110]
qsox1		2.88		2.66	Cell redox homeostasis [111]
glrx		2.33			Antioxidant defence [112]
gstp1		2.30		1.65	Antioxidant defence [113]
mgst1		3.17		2.74	Antioxidant defence [114]
cat				1.94	Antioxidant defence peroxissomal [104]
pex13			1.69	1.45	Antioxidant defence peroxissomal [115]
lonp2			1.50	1.75	Antioxidant defence peroxissomal ref
zgc:114079		5.50		4.91	Antioxidant defence peroxissomal [116]
zgc:162641		2.33		1.64	Antioxidant defence peroxissomal

2.4.7. Proteome instability impacts mitochondrial organization and function

The increase in oxidative stress and up regulation of DNA repair genes prompted us to investigate whether mistranslation increased DNA damage. We focused on the integrity of the mitochondrial and nuclear genomes in mistranslating zebrafish embryos and this was determined by QPCR [42] Mitochondrial damages accumulated in response to Ser-tRNA$_{CGC}^{Ala}$ (0.39 lesions/10Kb), Ser-tRNA$_{UCC}^{Gly}$ (0.82 lesions/10Kb), Ser-tRNA$_{CAC}^{Val}$ (0.77 lesions/10Kb) and Ser-tRNA$_{CAG}^{Leu}$ (1.62 lesions/10Kb). Nuclear genome damage was also observed in response to Ser-tRNA$_{CGC}^{Ala}$ (0.16 lesions/10Kb), Ser-tRNA$_{UCC}^{Gly}$ (0.36 lesions/10Kb), Ser-tRNA$_{CAC}^{Val}$ (0.34 lesions/10Kb) and Ser-tRNA$_{CAG}^{Leu}$ (0.52 lesions/10Kb), (Figure 2.7A). The higher level of damage of the mitochondrial DNA is likely related to reduced DNA repair capacity relative to repair of nuclear DNA and higher exposure to ROS [117-120].

The above data indicated that mistranslation induced proteotoxic stress likely had a major impact on mitochondrial function. To test this hypothesis we have characterized the mitochondrial membrane potential and mitochondrial morphology. Mitochondrial membrane potential was reduced by 35%, 33% and 46% in embryos expressing the Ser-$tRNA_{UCC}^{Gly}$, Ser-$tRNA_{CAC}^{Val}$ and Ser-$tRNA_{CAG}^{Leu}$ (Figure 2.7B), indicating that oxidative phosphorylation and ATP production were affected. Real-Time quantitative PCR (Figure 2.7C) analysis showed 28%, 55%, 50% and 70% increase in the levels of mitochondrial DNA in embryos expressing the $tRNA_{CGC}^{Ala}$, Ser-$tRNA_{UCC}^{Gly}$, Ser-$tRNA_{CAC}^{Val}$ and Ser-$tRNA_{CAG}^{Leu}$, respectively. And, the morphology of the mitochondrial network showed major alterations in embryos expressing the Ser-$tRNA_{CAG}^{Leu}$. Lower levels of alterations of the mitochondrial network were observed in the case of Ser-$tRNA_{CGC}^{Ala}$, Ser-$tRNA_{UCC}^{Gly}$ and Ser-$tRNA_{CAC}^{Val}$ embryos (Figure 2.7D).

Those alterations in the mitochondrial network were consistent with deregulation of expression of several mitochondrial genes (Figure 2.7E, Table 2.3). For example, *park2*/*parkin* which promotes mitochondrial degradation by facilitating their elimination by specific autophagy – mitophagy [121, 122] was 4.8 fold upregulated in embryos expressing the Ser-$tRNA_{CAG}^{Leu}$ (Figure 2.7E). Conversely, Park7/Dj-1 which protects against ROS and translocates to the mitochondrial membrane under mitochondrial oxidative stress [123, 124] was downregulated 1.5 fold in embryos expressing the Ser-$tRNA_{CAG}^{Leu}$ mutants (Figure 2.6D, Table 2.2), indicating increased susceptibility of mitochondria to ROS. Furthermore loss of Park7/Dj-1 elicits mitochondrial membrane potential reduction [125], an effect also observed in our samples. Genes related to mitochondrial network dynamics, namely *rhot2*, *zgc:63910*/*mtfp1* and *mff* [126-128] were upregulated. *zgc:63910* was 1.5 fold upregulated in embryos expressing the Ser-

$tRNA_{CAC}^{Val}$, *mff* was 1.2 fold upregulated in embryos expressing the Ser-$tRNA_{CAG}^{Leu}$ and *rhot2* was upregulated 1.9 fold in embryos expressing the Ser-$tRNA_{UCC}^{Gly}$ and 1.4 in Ser-$tRNA_{CAG}^{Leu}$ embryos. These three factors are activators of mitochondrial fission. Importantly Rhot2/Miro2 is a fission activator that responds to elevated Ca^{2+} signals in the cytoplasm [126], which are frequent during ER stress. Globally these results suggest that proteome instability produced by mRNA mistranslation increases the ratio of fission/fusion.

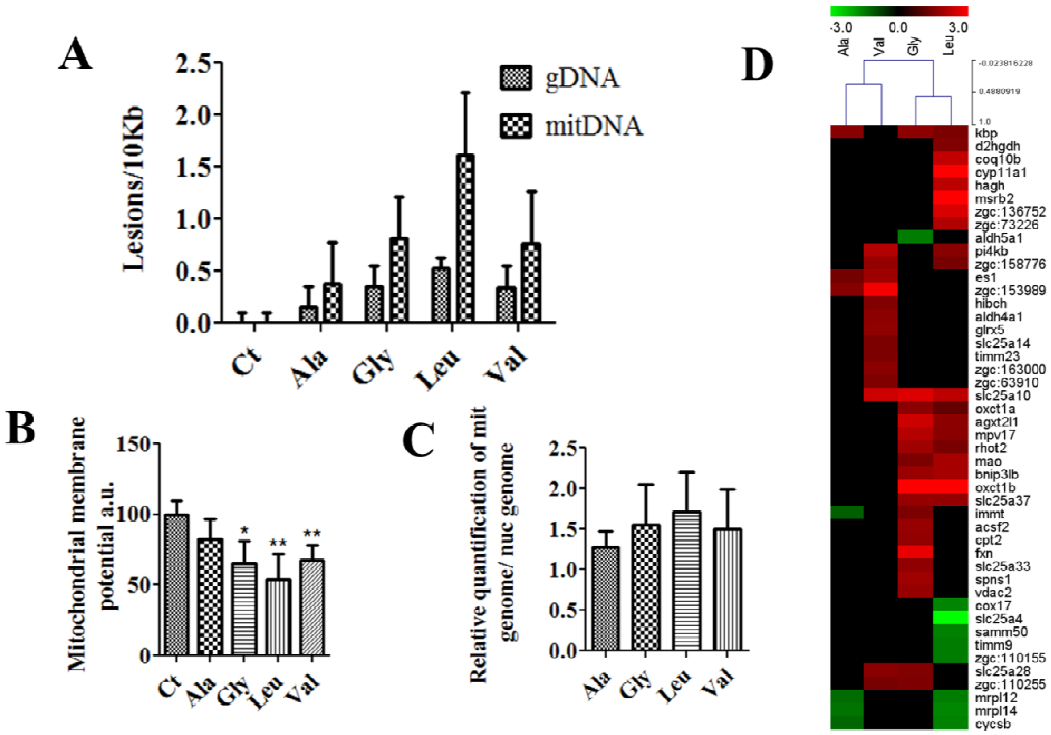

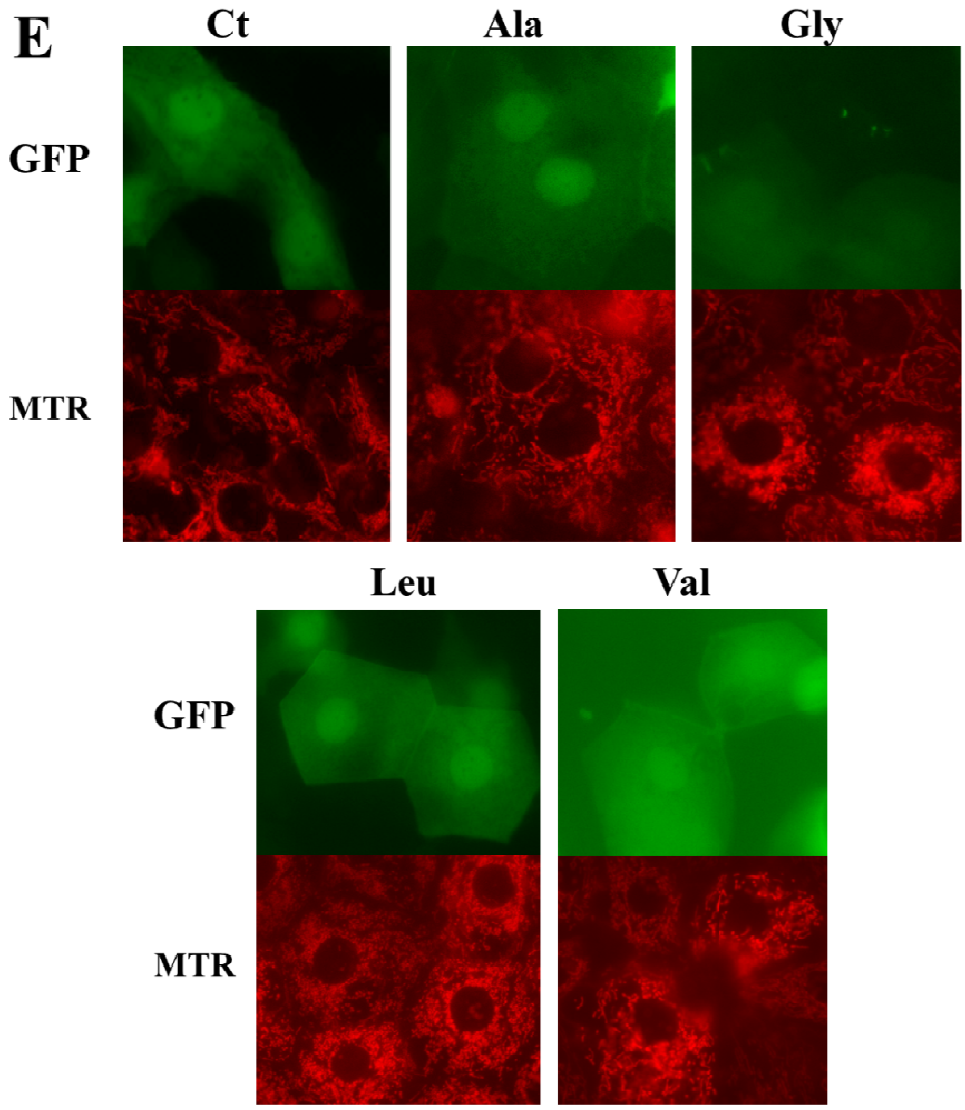

Figure 2.7. Mistranslation increases damage of mitochondrial and nuclear DNA and alters the mitochondrial morphology.

A) Quantification of DNA damage show that mistranslation leads to the accumulation of damages in both the nuclear and mitochondrial DNA. DNA damage was determined by qPCR. Values are expressed as lesions/10 kb of DNA. Data are presented as the mean ± SD (n =3). **B)** Mitochondrial membrane potential was assessed by JC-1 staining; fluorescence was measured on mitochondria purified from control and mistranslating embryos. Data are presented as the mean ± SD (n =3) (Student's unpaired t-test, *p<0.05, **p<0.01) Units are relative to control sample in percentage. **C)** Relative mtDNA copy number was measured by qRT-PCR, results show a tendency towards an increased mitochondrial abundance. Data are presented as the mean ± SD (n =3). **D)** Mistranslating embryos were labeled with Mito Tracker Red and observed with fluorescence microscopy. Mistranslation affected mitochondrial morphology, in particular the tubular structure of mitochondria was lost in mistranslating embryos. These differences in the shape of mitochondria were more pronounced in embryos expressing the Ser-$tRNA_{CAC}^{Val}$ and the Ser-$tRNA_{CAG}^{Leu}$. **E)** Cluster representation of mitochondrial genes deregulated in mistranslating embryos showing a trend towards up-regulation. The higher up-regulation was observed in embryos expressing the Ser-$tRNA_{UCC}^{Gly}$, Ser-$tRNA_{CAC}^{Val}$ and Ser-$tRNA_{CAG}^{Leu}$.

Several apoptosis and autophagy related genes were also upregulated (Table 2.3). For example *zgc:158776*/*smac*/*diablo* which is a mitochondrial protein related to apoptosis and caspase activation [129, 130] was upregulated by Ser-tRNA$_{CAC}^{Val}$ and by Ser-tRNA$_{CAG}^{Leu}$ expressing embryos. The *bnip3lb* gene encoding a mitochondrial outer membrane protein involved in autophagy and autophagic cell death [131] was also upregulated in Ser-tRNA$_{UCC}^{Gly}$ and Ser-tRNA$_{CAG}^{Leu}$ expressing embryos. Interestingly, the major zebrafish autophagic markers and autophagy related genes were coordinately expressed in our mistranslating embryos namely *lc3*/*map1lc3b*, *gabarap*, *becn1*, *atg10* and *atg4b* (Table 2.3) [132]. The *lc3*/*map1lc3b* gene was upregulated both in Ser-tRNA$_{UCC}^{Gly}$ and Ser-tRNA$_{CAG}^{Leu}$, *becn1* was upregulated in the three mutants, specifically in Ser-tRNA$_{UCC}^{Gly}$, Ser-tRNA$_{CAC}^{Val}$ and the Ser-tRNA$_{CAG}^{Leu}$ (See also Supplementary Table 6).

Table 2.3. Mitochondrial genes deregulated in mistranslating embryos.
Microarray data analysis was carried out using the MEV software [36, 37]. Significantly deregulated genes for each mutant tRNA were obtained with a t test analysis (p0.05) and a 1.5 fold change deregulation cut off. Fold change values are displayed.

Gene symbol	Ala	Gly	Val	Leu	Function
park2				4.8	Mitochondrial turnover [121]
cox17				-1.57	COX assembly
cycsb	-1.22			-1.52	Mitochondrial respiratory chain
bnip3lb		1.84		1.99	Apoptosis [130]
zgc:158776			1.76	1.42	Apoptosis (Eimon & Ashkenazi, 2010)
spns1		1.89			Apoptosis (Nakano et al, 2001)
mpv17		2.15		1.64	Response to ROS [133]
glrx5			1.69		Biogenesis of iron-sulfur clusters
msrb2				4.88	Response to ROS [134]
mrpl12	-1.26			-1.47	mitochondrial ribosomal protein
mrpl14	-1.36			-1.58	mitochondrial ribosomal protein
zgc:110255		1.51	1.43		mitochondrial ribosomal protein
zgc:63910			1.52		Mitochondrial fission [127]
mff				1.2	Mitochondrial fission [128]
rhot2		1.88		1.43	Mitochondrial dynamics [126]
samm50				-1.53	Ultrastructure organization [135]
atg10		1.5	1.5		Autophagy
atg4b		1.8			Autophagy
becn1		1.6	1.9	1.9	Autophagy
gabarap		1.9			Autophagy
map1lc3b		2.4		1.4	Autophagy

2.5. Discussion

2.5.1. Mistranslation induces proteome aggregation in zebrafish

We have destabilized the zebrafish proteome through low level proteome wide misincorporation of Ser. This lead to clearly visible accumulation of ubiquitinated protein aggregates in most embryos except in those expressing the Ser-$tRNA_{CGC}^{Ala}$ mutant where there was only a small increase in ubiquitination, carbonylation and protein aggregation (Figures 2.2.A, 2.2.B, 2.2.C). Compartmentalization of potentially toxic misfolded and aggregated proteins occurs according to their ubiquitination status and solubility, forming the juxtanuclear quality control (JUNQ) and the insoluble protein deposit (IPOD) [15]. Our results indicate that mRNA mistranslation produces misfolded proteins that form aggregates in the perinuclear region possibly in association with JUNQs since we detected perinuclear accumulation of poliubiquitinated proteins. The data is consistent with the differences in chemical properties between Ser and the targeted amino acids. Indeed, Ser and Ala are chemically similar and the Ser-$tRNA_{CGC}^{Ala}$ produced mild proteotoxic phenotypes while Ser misincorporations at the other amino acids (Gly<Val<Leu) sites produced increased levels of protein ubiquitination and aggregation, upregulated molecular chaperones and other components of the stress response. Despite the different levels of toxicity observed between the misreading tRNAs our data show that tRNA directed protein mutagenesis activates the ER-unfolded protein response (ER-UPR). Since the UPR coordinates several quality control mechanisms of the secretory pathway, which can either be adaptive or pro-apototic, and plays a role in several pathologies such as cancer, neurodegenerative, metabolic and inflammatory diseases [136], our data is consistent with the hypothesis that protein aggregation on its own has a strong impact on healthy ageing and ageing related diseases through ER stress. Indeed, ER stress signals extend

to the mitochondria, are associated with ROS production and activate JNK and TOR signaling pathways [6, 19]. In zebrafish, ER stress is associated with liver disease [137, 138] and it will be interesting to investigate in future studies whether mistranslating transgenic fish will develop liver disease and other protein conformational diseases.

Induction of the UPR increasess eIF2-α phosphorylation through activation of PERK, reducing the delivery of $tRNA^{iMet}$ to the ribosome and consequently decreasing translation rate [56-58]. Our data confirmed the down regulation of protein synthesis rate associated with increasing levels of eIF2-αP, depending on the chemical differences between Ser and the amino acids targeted by the misreading tRNAs. Studies from other laboratories show that protein aggregation does induce eIF2-αP and that long term down regulation of protein synthesis, rather than toxicity associated with aggregated proteins, is the main cause of neuronal cell death [139]. We have observed increased levels of apoptosis (data not shown) and it will be interesting to determine whether the latter is a direct result of down regulation of protein synthesis and can be alleviated through inhibition of eIF2-α phosphorylation.

2.5.2. Proteotoxic stress destabilizes the nuclear and mitochondrial genomes

Our data also showed remarkable negative impacts of mistranslation on both the nuclear and mitochondrial genomes, and up regulation of DNA repair and DNA damage response genes, but further studies are needed to clarify whether these negative phenotypes are a direct consequence of down regulation of protein synthesis and protein aggregation or are associated with oxidative damage or disruption of DNA replication, recombination and repair. In any case, the effect of proteome instability on the genome strongly suggests that proteotoxic stress has direct impacts on mutation rate and genome stability in general, which is of relevance to understand the role of age-associated

protein aggregation in cancer and degenerative diseases. Indeed, genomic instability is associated with natural ageing in several organisms and oxidative DNA damage potentiates genome instability and the mitochondria is believed to play an important role as a ROS generator [140, 141]. It is still unclear how mitochondrial metabolism impacts the ageing process, but it is likely that ROS produced at the mitochondrial level increases replication stress that mediates the effects of DNA oxidative damages and ageing [140]. Our observation that proteome aggregation has a strong negative impact on the mitochondrial genome suggests that proteotoxic stress may contribute to ageing by promoting mitochondrial genome instability.

Mitochondria form highly structured networks which are maintained through dynamic fusion and fission [142-144]. The shape of mitochondria can shift from the normal tubular shape to elongated structures by disruption of fission. Conversely, when fusion is impaired mitochondria assume short rod like or spherical shapes [142-144]. The dynamic balance between mitochondrial fusion and fission is crucial for diverse biological processes, namely apoptosis, embryonic development and human diseases [144-146]. Our transcriptome profiling data showed that mitochondrial fission processes are upregulated, suggesting that the observed fragmentation of the mitochondrial network is due to increased fission. Since the ER and mitochondria are interconnected at the mitochondria-associated membrane (MAM) and enable lipid, Ca^{2+} and ATP shuttling, it is possible that mRNA mistranslation affects mitochondrial function through elevated ER stress. Indeed, mitochondria and ER contacts increase under stress potentiating apoptosis activation [147, 148]. Furthermore, association of ER and mitochondrial membranes plays a role in mitochondrial dynamics and distribution due to their attachment to the cytoskeleton [148]. Prolonged ER stress increases the calcium flown from the stressed ER into the mitochondrial matrix through the MAM, and the

accumulation of Ca^{2+} in the mitochondrial matrix saturates its buffering capacity resulting in the opening of the mitochondrial permeability transition pore (mtPTP) and consequent apoptotic signalling [149]. Apoptosis and increased mitochondrial fission seem to be associated, although this association is not the only mandatory trigger of apoptosis, as perturbations in fusion and fission also increase it. In any case, increased mitochondrial fission, either through induction of fission stimulators or down regulation of fusion processes, is associated with cytochrome c release and apoptosome assembly [146, 150]. Modulation of the stress signal from the stressed ER to the mitochondria can also be executed by ROS and high levels of oxidative stress can deregulate Ca^{2+} signaling and homeostasis through oxidative damages to Ca^{2+} channels, namely SERCA and IP3R [151]. Therefore, our data is consistent with the hypothesis that ROS produced through protein aggregation may induce mitochondrial dysfunction through deregulated calcium signaling between the ER and the mitochondria [151].

The link between protein aggregation, mitochondrial disruption and oxidative stress in neurodegenerative diseases and ageing is still controversial. In particular, it is not yet clear whether ROS accumulation during ageing is the main cause of protein aggregation and mitochondrial dysfunction or whether protein aggregation is the triggering event of degenerative processes that culminate in ROS production and mitochondrial dysfunction [152-154]. Our data show unequivocally that proteome instability on its own is sufficient to disrupt the mitochondrial network, increase ROS, saturate the ER and down regulate protein synthesis. Considering the activation of the UPR and that the ER is a frequent source of ROS, it is likely that the observed increase in ROS in the mistranslating embryos may result from both ER and mitochondrial dysfunction. In any case, the data demonstrates that mistranslation and proteotoxic stress have a dominant effect on the mitochondrial network and are a major cause of

ROS accumulation, mimicking several of the major endpoints of neurodegenerative diseases [155].

2.5.3. Protein aggregation during ageing

Ageing is naturally accompanied by cellular senescence and has been frequently associated with protein aggregation, high levels of ROS and mitochondrial dysfunction [8, 16, 141]. Protein homeostasis is maintained by quality control mechanisms that function at different levels to maintain a stable proteome. In aged organisms there is reduced capacity to maintain a healthy proteome, and evidences are growing that this is due to loss of activity of the proteostasis networks [7]. Indeed, we observed increased protein aggregation in aged zebrafish. The influence of chaperone activity in the proteostasis network spreads out through multiple regulatory pathways, consequently deregulation of its activity can have profound effects on proteome [11]. Decreased chaperone activity has been observed in senescent fibroblasts and in vertebrates such as zebrafish [54, 156]. Furthermore, chaperone induction occurs in situations of caloric restriction, which prolongs life span, and has also been observed in centenarian human cells upon stress [3]. Chaperones and protein networks represent major preventive mechanisms in ageing associated diseases in humans, since accumulation of misfolded and aggregated proteins are related to several conformational diseases [1]. Additionally, different cellular types have proteome and proteostasis networks fitted to the cellular functions and this may partially explain why specific cell types, such as neurons, are particularly sensitive to ageing and disease [11]. Loss of proteostasis with concomitant protein aggregation is a common trait of human conformational diseases. This has several associated problems, namely chaperone sequestration, toxic gain of function and

improper protein trafficking, however the precise mechanisms that induce loss of proteostais and disease are still to be described [11].

In conclusion, the contribution of gene translational errors to protein misfolding/aggregation and proteotoxic stress is poorly understood, but our work raises the possibility that increased mRNA mistranslation during healthy ageing will promote protein aggregation and proteotoxic stress and it will be fascinating to quantify translational errors during healthy ageing zebrafish using mass-spectrometry or gain-of-function fluorescent reporter systems. Our data also raises the hypothesis that long term therapies that interfere with protein synthesis fidelity, environmental stressors, pathologies, mutations and other biological or environmental processes that interfere with the ribosome and translational factors will have direct impact on protein aggregation and consequently on proteotoxic stress and ageing. Finally, our data demonstrate that mutant misreading tRNAs are powerful tools to study the biology of proteome instability and proteotoxic stress. Since our misreading tRNAs can be applied to any organism and cell type we anticipate that this methodology will allow for deep dissection of eukaryotic proteotoxic stress networks and proteome aggregation during healthy ageing and in ageing related conformational diseases.

2.6. Supplementary data

Supplementary Table 1. Mutant tRNAs constructed in this study.

Name	Mutation	Affected Codon
$tRNA^{Ser}CGC$	Ala - Ser	GCG
$tRNA^{Ser}UCC$	Gly - Ser	GGA
$tRNA^{Ser}CAG$	Leu - Ser	CTG
$tRNA^{Ser}CAC$	Val - Ser	GTG

Supplementary Table 2. Characteristics of the amino acids and usage of the codons targeted in this study for Ser misincorporation.

Amino acid	Blossom 62 score X→S	Hidropathy	Polarity	Properties
Serine	-	-0,8	polar	reactive hydroxyl group
Alanine	1	1,8	non-polar	normal C-beta carbon
Glycine	0	-0,4	non-polar	side chain hydrogen
Valine	-2	4,2	non-polar	C-beta branched, aliphatic
Leucine	-2	3,8	non-polar	aliphatic

Codon	Nr codons	RSCU	% targeted genes
GCG - Ala	139402	0.524	89.69
GGA - Gly	397666	1.522	98.48
GUG - Val	393951	1.454	98.55
CUG - Leu	538477	1.773	98.98

Supplementary Table 3. Mutant reporter eGFP constructed in this study. These recombinant genes were cloned into the plasmid pCS2.

Reporter	Mutation eGFP 65
Positive ctrl	Ser
Alanine reporter	Ala - GCG
Alanine neg ctrl reporter	Ala - GCG
Glycine reporter	Gly - GGA
Glycine neg ctrl reporter	Gly - GGA
Leucine reporter	Leu - CTG
Leucine neg ctrl reporter	Leu - CTG
Valine reporter	Val - GTG
Valine neg ctrl reporter	Val - GTG

Supplementary Table 4. Oligos used in Real-time qPCR.

Target mRNA	Oligo
Tubulin (reference gene [157])	Fw 5'-CCTGCTGGGAACTGTATTGT-3' Rv 5'-TCAATGAGTTCCTTGCCAAT-3'
hsp70l	Fw 5'-CTGTCTCTGGGCATCGAGAC-3' Rv 5'-TGTCGGAGTAGGTGGTGAAG-3'
hsp90a.2	Fw 5'-GCTCTTATCCTCAGGCTTCA-3' Rv 5'-CGACAGGTCGTCCTCATCAA-3'
hspa5	Fw 5'-TGGAGGAGAAGATCGAGTGG-3' Rv 5'-CTGCCGTACAGTTTGCTGAC-3'
xbp-1	Fw 5'-CACCATGGATACTCACAGCC-3' Rv 5'- CTGAGGCTCCTGTGCTTCA-3'

Supplementary Figure 1. Insoluble proteins accumulate in aggregates during natural ageing in zebrafish. With age, proteins accumulate in insoluble aggregates in the zebrafish brain, eyes and heart. The panels show SDS-PAGE gels of the insoluble protein fraction profiles at six months, one and two years of age in the brain, eyes and heart. The 6 months samples were used as controls. Error bars represent the standard deviation of three independent experiments (Statistical analysis of the data was performed using one-way ANOVA followed by a Dunnet test with CI 95% relative to the six months control; **p<0.01, *p<0.05.

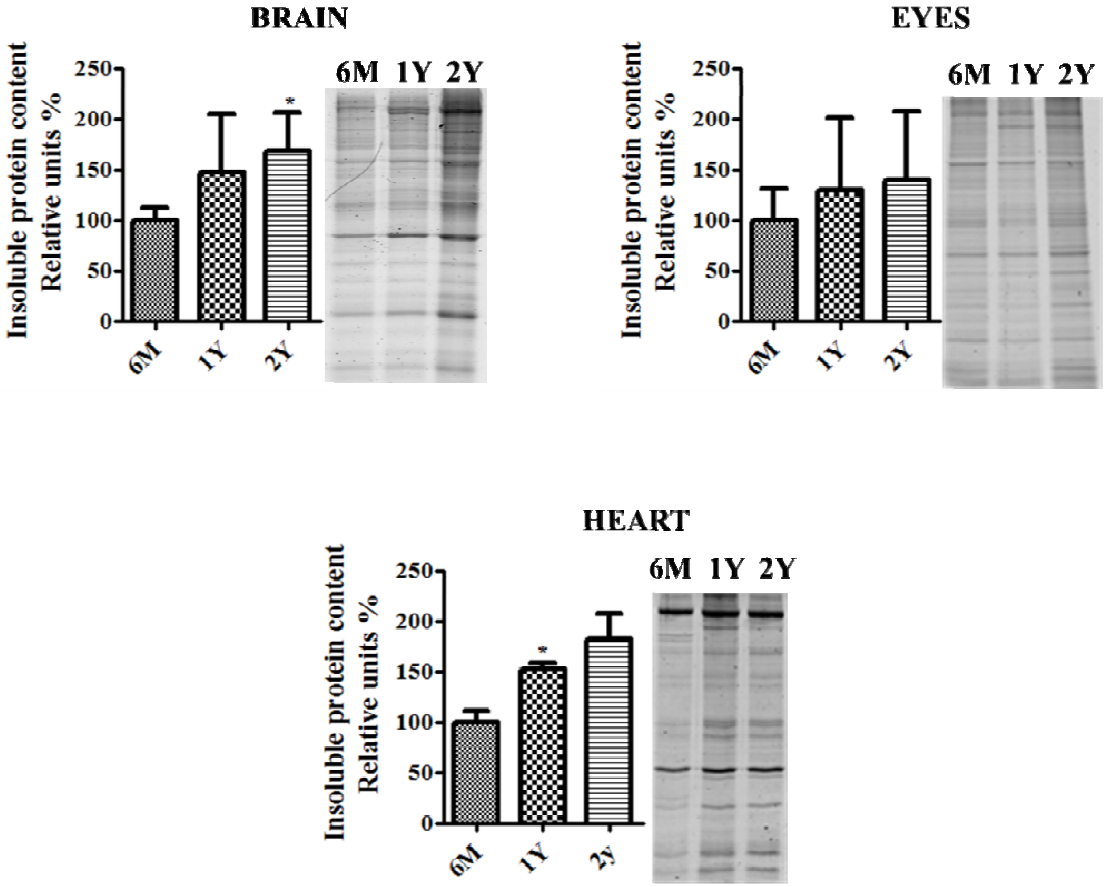

Supplementary Figure 2. Western blot analysis of puromycin levels in embryos expressing the mutant tRNAs.

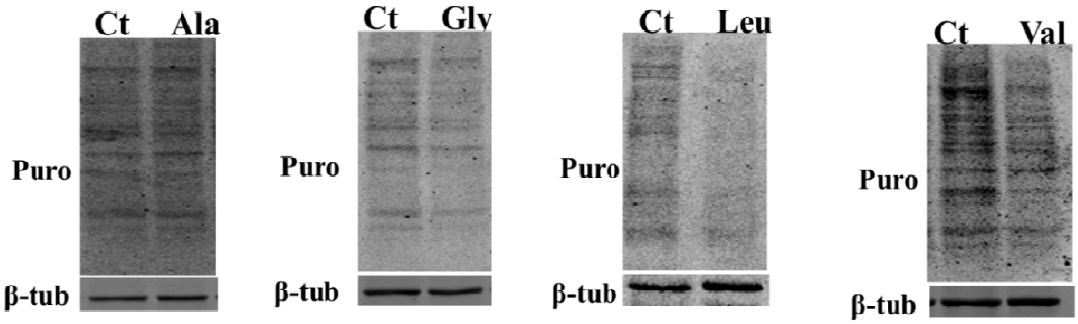

Supplementary Figure 3. Western blot analysis of total eif2α showing that the level of this protein is stable in embryos expressing the mutant tRNAs.

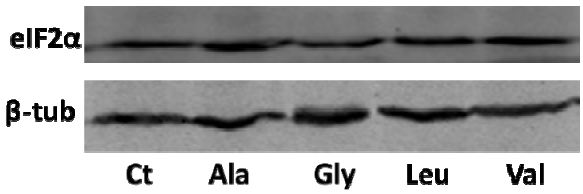

Supplementary Table 5. Comparative analysis of fold change values of *hsp70l, hsp90a.2, hspa5* and *xbp1* genes obtained by qpcr and microarray analysis.

Gene symbol		Ala	Gly	Leu	Val
hsp70l	qPCR	2.365	3.250	44.857	11.162
	microarray	-	-	38.320	34.168
hsp90a.2	qPCR	3.441	2.764	18.251	8.770
	microarray	-	-	9.396	7.541
hspa5	qPCR	1.880	1.349	5.762	2.513
	microarray	-	-	2.113	2.022
xpb1	qPCR	1.087	1.631	1.766	1.251
	microarray	-	-	1.537	1.702

Supplementary Table 6. ER metabolism genes that were deregulated in mistranslating embryos. Microarray data analysis was carried out using MEV software [36, 37]. Data was analyzed using M values (log2 ratios). Fold change values are displayed, t-test analysis p0.05.

Gene symbol	Ala	Gly	Val	Leu	GO BP
use1				1.63	protein transport
zgc:153032			3.88	2.46	protein thiol-disulfide exchange
cyp26a1			2.71	2.34	retinal metabolic process
dhcr7				1.54	cholesterol biosynthetic process
acer1				2.06	lipid metabolic process
agpat9l	4.10		5.58	7.98	phospholipid biosynthetic process
alg6				1.71	protein N-linked glycosylation
asah2				4.37	lipid metabolic process
extl2			1.81	1.37	metabolic process
hsd17b12a		1.76	1.63		lipid biosynthetic process
insig1				3.51	lipid metabolic process
mboat4				1.77	peptidyl-serine octanoylation
moxd1	-1.37	1.67		1.55	catecholamine metabolic process
ormdl1		1.87		1.46	ceramide metabolic process
p4ha1b		2.16			oxidation-reduction process
p4ha2		2.44		4.79	oxidation-reduction process
p4hb			2.09	1.77	glycerol ether metabolic process
pi4kb			2.13	1.62	phosphatidylinositol phosphorylation
plod3			1.74	1.87	oxidation-reduction process
rdh10b			1.61		oxidation-reduction process
sc4mol				2.78	lipid biosynthetic process
serinc5			2.06	1.65	lipid metabolic process
tmem195		1.87			fatty acid biosynthetic process
lpcat2				5.05	phospholipid biosynthetic process
tmem38b				7.36	ion transport
trpc4apa		1.59	1.73	1.41	_
rrbp1b				1.89	protein transport

Supplementary Table 7. Mitochondrial transport and metabolism genes deregulated in mistranslating embryos. Microarray data analysis was carried out using MEV software [36, 37]. Data was analyzed using M values (log2 ratios). Fold change values are displayed, after a t-test analysis p0,05.

Gene symbol	Ala	Gly	Val	Leu	GO BP
fxn		2.75			iron-sulfur cluster assembly
kbp	1.63	1.69		1.47	mitochondrial transport
slc25a14			1.48		mitochondrial transport
slc25a4				-5.03	transmembrane transport
slc25a10		2.60	2.42	2.23	mitochondrial transport
slc25a28		1.54	1.64		iron ion homeostasis
slc25a33		1.71			transmembrane transport
slc25a37		1.79		1.76	mitochondrial iron ion transport
vdac2		1.79			regulation of anion transport
slc25a47a				2.55	transmembrane transport
hibch			1.53		branched-chain amino acid catabolic process
oxct1a		1.65		1.18	ketone body catabolic process
d2hgdh				1.54	oxidation-reduction process
acsf2		1.79			lipid metabolic process
aldh4a1			1.65		oxidation-reduction process
cpt2		1.73			lipid metabolic process
cyp11a1				7.93	oxidation-reduction process
hagh				2.22	glutathione biosynthetic process
mao		1.48		1.98	catecholamine metabolic process
oxct1b		10.67		10.20	ketone body catabolic process

2.7. References

1. Chen, B., et al., *Cellular strategies of protein quality control.* Cold Spring Harb Perspect Biol, 2011. **3**(8): p. a004374.
2. Schroder, M. and R.J. Kaufman, *The mammalian unfolded protein response.* Annu Rev Biochem, 2005. **74**: p. 739-89.
3. Koga, H., S. Kaushik, and A.M. Cuervo, *Protein homeostasis and aging: The importance of exquisite quality control.* Ageing Res Rev, 2011. **10**(2): p. 205-15.
4. Yang, J.R., S.M. Zhuang, and J. Zhang, *Impact of translational error-induced and error-free misfolding on the rate of protein evolution.* Mol Syst Biol, 2010. **6**: p. 421.
5. Bukau, B., J. Weissman, and A. Horwich, *Molecular chaperones and protein quality control.* Cell, 2006. **125**(3): p. 443-51.
6. Malhotra, J.D. and R.J. Kaufman, *The endoplasmic reticulum and the unfolded protein response.* Semin Cell Dev Biol, 2007. **18**(6): p. 716-31.
7. Ben-Zvi, A., E.A. Miller, and R.I. Morimoto, *Collapse of proteostasis represents an early molecular event in Caenorhabditis elegans aging.* Proc Natl Acad Sci U S A, 2009. **106**(35): p. 14914-9.
8. David, D.C., et al., *Widespread protein aggregation as an inherent part of aging in C. elegans.* PLoS Biol, 2010. **8**(8): p. e1000450.
9. Reynolds, N.M., B.A. Lazazzera, and M. Ibba, *Cellular mechanisms that control mistranslation.* Nat Rev Microbiol, 2010. **8**(12): p. 849-56.
10. Hartl, F.U., A. Bracher, and M. Hayer-Hartl, *Molecular chaperones in protein folding and proteostasis.* Nature, 2011. **475**(7356): p. 324-32.
11. Morimoto, R.I., *Proteotoxic stress and inducible chaperone networks in neurodegenerative disease and aging.* Genes Dev, 2008. **22**(11): p. 1427-38.
12. Cui, H., Y. Kong, and H. Zhang, *Oxidative stress, mitochondrial dysfunction, and aging.* J Signal Transduct, 2012. **2012**: p. 646354.
13. Berlett, B.S. and E.R. Stadtman, *Protein oxidation in aging, disease, and oxidative stress.* J Biol Chem, 1997. **272**(33): p. 20313-6.
14. Tyedmers, J., A. Mogk, and B. Bukau, *Cellular strategies for controlling protein aggregation.* Nat Rev Mol Cell Biol, 2010. **11**(11): p. 777-88.
15. Kaganovich, D., R. Kopito, and J. Frydman, *Misfolded proteins partition between two distinct quality control compartments.* Nature, 2008. **454**(7208): p. 1088-95.
16. Hohn, A., J. Konig, and T. Grune, *Protein oxidation in aging and the removal of oxidized proteins.* J Proteomics, 2013.
17. Tabas, I. and D. Ron, *Integrating the mechanisms of apoptosis induced by endoplasmic reticulum stress.* Nat Cell Biol, 2011. **13**(3): p. 184-90.
18. Geslain, R., et al., *Chimeric tRNAs as tools to induce proteome damage and identify components of stress responses.* Nucleic Acids Res, 2010. **38**(5): p. e30.
19. Ron, D. and P. Walter, *Signal integration in the endoplasmic reticulum unfolded protein response.* Nat Rev Mol Cell Biol, 2007. **8**(7): p. 519-29.
20. Paredes, J.A., et al., *Low level genome mistranslations deregulate the transcriptome and translatome and generate proteotoxic stress in yeast.* BMC Biol, 2012. **10**(1): p. 55.
21. Kimmel, C.B., et al., *Stages of embryonic development of the zebrafish.* Dev Dyn, 1995. **203**(3): p. 253-310.
22. Kim, H.Y., et al., *Establishment of the expression system for studying the function of active caspase-3 in zebrafish.* Mol Biol Rep, 2009. **36**(2): p. 405-13.
23. Betts, M.J. and R.B. Russell, *Amino acid properties and consequences of subsitutions*. Bioinformatics for Geneticists, ed. M.R.B.a.I.C. Gray2003: John Wiley & Sons, Ltd.
24. Berleant, D., et al., *The genetic code--more than just a table.* Cell Biochem Biophys, 2009. **55**(2): p. 107-16.

25. Henikoff, S. and J.G. Henikoff, *Amino acid substitution matrices from protein blocks.* Proc Natl Acad Sci U S A, 1992. **89**(22): p. 10915-9.
26. Haig, D. and L.D. Hurst, *A quantitative measure of error minimization in the genetic code.* J Mol Evol, 1991. **33**(5): p. 412-7.
27. Taylor, W.R., *The classification of amino acid conservation.* J Theor Biol, 1986. **119**(2): p. 205-18.
28. Moura, G., et al., *Comparative context analysis of codon pairs on an ORFeome scale.* Genome Biol, 2005. **6**(3): p. R28.
29. Link, V., A. Shevchenko, and C.P. Heisenberg, *Proteomics of early zebrafish embryos.* BMC Dev Biol, 2006. **6**: p. 1.
30. Urasaki, A., G. Morvan, and K. Kawakami, *Functional dissection of the Tol2 transposable element identified the minimal cis-sequence and a highly repetitive sequence in the subterminal region essential for transposition.* Genetics, 2006. **174**(2): p. 639-49.
31. Wu, Y.L., et al., *Development of a heat shock inducible gfp transgenic zebrafish line by using the zebrafish hsp27 promoter.* Gene, 2008. **408**(1-2): p. 85-94.
32. Schmidt, E.K., et al., *SUnSET, a nonradioactive method to monitor protein synthesis.* Nat Methods, 2009. **6**(4): p. 275-7.
33. Goodman, C.A., et al., *Novel insights into the regulation of skeletal muscle protein synthesis as revealed by a new nonradioactive in vivo technique.* FASEB J, 2011. **25**(3): p. 1028-39.
34. Grune, T., et al., *Peroxynitrite increases the degradation of aconitase and other cellular proteins by proteasome.* J Biol Chem, 1998. **273**(18): p. 10857-62.
35. Demasi, M., G.M. Silva, and L.E. Netto, *20 S proteasome from Saccharomyces cerevisiae is responsive to redox modifications and is S-glutathionylated.* J Biol Chem, 2003. **278**(1): p. 679-85.
36. Saeed, A.I., et al., *TM4 microarray software suite.* Methods Enzymol, 2006. **411**: p. 134-93.
37. Saeed, A.I., et al., *TM4: a free, open-source system for microarray data management and analysis.* Biotechniques, 2003. **34**(2): p. 374-8.
38. Carmona-Saez, P., et al., *GENECODIS: a web-based tool for finding significant concurrent annotations in gene lists.* Genome Biol, 2007. **8**(1): p. R3.
39. Nogales-Cadenas, R., et al., *GeneCodis: interpreting gene lists through enrichment analysis and integration of diverse biological information.* Nucleic Acids Res, 2009. **37**(Web Server issue): p. W317-22.
40. Pfaffl, M.W., *A new mathematical model for relative quantification in real-time RT-PCR.* Nucleic Acids Res, 2001. **29**(9): p. e45.
41. Pfaffl, M.W., G.W. Horgan, and L. Dempfle, *Relative expression software tool (REST) for group-wise comparison and statistical analysis of relative expression results in real-time PCR.* Nucleic Acids Res, 2002. **30**(9): p. e36.
42. Hunter, S.E., et al., *The QPCR assay for analysis of mitochondrial DNA damage, repair, and relative copy number.* Methods, 2010. **51**(4): p. 444-51.
43. Hu, M.C., et al., *XBP-1, a key regulator of unfolded protein response, activates transcription of IGF1 and Akt phosphorylation in zebrafish embryonic cell line.* Biochem Biophys Res Commun, 2007. **359**(3): p. 778-83.
44. Ayala-Torres, S., et al., *Analysis of gene-specific DNA damage and repair using quantitative polymerase chain reaction.* Methods, 2000. **22**(2): p. 135-47.
45. Lenhard, B., et al., *tRNA recognition and evolution of determinants in seryl-tRNA synthesis.* Nucleic Acids Res, 1999. **27**(3): p. 721-9.
46. Cusack, S., A. Yaremchuk, and M. Tukalo, *The crystal structure of the ternary complex of T.thermophilus seryl-tRNA synthetase with tRNA(Ser) and a seryl-adenylate analogue reveals a conformational switch in the active site.* EMBO J, 1996. **15**(11): p. 2834-42.

47. Rocha, R., et al., *Unveiling the structural basis for translational ambiguity tolerance in a human fungal pathogen.* Proc Natl Acad Sci U S A, 2011. **108**(34): p. 14091-6.
48. White, S.H., *Amino acid preferences of small proteins. Implications for protein stability and evolution.* J Mol Biol, 1992. **227**(4): p. 991-5.
49. Reid, B.G. and G.C. Flynn, *Chromophore formation in green fluorescent protein.* Biochemistry, 1997. **36**(22): p. 6786-91.
50. Cody, C.W., et al., *Chemical structure of the hexapeptide chromophore of the Aequorea green-fluorescent protein.* Biochemistry, 1993. **32**(5): p. 1212-8.
51. Dalle-Donne, I., et al., *Protein carbonyl groups as biomarkers of oxidative stress.* Clin Chim Acta, 2003. **329**(1-2): p. 23-38.
52. Ojha, J., et al., *Sequestration of toxic oligomers by HspB1 as a cytoprotective mechanism.* Mol Cell Biol, 2011. **31**(15): p. 3146-57.
53. Bryantsev, A.L., et al., *Regulation of stress-induced intracellular sorting and chaperone function of Hsp27 (HspB1) in mammalian cells.* Biochem J, 2007. **407**(3): p. 407-17.
54. Murtha, J.M. and E.T. Keller, *Characterization of the heat shock response in mature zebrafish (Danio rerio).* Exp Gerontol, 2003. **38**(6): p. 683-91.
55. Paredes, J.A., et al., *Low level genome mistranslations deregulate the transcriptome and translatome and generate proteotoxic stress in yeast.* BMC Biol, 2012. **10**: p. 55.
56. Proud, C.G., *eIF2 and the control of cell physiology.* Semin Cell Dev Biol, 2005. **16**(1): p. 3-12.
57. Raven, J.F. and A.E. Koromilas, *PERK and PKR: old kinases learn new tricks.* Cell Cycle, 2008. **7**(9): p. 1146-50.
58. Krishnamoorthy, T., et al., *Tight binding of the phosphorylated alpha subunit of initiation factor 2 (eIF2alpha) to the regulatory subunits of guanine nucleotide exchange factor eIF2B is required for inhibition of translation initiation.* Mol Cell Biol, 2001. **21**(15): p. 5018-30.
59. Zhang, Y., et al., *Heat shock factor-4 (HSF-4a) is a repressor of HSF-1 mediated transcription.* J Cell Biochem, 2001. **82**(4): p. 692-703.
60. Marzec, M., D. Eletto, and Y. Argon, *GRP94: An HSP90-like protein specialized for protein folding and quality control in the endoplasmic reticulum.* Biochim Biophys Acta, 2012. **1823**(3): p. 774-87.
61. Gething, M.J., *Role and regulation of the ER chaperone BiP.* Semin Cell Dev Biol, 1999. **10**(5): p. 465-72.
62. Harding, H.P., Y. Zhang, and D. Ron, *Protein translation and folding are coupled by an endoplasmic-reticulum-resident kinase.* Nature, 1999. **397**(6716): p. 271-4.
63. Berlanga, J.J., S. Herrero, and C. de Haro, *Characterization of the hemin-sensitive eukaryotic initiation factor 2alpha kinase from mouse nonerythroid cells.* J Biol Chem, 1998. **273**(48): p. 32340-6.
64. Yoshida, H., et al., *XBP1 mRNA is induced by ATF6 and spliced by IRE1 in response to ER stress to produce a highly active transcription factor.* Cell, 2001. **107**(7): p. 881-91.
65. Schafer, A. and D.H. Wolf, *Sec61p is part of the endoplasmic reticulum-associated degradation machinery.* EMBO J, 2009. **28**(19): p. 2874-84.
66. Lang, S., et al., *Sec61 complexes form ubiquitous ER Ca2+ leak channels.* Channels (Austin), 2011. **5**(3): p. 228-35.
67. Oda, Y., et al., *Derlin-2 and Derlin-3 are regulated by the mammalian unfolded protein response and are required for ER-associated degradation.* J Cell Biol, 2006. **172**(3): p. 383-93.
68. Belmont, P.J., et al., *Roles for endoplasmic reticulum-associated degradation and the novel endoplasmic reticulum stress response gene Derlin-3 in the ischemic heart.* Circ Res, 2010. **106**(2): p. 307-16.

69. Kim, T.Y., et al., *Herp enhances ER-associated protein degradation by recruiting ubiquilins.* Biochem Biophys Res Commun, 2008. **369**(2): p. 741-6.
70. Wakana, Y., et al., *Bap31 is an itinerant protein that moves between the peripheral endoplasmic reticulum (ER) and a juxtanuclear compartment related to ER-associated Degradation.* Mol Biol Cell, 2008. **19**(5): p. 1825-36.
71. Rutkowski, D.T., et al., *The role of p58IPK in protecting the stressed endoplasmic reticulum.* Mol Biol Cell, 2007. **18**(9): p. 3681-91.
72. Chuang, J.Z., et al., *Characterization of a brain-enriched chaperone, MRJ, that inhibits Huntingtin aggregation and toxicity independently.* J Biol Chem, 2002. **277**(22): p. 19831-8.
73. Qiu, X.B., et al., *The diversity of the DnaJ/Hsp40 family, the crucial partners for Hsp70 chaperones.* Cell Mol Life Sci, 2006. **63**(22): p. 2560-70.
74. Braun, J.E., S.M. Wilbanks, and R.H. Scheller, *The cysteine string secretory vesicle protein activates Hsc70 ATPase.* J Biol Chem, 1996. **271**(42): p. 25989-93.
75. Fortier, S., et al., *Base excision repair in early zebrafish development: evidence for DNA polymerase switching and standby AP endonuclease activity.* Biochemistry, 2009. **48**(23): p. 5396-404.
76. Bladen, C.L., et al., *DNA damage response and Ku80 function in the vertebrate embryo.* Nucleic Acids Res, 2005. **33**(9): p. 3002-10.
77. Ringvoll, J., et al., *AlkB homologue 2-mediated repair of ethenoadenine lesions in mammalian DNA.* Cancer Res, 2008. **68**(11): p. 4142-9.
78. Wood, R.D., *Mammalian nucleotide excision repair proteins and interstrand crosslink repair.* Environ Mol Mutagen, 2010. **51**(6): p. 520-6.
79. Kawahara, A., et al., *Zebrafish GADD45beta genes are involved in somite segmentation.* Proc Natl Acad Sci U S A, 2005. **102**(2): p. 361-6.
80. Takekawa, M. and H. Saito, *A family of stress-inducible GADD45-like proteins mediate activation of the stress-responsive MTK1/MEKK4 MAPKKK.* Cell, 1998. **95**(4): p. 521-30.
81. Elicker, K.S. and L.D. Hutson, *Genome-wide analysis and expression profiling of the small heat shock proteins in zebrafish.* Gene, 2007. **403**(1-2): p. 60-9.
82. van Huizen, R., et al., *P58IPK, a novel endoplasmic reticulum stress-inducible protein and potential negative regulator of eIF2alpha signaling.* J Biol Chem, 2003. **278**(18): p. 15558-64.
83. Panaretou, B., et al., *Activation of the ATPase activity of hsp90 by the stress-regulated cochaperone aha1.* Mol Cell, 2002. **10**(6): p. 1307-18.
84. Jin, H.O., et al., *Nuclear protein 1 induced by ATF4 in response to various stressors acts as a positive regulator on the transcriptional activation of ATF4.* IUBMB Life, 2009. **61**(12): p. 1153-8.
85. Nakai, A., et al., *HSF4, a new member of the human heat shock factor family which lacks properties of a transcriptional activator.* Mol Cell Biol, 1997. **17**(1): p. 469-81.
86. Swan, C.L., et al., *Zebrafish HSF4: a novel protein that shares features of both HSF1 and HSF4 of mammals.* Cell Stress Chaperones, 2012. **17**(5): p. 623-37.
87. Fukuda, S., et al., *Murine and human SDF2L1 is an endoplasmic reticulum stress-inducible gene and encodes a new member of the Pmt/rt protein family.* Biochem Biophys Res Commun, 2001. **280**(1): p. 407-14.
88. Ikeda, J., et al., *Cloning and expression of cDNA encoding the human 150 kDa oxygen-regulated protein, ORP150.* Biochem Biophys Res Commun, 1997. **230**(1): p. 94-9.
89. Nishikawa, M., et al., *Identification and characterization of endoplasmic reticulum-associated protein, ERp43.* Gene, 2007. **386**(1-2): p. 42-51.
90. Linnik, K.M. and H. Herscovitz, *Multiple molecular chaperones interact with apolipoprotein B during its maturation. The network of endoplasmic reticulum-resident chaperones*

(ERp72, GRP94, calreticulin, and BiP) interacts with apolipoprotein b regardless of its lipidation state. J Biol Chem, 1998. **273**(33): p. 21368-73.
91. Jessop, C.E., et al., *Protein disulphide isomerase family members show distinct substrate specificity: P5 is targeted to BiP client proteins.* J Cell Sci, 2009. **122**(Pt 23): p. 4287-95.
92. Treves, S., et al., *Junctate is a key element in calcium entry induced by activation of InsP3 receptors and/or calcium store depletion.* J Cell Biol, 2004. **166**(4): p. 537-48.
93. Arnaudeau, S., et al., *Calreticulin differentially modulates calcium uptake and release in the endoplasmic reticulum and mitochondria.* J Biol Chem, 2002. **277**(48): p. 46696-705.
94. Krause, K.H. and M. Michalak, *Calreticulin.* Cell, 1997. **88**(4): p. 439-43.
95. Michalak, M., et al., *Calreticulin: one protein, one gene, many functions.* Biochem J, 1999. **344 Pt 2**: p. 281-92.
96. Ashworth, R., et al., *Molecular and functional characterization of inositol trisphosphate receptors during early zebrafish development.* J Biol Chem, 2007. **282**(19): p. 13984-93.
97. Voeltz, G.K., et al., *A class of membrane proteins shaping the tubular endoplasmic reticulum.* Cell, 2006. **124**(3): p. 573-86.
98. Terentyev, D., et al., *Protein protein interactions between triadin and calsequestrin are involved in modulation of sarcoplasmic reticulum calcium release in cardiac myocytes.* J Physiol, 2007. **583**(Pt 1): p. 71-80.
99. Malhotra, J.D., et al., *Antioxidants reduce endoplasmic reticulum stress and improve protein secretion.* Proc Natl Acad Sci U S A, 2008. **105**(47): p. 18525-30.
100. Harding, H.P., et al., *An integrated stress response regulates amino acid metabolism and resistance to oxidative stress.* Mol Cell, 2003. **11**(3): p. 619-33.
101. Haynes, C.M., E.A. Titus, and A.A. Cooper, *Degradation of misfolded proteins prevents ER-derived oxidative stress and cell death.* Mol Cell, 2004. **15**(5): p. 767-76.
102. Tu, B.P. and J.S. Weissman, *Oxidative protein folding in eukaryotes: mechanisms and consequences.* J Cell Biol, 2004. **164**(3): p. 341-6.
103. Dikalov, S., K.K. Griendling, and D.G. Harrison, *Measurement of reactive oxygen species in cardiovascular studies.* Hypertension, 2007. **49**(4): p. 717-27.
104. Chance, B., H. Sies, and A. Boveris, *Hydroperoxide metabolism in mammalian organs.* Physiol Rev, 1979. **59**(3): p. 527-605.
105. Grune, T., et al., *Decreased proteolysis caused by protein aggregates, inclusion bodies, plaques, lipofuscin, ceroid, and 'aggresomes' during oxidative stress, aging, and disease.* Int J Biochem Cell Biol, 2004. **36**(12): p. 2519-30.
106. Nystrom, T., *Role of oxidative carbonylation in protein quality control and senescence.* EMBO J, 2005. **24**(7): p. 1311-7.
107. Bretaud, S., et al., *p53-dependent neuronal cell death in a DJ-1-deficient zebrafish model of Parkinson's disease.* J Neurochem, 2007. **100**(6): p. 1626-35.
108. Baulac, S., et al., *Increased DJ-1 expression under oxidative stress and in Alzheimer's disease brains.* Mol Neurodegener, 2009. **4**: p. 12.
109. Chen, J. and M.J. Berry, *Selenium and selenoproteins in the brain and brain diseases.* J Neurochem, 2003. **86**(1): p. 1-12.
110. Xu, X.M., et al., *Evidence for direct roles of two additional factors, SECp43 and soluble liver antigen, in the selenoprotein synthesis machinery.* J Biol Chem, 2005. **280**(50): p. 41568-75.
111. Chakravarthi, S., et al., *Intracellular catalysis of disulfide bond formation by the human sulfhydryl oxidase, QSOX1.* Biochem J, 2007. **404**(3): p. 403-11.
112. Saeed, U., et al., *Knockdown of cytosolic glutaredoxin 1 leads to loss of mitochondrial membrane potential: implication in neurodegenerative diseases.* PLoS One, 2008. **3**(6): p. e2459.
113. Raza, H., *Dual localization of glutathione S-transferase in the cytosol and mitochondria: implications in oxidative stress, toxicity and disease.* FEBS J, 2011. **278**(22): p. 4243-51.

114. Kelner, M.J., et al., *Structural organization of the microsomal glutathione S-transferase gene (MGST1) on chromosome 12p13.1-13.2. Identification of the correct promoter region and demonstration of transcriptional regulation in response to oxidative stress.* J Biol Chem, 2000. **275**(17): p. 13000-6.
115. Gould, S.J., et al., *Pex13p is an SH3 protein of the peroxisome membrane and a docking factor for the predominantly cytoplasmic PTs1 receptor.* J Cell Biol, 1996. **135**(1): p. 85-95.
116. Koch, J., et al., *PEX11 family members are membrane elongation factors that coordinate peroxisome proliferation and maintenance.* J Cell Sci, 2010. **123**(Pt 19): p. 3389-400.
117. Santos, J.H., B.S. Mandavilli, and B. Van Houten, *Measuring oxidative mtDNA damage and repair using quantitative PCR.* Methods Mol Biol, 2002. **197**: p. 159-76.
118. Mandavilli, B.S., J.H. Santos, and B. Van Houten, *Mitochondrial DNA repair and aging.* Mutat Res, 2002. **509**(1-2): p. 127-51.
119. Van Houten, B., V. Woshner, and J.H. Santos, *Role of mitochondrial DNA in toxic responses to oxidative stress.* DNA Repair (Amst), 2006. **5**(2): p. 145-52.
120. Cline, S.D., *Mitochondrial DNA damage and its consequences for mitochondrial gene expression.* Biochim Biophys Acta, 2012. **1819**(9-10): p. 979-91.
121. Narendra, D.P. and R.J. Youle, *Targeting mitochondrial dysfunction: role for PINK1 and Parkin in mitochondrial quality control.* Antioxid Redox Signal, 2011. **14**(10): p. 1929-38.
122. Springer, W. and P.J. Kahle, *Regulation of PINK1-Parkin-mediated mitophagy.* Autophagy, 2011. **7**(3): p. 266-78.
123. Ved, R., et al., *Similar patterns of mitochondrial vulnerability and rescue induced by genetic modification of alpha-synuclein, parkin, and DJ-1 in Caenorhabditis elegans.* J Biol Chem, 2005. **280**(52): p. 42655-68.
124. Canet-Aviles, R.M., et al., *The Parkinson's disease protein DJ-1 is neuroprotective due to cysteine-sulfinic acid-driven mitochondrial localization.* Proc Natl Acad Sci U S A, 2004. **101**(24): p. 9103-8.
125. Giaime, E., et al., *Loss of DJ-1 does not affect mitochondrial respiration but increases ROS production and mitochondrial permeability transition pore opening.* PLoS One, 2012. **7**(7): p. e40501.
126. Saotome, M., et al., *Bidirectional Ca2+-dependent control of mitochondrial dynamics by the Miro GTPase.* Proc Natl Acad Sci U S A, 2008. **105**(52): p. 20728-33.
127. Tondera, D., et al., *The mitochondrial protein MTP18 contributes to mitochondrial fission in mammalian cells.* J Cell Sci, 2005. **118**(Pt 14): p. 3049-59.
128. Gandre-Babbe, S. and A.M. van der Bliek, *The novel tail-anchored membrane protein Mff controls mitochondrial and peroxisomal fission in mammalian cells.* Mol Biol Cell, 2008. **19**(6): p. 2402-12.
129. Inohara, N. and G. Nunez, *Genes with homology to mammalian apoptosis regulators identified in zebrafish.* Cell Death Differ, 2000. **7**(5): p. 509-10.
130. Eimon, P.M. and A. Ashkenazi, *The zebrafish as a model organism for the study of apoptosis.* Apoptosis, 2010. **15**(3): p. 331-49.
131. Chinnadurai, G., S. Vijayalingam, and S.B. Gibson, *BNIP3 subfamily BH3-only proteins: mitochondrial stress sensors in normal and pathological functions.* Oncogene, 2008. **27 Suppl 1**: p. S114-27.
132. He, C., et al., *Assaying autophagic activity in transgenic GFP-Lc3 and GFP-Gabarap zebrafish embryos.* Autophagy, 2009. **5**(4): p. 520-6.
133. Iida, R., M. Ueki, and T. Yasuda, *Identification of Rhit as a novel transcriptional repressor of human Mpv17-like protein with a mitigating effect on mitochondrial dysfunction, and its transcriptional regulation by FOXD3 and GABP.* Free Radic Biol Med, 2012. **52**(8): p. 1413-22.

134. Cabreiro, F., et al., *Overexpression of mitochondrial methionine sulfoxide reductase B2 protects leukemia cells from oxidative stress-induced cell death and protein damage.* J Biol Chem, 2008. **283**(24): p. 16673-81.
135. Alkhaja, A.K., et al., *MINOS1 is a conserved component of mitofilin complexes and required for mitochondrial function and cristae organization.* Mol Biol Cell, 2012. **23**(2): p. 247-57.
136. Wang, S. and R.J. Kaufman, *The impact of the unfolded protein response on human disease.* J Cell Biol, 2012. **197**(7): p. 857-67.
137. Thakur, P.C., et al., *Lack of de novo phosphatidylinositol synthesis leads to endoplasmic reticulum stress and hepatic steatosis in cdipt-deficient zebrafish.* Hepatology, 2011. **54**(2): p. 452-62.
138. Cinaroglu, A., et al., *Activating transcription factor 6 plays protective and pathological roles in steatosis due to endoplasmic reticulum stress in zebrafish.* Hepatology, 2011. **54**(2): p. 495-508.
139. Moreno, J.A., et al., *Sustained translational repression by eIF2alpha-P mediates prion neurodegeneration.* Nature, 2012. **485**(7399): p. 507-11.
140. Burhans, W.C. and M. Weinberger, *DNA replication stress, genome instability and aging.* Nucleic Acids Res, 2007. **35**(22): p. 7545-56.
141. Balaban, R.S., S. Nemoto, and T. Finkel, *Mitochondria, oxidants, and aging.* Cell, 2005. **120**(4): p. 483-95.
142. Chen, H. and D.C. Chan, *Emerging functions of mammalian mitochondrial fusion and fission.* Hum Mol Genet, 2005. **14 Spec No. 2**: p. R283-9.
143. Chen, H., A. Chomyn, and D.C. Chan, *Disruption of fusion results in mitochondrial heterogeneity and dysfunction.* J Biol Chem, 2005. **280**(28): p. 26185-92.
144. Chen, H., et al., *Mitofusins Mfn1 and Mfn2 coordinately regulate mitochondrial fusion and are essential for embryonic development.* J Cell Biol, 2003. **160**(2): p. 189-200.
145. Suen, D.F., K.L. Norris, and R.J. Youle, *Mitochondrial dynamics and apoptosis.* Genes Dev, 2008. **22**(12): p. 1577-90.
146. Detmer, S.A. and D.C. Chan, *Functions and dysfunctions of mitochondrial dynamics.* Nat Rev Mol Cell Biol, 2007. **8**(11): p. 870-9.
147. Bravo, R., et al., *Increased ER-mitochondrial coupling promotes mitochondrial respiration and bioenergetics during early phases of ER stress.* J Cell Sci, 2011. **124**(Pt 13): p. 2143-52.
148. Raturi, A. and T. Simmen, *Where the endoplasmic reticulum and the mitochondrion tie the knot: The mitochondria-associated membrane (MAM).* Biochim Biophys Acta, 2012.
149. Grimm, S., *The ER-mitochondria interface: the social network of cell death.* Biochim Biophys Acta, 2012. **1823**(2): p. 327-34.
150. Sheridan, C. and S.J. Martin, *Mitochondrial fission/fusion dynamics and apoptosis.* Mitochondrion, 2010. **10**(6): p. 640-8.
151. Csordas, G. and G. Hajnoczky, *SR/ER-mitochondrial local communication: calcium and ROS.* Biochim Biophys Acta, 2009. **1787**(11): p. 1352-62.
152. Gandhi, S. and A.Y. Abramov, *Mechanism of oxidative stress in neurodegeneration.* Oxid Med Cell Longev, 2012. **2012**: p. 428010.
153. Ross, C.A. and M.A. Poirier, *Protein aggregation and neurodegenerative disease.* Nat Med, 2004. **10 Suppl**: p. S10-7.
154. Gidalevitz, T., E.A. Kikis, and R.I. Morimoto, *A cellular perspective on conformational disease: the role of genetic background and proteostasis networks.* Curr Opin Struct Biol, 2010. **20**(1): p. 23-32.
155. Federico, A., et al., *Mitochondria, oxidative stress and neurodegeneration.* J Neurol Sci, 2012.
156. Fargnoli, J., et al., *Decreased expression of heat shock protein 70 mRNA and protein after heat treatment in cells of aged rats.* Proc Natl Acad Sci U S A, 1990. **87**(2): p. 846-50.

157. McCurley, A.T. and G.V. Callard, *Characterization of housekeeping genes in zebrafish: male-female differences and effects of tissue type, developmental stage and chemical treatment.* BMC Mol Biol, 2008. **9**: p. 102.

Chapter 3 - Proteotoxic stress induces developmental malformations and deregulates specific microRNAs in zebrafish mistranslating embryos

Marisa Reverendo, Ana Soares, Patrícia Pereira, Laura Carreto, Manuel Santos

Manuscript in preparation

3. Proteotoxic stress induces developmental malformations and deregulates specific microRNAs in zebrafish mistranslating embryos

3.1. Abstract

The accumulation of misfolded proteins leads to proteotoxic stress, which has a strong impact on cell homeostasis. However, it is not yet clear how this phenomenon affects gene expression and if microRNAs play a role in the proteotoxic stress response during vertebrate development. To clarify this issue, we generated zebrafish embryos that mistranslate mRNA at low level, due to the expression of engineered transfer RNAs that introduce random mutations at the proteome level. This activates the stress response in response to protein enabling the study of the effects of proteotoxic stress during vertebrate development. Our data show that proteotoxic stress induces developmental malformations, reduces embryo viability, and deregulates apoptosis, Hedgehog, Wnt and Notch signaling pathways. It also up-regulates miR-145, miR-2195, miR-190b and miR-365 and down-regulates miR-17a*, miR-27c, miR-735, miR-1, miR-16c and let-7g. Interestingly, some putative targets of these molecules are deregulated at the mRNA level and are mainly involved in embryo development and apoptosis, indicating that the observed embryo malformations may be associated with miRNA deregulation.

.

3.2. Introduction

The maintenance of a functional proteome is fundamental to life. Translational errors that occur naturally at a frequency of 10^{-4} are not associated with cell degeneration, however small increases in the level of error are detrimental [1]. Indeed, the accuracy of protein synthesis [2] and protein quality control mechanisms (PQC) promote correct protein folding and modification allowing proteins to reach their native conformation, thus contributing to proteome balance [3, 4]. These PQC systems are composed by molecular chaperones, endoplasmic reticulum associated degradation (ERAD), autophagy and the ubiquitin proteasome pathway (UPP). These mechanisms reduce proteotoxic stress by minimizing the production of abnormal proteins and removing those that are terminally aberrant [5, 6]. Chaperones take part in several processes in the cell, especially in the folding/refolding and assembly steps and also in the deposition and degradation of aggregated and misfolded proteins [7-9]. Endoplasmic reticulum (ER) saturation with misfolded proteins triggers the activation of apoptotic pathways [10, 11], increase oxidative stress, induces calcium leakage from the stressed ER and subsequent activation of cytosolic proteases and death effectors of the BCL-2 family [11, 12]. The latter signal apoptosis through the mitochondrial pathway, however these mechanisms remain poorly understood and how apoptotic signaling is initiated is still a matter of debate [11, 12].

MicroRNA regulation plays a critical role in the control of vertebrate embryo development. Since the first evidences of miRNA regulated gene expression *in Caenorhabditis elegans* by lin-4 and let-7 it has been shown that these small RNAs intervene in the regulation of most of the biological processes [13]. Importantly, specific miRNAs regulate vertebrate cellular differentiation and developmental progression and

patterning [14]. In the case of zebrafish, miRNAs have a pivotal role during development by regulating tissue differentiation and organogenesis [15-23]. For instance, miR-1 and miR-133 play fundamental roles is sarcomeric organization allowing for proper muscle tissue development [15]. And the tumor suppressor miR-145 is responsible for zebrafish gut development by targeting the transcription factor *gata6* [21]. Several studies have also shown that miRNAs can play an important role in mediating cellular stress responses. Indeed, endoplasmic stress response factor XBP1 can be targeted by miR-30c-2-3p and induce the expression of miR-346 under ER stress conditions to mediate adaptive responses to ER stress [24, 25]. The ER-UPR factor IREα can also intervene in miRNA dynamics at the biogenesis levels, since this factor can cleave several miRNAs (miR-17, miR-34a, miR-96, miR-125b) to stimulate apoptosis following ER stress [26].

Several strategies based on chemical stressors or overexpression of aggregation prone proteins have been used to generate proteome imbalance [27-29]. A new method based on misreading tRNAs has been tested in yeast, mammalian cells and chick embryos and the results indicate that it is possible to induce the activation of the stress response in the ER without exposing cells to chemicals [30-32]. Our laboratory has established a zebrafish system based on misreading serine tRNAs that created proteome instability; we observed increased protein ubiquitination and activation of the UPP and UPR, increased reactive oxygen species (ROS) production, down-regulation of protein biosynthesis and mitochondrial dysfunction (chapter 2). Zebrafish is a vertebrate model system with many advantages over other vertebrate models, since it has high fecundity, transparent embryos, and external development. Thus, it is easily visualized and experimentally manipulated at early developmental stages. All these features, previously found mainly in invertebrate models, facilitate genetic and functional studies.

Importantly, the zebrafish model system allows the evaluation of proteotoxic stress response in a whole organism at early development stage by expressing mutant tRNAs in zebrafish embryos.

Our approach targets the whole proteome with different mutations that activate several quality control mechanisms and trigger ER stress. These misreading tRNAs caused embryo malformation and reduced survival. To elucidate whether miRNAs are implicated in this phenotype we have used miRNA profiling to identify deregulated miRNAs. Protetoxic stress induced by the misreading tRNAs upregulated expression of miR-145, miR-2195, miR-190b and miR-365, and downregulated miR-17a*, miR-27c, miR-732, miR-1, miR-16c and let-7g. Several putative targets of these miRNAs were also deregulated. We also performed gene expression microarrays to explore transcriptome reprograming and proteotoxic stress responsive genes. We show that misreading tRNAs activate the apoptotic pathways, and also that this activation is dependent on the type of mutations introduced into the proteome. Our data shows that early zebrafish development is strongly affected by the misreading tRNAs; thus opening the door creating to study vertebrate developmental progression under proteotoxic stress conditions.

3.3. Methods

3.3.1. Zebrafish husbandry and mutant serine tRNA microinjection

Zebrafish were maintained at 28ºC on a 14 h-light/10 h-dark cycle. Stages of embryonic development were determined based on the number of hours after fertilization and morphological standards [33]. Zebrafish maintenance followed the Portuguese law for animal experimentation (Regulatory Guideline nº 1005/92, October 23rd, 1992). Mutant tRNA constructs described in the previous chapter were injected into zebrafish embryos at one-cell stage. 65 ng/µL of plasmid in phenol red/KCl were injected in one-cell stage embryos and embryos were staged in system water and observed under a stereo-microscope equipped for fluorescence measurements (Nikon).

3.3.2. Alcian blue staining

For the alcian blue staining of craniofacial cartilage, 5 dpf larvae were euthanized in tricane and fixed overnight at 4ºC in 4% paraformaldehyde and maintained in 100% ethanol at -20ºC. Fixed larvae were washed with PBT, bleached in hydrogen peroxide and potassium. Staining was performed overnight in 0.1% Alcian Blue in acid-alcohol (5% concentrated hydrochloric acid, 70% ethanol) and larvae were washed several times with the same solution of acid-alcohol. Finally larvae were rehydrated and mounted with glycerol-KOH.

3.3.3. ROS scavengers

Zebrafish embryos were injected with the mutant tRNA contructs and were maintained in scavenger solutions. Namely, ascorbic acid (500µM), gluthatione (100µM) and d-methionine (20µM). Scavenger solutions were prepared with system

water and solution pH was corrected. Embryos were observed under a stereo-microscope equipped for fluorescence measurements (Nikon). Stages of embryonic development were determined based on the number of hours after fertilization and morphological standards [33].

3.3.4. Total RNA extraction

Total RNA was extracted using Trizol® according to manufacturer´s instructions. Briefly, 200 24hpf embryos were collected, dechorionated and stored at -80ºC. Frozen embryo pellets were ressuspended in 1mL of TRIZOL and disrupted using precellys 24 (Bertin technologies). The total extracts were incubated at room temperature for 5 minutes and further extracted with chlorophorm and isopropyl alcohol. Total RNA pellets were washed with 75% ethanol and ressuspended in milliQ water. To remove contaminating DNA, samples were treated with DNAseI (Fermentas) following the manufacturer instructions and stored at -80ºC. RNA was quantified using Nanodrop 1000 Spectrophotometer (Thermo Scientific) and quality was verified using the Agilent 2100 Bioanalyzer.

3.3.5. MicroRNA microarrays

MiRNA microarrays were performed using the miRNA Chip (miRNAChip_MS_V1) which was printed at the Portuguese National DNA Microarrays Facility, at the University of Aveiro. Arrays were printed with 1164 probes in quadruplicate, probes targeted the known mature miRNAs present in the Sanger miRBase Sequence Database, Release 9.0 (features human, mouse, rat, *Drosophila melanogaster*, *Caenorhabditis elegans*, and zebrafish). Mismatch controls and Ncode Positive Control were also included. These probes control hybridization and labeling

quality determination and also improve spot location. An additional set of 24 probes was included; these probes correspond to novel zebrafish miRNAs identified by Soares and colleages [34]. Sample labeling was carried out with ULS microRNA labeling kit (Kreatech) following manufacturer's instructions. 2µg of total RNA was labeled with Cy3-ULS at 85ºC for 15min. After this, labeled samples were purified and dye incorporation was monitored using ultraviolet-visible spectroscopy. Samples were hybridized to the miRNA Chips at 42ºC for 16h. Following hybridization slides were immediately washed and scanned with the Agilent G2565AA microarrays scanner.

3.3.6. MicroRNA microarray data extraction and analysis

Probes signal were extracted from microarray scan data and analyzed using Agilent Feature Extraction Software (Agilent). Briefly, median pixel intensity values were normalized and background subtracted. Data was normalized using BRB Array tool v3.4.0 software to do a global median normalization for each miRNA. Normalized data was log transformed (base 2) and further analyzed with MEV software (TM4 Microarray Software Suite) [35, 36]. A t-test ($p<0.05$) was applied to identify miRNAs that showed statistically significant differences in expression between control and mutant tRNA samples.

3.3.7. Real-Time Quantitative PCR

Quantification of miRNA expression was carried out using NCode™ miRNA First-Strand cDNA module and Platinum® SYBR® Green qPCR Super Mix-UDG (Invitrogen). Total RNA was extracted using Trizol® and treated with DNAseI. Total RNA was polyadenylated and used to produce the cDNA. cDNA was prepared from 500ng of total polyadenylated RNA using Superscript III (Invitrogen) according to the

manufacturer´s instructions. Real-time Quantitative PCR was carried out using the ABI Prism 7500 Sequence Detector System (Applied Biosystems). The reactions were carried out at 95ºC for 2 min, 95ºC for 15s and 60ºC for 30s with 50 repetitions. The threshold cycle data (CT) and baselines were determined using auto settings. All assays, including no template controls, were performed in triplicate and relative quantification of gene expression was calculated by the $2-\Delta\Delta CT$ method [37] where the control sample was the endogenous serine tRNA and the experimental internal control was U6 small RNA (RNU6B). Probes were U6: 5'-GACACGCAAATTCGTGAAGCGTTCC ATA-3', mir-145: 5'-GTCCAGTTTTCCCAGGAATCCC-3', mir-1: 5'TGGAATGT AAAGAAGTATGTAT-3' and mir-27c: 5'-TTCACAGTGGTTAAGTTCTGC-3'. All the analyses were carried out using REST-MCS tool [38].

3.3.7. MiRNA target prediction

miRNA targets were identified with the Eimmo (MirZ), miRBASE Targets and TargetScan Fish databases. The computational targets were considered when they were retrieved from at least two of the algorithms. GO terms were identified using DAVID database and manually curated to remove redundant terms [39, 40].

3.3.8. Gene expression microarrays

Gene expression microarrays were performed following the Agilent protocol for One-Color Microarray-Based Gene Expression Analysis Quick Amp Labeling v5.7 (Agilent Technologies). Briefly, cDNA was synthesized from 600ng of total RNA using Agilent T7 Promoter Primer and T7 RNA Polymerase Blend and labeled with Cyanine 3-CTP. Labeled cDNA was purified with RNAeasy mini spin columns (QIAGEN) to remove residual Cyanine 3-CTP. Dye incorporation and quantification was monitored

using the Nanodrop 1000 Spectrophotometer. Agilent zebrafish (v2) microarrays were hybridized with 1.65 μg of labeled cDNA. Hybridizations were carried out using Agilent gasket slides in a rotating oven for 17hr at 65ºC. After hybridization, microarrays were washed using the wash procedure with stabilization and drying solution following the manufacture's recommendations (Agilent). Slides were immediately scanned using an Agilent G2565AA microarrays scanner (Agilent).

3.3.9. Gene expression microarray data extraction and analysis

Probes signal values were extracted from microarray scan data using Agilent Feature Extraction Software (Agilent). The microarray raw data was submitted to the GEO Database and has been given the following accession number: GSE50090. Data was normalized using median centering of signal distribution with Biometric Research Branch BRB-Array tools v3.4.o software. Microarray data analysis was carried out with MEV software (TM4 Microarray Software Suite) [35, 36]. A t-test ($p<0.05$) was applied to identify genes that showed statistically significant differences in expression between control and mutant tRNA samples. GO term enrichment analysis for total statistically significant gene lists for all the mutants was carried out using a hypergeometric test in GeneCodis 2.0 [41, 42].

3.3.10. Cell death assay

Acridine orange (AO) is a cell permeable nucleic acid dye which is sequestered by lysosomes and does not enter the nucleus. However, upon cell death intracellular pH changes and AO is released into the cytoplasm. For cell death staining, 24hpf embryos were washed and dechorionated. Live embryos were stained for apoptotic cells with 5μg/ml AO for 30 min in the dark. After incubation, embryos were washed with system

water and photographed using an epifluorescence microscopy. Fluorescent images were obtained using an Imager.Z1 (Zeiss), AxioCam HRm camera (Zeiss) and AxioVision software (Zeiss).

3.3.11. Caspase activity assays

For caspase activity measurements 20 embryos (24hpf) were dechorionated and stored at -80º C, resuspended in 100µL of buffer and lysed by passing them through a 26.5 gauge needle, then incubated on ice for 30 minutes and centrifuged at 10 000 rpm for 15 minutes at 4ºC. Caspase activation was assessed after measuring the release of aminoluciferin from a caspase substrate (ZDEVD-AML) using the Caspase-Glo® Luminescence kit (Promega, Madison, WI). Kits for Caspase 3/7, 8 and 9 were used. For the assays, 10 µL of the supernatant was diluted with 90µL of room temperature lysis buffer and 100µL of the Caspase-Glo reagent was added. The reactions were carried out on white 96 well plates and incubated at room temperature for 2 hours. After incubation luminescence was measured in a luminometer (Synergy2 BioTek).

3.3.12. Statistical analysis

Data was analyzed using GraphPad Prism. The differences between control and conditioned embryos were assessed by Student's t-test or ANOVA with post-test Dunnett's Multiple Comparison Test. In all cases, p values < 0.05 were considered statistically significant.

3.4. Results

3.4.1. Impact of proteome instability on zebrafish embryo development

In this study we describe the impact on zebrafish development of proteotoxic stress generated by mutant tRNAs described in chapter 2. These mutant tRNAs are able to misincorporate serine at low level into proteins on a proteome wide scale. Importantly, zebrafish embryos at 24hpf show already most of their organ systems differentiated. The brain is already divided into five lobes, and neurons are organized and localized to positions that are maintained up to adulthood [33, 43, 44]. The main muscular and skeletal structures are already present or starting to differentiate, like for instance the vascular system [33]. Therefore this time point is adequate to evaluate the influence of mRNA mistranslation on early larval development. The effects of the expression of mutant tRNAs were analyzed at 24hpf regarding embryo development and morphological alterations. Embryos suffered a strong reduction in viability, especially in the case of the embryos expressing the Ser-tRNA$_{CAG}^{Leu}$, only 5% survived (Figure 3.1A, Supplementary Table 1). The reduction of viability was accompanied by an increase in developmental malformations (Figure 3.1B). Embryos developed several morphological alterations, which were particularly severe in the embryos expressing the Ser-tRNA$_{UCC}^{Gly}$, Ser-tRNA$_{CAC}^{Val}$ and Ser-tRNA$_{CAG}^{Leu}$. Visible alterations to development ranged from undeveloped head and spinal region, tail shortening, longitudinal symmetry loss and also developmental arrest (Figure 3.1C). Cartilage staining of 5dpf larvae showed craniofacial malformations that affected the jaw and also the branchial arches. All mutant tRNAs caused alterations on zebrafish craniofacial cartilage organization and development (Figure 3.1D). However, strongest impact was

observed in the Ser-tRNA$_{CAG}^{Leu}$ expressing embryos, with affected embryo patterning and nervous system development and also craniofacial cartilage organization.

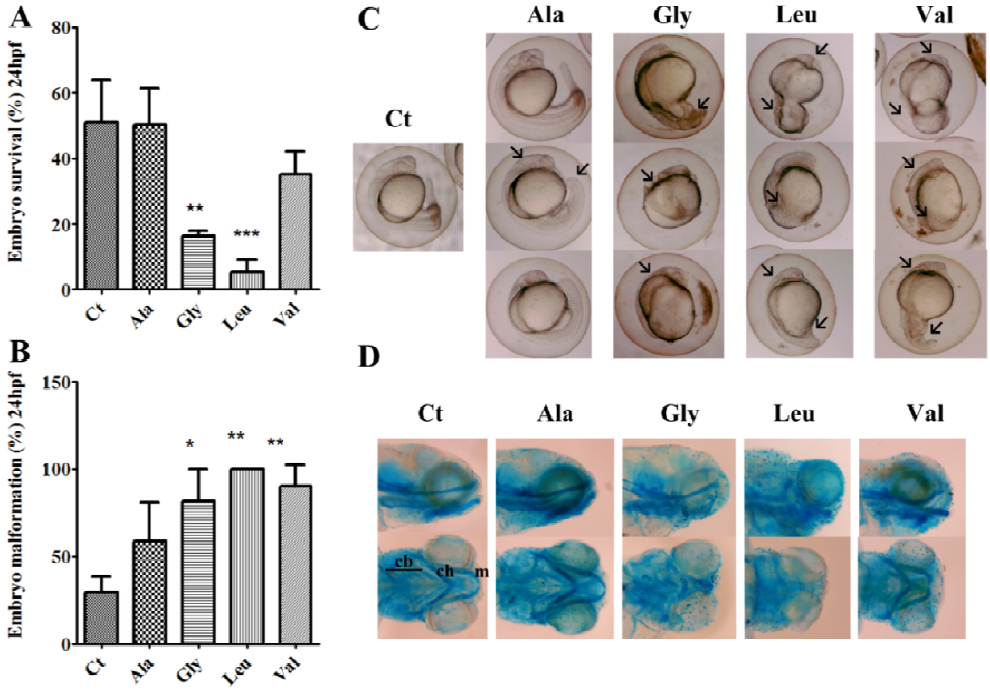

Figure 3.1. Impact of mRNA mistranslation on early zebrafish development.
A) Mutant tRNAs strongly decreased embryos survival at 24hpf. Errors bars represent the standard deviation of three independent experiments. (Student's unpaired t-test, **p<0.05, ***p<0.0001) **B**) Mutant tRNAs have a strong effect on embryo development and cause morphological alterations. This graph illustrates the percentage of embryos displaying morphological alterations Data are presented as the mean ± SD (n =3) (Student's unpaired t-test against control sample, *p<0.05, **p<0.01). **C**) Morphological alterations caused by mutant tRNAs. Control embryos (microinjected with endogenous serine tRNA) show normal development. Embryos expressing the mutant misreading tRNAs show various morphological alterations, namely: longitudinal symmetry loss, undeveloped head and spinal region, and also developmental arrest (data not shown). **D**) mRNA mistranslation leads to craniofacial defects in developing zebrafish. Representative lateral and ventral views of 5dpf stained larvae show craniofacial abnormalities, particularly malformations of the cartilages of the jaw and branchial arches. m, Meckel's cartilage; ch, ceratohyal cartilage; cb 1-5, ceratobranchial cartilage arches 1-5.

As discussed in chapter 2, our proteotoxic stress system leads to the accumulation of reactive oxygen species (ROS) and oxidative stress mediates the impact of mRNA mistranslation at the cellular level. This prompted us to investigate the effect of oxidative stress in embryo development, for this we incubated the mistranslating

embryo with ROS scavengers. Interestingly, ROS scavengers were able to ameliorate the effects of mRNA mistranslation, improving embryo survival especially in the case of embryos expressing the Ser-$tRNA_{CAG}^{Leu}$ up to 16% with Ascorbic acid (500µM), up to 18% with Gluthatione (100µM) and up to 42% with D-methionine (20µM) (Figure 3.2A) and reducing the number of embryos with developmental alterations (Figure 3.2B, Supplementary Figures 1-3).

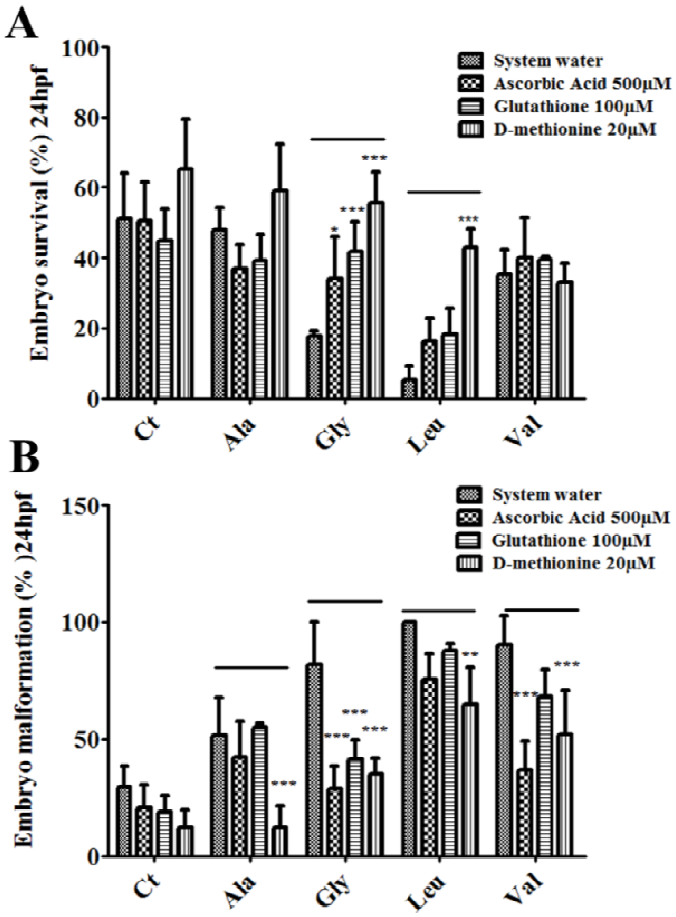

Figure 3.2. ROS scavengers ameliorate mistranslation effects on zebrafish survival and developmental phenotypes.
Zebrafish embryos were incubated in three different ROS scavengers, namely Ascorbic acid (500µM), Glutathione (100µM) and Methionine (20µM). **A)** Scavengers rescued mutant embryo survival. Errors bars represent the standard deviation of five independent experiments. (Data statistical analysis two-way ANOVA was performed followed by a Bonferroni post-test with CI 95% relative to Ct; ***p<0.001, *p<0.05). **B)** Scavengers decreased the number of embryos with mistranslation phenotypes. Error bars represent the standard deviation of five independent experiments. (Data statistical analysis two-way ANOVA was performed followed by a Bonferroni post-test with CI 95% relative to Ct; ***p<0.001, **p<0.01).

3.4.2. MiRNA expression in response to mRNA mistranslation

Analysis of miRNA microarray profiling data showed that proteotoxic stress coordinately deregulated miRNAs in 24hfp zebrafish embryos (Figure 3.3A). After the application of a 1.5 fold change cut off we determined that the expression of the Ser-tRNA$_{CGC}^{Ala}$ deregulated 17 miRNAs, the Ser-tRNA$_{UCC}^{Gly}$ deregulated 10 miRNAs, the Ser-tRNA$_{CAC}^{Val}$ deregulated 21 miRNAs and finally the expression of the Ser-tRNA$_{CAG}^{Leu}$ induced the deregulation of 12 miRNAs (Figure 3.3B, Supplementary Table 2). Several miRNAs were common to the different mRNA mistranslation conditions (Figure 3.3C, D). In the group of upregulated miRNAs the miR-145, which is involved in the regulation of cell proliferation, differentiation and apoptosis [21, 45-48], was deregulated in the four mutants. MiR-2195 and miR-15a* were induced by both the Ser-tRNA$_{CAC}^{Val}$ and the Ser-tRNA$_{CAG}^{Leu}$. MiR-150, a regulator of cellular proliferation [49], was induced by the tRNAs that misincorporate at alanine, glycine and leucine codons. MiR-130c, miR-155, miR-1388 and miR-153a were induced by both Ser-tRNA$_{CGC}^{Ala}$ and Ser-tRNA$_{CAC}^{Val}$. MiR-196a was upregulated by the Ser-tRNA$_{UCC}^{Gly}$ and Ser-tRNA$_{CGC}^{Ala}$; and finally miR-30c was induced by both Ser-tRNA$_{UCC}^{Gly}$ and Ser-tRNA$_{CAC}^{Val}$. There were also miRNAs deregulated in one mRNA mistranslation condition only (Supplementary Table 2). For instance, the mutant Ser-tRNA$_{CGC}^{Ala}$ upregulated miR-144, miR-152, miR-190b, miR-26a and miR-457b. The mutant Ser-tRNA$_{UCC}^{Gly}$ upregulated let-7h, miR-10b, miR-135b, miR-18b and miR-365. The mutant Ser-tRNA$_{CAC}^{Val}$ upregulated miR-101b, miR-133c, miR-190, miR-200b, miR-206, miR-301b and miR-726. Finally, the mutant Ser-tRNA$_{CAG}^{Leu}$ induced the expression of miR-222b, miR-27a and miR-454b. To a smaller extent, proteotoxic stress also repressed several miRNAs (Figure 3.3D). MiR-27c was repressed by the Ser-tRNA$_{UCC}^{Gly}$, the Ser-tRNA$_{CAC}^{Val}$ and the Ser-tRNA$_{CAG}^{Leu}$. MiR-17a* was

downregulated by Ser-tRNA$_{CGC}^{Ala}$, Ser-tRNA$_{CAC}^{Val}$ and Ser-tRNA$_{CAG}^{Leu}$. The Ser-tRNA$_{CGC}^{Ala}$ and the Ser-tRNA$_{CAG}^{Leu}$ decreased expression of the miR-27b, a regulator of angiogenesis [50]. Again, there were also unique profiles of silenced miRNAs (Supplementary Table 2), for example, the mutant Ser-tRNA$_{CGC}^{Ala}$ repressed miR-203b and let-7g. In the case of the mutant Ser-tRNA$_{CAC}^{Val}$, miR-10b, miR-16b, miR-261b and miR-732 were downregulated. Finally, the mutant Ser-tRNA$_{CAG}^{Leu}$ repressed miR-16c and miR-1. MiR-1 is involved is embryonic muscle development in zebrafish and can also play a role in angiogenesis [15, 51]. We confirmed miRNA deregulation by qPCR (Figure 3.4) for the embryos expressing the mutant Ser-tRNA$_{CAG}^{Leu}$. Expression levels of miR-145, miR-1 and miR-27c measured by qPCR were coincident with the microarray data, namely miR-1 and miR-27c were downregulated and miR-145 was upregulated, although for this miRNA the upregulation was less extensive than that detected using the microarrays.

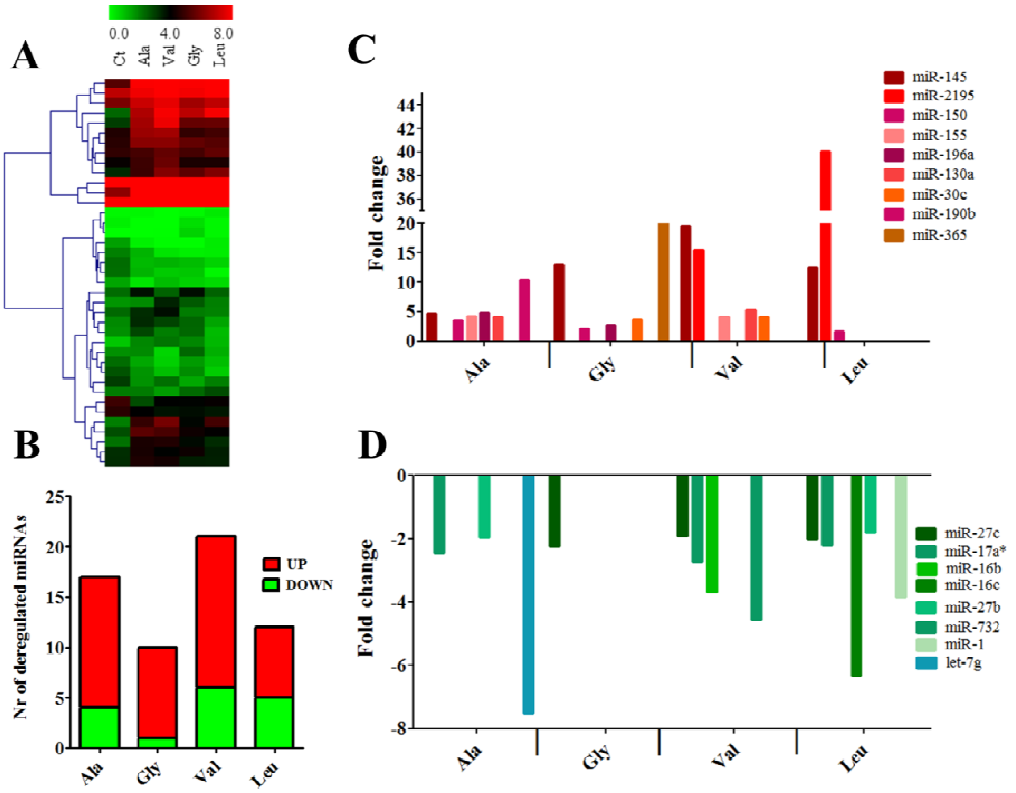

Figure 3.3. MiRNAs deregulated by proteotoxic stress.

A) Hierarchical clustering of globally deregulated miRNAs retrived through the application of a Student´s t-test $p<0.05$. Replicate intensities (log2 scale) were averaged for each condition **B**) Number of deregulated miRNAs by the four proteotoxic stress conditions tested after the application of a 1.5 expression cut off. The deregulated miRNAs are mainly upregulated by the misreading tRNAs. **C**) MiRNAs whose expression was highly induced and shared between several proteotoxic stress conditions studied. **D)** MiRNAs that were downregulated in all proteotoxic stress conditions tested.

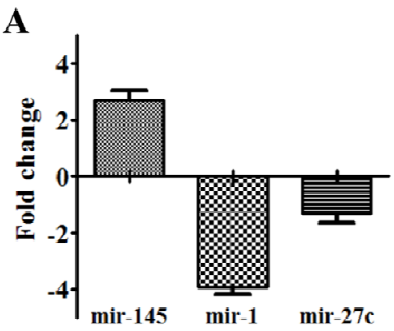

B

	Mir-145	Mir-1	Mir-27c
microarray	12.6	-3.8	-2
qPCR	2.7	-3.9	-1.3

Figure 3.4. qPCR validation of miRNA microarrays.

A) We used qPCR to confirm miRNA deregulation in the embryos expressing the mutant Ser-$tRNA_{CAG}^{Leu}$. **B)** MiRNA microarrays were validated by qPCR, even though qPCR results show less extensive upregulation of mir-145 and confirm downregulation of mir-1 and mir-27c. qPCR results were analyzing using the REST-MCS tool using small RNA (RNU6B) as the internal control.

3.4.3. Target Prediction for miRNAs deregulated by proteotoxic stress

Knowing that miRNAs regulate gene expression at the post transcriptional level and that their expression is sensitive to developmental stage and tissue type; we assessed the biological meaning of miRNA deregulation induced by proteotoxic stress. For this, we have performed miRNA target prediction. Potential targets were predicted using the Eimmo, Miranda and TargetScan Fish algorithms. Putative targets were considered only when they were identified by at least two of these databases. Proteotoxic stress deregulated the expression of 27 miRNAs. The most representative induced miRNAs were miR-2195, which was deregulated by both Ser-$tRNA_{CAC}^{Val}$ and Ser-$tRNA_{CAG}^{Leu}$, and miR-145, whose expression was altered by four mutant tRNAs; miR-365 was most upregulated by Ser-$tRNA_{UCC}^{Gly}$ and miR-190b showed high expression level in the Ser-$tRNA_{CGC}^{Ala}$ embryos. Putative targets of miR-190b (Supplementary Table 3) such as *mad1l1* and *sept2* are involved in cell cycle, *fezf1*, *pou4f3*, and *mef2a* are involved in regulation of transcription and patterning, such as *gli1*, which is a regulator of Hedgehog signaling [52-54]. The predicted targets for miR-365 (Supplementary Table 4) were mainly related to protein handling processes, cell morphogenesis, transcription and embryo development, namely *fzd8a*, a Wnt signaling element [55]; *neurod4*, *igf2a*, *igf2b* and *robo3a*, which are regulators of nervous system development [56, 57]; *numbl* that regulates left/right symmetry establishment [58], and *smo* an important factor in Hedgehog signaling [59]. The expression pattern of miR-2195 and miR-145 suggests that they represent a generalized inductive response to proteotoxic stress. Putative target analysis for these miRNAs (Table 3.1, Table 3.2) shows that the main processes where they are involved are transcription, cellular and development processes, and angiogenesis. Interestingly, *furina* which is involved in craniofacial development [60], the transcriptional factor *foxc1* that participates in vessel

morphogenesis and somitogenesis [61, 62] and *nlk1* and *nlk2*, Wnt co-activators, are putative targets for miR-2195 (Table 3.1). As for miR-145, possible targets (Table 3.2) were notch component *dll4*, which is related to angiogenesis [63], *unc5b* that participates in axon guidance processes [64] and *plxna4* a regulator of embryonic brain development [65]. Finally, the *rbpja*, a co-activator of notch signaling target hairy and Enhancer of split genes, was retrieved as a miR-145 potential target [66].

Table 3.1. Putative targets of miR-2195.
miRNA targets were identified with the Eimmo (MirZ), miRBASE Targets and TargetScan Fish databases. The computational targets were considered when they were retrieved from at least two of the algorithms. GO terms were identified using DAVID database and manually curated to remove redundant terms.

miR-2195	
Target	**GO Term – Biological Process**
celsr3, itgb1b.1	Cell adhesion
sept6, sesn3, chek1	Cell cycle
dvl2	Cell migration, embryonic morphogenesis
olfm1b	Cell morphogenesis, neuron differentiation,
cxcr3.1, oprd1a	Cell surface receptor linked signal transduction
hdac9b	Chromatin organization, transcription
ogdh	Citrate cycle (TCA cycle), Lysine degradation, Tryptophan metabolism,
zgc:162576	Cytoskeleton organization
ppm1e	Dephosphorylation
pik3r2	Erbb signaling pathway, mtor signaling pathway, Apoptosis, VEGF signaling pathway
sc5dl	Fatty acid metabolic process, oxidation reduction
fads2	Generation of precursor metabolites and energy oxidation reduction
cnih2, net1	Intracellular signaling cascade
dot1l	Lysine degradation
cacna1ab	MAPK signaling pathway, Calcium signaling pathway,
dhrs13	Oxidation reduction
st6gal1	Protein amino acid glycosylation
adrm1b	Protein complex assembly
tgfbr1a, nlk1, nlk2	Protein modification process, phosphorylation
ube2e3	Proteolysis
otud5a	RIG-I-like receptor signaling pathway
nxf1	RNA localization
furina	Skeletal system development, proteolysis, cartilage development
foxc1a	Somitogenesis , regulation of transcription
si:dkeyp-27e10.3, atf7b, mta3, runx2a, crsp7, rxrba, srebf1, nr3c2	Transcription, regulation of transcription
stxbp5a	Vesicle-mediated transport

Table 3.2. Putative targets of miR-145.
miRNA targets were identified with the Eimmo (MirZ), miRBASE Targets and TargetScan Fish databases. The computational targets were considered when they were retrieved from at least two of the algorithms. GO terms were identified using DAVID database and manually curated to remove redundant terms.

miR-145	
Target	**GO Term –Biological Process**
snx14	Cell communication
dll4, unc5b, hspa12b, fli1a, rbpja	Angiogenesis
loc554469	Cell cycle, regulation of transcription
plxna4, sema3aa, tfap2a	Cell morphogenesis, nervous system development
cib2, zgc:158263	Cell surface receptor linked signal transduction
atoh7, sox2, pax6b	Eye development, transcription, multicellular organismal development
hs3st1	Heparan sulfate biosynthesis
tlr3	Immune system process, Toll-like receptor signaling pathway
slc30a7	Ion transport
cd63	Lysosome
zgc:114200	Metabolic process, gene expression, Notch signaling pathway
pgd, cyp1a, mtmr6, lpl, chka, psat1, gys2, st6galnac5, hmgcra	Metabolism
eef2k	Mitotic cell cycle, mitotic spindle organization
clptm1, spata18, skib, fgf24, msxd, dmd	Multicellular organismal development, cell differentiation
pnrc2	Nuclear-transcribed mrna catabolic process, nonsense-mediated decay, transcription,
sod1	Oxygen and reactive oxygen species metabolic process
zic2a	Pattern specification process, nervous system development , Hedgehog signaling pathway
si:dkey-121j17.5, src, grk1a	Phosphorylation, protein modification process
ptk2.1	Protein complex assembly, erbb signaling pathway, VEGF signaling pathway, Regulation of actin cytoskeleton
calrl2	Protein folding, protein metabolic process
ptp4a1, opn1lw2	Protein modification process, dephosphorylation
mbtps1, cul1b, ube4b, pias2	Proteolysis
sppl3	Regulation of apoptosis
carhsp1, irx6a, mta2, pou2f1b, si:dkey-109n11.1, gata6, med25, nr2f1a, sox19a	Transcription, regulation of transcription
mknk2b	Regulation of translation, response to stress, MAPK signaling pathway
apex1	Response to DNA damage stimulus, regulation of apoptosis, Base excision repair
xrn2	RNA degradation
hnrpl, utp15	RNA processing
rhpn2, arrb1	Signal transduction
vcanb	Skeletal system development, ossification, multicellular organismal development,
mrrf	Translation
ergic3, rh50, ttpa, apoeb, chrne	Transport
slc25a14	Transport, mitochondrial transport
aars	Trna metabolic process, Aminoacyl-trna biosynthesis
wnt10a	Wnt receptor signaling pathway, calcium modulating pathway, Hedgehog signaling pathway

Proteotoxic stress repressed the expression of 11 miRNAs from which miR-27c and miR1-17* were coordinately deregulated by several mutant tRNAs; let-7g, miR-732, miR-1 and miR-16b were the miRNAs most represed by the Ser-$tRNA_{CGC}^{Ala}$, Ser-$tRNA_{CAC}^{Val}$ and Ser-$tRNA_{CAG}^{Leu}$, respectively. The predicted targets for miR-27c are related to cell cycle and cellular processes, development and patterning, transcription and apoptosis (Table 3.3). For instance, the apoptosis related putative targets were *apaf1*, *fas*, *bad*, *dffb*, and *bcl2*. the notch signaling factor *axin1* was also a putative target of miR-27c. Putative targets for miR-17a* were not considered here since they were retrieved by one algorithm only. In the case of let-7g, which was the most repressed miRNA in Ser-$tRNA_{CGC}^{Ala}$ embryos, the predicted preferential targets were essentially related to apoptosis, embryo and cell morphogenesis, development and transcription (Supplementary Table 5). The development related targets genes were *nrarpa* that articulates Notch and Wnt signaling during angiogenesis [67] and *pbx2* which is essential for hindbrain patterning [68]. The putative targets of miR-732 (Supplementary Table 6), miR-16c (Supplementary Table 7) and miR-1 (Supplementary Table 8) were also related to embryo and cell morphogenesis, development and transcription. *bad* was again targeted, by miR-732, as were notch receptors *fzd3* and *fzd4*, hedgehog factor *smo* and the transcription factor *hey2* that are activated by Notch signaling. Furthermore, *nrarpa*, *psen2*, *dla*, *dld* were retrieved as miR-16c putative targets. These genes are regulators of Notch signaling and are involved in angiogenesis and neurogenesis [69, 70]. Our target prediction for the miR-1 retrieved the previously validated targets *arpc4l*, *pfn2l* and *copz1* mainly involved in actin binding and vesicular transport [15] and several genes involved in embryo segmentation and patterning, namely *igf2b*, *igf2a*, *her7*, *bmpr2a* [71-73].

Table 3.3. Putative targets of mir 27c.

miRNA targets were identified with the Eimmo (MirZ), miRBASE Targets and TargetScan Fish databases. The computational targets were considered when they were retrieved from at least two of the algorithms. GO terms were identified using DAVID database and manually curated to remove redundant terms.

miR-27c	
Target	**GO Term –Biological Process**
tbx16, ptenb	Angiogenesis
apaf1, faz, bad, dffb, traf4b, bcl2	Apoptosis
tpm1	Cardiac muscle contraction
cdh11, cd36	Cell adhesion
mlh1, sesn2, cth1	Cell cycle
b4galt1	Cell motion
zgc:152951	Cell redox homeostasis
mc4r, gpr98	Cell surface receptor linked signal transduction
setd1ba	Chromatin organization
snap25a	Cytokinesis, cell division
nfia, kbtbd5, dnase1l3l,	DNA metabolic process
disc1	Embryonic morphogenesis
col2a1a, eya1	Embryonic organ development
rdh5, atoh7, ctbp2, prkci	Eye development
cx43	Heart development , embryonic organ development
dvl2	Hindbrain development , Wnt signaling pathway, Notch signaling pathway
il22, zgc:136614, si:ch211-234p6.13	Immune response
arl3l2, arl5a	Intracellular signaling cascade
nup50	Intracellular transport
abcc9, cacng2a, trpc6, slc34a2a, slc25a28	Ion transport
xdh, aanat1, pdss1, amt, psat1, sult1st3, nt5e, pla2g6, c1galt1c1, atic, atp13a	Metabolism
lhb	Neuroactive ligand-receptor interaction, gnrh signaling pathway
acadvl	Oxidation reduction
cygb2	Oxygen transport
sox4b	Pancreas development
bmpr2a, aldh1a2, eng2a, bmpr1aa, bmpr1ab	Pattern specification process
prkcq, stk35, prkg1a, stk33, pdpk1b, axin1, ephb4a	Phosphorylation
fabp2	PPAR signaling pathway
st3gal2l, st3gal5l, gyltl1b	Protein amino acid glycosylation
tuba7l, zgc:153426	Protein complex assembly
cct7, hsp90b1	Protein folding
malt1, usp2a, ubr5	Proteolysis
zgc:63523	Regulation of cell shape
bms1l	Ribosome biogenesis
ddx3	RIG-I-like receptor signaling pathway
qk, rbm39b, dus1l, nxf1	RNA processing
crsp7, vsx1, hoxc13a, pou3f3b, bhlhe40, hoxc11a, nr1i2, rfx2, rybpb, thrap6, nkx6.1, ef1, nkx1.2la, dbx2, foxd1, pknox2, sfmbt2, per3, tbpl2, isl1	Transcription , regulation of transcription
qrsl1, si:ch211-216l23.2, rps15a, mknk2b	Translation
oat	Transmembrane transport

3.4.4. Transcriptional profiles of zebrafish embryos

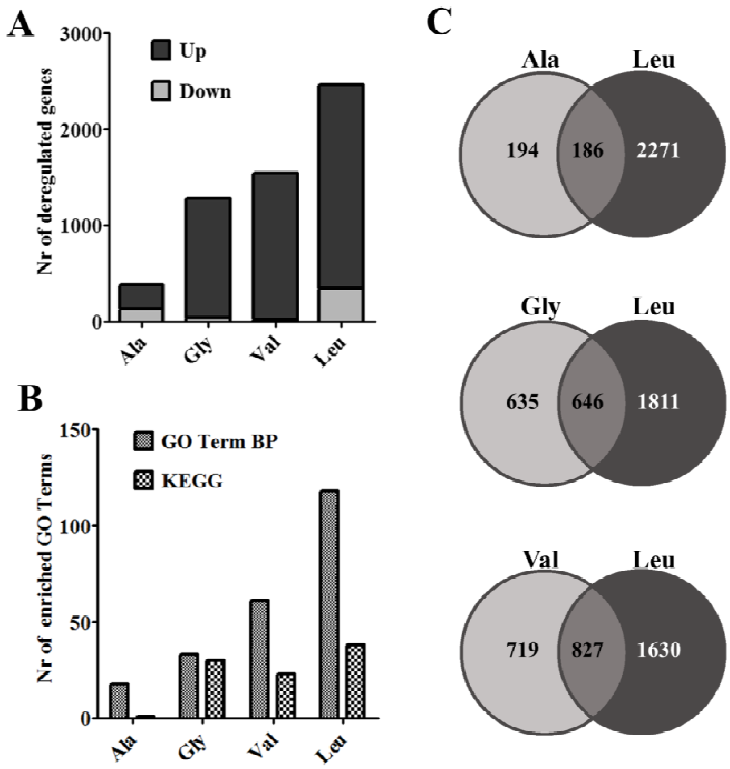

Figure 3.5. Mistranslation strongly deregulates gene expression.
A) Total number of deregulated genes show a marked tendency towards gene up regulation. (Student´s t-test $p<0.05$; only known probes with fold change values lower than -1.5 or higher than 1.5 in each mistranslation condition are present in the dataset) **B)** GO term enrichment analysis for Biological Processes and KEGG pathways was done with Gene Codis 2.0. (Hypergeometric test, only known probes with fold change values lower than -1.5 or higher than 1.5 in each mistranslation condition are present in the dataset). **C)** Shared genes between mistranslation mutants. Common genes represent 50% of the alanine and glycine gene set and valine shows 53% of common genes. Comparisons were made against the leucine mutant, the most toxic mistranslation mutant.

Transcriptional responses to mRNA mistranslation were analysed through mRNA profiling of the embryos expressing Ser-tRNA$_{CGC}^{Ala}$, Ser-tRNA$_{UCC}^{Gly}$, Ser-tRNA$_{CAC}^{Val}$ and Ser-tRNA$_{CAG}^{Leu}$ mutants. Results were obtained through the application of a t-test with p value<0.05 and a 1.5 cutoff. This analysis shows that mRNA mistranslation has a big impact on gene expression patterns. The overall response to codon mistranslation is gene expression up regulation (Figure 3.5A) and interestingly the number of deregulated genes

correlates with the amino exchange toxicity, for example the Ser-$tRNA_{CAG}^{Leu}$ mutant can be considered the most toxic of our mutants and this was the case that produced the highest numbers of deregulated genes. Accordingly, this mutant also has the highest number of enriched GO BP and KEGG terms (Figure 3.5B). A common response was observed in the different mistranslation situations. Indeed, the embryos expressing the Ser-$tRNA_{CGC}^{Ala}$, Ser-$tRNA_{UCC}^{Gly}$, and the Ser-$tRNA_{CAC}^{Val}$ shared 50, 50 and 53% of the deregulated genes with the embryos expressing the Ser-$tRNA_{CAG}^{Leu}$, respectively (Figure 3.5C).

Interestingly, a gene enrichment analysis (GO term biological processes) of the main deregulated clusters (Figure 3.6) showed down regulation of transport, oxidation-reduction processes, regulation of transcription and cytoskeleton organization. For the highest levels of gene expression up-regulation were observed for regulation of transcription, DNA-dependent and oxidation-reduction processes and also proteolysis, apoptotic processes, dorsal/ventral pattern formation, phosphorylation, response to stress, anterior/posterior pattern specification and somitogenesis.

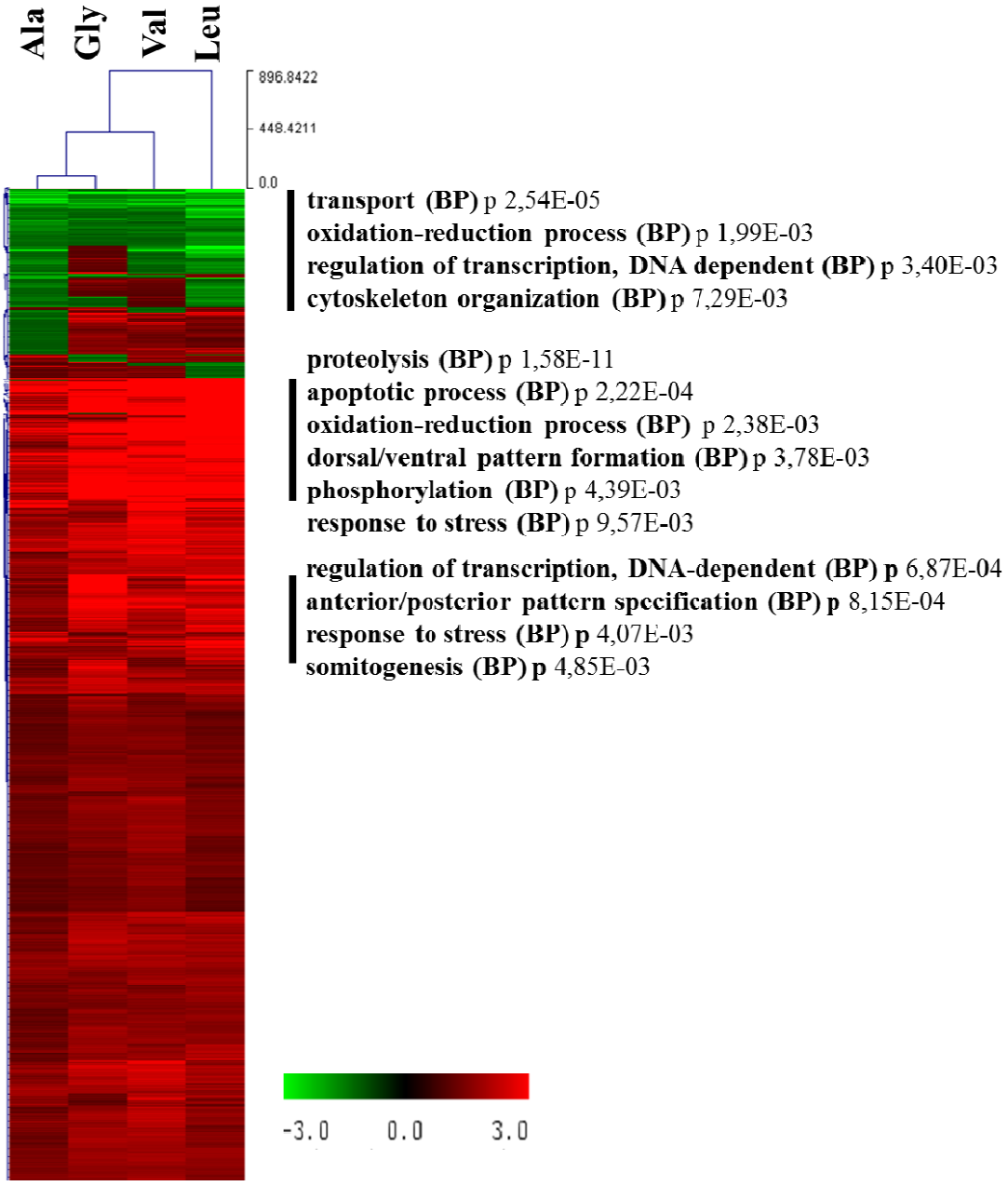

Figure 3.6. Global transcriptional signature of mistranslation in zebrafish embryos.
Global gene expression profiling was done by clustering individual globally deregulated gene sets. Cluster analysis was carried out with MEV software (TM4 Microarray Software Suite). Expression values are normalized Log2 fold change values.

In order to obtain a general and more representative overview of gene expression deregulation by mistranslation we carried out individual enrichment analysis of globally deregulated genes. A GO term (biological process - BP) enrichment analysis of all deregulated genes showed that mRNA mistranslation deregulates a wide variety of cellular and developmental processes (Table 3.4). At the cellular level, enriched BP terms were mainly regulation of transcription, phosphorylation, oxidation-reduction process, response to stress, cell differentiation, apoptosis and cell adhesion. In addition, development related terms, namely somitogenesis, determination of left/right symmetry, cartilage development, pattern specification process and heart morphogenesis were also enriched. After the application of a 1.5 fold cut off of the gene expression data we performed a similar analysis for KEGG terms and obtained enrichment of protein processing in the endoplasmic reticulum, Wnt signaling pathway, Hedgehog signaling pathway, VEGF signaling pathway, apoptosis, and also various metabolism related pathways (Table 3.5).

Table 3.4. General overview of enriched GO terms for mistranslation conditions.
Individual globally deregulated gene sets were analyzed with GeneCodis 3.0 using a hypergeometric test. Selected GO terms have a p value lower than 10^{-3} and redundant terms were removed manually.

GO Term BP	Genes in term	Ala genes	P value	Gly genes	P value	Val genes	P value	Leu genes	P value
regulation of transcription, DNA-dependent	913	3E-04	24	2E-11	62	3E-35	145	3E-35	145
multicellular organismal development	437	4E-02	10	9E-04	26	9E-20	75	9E-20	75
transport	625	3E-03	17	4E-06	39	3E-19	91	3E-19	91
phosphorylation	431	5E-02	9	9E-04	26	3E-13	63	3E-13	63
proteolysis	319	3E-03	12	5E-14	38	9E-13	52	9E-13	52
oxidation-reduction process	456			3E-16	49	1E-11	62	1E-11	62
somitogenesis	66					2E-10	21	2E-10	21
carbohydrate metabolic process	94	3E-02	4	8E-09	17	8E-10	24	8E-10	24
determination of left/right symmetry	72					8E-09	20	8E-09	20
response to chemical stimulus	61			1E-02	7	2E-08	18	2E-08	18
protein phosphorylation	383					7E-08	48	7E-08	48
lipid metabolic process	76			2E-05	12	1E-07	19	1E-07	19
small GTPase mediated signal transduction	170	4E-03	8	7E-03	13	6E-07	28	6E-07	28
transmembrane transport	264					8E-07	36	8E-07	36
response to stress	53					9E-07	15	9E-07	15
cell differentiation	109	3E-02	5			2E-06	21	2E-06	21
melanocyte differentiation	19					4E-06	9	4E-06	9
cartilage development	60			3E-03	8	3E-05	14	3E-05	14
positive regulation of apoptotic process	30	4E-03	4			3E-05	10	3E-05	10
embryonic heart tube development	38					4E-05	11	4E-05	11
dorsal/ventral pattern formation	71					4E-05	15	4E-05	15
anterior/posterior pattern specification	55					5E-05	13	5E-05	13
ion transport	193	2E-02	7	5E-02	11	6E-05	26	6E-05	26
regulation of sequence-specific DNA binding transcription factor activity	41			1E-02	6	8E-05	11	8E-05	11
mesoderm development	15					9E-05	7	9E-05	7
apoptotic process	61			1E-02	7	2E-04	13	2E-04	13
cell adhesion	171			3E-02	11	6E-04	22	6E-04	22
sympathetic nervous system development	5			4E-02	2	6E-04	4	6E-04	4
pattern specification process	35			9E-04	7	7E-04	9	7E-04	9
heart morphogenesis	28			4E-02	4	8E-04	8	8E-04	8

Table 3.5. General overview of enriched KEGG pathways for mistranslation conditions. Individual globally deregulated gene sets were analyzed with GeneCodis 2.0 using a hypergeometric test. KEGG pathways were selected for p values lower than 10-4 or if they were present in at least two conditions. Redundant terms were removed manually. Pathway enrichment was done using the database GeneCodis 2.0 using a hypergeometric test.

KEGG	Genes in term	Ala genes	P value	Gly genes	P value	Val genes	P value	Leu genes	P value
Regulation of actin cytoskeleton	209			15	3E-04	12	3E-02	30	5E-08
Focal adhesion	194			12	4E-03	14	8E-03	25	3E-06
Fructose and mannose metabolism	44			4	4E-02			12	3E-06
Insulin signaling pathway	142			10	4E-03			21	4E-06
Amino sugar and nucleotide sugar metabolism	49			9	2E-05			12	5E-06
Tight junction	140			8	3E-02	11	1E-02	20	7E-06
Protein processing in endoplasmic reticulum	157					21	4E-08	21	9E-06
Lysosome	121			17	3E-08	13	4E-04	18	1E-05
Wnt signaling pathway	162					11	2E-02	21	1E-05
Pentose phosphate pathway	31			7	4E-05		3E-02	9	2E-05
Hedgehog signaling pathway	62							12	3E-05
Glycolysis / Gluconeogenesis	64			10	1E-05			12	4E-05
ECM-receptor interaction	59							11	1E-04
Starch and sucrose metabolism	35							8	4E-04
Adherens junction	82					7	2E-02	12	5E-04
Phagosome	125			9	5E-03			15	6E-04
TGF-beta signaling pathway	86			6	3E-02	8	1E-02	12	7E-04
Sphingolipid metabolism	48			7	5E-04			8	3E-03
VEGF signaling pathway	75					7	2E-02	10	3E-03
Drug metabolism - cytochrome P450	29			4	1E-02			6	4E-03
Nitrogen metabolism	20					4	1E-02	5	4E-03
Alanine, aspartate and glutamate metabolism	35			8	2E-05	6	5E-03	6	9E-03
Arginine and proline metabolism	64			10	1E-05	6	3E-02	8	1E-02
Phosphatidylinositol signaling system	66					6	3E-02	8	1E-02
Purine metabolism	158			11	3E-03			13	3E-02
PPAR signaling pathway	61			6	7E-03			7	3E-02
Apoptosis	85					8	1E-02	8	5E-02
Valine, leucine and isoleucine degradation	46			8	5E-05	5	3E-02		
Pyruvate metabolism	37			6	9E-04				
Endocytosis	225	7	4E-03	12	9E-03	14	1E-02		
p53 signaling pathway	61					10	1E-04		

With this reduced dataset we repeated the BP terms enrichment in order to obtain an overview of the more severe gene expression deregulation by mRNA mistranslation conditions. Focusing on development related terms (Figure 3.7. Development related BP terms enrichment analysis., Supplementary Tables 9-12). The enrichment analysis showed that mRNA mistranslation generated proteotoxic stress, deregulated several developmental

signaling pathways and also specific organ developmental processes. Signaling pathways such as Wnt and Notch were enriched and also organogenesis related terms such as cartilage development, heart formation, central nervous system development, and muscle organ development were also enriched. Analysis of the enriched GO terms related to cellular processes in response to proteotoxic stress showed that proteome dysfunction has deep impact in signaling pathways pivotal to embryo development and in embryo shaping processes, such as apoptosis (Supplementary Tables 13-16).

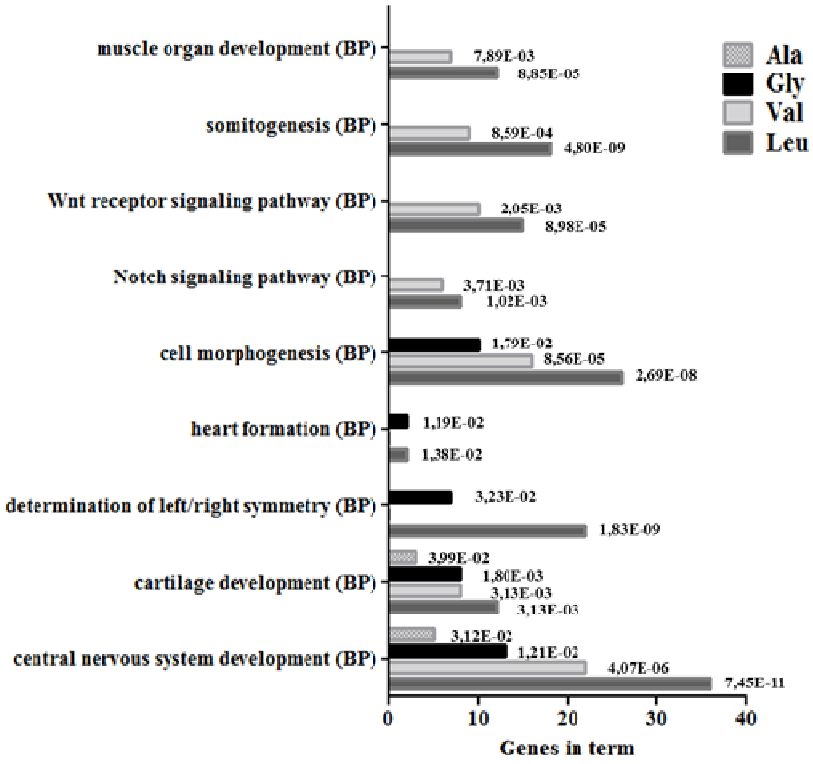

Figure 3.7. Development related BP terms enrichment analysis.
Representation of selected enriched GO Terms shows a transversal enrichment for pathways such as Wnt and Notch signaling and also processes related to organ development. Pathway enrichment was done using the database GeneCodis 2.0 using a hypergeometric

3.4.5. Deregulation of apoptotic genes by proteotoxic stress

A large set of apoptosis genes was deregulated at the gene expression level by proteotoxic stress (Figure 3.8A, supplementary Table 17). Components of the extrinsic

apoptotic pathway, namely *tnfrsfa*, *tnfsf10l*, *fas* and *casp8* were upregulated [74]. *tnfrsfa* and *fas* are death receptors and both were induced in embryos expressing the Ser-$tRNA_{CAG}^{Leu}$ by 2 and 4 fold, respectively. *tnfrsfa* was induced 2 fold in embryos expressing the Ser-$tRNA_{CGC}^{Ala}$ and *fas* was induced 3.2 fold by the expression of Ser-$tRNA_{CAC}^{Val}$. The death ligand *tnfsf10l* was upregulated 4 and 3.5 fold in embryos expressing the Ser-$tRNA_{UCC}^{Gly}$ and Ser-$tRNA_{CAG}^{Leu}$, respectively. *casp8* was induced 2.4 and 2.6 fold in embryos expressing the Ser-$tRNA_{CGC}^{Ala}$ and the Ser-$tRNA_{CAC}^{Val}$. The extrinsic apoptosis pathway is an important regulator of the immune system, at least in mammals. However, this pathway is activated under liver damage by ethanol toxicity and neuropathological processes, and is also involved in the establishment of hematopoietic cell lineages [75, 76]. Bcl-2 family members are major regulators of apoptosis and several of these factors were upregulated by proteotoxic stress, namely *bcl2l*, *bbc3*, *bad*, *baxa*, *bnip3l*, *bmf1*, *boka*, other apoptosis related genes, such as *xiap*, *bag3*, *tp53*, *tp63*, *zgc:158776/diablo*, *perp*, *mdm2* [75] were also deregulated. The pro-survival *bcl2l* was upregulated 2 and 2.8 fold by Ser-$tRNA_{CAC}^{Val}$ and Ser-$tRNA_{CAG}^{Leu}$. The pro-apoptotic *bbc3* was induced 2.9 fold by Ser-$tRNA_{CAG}^{Leu}$, and pro-apoptptic *bad* and 2.2 and 2 fold induced by Ser-$tRNA_{CAC}^{Val}$ and Ser-$tRNA_{CAG}^{Leu}$. *baxa* was induced in the embryos expressing the Ser-$tRNA_{CGC}^{Ala}$, the Ser-$tRNA_{CAC}^{Val}$ and the Ser-$tRNA_{CAG}^{Leu}$ by 1.2, 1.8 and 1.8 fold, respectively

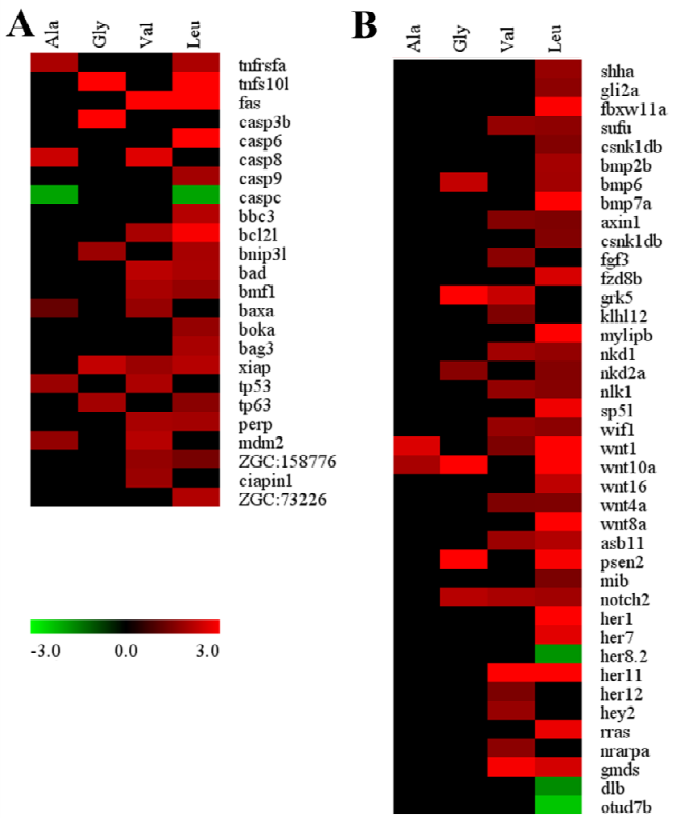

Figure 3.8. Mistranslation has a strong impact on gene expression.
Functional enrichment analysis of genes deregulated in mistranslation conditions showing that the enriched GO Terms have a transversal enrichment for pathways such as apoptosis, Wnt and Notch signaling. **A)** Cluster representation of apoptosis related genes deregulated in mistranslation conditions shows that these genes are mainly upregulated. Gene expression values are normalized Log_2 fold change values. **B)** Cluster representation of Hedgehog, Wnt and Notch signaling shows that components of these pathways are mainly upregulated in all mistranslation conditions studied. Gene expression values are normalized Log_2 fold change values.

Bbc3 and Bad transmit the apoptotic stimuli through their interaction with Baxa which mediates mitochondrial outer membrane permeabilization with subsequent cytochrome c release [77]. ZGC:158776/DIABLO is a mitochondrial proapototic protein that is released with cytochrome c in response to apoptotic stimuli that promotes effector caspase activation [78]. This factor was induced 1.7 and 1.4 fold in embryos expressing the Ser-$tRNA_{CAC}^{Val}$ and Ser-$tRNA_{CAG}^{Leu}$, respectively. The effector caspases were differentially deregulated by proteotoxic stress, *casp3b* was induced 5 fold by the

expression of the Ser-tRNA$_{UCC}^{Gly,}$ *casp6* and 9 were 4 and 1.9 fold induced by the Ser-tRNA$_{CAG}^{Leu}$, respectively. Tp53 and Tp63, which are important regulators of the ER stress induced apoptosis [79-81], showed also deregulation. *tp53* was induced 1.8 and 2 fold in Ser-tRNA$_{CGC}^{Ala}$ and Ser-tRNA$_{CAC}^{Val}$ conditions, whereas *tp63* was 1.9 and 1.6 induced by the Ser-tRNA$_{UCC}^{Gly}$ and Ser-tRNA$_{CAG}^{Leu}$.

3.4.6. Apoptotic pathways are activated by proteotoxic stress

The apoptotic stimuli are integrated in two signaling pathways, namely the intrinsic and extrinsic and contribute to tissue homeostasis and embryo development. Therefore, the phenotypes observed in zebrafish embryos expressing the mutant Serine tRNAs and the deregulation at the gene expression level of apoptotic factors prompted us to study the activation of apoptosis in response to proteotoxic stress. For this, we performed staining of apoptotic cells with acridine orange, which revealed a sharp increase in cell death for the embryos expressing the Ser-tRNA$_{CGC}^{Ala}$ (50%), Ser-tRNA$_{UCC}^{Gly}$ (460%), Ser-tRNA$_{CAC}^{Val}$ (390%) and Ser-tRNA$_{CAG}^{Leu}$ (540%) mutants (Figure 3.9A). The pattern of apoptotic activation correlates with the results previously described in chapter two, in assays to determine the activation of stress responses; increased proteotoxic stress lead to increased apoptosis levels especially in embryos expressing Ser-tRNA$_{UCC}^{Gly}$, Ser-tRNA$_{CAC}^{Val}$ and Ser-tRNA$_{CAG}^{Leu}$. We further investigated several components of apoptotic cascades, namely the activity of caspases 8, 9, and 3-7 (Figure 3.9B-D). The data shows activation of the caspases 8, 9, and 3-7, particularly in embryos expressing Ser-tRNA$_{UCC}^{Gly}$, Ser-tRNA$_{CAC}^{Val}$ and Ser-tRNA$_{CAG}^{Leu}$. Activation levels for caspase 8 and caspases 3/7 where the highest for the Ser-tRNA$_{CAG}^{Leu}$ mutant, whereas for caspase 9, the activation levels were similar for Ser-tRNA$_{UCC}^{Gly}$, Ser-tRNA$_{CAC}^{Val}$ and Ser-tRNA$_{CAG}^{Leu}$ mutants. We determined that the

misreading tRNAs were able to trigger both the intrinsic and extrinsic apoptotic pathways since they activate effector caspases 8 and 9 belonging to these two pathways [75]. The gene expression results correlate with the apoptotic states described above, indeed gene expression up-regulation of both apoptotic pathways correlates with the caspase activation results, and also with the elevated apoptosis levels detected in zebrafish embryos expressing the mutant Serine tRNAs. Since apoptosis plays a pivotal role during embryo development and increases in apoptotic levels can lead to deficient embryogenesis, our results suggest that proteotoxic stress can interfere with developmental progression by exacerbating cell death [82].

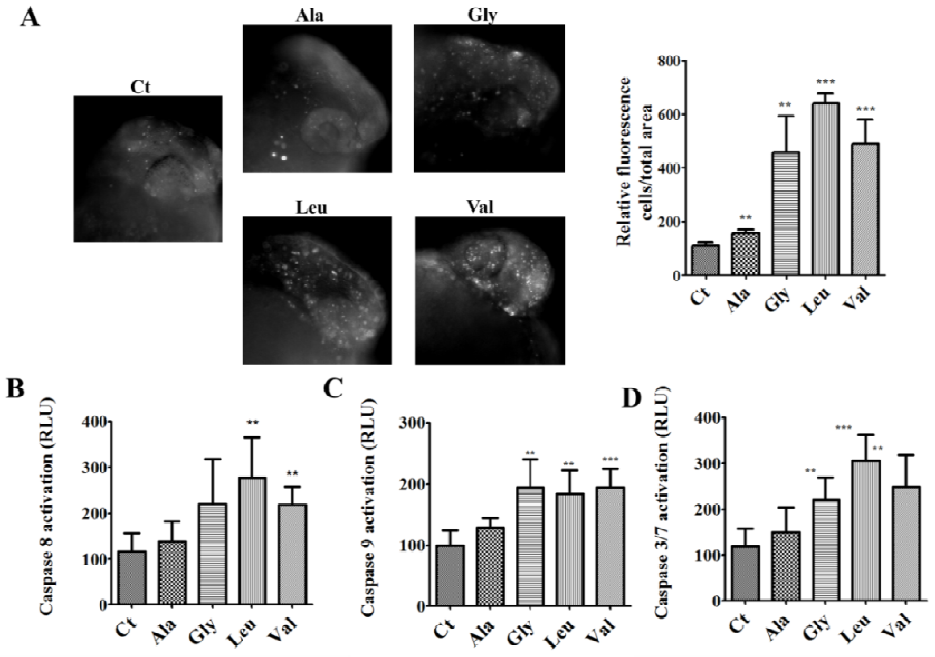

Figure 3.9. Mistranslation strongly induces apoptosis.
A) Acridine orange staining shows a strong increase in apoptosis especially in embryos expressing mutant tRNAs for glycine, leucine and valine. Embryos were imaged at 24hpf and fluorescence was analyzed with ImageJ software. Graphs depict the mean ± SD (n = 4) (Student's unpaired t-test against control sample, **p<0.05, ***p<0.001). Units are relative to control sample in percentage. **B-D)** Mistranslation activates extrinsic and intrinsic apoptotic pathways. Induction of apoptosis in embryos expressing mutant tRNAs was monitored by measuring caspase activity. Data are presented as the mean ± SD (n = 6). ((Student's unpaired t-test, Caspase 8 **p<0.005; Caspase 9 **p<0.005, ***p<0.001; Caspase 3/7 **p<0.005, ***p<0.0001). RLU – relative light units. Units are relative to control sample in percentage.

3.4.7. Proteotoxic stress deregulates genes associated with Hedgehog, Wnt and Notch signaling

Proteotoxic stress deregulated several groups of genes involved in embryo development. Components of the signaling pathways Hedgehog, Wnt and Notch (Figure 3.8B, supplementary table 18) were deregulated. Hedgehog signaling pathway was affected at various levels. Indeed, several components of this signaling pathway were upregulated by the Ser-$tRNA_{CAG}^{Leu}$. Core components, such as Hedgehog ligand *shha*, the gli transcription factor *gli2a*, and the pathway inhibitors *fbxw11a*, *csnk1db* and *sufu* were induced by 1.8, 1.7, 2.8, 1.5 and 1.7 fold, respectively. Various Wnt ligands and one of the frizzled receptors were u- regulated, namely *wnt1*, *wnt10a*, *wnt16*, *wnt4a*, *wnt8a* and *fzd8b*. However, several downstream negative regulators of this signaling pathway showed also up regulation, namely *axin1*, *klhl12*, *nkd1*, *nkd2a* and *wif1*. Axin1 integrates the complex that phosphorylates β-catenin thus inhibiting Wnt signaling, and regulates embryo axis formation [83]. This factor was induced by 1.5 fold by both Ser-$tRNA_{CAC}^{Val}$ and Ser-$tRNA_{CAG}^{Leu}$. *klhl12* was 1.5 fold induced by the Ser-$tRNA_{CAC}^{Val}$. *nkd1* was induced by the Ser-$tRNA_{CAC}^{Val}$ and Ser-$tRNA_{CAG}^{Leu}$ 1.9 and 1.7 fold respectively, in the case of *nkd2a* induction was 1.6 and 1.5 in response to the Ser-$tRNA_{UCC}^{Gly}$ and Ser-$tRNA_{CAG}^{Leu}$, respectively. These two factors reduce Wnt signaling levels by modulating β-catenin levels [84, 85]. Wif1 is a Wnt signaling antagonist since it binds Wnt proteins preventing them from interacting with their receptors [86], it showed 1.8 and 1.7 fold induction by the Ser-$tRNA_{CAC}^{Val}$ and Ser-$tRNA_{CAG}^{Leu}$, respectively. Notch signaling pathway elements were also coordinately deregulated by proteotoxic stress. The receptor *notch2* was induced 2.1, 2 and 1.9 fold by the Ser-$tRNA_{UCC}^{Gly}$, Ser-$tRNA_{CAC}^{Val}$ and Ser-$tRNA_{CAG}^{Leu}$, respectively. The canonical Notch activators *asb11*, *mib* and *psen2* [69, 87, 88] were induced as well; *asb11*was induced

1.8 and 2 fold by Ser-tRNA$_{CAC}^{Val}$ and Ser-tRNA$_{CAG}^{Leu}$, *mib* was induced 1.5 fold by the Ser-tRNA$_{CAG}^{Leu}$, and finally *psen2* was induced by Ser-tRNA$_{UCC}^{Gly}$ and Ser-tRNA$_{CAG}^{Leu}$ 3.5 and 2.9 fold, respectively. The genes *dlb* and *otud7b* were upregulated 1.6 and 3.3 fold in the Ser-tRNA$_{CAG}^{Leu}$. Not only components of this signaling pathway were induced, indeed transcriptional targets were also upregulated by proteotoxic stress; namely, *her1*, *her7*, *her11*, *her12*, *hey2*, *nrarpa* and *rras*. Most of these activated targets regulate embryonic processes such as somitogenesis, patterning and angiogenesis [66, 67, 89]. The deregulation of these pathways showed significant term enrichment suggesting that the phenotypic aspects of proteotoxic stress on zebrafish development may be related to the deregulated signaling of these developmental pathways.

3.4.8. Putative targets of the deregulated miRNAs are deregulated at the gene expression level

Alterations in miRNA levels can affect the levels of expression of hundreds of different proteins, and albeit the fact that miRNAs repression can occur without detectable alteration in mRNA levels, in situations of more severe translational silencing mRNA levels can also be destabilized [90]. Interestingly, a miRNA targeting site enrichment analysis of the highly deregulated genes clusters (Figure 3.6, Supplementary Table 19) correlated with the most differentially expressed genes both down and upregulated. The set of down deregulated genes are enriched for the binding of miR-145, miR-150, miR155 and miR-196a. Furthermore, highly upregulated genes were also enriched for the deregulated miRNAs, namely miR-27b, miR-10b, miR-27c, miR-17a*, miR-203b, miR-216b, miR-16b, miR-1, miR-732, miR-16c, let-7g. Moreover, several putative targets of deregulated miRNAs were deregulated at the gene expression level and these were mainly deregulated in the Ser-tRNA$_{CAG}^{Leu}$ mutant embryos (Table 3.6). The other mutant tRNAs had less

extensive putative target deregulation at the gene expression level (Supplementary Table 20). The embryos expressing Ser-tRNA$_{CAG}^{Leu}$ had extensive gene expression deregulation that reflected the apoptotic state and phenotypic aspects of the mutant embryos. In agreement with this, our data show that deregulation of miRNA may affect some of its putative targets that participate in developmental signaling and apoptosis. We observed silencing of *tspan12* which is involved in vascularization of the retina and nonamyloidogenic proteolysis of APP [91, 92], of *hic1* which is a tumor suppressor [93], of *plxna4* which is a regulator of axon branching and patterning in brain development and Notch factors *otud7b* which are putative targets of miR-145 and *dbx1a* [94, 95] which is a putative target of mir-2195. Silenced miRNA expression may also be responsible for the increased gene expression levels of several putative targets (Table 3.6) namely Notch signaling component *axin1*, apoptosis related factors *bad* and *fas*, endoplasmic reticulum chaperone *hsp90b1*/*grp98* and transcription factors, such as *hoxc11a*, *rfx2*, *foxd1* and *efl* are putative targets of miR-27c. Up-regulated putative targets of miR-1 were the ER co-chaperones *dnajc3* and *zgc:56419*/*serp1*, the transcription factors *her7* and *hoxa39*, the and the actin binding *pfn2l*, *cnn3a*, *cnn3b*, *cnn2*, *pdlim1* and *sec23b* [15]. Finally, we also detected several putative targets of miR-16c that were induced at the gene expression level. In particular these were *sox32* and *vox* which are involved in embryo development [96, 97]; *psen2* that regulate Notch signaling [69], *fgf8a* which is involved in heart and forelimb development; and also transcription factors such as *hoxc11a* and *hoxa3a*. Globally, this group of deregulated putative miRNA targets includes several factors that can participate in embryo development and apoptosis, among other processes, showing that expression reprograming is present during proteotoxic stress.

Table 3.6. Putative targets deregulated by proteotoxic stress.

From the group of putative targets we determined for the deregulated miRNAs, we obtained a group of genes deregulated at the gene expression level in the Ser-$tRNA_{CAG}^{Leu}$ mutant embryos.

MiRNA	Genes deregulated in Leu
miR-2195	*tspan12, zgc:85746, gpib, ckmb, dbx1a, si:ch211-250g4.1, phactr4, zgc:56304*
miR-145	*tspan12, otud7b, zgc:112300, chrne, plxna4, mta2, hic1, zgc:158268, rtn1b, ppox, zgc:92710, pnrc2*
miR-150	*tspan12, zgc:165525, vat1, tubb5, sod2, zgc:158268, cav3, efr3a,*
miR-27c	*cd36, arl3l2, faz, mknk2b, oat, sesn2, zfand5a, sult1st3, hsp90b1, rfx2, hoxc11a, klf11b, bad, si:ch211-216l23.2, cth1, amt, rbm39b, fabp2, st3gal2l, nxf1, foxd1, ef1, axin1, gpr98, rybpb, stk33, thrap6, malt1, qk*
miR-1	*bhmt, paics, dnajc3, zgc:153896, her7, vtg3, snx14, anxa4, zgc:136871, hoxa3a, pdlim1, entpd1, kctd10, pax2a, mcfd2, cd63, dhrs1, zgc:56419, tagln2, zgc:112263, rpia, gnl1, tbp, pfn2l, cnn3a, cnn3b, cnn2, pdlim1, sec23b*
miR-16c	*pc, mknk2b, sox32, slc26a5, glud1a, vox, ptges, psen2, sybl1, fn1b, klf11a, sec23b, hoxc11a, hoxa3a, snx4, zgc:158263, fgf8a, myoc, nxf1, arl6, zgc:113030, zar1, tube1, stk33, wipi2, tnfaip1, anapc5*

3.5. Discussion

Our data show that proteotoxic stress affects zebrafish early development leading to severely malformed embryos, with poorly developed head and caudal regions accompanied by low survival rates. We observed that deregulated proteostasis has an impact on miRNA expression and our work suggests that miRNAs are important mediators. The general miRNA expression profile demonstrates that stress differentially deregulates specific miRNAs, however some miRNAs are coordinately deregulated by stress. MiR-190b was the most upregulated miRNA by Ser-tRNA$_{CGC}^{Ala}$; miR-365 was highly induced by Ser-tRNA$_{UCC}^{Gly}$; miR-2195 was highly induced by Ser-tRNA$_{CAC}^{Val}$ and Ser-tRNA$_{CAG}^{Leu}$, and miR-145 showed high up-regulation in embryos expressing the four misreading tRNAs. Mistranslation also downregulated some miRNAs. We were able to detect miRNAs coordinately deregulated by the four tRNAs and miRNAs that were deregulated in a tRNA specific manner. Let-7g was the most repressed miRNA in the Ser-tRNA$_{CGC}^{Ala}$ embryos, miR-732 was also highly repressed by Ser-tRNA$_{CAC}^{Val}$, and miR-16c and miR-1 were the most downregulated by the Ser-tRNA$_{CAG}^{Leu}$ mutant. Finally, miR-27c was coordinately repressed by three of the mutant tRNAs, namely the mutants Ser-tRNA$_{UCC}^{Gly}$, Ser-tRNA$_{CAC}^{Val}$ and Ser-tRNA$_{CAG}^{Leu}$. The putative targets of the deregulated miRNAs belong mainly to protein handling processes, cell cycle and morphogenesis, apoptosis, transcription and embryo development such as nervous system development, somitogenesis, patterning and angiogenesis.

Interestingly, our mRNA profiling results show that proteotoxic stress in zebrafish embryos activates apoptosis at the levels of death receptors, of caspases and of the Bcl-2 family, unveiling the potential activation of mitochondrial apoptosis dependent on ER. The latter is mediated by Bbc3/Puma, a known ER stress signal

adaptor that mediates the apoptotic signal from the ER to the mitochondria [79, 80, 98]. We have observed that proteotoxic stress coordinately activates the apoptotic pathways, which may partially be responsible for abnormal developmental patterns and low survival. Apoptosis plays an important role during organogenesis because this process shapes tissue and organ size and morphology by precisely removing unnecessary cells [99]. The activation of extrinsic cell death is of particular interest considering embryonic development, since zebrafish extrinsic pathway mediators are present in several tissues including the developing central nervous system [75]. Therefore, our data suggests that apoptosis is adjusting to balance the effects of aberrant polypeptides being produced as a result of the expression of mutant tRNAs. Given, the important role of apoptosis on developmental progression this deregulation in apoptosis can interfere with developmental and embryo shaping processes. Our gene expression profiling also indicates that deficient embryos morphogenesis under proteotoxic stress conditions happens through the deregulation, at the gene expression level, of several developmental signaling pathways, namely Hh, Wnt and Notch signaling. Signaling by Hh, Wnt and Notch family proteins plays a fundamental role in the development of vertebrates, since they regulate both cell fate specification and cell proliferation. These are pleiotropic pathways crucial to cell-cell communication, cell fate diversification, development and cell maintenance [100-102]. Hh and Notch signaling pathways are pivotal during embryo development by regulating spinal cord patterning and neural development; the Notch pathway is also involved in vascular development [103, 104]. Hh helps patterning the ventral spinal cord through the activation of Gli transcription factors. Importantly, Hh ligands are expressed in many vertebrate tissues, such as the developing central and peripheral nervous system and, several epithelia tissues, reproductive tissues and bone [102]. Wnt signaling is also involved in mitogenic

stimulation, cellular proliferation and differentiation. This pathway helps to establish cell and organism polarity through signaling gradients. The Wnt signals are pleiotropic and can activate three pathways, the best understood is the Wnt/β-catenin or canonical pathway [100, 105, 106]. Deregulation at the gene expression level of Hh signaling, namely *fbxw11a*, *csnk1db* and *sufu*, suggests that deregulated silencing occured. Wnt signaling was also affected, since we found several upregulated genes belonging to this pathway. Several ligands and also negative regulators such as, *wif1*, *nkd1*, *nkd2a*, indicating that this pathway may be silenced to some extent. In the case of Notch signaling, up regulation of positive regulators, namely *psen2*, *asb11* and *mib* points towards sustained activation of this signaling pathway [69, 88]. During development Wnt and Notch pathways have opposing effects promoting growth and repressing neural development, respectively. Concerted deregulation of developmental gene programming suggests a reduction in cellular identity establishment and tissue differentiation that correlates with the phenotypes that we observed at 24hfp, as embryos showed developmental delay and several undeveloped body regions and in some cases loss of body symmetry.

Our model of proteotoxic stress is a potent ROS and oxidative stress generator; and our previous work showed that oxidative damages to the DNA accumulate under mRNA mistranslation. In addition, oxidative stress also contributes to the phenotypic aspects of proteotoxic stress in zebrafish. Indeed, ROS scavengers were able to ameliorate embryos survival and malformations. Upon accumulation of DNA damage, p53 modulates miR-145 processing to modulate cell proliferation and apoptosis [107]. Therefore, in zebrafish embryos it is most likely that oxidative DNA damage drives miR-145 processing. MiR-145 and miR-2195 mainly potentialy target genes involved in angiogenesis, cell cycle and differentiation, embryo development and transcription

regulation. The genes *furina*, *foxc1*, *nlk1*, *nlk2*, *dll4*, *unc5b*, *rbpja*, *plxna4*, *nr2f1a*, *otud7b*, *dbx1a* and *arl13b* were established as putative targets and can be associated with the phenotypic alterations displayed by the embryos expressing the mutants tRNAs since these genes are involved in several embryonic developmental processes. Given the importance of miR-1 in zebrafish muscle tissue development, regulating sarcomeric actin organization at the gene expression level, down regulation of this particular miRNA indicates that sarcomere disorganization can be one of the aspects that shape the observed morphological alterations in Ser-tRNA$_{CAG}^{Leu}$ mutants. This suggests that the inhibition of this miRNA may stand as an important effector of proteotoxic stress in zebrafish embryos. Moreover, we hypothesize that repression of miR-27c probably alleviates silencing of fundamental genes involved in ER stress, namely *hsp90b1*/*grp98*, *fas*, *bad*, *dffb*, and *bcl2*, as observed by target prediction and microarray data. The ER stress response is the primary adaptive mechanism that alleviates ER stress by increasing the protein folding capacity while reducing the influx of nascent polypeptides into the ER through attenuated protein synthesis levels. However, under prolonged stress when the ER folding capacity is overwhelmed apoptosis is activated. Therefore, reduced levels of miR-27c may facilitate apoptotic progression in mistranslating zebrafish embryos. Several studies have shown that ER-stress intervenes in miRNA regulation through factors such as, XBP1 and IREα, our data expands this notion of proteotoxic stress responsive miRNAs that may facilitate apoptosis activation.

In conclusion, proteotoxic stress impacts embryo development through the deregulation of miRNA expression. The miRNA deregulation signature includes miR-2195, miR-145, miR27c, miR-1 and is very relevant in a developmental background as several putative targets are related to developmental signaling pathways. Since these miRNAs are present in adult tissues, this miRNA deregulation is very likely to affect

zebrafish in adult stages as well [17, 34, 108]. Therefore, our approach is a potent apoptosis activator that can be used to study early vertebrate development and tissue differentiation in a stressful background. And, given the impact of proteotoxic stress on miRNA regulation during zebrafish development, our methodology should help tackle the biology of miRNA biogenesis and processing driven by proteome destabilization and proteotoxic stress conditions.

3.6. Supplementary data

Supplementary Figure 1. Morphological alterations caused by mutant tRNAs. Control embryos (microinjected with endogenous serine tRNA) display normal development.

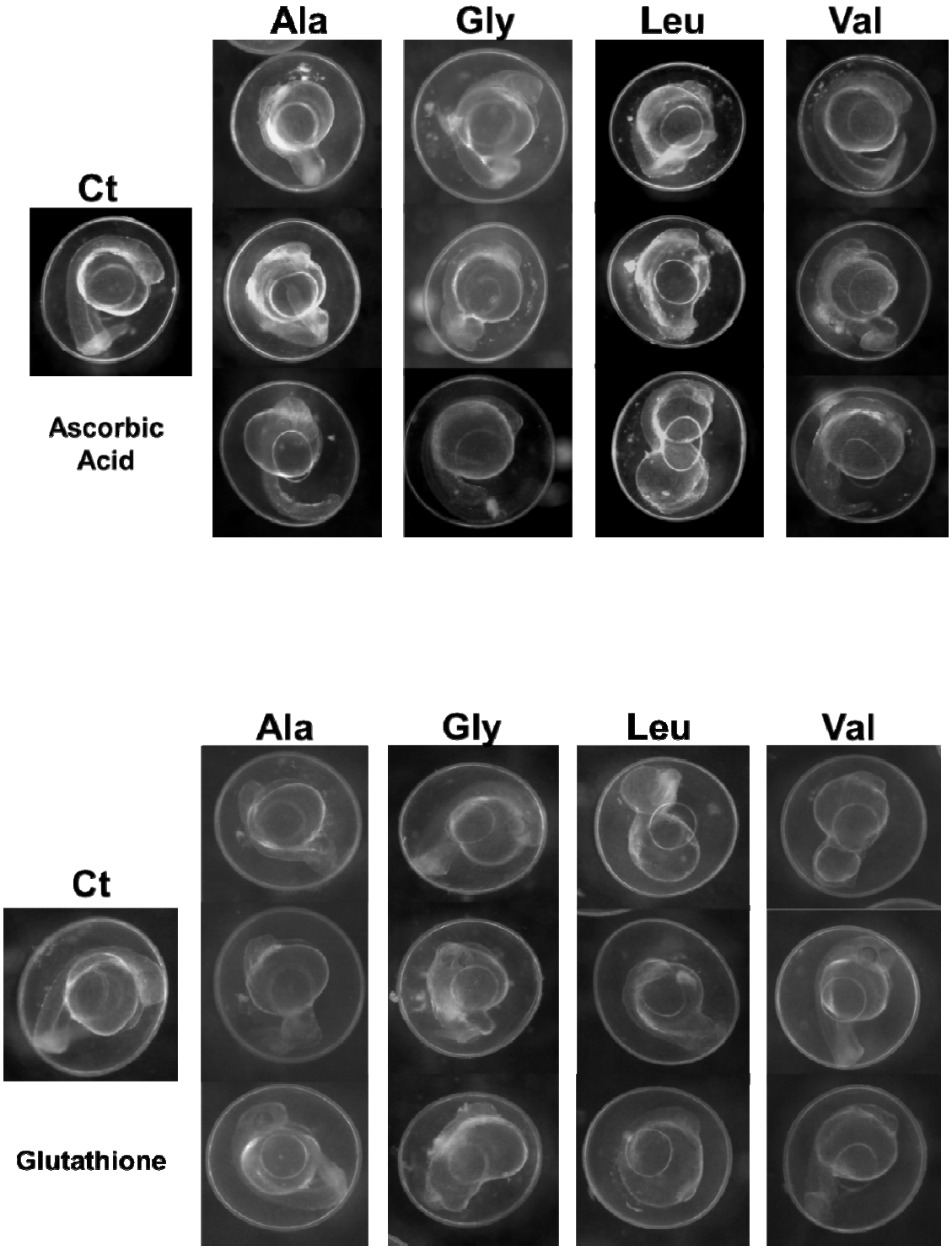

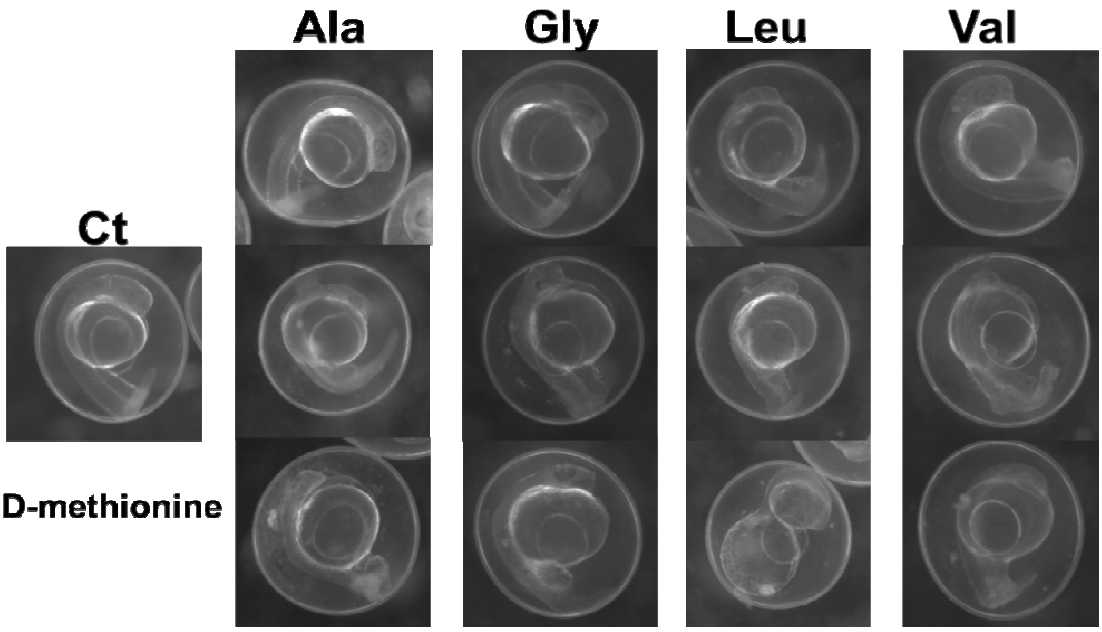

Supplementary Table 1. Embryo survival from 48hfp until 120hpf/5dpf. Data are represented by mean ± SD (n = 4).

	Embryo Survival %			
	48 hpf	**72 hpf**	**96 hpf**	**120 hpf**
Ct	50.5% ± 12.45	49.5% ± 11.6	49.1% ± 11.4	48.9% ± 11.2
Ala	38.6% ± 4.9	32.9% ± 6.7	32.0% ± 6.7	31.0% ± 7.5
Gly	14.6% ± 3.0	14.6% ± 3.5	11.6% ± 1.7	11.6% ± 1.7
Leu	3.4% ± 2.7	2.3% ± 2.6	2.3% ± 2.6	1.9% ± 2.2
Val	24.7% ± 5.9	17.1% ± 3.1	16.4% ± 2.4	15.7% ± 2.1

Supplementary Table 2. Log_2 fold change of miRNAs deregulated by proteotoxic stress. MiRNAs deregulated by proteotoxic stress. MiRNA were considered deregulated fold change higher than 1.5 and lower than -1.5. Displayed results are Log_2 fold change values.

	ALA	GLY	VAL	LEU
miR-365		**20.00**		
miR-190b	**10.38**			
miR-2195			**15.53**	**40.03**
miR-145	**4.63**	**13.00**	**19.48**	**12.67**
miR-101b			9.49	
miR-196[a]	**4.78**	**2.66**		
miR-130[a]	**4.17**		**5.24**	
miR-155	**4.27**		**4.11**	
miR-30c		**3.73**	**4.11**	
miR-726			**4.04**	
miR-301b			**3.77**	
miR-190			**3.65**	
miR-150	**3.50**	**2.10**		**1.65**
miR-457b	3.31			
miR-200b			2.99	
miR-18b		2.90		
miR-133c			2.82	
miR-135b		2.41		
miR-144	2.38			
miR-27a				2.28
miR-1388	2.26		2.13	
miR-153a	2.26		1.65	
miR-26a	2.18			
miR-206			2.07	
miR-152	2.05			
miR-454b				2.04
let-7h		1.73		
miR-10b		1.70		
mir-222b				1.64
miR-15a*			1.64	1.61
miR-27b	**-1.96**			**-1.79**
miR-10b			**-1.75**	
miR-27c		**-2.25**	**-1.91**	**-2.01**
miR-17a*	**-2.45**		**-2.72**	**-2.22**
miR-203b	**-2.97**			
miR-216b			**-3.37**	
miR-16b			**-3.68**	
miR-1				**-3.85**
miR-732			**-4.55**	
miR-16c				**-6.33**
let-7g	**-7.51**			

Supplementary Table 3. Putative targets of miR-190b. miRNA targets were identified with the Eimmo (MirZ), miRBASE Targets and TargetScan Fish databases. The computational targets were considered when they were retrieved from at least two of the algorithms. GO terms were identified using DAVID database and manually curated to remove redundant terms.

miR-190b	
Target	**GO Term –Biological Process**
pycard	Apoptosis
mad1l1, sept2	Cell cycle
grin1b	Ion transport, calcium signaling pathway neuroactive ligand-receptor interaction
ncbp2	RNA processing, spliceosome
gli1, pou4f3, mef2a, fezf1	Transcription
nrp2a	Vasculogenesis, neural crest cell migration,

Supplementary Table 4. Putative targets of miR-365. miRNA targets were identified with the Eimmo (MirZ), miRBASE Targets and TargetScan Fish databases. The computational targets were considered when they were retrieved from at least two of the algorithms. GO terms were identified using DAVID database and manually curated to remove redundant terms.

miR-365	
Target	**GO Term –Biological Process**
slc7a3	Amino acid transport
fli1a	Blood vessel development, regulation of transcription
cldn10	Cell adhesion molecules (cams), Tight junction
cxcl12a, kif1b, erbb3b	Cell morphogenesis
oprd1b, tgfb3	Cell surface receptor linked signal transduction
fzd8a	Cell surface receptor linked signal transduction, Wnt signaling pathway, Melanogenesis
si:ch211-15p9.2	Dephosphorylation
rag2	DNA metabolic process
dnmt4	DNA methylation, Cysteine and methionine metabolism
zgc:66475	DNA repair, cellular response to stress,
neurod4	Embryonic morphogenesis, regulation of nervous system development
pik3r3	Erbb signaling pathway, mtor signaling pathway, Apoptosis, VEGF signaling pathway
arl3l1, zgc:63637,rhogb	Intracellular signaling cascade
clic1, clica, kcnj13	Ion transport
zgc:114174	Macromolecule catabolic process
eif4g2b	Mesoderm development
cdipt, adkb, agpat4, ggps1	Metabolism
slc15a2	Oligopeptide transport, peptide transport
numbl, robo3	Pattern specification process
pdgfra limk2	Phosphorylation
st3gal2l, st6galnac3	Protein amino acid glycosylation
ppif	Protein folding
xpo4, vps26b, srp72	Protein localization
sec22bb	Protein localization, SNARE interactions in vesicular transport
mtx1b, mtx3	Protein targeting to mitochondrion
hectd1	Proteolysis, protein ubiquitination
atp13a	Purine nucleotide biosynthetic process
adarb1	RNA processing
mbtps2, smo	Skeletal system development
igf2a, igf2b	Somitogenesis
maf1, pax9, taf6, sox21a, irf7, hoxc3a, mafba, pnx, snd1, vsx1, papolb	Transcription, regulation of transcription

Supplementary Table 5. Putative targets of let-7g. miRNA targets were identified with the Eimmo (MirZ), miRBASE Targets and TargetScan Fish databases. The computational targets were considered when they were retrieved from at least two of the algorithms. GO terms were identified using DAVID database and manually curated to remove redundant terms.

let-7g	
Target	**GO Term –Biological Process**
zgc:77651	Acyl-coa metabolic process , coenzyme metabolic process, cofactor metabolic process
lbr	Ameboidal cell migration cell motion
zgc:153993, casp8l2, clu	Apoptosis, cell death
foxh1	Blood vessel development, regionalization, transcription, pattern specification process
pbx1a	Cell morphogenesis, regulation of transcription, DNA-dependent
drd2a	Cell surface receptor linked signal transduction
gng5, zgc:110292	Chromatin organization, chromosome organization
dclre1c, dnmt7, pold1	DNA metabolic process
dfna5	Embryonic morphogenesis
pbx2	Eye development, regulation of transcription, DNA-dependent, muscle cell development,
col1a1b	Focal adhesion
tarbp2	Gene silencing
atp2a2a	Heart morphogenesis, purine nucleotide metabolic proces , ion transport , Calcium signaling pathway
zgc:114118	Intracellular signaling cascade
slc25a22, grin1b, slc9a6a, rhag	Ion transport
fgf6a	MAPK signaling pathway, Regulation of actin cytoskeleton
pde10a, atp1b1b, atp2a2b, gatm, tpi1a, idh2, rdh10a	Metabolism
paqr5b	Multicellular organism reproduction
slc6a13, zgc:103663, stx3a	Neurotransmitter transport
nrarpa	Notch signaling pathway,
prdm1a, acvr1b, dzip1, nr6a1a	Pattern specification process
prkcq, nek1, zgc:101572, zgc:113355, zgc:153997	Protein amino acid phosphorylation, phosphorylation
fga	Protein complex assembly, blood coagulation
wasla, waslb	Protein complex assembly, cytoskeleton organization
fkbp11	Protein folding
sar1a, stx7l, napa, trpc4apa, serac1	Protein localization, protein transport
mtx1b	Protein targeting, protein targeting to mitochondrion
fbxl14a	Protein ubiquitination
capn3, usp44	Proteolysis
col1a1a	Regulation of ossification
igf2bp3	Regulation of translation
ngb	Response to hypoxia
lipf	Response to hypoxia
zorba, rbm22, hspa8	RNA processing
coe2, hoxa1a, sox19b, cebpd, pou2f1b, zgc:158291	Transcription, regulation of transcription

Supplementary Table 6. Putative targets of miR-732. miRNA targets were identified with the Eimmo (MirZ), miRBASE Targets and TargetScan Fish databases. The computational targets were considered when they were retrieved from at least two of the algorithms. GO terms were identified using DAVID database and manually curated to remove redundant terms.

miR-732	
Target	**GO Term –Biological Process**
ntn1a	Angiogenesis, pattern specification process
bad	Apoptosis, VEGF signaling pathway
arg2	Arginine and proline metabolism
hey2	Blood vessel development, transcription, Notch signaling pathway
itgb1a, ncam2	Cell adhesion
fzd2	Cell morphogenesis, Wnt receptor signaling pathway, calcium modulating pathway, pattern specification process
fzd4	Cell surface receptor linked signal transduction, Wnt receptor signaling pathway
tln1	Cytoskeleton organization
cav3	Cytoskeleton organization, cell fate commitment, embryonic organ development
lhx5	Eye development, transcription
tnw	Focal adhesion, ECM-receptor interaction
si:dkey-217m5.3, si:dkeyp-59a8.1, si:dkeyp-59a8.2, si:dkeyp-59a8.3, zgc:171266	Immune response
rap2c, si:dkey-206f10.1	Intracellular signaling cascade
sfxn1, clic5	Ion transport
si:dkey-159a18.1	Lysosome
map4k3	MAPK signaling pathway
sepn1, noc3l	Muscle organ development
aldh1a3, si:dkey-180p18.9, hmox1	Oxidation reduction
ndufs1	Oxidative phosphorylation , oxidation reduction
smo	Pattern specification process, embryonic organ development
pxk, eif2ak1, tnika	Protein amino acid phosphorylation, phosphorylation
tuba7l	Protein complex assembly
ppif	Protein folding
ipo9	Protein localization
kpna4, bcap31, mrpl45	Protein localization, protein transport
timm23	Protein targeting, protein targeting to mitochondrion
zgc:112038, mdm2, fancl	Proteolysis
plk4	Regulation of cell cycle process regulation of centrosome cycle
extl3	Regulation of cell growth,
vasa	Reproductive developmental process
paqr8, cyp19a1a	Response to hormone stimulus
dbr1	RNA processing
hspa8	Spliceosome, MAPK signaling pathway, Endocytosis
dhdds	Terpenoid backbone biosynthesis
ar, rarga, edf1, barhl1.1, mycn, polr3e, th1l, onecut1	Transcription, regulation of transcrition
eef1g	Translation
slc25a1	Transmembrane transport

Supplementary Table 7. Putative targets of miR-16c. miRNA targets were identified with the Eimmo (MirZ), miRBASE Targets and TargetScan Fish databases. The computational targets were considered when they were retrieved from at least two of the algorithms. GO terms were identified using DAVID database and manually curated to remove redundant terms.

miR-16c	
Target	**GO Term –Biological Process**
sox32, ptges	Ameboidal cell migration regulation of transcription, DNA-dependent, pattern specification process
ntn1a	Angiogenesis
gfra1b	Autonomic nervous system development, enteric nervous system development
spred1, flt1, ptenb	Blood vessel development
btbd9	Cell adhesion
sept6, anapc5, ccnb2, sesn1	Cell cycle
clu	Cell death
tnr, arl6	Cell morphogenesis
cmklr1, zgc:158263	Cell surface receptor linked signal transduction
tnfaip1, top2a, chaf1a, poll, rnaseh1	DNA metabolic process , DNA repair
sec23b, mab21l2	Embryonic organ developmen, eye development
sh3gl2	Endocytosis
bmp5	Hedgehog signaling pathway TGF-beta signaling pathway
zgc:123107, sptb	Immune response
asb16,m spsb4a, arl4d	Intracellular signaling cascade
kctd6, slc26a5, apol1	Ion transport
fgf6a	MAPK signaling pathway, Regulation of actin cytoskeleton,
sybl1, th, atp6v1b2, evla, pc	Metabolism
nek8, zw10	Mitotic cell cycle
cab39, pik3r3	Mtor signaling pathway
pthlh	Multicellular organism reproduction,
nrarpa, psen2, dla, dld	Notch signaling pathway
tbxas1, glud1a	Oxidation reduction
sox4b	Pancreas development
fgf8a	Pattern specification process, regulation of Wnt receptor signaling pathway,
cpox, has3, cbsa, chka, hmgcs1	Protein amino acid phosphorylation , phosphorylation, Cell cycle
cdk2, stk33	Protein catabolic process, Proteasome
psmc3	Protein complex assembly
tube1, zgc:112335	Protein folding
pfdn5, scamp2	Protein localization, protein transport
illr4, usp25, usp2a, napa	Proteolysis
ctsk	Regulation of cell death, regulation of apoptosis
plrg1	Regulation of gtpase activity, regulation of Ras protein signal transduction
tbc1d19	RIG-I-like receptor signaling pathway
pl10	RNA processing
zmat5, nxf1	Sensory organ development, neurological system process
myo6b	Spliceosome
crsp7, bhlhe40, hoxa3a, hoxc11a, sap30l, znf367, olig4, vox, cdc5l, tarbp2	Transcription , regulation of transcription
nfat5	Transcription, Wnt signaling pathway, VEGF signaling pathway
sf3b5, smn1	Translation, regulation of translation
eif1b, eef1db, eef1da, etf1, mknk2b, slc25a33, zgc:73228	Transmembrane transport, vesicle-mediated transport

Supplementary Table 8. Putative targets of miR-1. miRNA targets were identified with the Eimmo (MirZ), miRBASE Targets and TargetScan Fish databases. The computational targets were considered when they were retrieved from at least two of the algorithms. GO terms were identified using DAVID database and manually curated to remove redundant terms.

miR-1	
Target	**GO Term –Biological Process**
hs6st2	Angiogenesis, blood vessel development
notch1b	Blood vessel development, Notch signaling pathway,
calm1b, calm1a, calm2b, calm3a, calm3b	Calcium signaling pathway
nrxn2a	Cell adhesion molecules (cams)
nadl1.1, cxcl12a	Cell morphogenesis
tagln2, pfn2l	Cell morphogenesis, cytoskeleton organization
mtnr1c	Cell surface receptor linked signal transduction
snap25a	Cytokinesis, cell division
arpc4l	Cytoskeleton organization
zgc:165555	DNA packaging, chromatin organization
paics	Eye development, metabolism
copz1	Eye development, protein localization
hs3st3b1b	Glycosaminoglycan degradation, Heparan sulfate biosynthesis
ak2	Immune system development
asb4, arf1l, rabif	Intracellular signaling cascade
slc40a1, slc39a13, kctd10	Ion transport
vtg3	Lipid transport
cd63	Lysosome
rpia, atic, dpyd, ddost, alg8, arg2, azin1b, zgc:136871, entpd1, acat2, hccsa, nudt9, zgc:153896, ass1, bhmt, adh8b	Metabolism
cbr1l, dhrs1, idh1	Oxidation reduction
atp6v1c1a	Oxidative phosphorylation, proton transport
ccng2	P53 signaling pathway
bmpr2a	Pattern specification process
bsk146, dyrk2, prkacab	Protein amino acid phosphorylation, phosphorylation
tuba8l4	Protein complex assembly
fkbp9	Protein folding
ppih	Protein folding, Spliceosome
m6pr	Protein targeting to lysosome
zgc:136971	Proteolysis
fancd2	Regulation of cell death, regulation of apoptosis
eif5a	Regulation of translation
amh	Reproductive developmental process,
igf2b, igf2a, her7	Somitogenesis, pattern specification process
hnrpkl	Spliceosome
tbp, hoxa3a, hoxb2a, nr4a3, meis3, dlx2b, elk4, hsf2, cnot3a, pax2a	Transcription, regulation of transcription
slc25a27	Transmembrane transport
wnt4b, cacybp	Wnt signaling pathway

Supplementary Tables 9-12. Enriched GO Biological Processes (BP). Terms related to development in mistranslation mutants were obtained with GeneCodis v3.0. Genes in term refers the number of genes in the dataset that belong to the respective BP. Hyp_c refers to corrected p values obtained with the application of a hypergeometric test.

9 - ALANINE GO Term BP development	Genes in Term	Hyp_c
regulation of neuron apoptosis (BP)	2(147)	2.57E-02
central nervous system development (BP)	5(147)	3.12E-02
cartilage development (BP)	3(147)	3.99E-02
positive regulation of cell differentiation (BP)	2(147)	4.08E-02

10 - GLYCINE GO Term BP development	Genes in Term	Hyp_c
liver development (BP)	8(641)	5.72E-06
morphogenesis of an epithelium (BP)	12(641)	1.77E-03
cartilage development (BP)	8(641)	1.80E-03
ameboidal cell migration (BP)	8(641)	8.40E-03
pectoral fin development (BP)	5(641)	9.69E-03
heart formation (BP)	2(641)	1.19E-02
central nervous system development (BP)	13(641)	1.21E-02
cell morphogenesis (BP)	10(641)	1.79E-02
pancreas development (BP)	5(641)	2.14E-02
hemopoiesis (BP)	7(641)	2.21E-02
gastrulation (BP)	8(641)	3.21E-02
determination of left/right symmetry (BP)	7(641)	3.23E-02
digestive tract development (BP)	4(641)	3.23E-02

11 - VALINE GO Term BP development	Genes in Term	Hyp_c
cardiovascular system development (BP)	30(798)	1.14E-08
anterior/posterior pattern formation (BP)	18(798)	7.78E-08
sensory organ development (BP)	23(798)	1.16E-06
morphogenesis of an epithelium (BP)	18(798)	3.23E-06
central nervous system development (BP)	22(798)	4.07E-06
embryonic organ morphogenesis (BP)	13(798)	4.05E-05
cell morphogenesis (BP)	16(798)	8.56E-05
fin morphogenesis (BP)	10(798)	1.10E-04
vasculature development (BP)	15(798)	1.27E-04
forebrain anterior/posterior pattern formation (BP)	3(798)	2.39E-04

neurogenesis (BP)	19(798)	2.46E-04
segmentation (BP)	10(798)	4.82E-04
dorsal/ventral pattern formation (BP)	10(798)	5.23E-04
branching morphogenesis of a tube (BP)	4(798)	5.64E-04
hindbrain development (BP)	9(798)	6.45E-04
somitogenesis (BP)	9(798)	8.59E-04
neural tube development (BP)	7(798)	1.65E-03
skeletal system morphogenesis (BP)	6(798)	1.91E-03
Wnt receptor signaling pathway (BP)	10(798)	2.05E-03
determination of left/right symmetry (BP)	10(798)	2.16E-03
cartilage development (BP)	8(798)	3.13E-03
neuromast development (BP)	4(798)	3.63E-03
Notch signaling pathway (BP)	6(798)	3.71E-03
intestinal cholesterol absorption (BP)	2(798)	3.82E-03
parasympathetic nervous system development (BP)	2(798)	3.82E-03
muscle organ development (BP)	7(798)	7.89E-03
regulation of Wnt receptor signaling pathway (BP)	4(798)	2.64E-02

12 - LEUCINE GO Term BP development	Genes in Term	Hyp_c
chordate embryonic development (BP)	36(1216)	1.42E-16
sensory organ development (BP)	40(1216)	1.17E-13
anterior/posterior pattern formation (BP)	27(1216)	6.42E-12
cardiovascular system development (BP)	42(1216)	3.37E-11
central nervous system development (BP)	36(1216)	7.45E-11
determination of left/right symmetry (BP)	22(1216)	1.83E-09
brain development (BP)	29(1216)	3.16E-09
somitogenesis (BP)	18(1216)	4.80E-09
segmentation (BP)	19(1216)	4.99E-09
heart development (BP)	28(1216)	5.67E-09
cell morphogenesis (BP)	26(1216)	2.69E-08
eye development (BP)	26(1216)	2.96E-08
neurogenesis (BP)	31(1216)	1.43E-07
morphogenesis of an epithelium (BP)	24(1216)	2.33E-07
hemopoiesis (BP)	18(1216)	3.52E-07
hindbrain development (BP)	14(1216)	4.15E-06
dorsal/ventral pattern formation (BP)	15(1216)	7.29E-06
ameboidal cell migration (BP)	16(1216)	8.26E-06
skeletal system morphogenesis (BP)	10(1216)	8.41E-06
endoderm formation (BP)	8(1216)	1.11E-05
digestive tract development (BP)	9(1216)	5.09E-05
muscle organ development (BP)	12(1216)	8.85E-05
Wnt receptor signaling pathway (BP)	15(1216)	8.98E-05
erythrocyte differentiation (BP)	8(1216)	1.09E-04

forebrain development (BP)	11(1216)	1.27E-04
liver development (BP)	8(1216)	1.33E-04
smoothened signaling pathway (BP)	6(1216)	1.46E-04
cartilage development (BP)	12(1216)	1.49E-04
muscle cell development (BP)	11(1216)	2.79E-04
fin morphogenesis (BP)	11(1216)	3.55E-04
ventral midline development (BP)	5(1216)	3.76E-04
autonomic nervous system development (BP)	5(1216)	3.76E-04
blood vessel development (BP)	17(1216)	3.77E-04
heart looping (BP)	10(1216)	4.94E-04
notochord development (BP)	8(1216)	6.17E-04
epidermal cell differentiation (BP)	4(1216)	8.59E-04
Notch signaling pathway (BP)	8(1216)	1.02E-03
neuron fate commitment (BP)	5(1216)	1.48E-03
mesoderm formation (BP)	6(1216)	2.06E-03
skeletal muscle organ development (BP)	7(1216)	2.06E-03
striated muscle cell development (BP)	9(1216)	2.29E-03
nerve development (BP)	5(1216)	2.43E-03
epithelial cell differentiation (BP)	5(1216)	2.43E-03
pancreas development (BP)	8(1216)	2.54E-03
mesenchymal cell development (BP)	8(1216)	3.54E-03
melanocyte differentiation (BP)	4(1216)	3.80E-03
neural crest cell development (BP)	7(1216)	3.88E-03
regulation of Wnt receptor signaling pathway (BP)	6(1216)	5.05E-03
parasympathetic nervous system development (BP)	2(1216)	6.02E-03
notochord cell development (BP)	2(1216)	6.02E-03
lateral line system development (BP)	6(1216)	7.22E-03
gastrulation with mouth forming second (BP)	5(1216)	8.39E-03
endocrine pancreas development (BP)	4(1216)	9.84E-03
neuromast development (BP)	4(1216)	9.84E-03
regulation of smoothened signaling pathway (BP)	3(1216)	9.90E-03
otic vesicle morphogenesis (BP)	5(1216)	1.15E-02
forebrain anterior/posterior pattern formation (BP)	2(1216)	1.38E-02
heart formation (BP)	2(1216)	1.38E-02
non-canonical Wnt receptor signaling pathway (BP)	5(1216)	1.39E-02
spinal cord development (BP)	5(1216)	1.60E-02
enteric nervous system development (BP)	3(1216)	1.69E-02
kidney development (BP)	6(1216)	4.48E-02
central nervous system segmentation (BP)	2(1216)	4.82E-02
gliogenesis (BP)	4(1216)	4.98E-02

Supplementary Tables 13-16. Enriched GO Biological Processes (BP) Terms related to cellular processes in mistranslation mutants were obtained with GeneCodis v3.0. Genes in term refers the number of genes in the dataset that belong to the respective BP. Hyp_c refers to corrected p values obtained with the application of a hypergeometric test.

13 - ALANINE GO Term BP	Genes in Term	Hyp_c
regulation of gene expression (BP)	17(147)	2.03E-04
metal ion transport (BP)	8(147)	3.64E-04
RNA metabolic process (BP)	17(147)	1.13E-03
regulation of apoptosis (BP)	5(147)	2.90E-03
steroid hormone mediated signaling pathway (BP)	4(147)	3.81E-03
DNA catabolic process (BP)	2(147)	5.70E-03
positive regulation of apoptosis (BP)	3(147)	9.67E-03
phosphorylation (BP)	9(147)	1.52E-02
carboxylic acid biosynthetic process (BP)	3(147)	3.39E-02
protein phosphorylation (BP)	7(147)	3.41E-02
calcium ion transmembrane transport (BP)	2(147)	4.08E-02
glycerolipid metabolic process (BP)	2(147)	4.13E-02
regulation of cell cycle process (BP)	2(147)	4.31E-02
protein modification process (BP)	9(147)	4.44E-02

14 - GLYCINE GO Term BP	Genes in Term	Hyp_c
carboxylic acid metabolic process (BP)	22(641)	3.41E-09
monosaccharide metabolic process (BP)	12(641)	1.01E-06
nucleotide metabolic process (BP)	21(641)	1.30E-06
regulation of gene expression (BP)	49(641)	2.10E-06
cellular carbohydrate catabolic process (BP)	8(641)	8.08E-05
membrane lipid metabolic process (BP)	5(641)	1.73E-04
phosphorylation (BP)	28(641)	3.31E-04
glycerol metabolic process (BP)	4(641)	5.76E-04
convergent extension (BP)	8(641)	1.70E-03
fatty acid metabolic process (BP)	6(641)	1.88E-03
protein modification process (BP)	31(641)	2.25E-03
cellular carbohydrate biosynthetic process (BP)	4(641)	5.55E-03
glycolipid metabolic process (BP)	3(641)	5.78E-03
protein transport (BP)	13(641)	7.43E-03
purine nucleoside metabolic process (BP)	4(641)	7.78E-03

cellular lipid catabolic process (BP)	3(641)	9.44E-03
protein glycosylation (BP)	6(641)	9.83E-03
cellular biogenic amine metabolic process (BP)	4(641)	1.19E-02
small GTPase mediated signal transduction (BP)	11(641)	1.51E-02
integrin-mediated signaling pathway (BP)	4(641)	1.85E-02
regulation of ubiquitin-protein ligase activity (BP)	2(641)	1.87E-02
protein phosphorylation (BP)	18(641)	1.87E-02
sterol transport (BP)	2(641)	2.55E-02
isoprenoid metabolic process (BP)	3(641)	3.20E-02
coenzyme biosynthetic process (BP)	4(641)	3.23E-02
regulation of organelle organization (BP)	4(641)	3.31E-02
positive regulation of macromolecule metabolic process (BP)	6(641)	3.82E-02
retinoid metabolic process (BP)	2(641)	4.29E-02
regulation of protein metabolic process (BP)	6(641)	4.74E-02
steroid biosynthetic process (BP)	3(641)	4.90E-02

15 - VALINE GO Term BP	**Genes in Term**	**Hyp_c**
RNA metabolic process (BP)	86(798)	3.24E-15
regulation of gene expression (BP)	75(798)	6.20E-14
protein modification process (BP)	52(798)	2.62E-09
phosphorylation (BP)	43(798)	9.25E-09
protein phosphorylation (BP)	32(798)	1.03E-06
regulation of cellular protein metabolic process (BP)	14(798)	1.03E-06
protein transport (BP)	22(798)	1.30E-06
metal ion transport (BP)	20(798)	2.51E-06
carboxylic acid metabolic process (BP)	18(798)	9.13E-06
negative regulation of macromolecule metabolic process (BP)	12(798)	1.05E-05
regulation of apoptosis (BP)	14(798)	1.57E-05
positive regulation of cell communication (BP)	7(798)	3.59E-04
positive regulation of apoptosis (BP)	7(798)	6.27E-04
negative regulation of cell cycle (BP)	6(798)	7.67E-04
mRNA metabolic process (BP)	10(798)	8.72E-04
regulation of phosphorus metabolic process (BP)	7(798)	1.49E-03
negative regulation of cellular protein metabolic process (BP)	4(798)	2.32E-03
protein folding (BP)	9(798)	3.83E-03
ameboidal cell migration (BP)	9(798)	3.87E-03
RNA processing (BP)	12(798)	4.24E-03
regulation of peptidase activity (BP)	4(798)	6.33E-03
phospholipid biosynthetic process (BP)	4(798)	9.30E-03
negative regulation of cell communication (BP)	6(798)	1.00E-02
posttranscriptional regulation of gene expression (BP)	5(798)	1.48E-02
glycerolipid metabolic process (BP)	4(798)	1.63E-02

organic acid transport (BP)	4(798)	1.63E-02
carboxylic acid transport (BP)	4(798)	1.63E-02
DNA damage response, signal transduction by p53 class mediator (BP)	2(798)	2.13E-02
regulation of cell development (BP)	5(798)	2.63E-02
dephosphorylation (BP)	7(798)	2.78E-02
mesendoderm development (BP)	2(798)	2.83E-02
protein glycosylation (BP)	5(798)	3.71E-02
protein dephosphorylation (BP)	6(798)	4.47E-02
gene silencing (BP)	3(798)	4.66E-02

16 - LEUCINE GO Term BP	**Genes in Term**	**Hyp_c**
MAPKKK cascade (BP)	4(1216)	2.88E-03
monosaccharide metabolic process (BP)	18(1216)	5.78E-10
protein complex assembly (BP)	8(1216)	2.47E-02
protein modification process (BP)	78(1216)	7.04E-14
protein phosphorylation (BP)	49(1216)	1.47E-10
protein glycosylation (BP)	6(1216)	4.76E-02
glutamine metabolic process (BP)	4(1216)	3.80E-03
membrane lipid metabolic process (BP)	6(1216)	1.10E-04
steroid biosynthetic process (BP)	7(1216)	1.11E-04
mitochondrial transport (BP)	3(1216)	3.78E-02
amino acid transport (BP)	3(1216)	2.63E-02
endocytosis (BP)	4(1216)	1.60E-02
cytoskeleton organization (BP)	17(1216)	7.52E-05
small GTPase mediated signal transduction (BP)	25(1216)	1.05E-06
Ras protein signal transduction (BP)	5(1216)	1.32E-02
cholesterol metabolic process (BP)	3(1216)	1.37E-03
nucleotide metabolic process (BP)	23(1216)	2.91E-04
catechol metabolic process (BP)	5(1216)	1.46E-04
positive regulation of signal transduction (BP)	10(1216)	8.41E-06
negative regulation of signal transduction (BP)	8(1216)	4.22E-03
regulation of gene expression (BP)	115(1216)	4.53E-22
protein transport (BP)	17(1216)	1.52E-02
organic acid transport (BP)	4(1216)	4.60E-02
sterol transport (BP)	3(1216)	2.80E-03
cell growth (BP)	7(1216)	3.74E-02
RNA metabolic process (BP)	117(1216)	3.29E-18
phosphorylation (BP)	74(1216)	2.68E-18
regulation of phosphate metabolic process (BP)	8(1216)	2.27E-03
carboxylic acid metabolic process (BP)	20(1216)	1.10E-04
water homeostasis (BP)	2(1216)	1.38E-02
extracellular matrix organization (BP)	4(1216)	7.81E-03

regulation of transporter activity (BP)	4(1216)	1.42E-02
regulation of organelle organization (BP)	5(1216)	3.08E-02
ion transmembrane transport (BP)	12(1216)	3.17E-03
cellular response to reactive oxygen species (BP)	2(1216)	6.02E-03
maintenance of protein localization in endoplasmic reticulum (BP)	2(1216)	1.38E-02
response to hydrogen peroxide (BP)	3(1216)	2.80E-03
muscle cell fate commitment (BP)	6(1216)	3.78E-07
regulation of apoptosis (BP)	14(1216)	5.98E-04
steroid hormone mediated signaling pathway (BP)	8(1216)	1.41E-02
regulation of kinase activity (BP)	7(1216)	3.49E-03
cellular carbohydrate catabolic process (BP)	8(1216)	1.79E-03
negative regulation of cell differentiation (BP)	5(1216)	1.81E-02
positive regulation of cell differentiation (BP)	4(1216)	2.50E-02
carboxylic acid biosynthetic process (BP)	10(1216)	1.15E-03
glycerolipid metabolic process (BP)	6(1216)	2.44E-03
phosphatidylinositol metabolic process (BP)	5(1216)	5.98E-03
response to copper ion (BP)	4(1216)	5.06E-03
Golgi vesicle transport (BP)	4(1216)	9.84E-03
regulation of protein metabolic process (BP)	11(1216)	2.82E-03
regulation of cytoskeleton organization (BP)	4(1216)	4.09E-02
regulation of peptidase activity (BP)	4(1216)	1.60E-02
convergent extension (BP)	9(1216)	6.12E-03
regulation of transmembrane receptor protein serine/threonine kinase signaling pathway (BP)	6(1216)	5.05E-03

Supplementary table 17. Log_2 fold change of apoptosis related genes deregulated by proteotoxic stress. Genes involved in apoptosis deregulated by proteotoxic stress. Genes were considered deregulated fold change higher than 1.5 and lower than -1.5. Displayed results are Log_2 fold change values.

	Ala	Gly	Val	Leu
tnfrsfa	2.02			2.04
tnfs10l		4.01		3.52
fas			3.22	4.13
casp3b		5.17		
casp6				4.01
casp8	2.39		2.64	
casp9				1.93
caspc	-1.93			-1.93
bbc3				2.15
bcl2l			1.99	2.94
bnip3l		1.84		1.99
bad			2.20	2.01
bmf1			2.00	1.78
baxa	1.21		1.79	1.79
boka				1.77
bag3				1.99
xiap		2.29	1.82	2.14
tp53	1.83		2.04	
tp63		1.93		1.64
perp			1.99	1.94
mdm2	1.75		2.15	
zgc:158776			1.76	1.42
ciapin1			1.83	
zgc:73226				2.10

Supplementary table 18. Log_2 fold change of developmental signalling related genes deregulated by proteotoxic stress. Genes involved in developmental signalling pathways Hedgehog, Wnt and Notch deregulated by proteotoxic stress. Genes were considered deregulated fold change higher than 1.5 and lower than -1.5. Displayed results are Log_2 fold change values.

	Ala	Gly	Val	Leu
shha				1.78
gli2a				1.67
fbxw11a				2.99
sufu			1.76	1.69
csnk1db				1.54
bmp2b				1.95
bmp6		2.31		1.92
bmp7a				3.88
axin1			1.57	1.50
csnk1db				1.54
fgf3			1.64	
fzd8b				2.55
grk5		4.38	2.36	
klhl12			1.50	
mylipb				4.12
nkd1			1.92	1.76
nkd2a		1.62		1.56
nlk1			1.75	1.60
sp5l				2.84
wif1			1.79	1.67
wnt1	2.59		1.49	3.41
wnt10a	2.00	3.05		3.77
wnt16				2.26
wnt4a			1.50	1.51
wnt8a				4.23
asb11			1.85	2.12
psen2		3.52		2.93
mib				1.46
notch2		2.17	2.01	1.91
her1				3.47
her7				2.68
her8.2				-1.74
her11			3.21	3.73
her12			1.48	
hey2			1.79	
rras				2.78
nrarpa			1.67	
gmds			2.92	2.50
dlb				-1.65
otud7b				-2.34

Supplementary Table 19. Enriched miRNAs target sites. Genes contained in the 3 major clusters of gene expression profiling results (figure 5) were analyzed with GeneCodis v2.0 for microRNA target site enrichment. The miRNAs deregulated in this study that were present in the GeneCodis analysis were selected from the total lists and are shown in the table.

MicroRNA	Nbr targeted genes	Hyp_c
Cluster 1		
dre-miR-150	11	4,80E-06
dre-miR-155	10	4,94E-05
dre-miR-145	8	3,27E-04
dre-miR-196a	8	8,62E-04
dre-miR-15a*	4	4,73E-02
Cluster 2		
dre-let-7g	10	4,69E-04
dre-miR-27b	7	2,98E-03
dre-miR-16b	7	3,11E-03
dre-miR-10b	7	5,01E-03
dre-miR-16c	6	8,69E-03
dre-miR-27c	5	2,61E-02
dre-miR-17a*	4	2,95E-02
Cluster 3		
dre-miR-1	13	1,88E-06
dre-miR-10b	10	1,91E-04
dre-miR-216b	8	6,53E-03
dre-miR-732	6	1,64E-02
dre-miR-203b	5	3,10E-02
dre-miR-27b	5	3,88E-02
dre-miR-16b	5	3,88E-02

Supplementary Table 20. Putative targets deregulated by proteotoxic stress (Ala, Gly and Val mutants).

From the group of putative targets we determined for the deregulated miRNAs, we obtained a group of genes deregulated at the gene expression level in the Ala, Gly and Val mutant embryos.

MicroRNA	Putative target genes deregulated in Ala
miR-190b	*ncbp2*
miR-145	*tspan12, hic1, cxcr3.1,*
miR-130a	*elovl6*
miR-150	*rplp1, pik3r3, sod2, elovl6, tspan12*
miR-155	*lim2.4*
miR-203b	*sucla2*
let-7g	*zgc:110410, slc9a6a, fkbp11, pde10a, zgc:153997*

MicroRNA	Putative target genes deregulated in Gly
mir-145	*myom1a, mybpc1, mtnr1c*
mir-27c	*sult1st3, entpd2a.2, atic, nxf1, zgc:66484, b4galt1, si:ch211-216l23.2, ef1, fabp2, gyltl1b, slc25a28, hoxc13a, thrap6, aldh1a2, hoxc11a*

MicroRNA	Putative target genes deregulated in Val
mir-27c	*hsp90b1, sesn2, faz, zfand5a, mknk2b, rfx2, cth1, hoxc11a, bad, si:ch211-216l23.2, nfia, rbm39b, es1, ef1, nrarpa, nt5e, sdf2l1, slc25a28, arl3l2, axin1, nr1i2, qrsl1, gyltl1b, dus1l, qk, hoxc13a*
mir-732	*si:ch211-129c21.1, vasa, mospd2, bad, mdm2, bcap31, hey2, si:dkey-159a18.1, kpna4, tln1, smo, timm23, zgc:66433, nipa2, zar1, dbr1, edf1*

3.7. References

1. Drummond, D.A. and C.O. Wilke, *The evolutionary consequences of erroneous protein synthesis.* Nat Rev Genet, 2009. **10**(10): p. 715-24.
2. Reynolds, N.M., B.A. Lazazzera, and M. Ibba, *Cellular mechanisms that control mistranslation.* Nat Rev Microbiol, 2010. **8**(12): p. 849-56.
3. Koga, H., S. Kaushik, and A.M. Cuervo, *Protein homeostasis and aging: The importance of exquisite quality control.* Ageing Res Rev, 2011. **10**(2): p. 205-15.
4. Schroder, M. and R.J. Kaufman, *The mammalian unfolded protein response.* Annu Rev Biochem, 2005. **74**: p. 739-89.
5. Yang, J.R., S.M. Zhuang, and J. Zhang, *Impact of translational error-induced and error-free misfolding on the rate of protein evolution.* Mol Syst Biol, 2010. **6**: p. 421.
6. Bukau, B., J. Weissman, and A. Horwich, *Molecular chaperones and protein quality control.* Cell, 2006. **125**(3): p. 443-51.
7. Hageman, J., et al., *Comparison of intra-organellar chaperone capacity for dealing with stress-induced protein unfolding.* J Biol Chem, 2007. **282**(47): p. 34334-45.
8. Kaganovich, D., R. Kopito, and J. Frydman, *Misfolded proteins partition between two distinct quality control compartments.* Nature, 2008. **454**(7208): p. 1088-95.
9. Tyedmers, J., A. Mogk, and B. Bukau, *Cellular strategies for controlling protein aggregation.* Nat Rev Mol Cell Biol, 2010. **11**(11): p. 777-88.
10. Tabas, I. and D. Ron, *Integrating the mechanisms of apoptosis induced by endoplasmic reticulum stress.* Nat Cell Biol, 2011. **13**(3): p. 184-90.
11. Ron, D. and P. Walter, *Signal integration in the endoplasmic reticulum unfolded protein response.* Nat Rev Mol Cell Biol, 2007. **8**(7): p. 519-29.
12. Malhotra, J.D. and R.J. Kaufman, *The endoplasmic reticulum and the unfolded protein response.* Semin Cell Dev Biol, 2007. **18**(6): p. 716-31.
13. Bushati, N. and S.M. Cohen, *microRNA functions.* Annu Rev Cell Dev Biol, 2007. **23**: p. 175-205.
14. Farh, K.K., et al., *The widespread impact of mammalian MicroRNAs on mRNA repression and evolution.* Science, 2005. **310**(5755): p. 1817-21.
15. Mishima, Y., et al., *Zebrafish miR-1 and miR-133 shape muscle gene expression and regulate sarcomeric actin organization.* Genes Dev, 2009. **23**(5): p. 619-32.
16. Giraldez, A.J., et al., *MicroRNAs regulate brain morphogenesis in zebrafish.* Science, 2005. **308**(5723): p. 833-8.
17. Wienholds, E., et al., *MicroRNA expression in zebrafish embryonic development.* Science, 2005. **309**(5732): p. 310-1.
18. Soares, A.R., et al., *Dre-miR-2188 targets Nrp2a and mediates proper intersegmental vessel development in zebrafish embryos.* PLoS One, 2012. **7**(6): p. e39417.
19. Fish, J.E., et al., *miR-126 regulates angiogenic signaling and vascular integrity.* Dev Cell, 2008. **15**(2): p. 272-84.
20. Li, N., et al., *Regulation of endoderm formation and left-right asymmetry by miR-92 during early zebrafish development.* Development, 2011. **138**(9): p. 1817-26.
21. Zeng, L., A.D. Carter, and S.J. Childs, *miR-145 directs intestinal maturation in zebrafish.* Proc Natl Acad Sci U S A, 2009. **106**(42): p. 17793-8.
22. Morton, S.U., et al., *microRNA-138 modulates cardiac patterning during embryonic development.* Proc Natl Acad Sci U S A, 2008. **105**(46): p. 17830-5.
23. Flynt, A.S., et al., *Zebrafish miR-214 modulates Hedgehog signaling to specify muscle cell fate.* Nat Genet, 2007. **39**(2): p. 259-63.
24. Bartoszewski, R., et al., *The unfolded protein response (UPR)-activated transcription factor X-box-binding protein 1 (XBP1) induces microRNA-346 expression that targets the human*

antigen peptide transporter 1 (TAP1) mRNA and governs immune regulatory genes. J Biol Chem, 2011. **286**(48): p. 41862-70.

25. Byrd, A.E., I.V. Aragon, and J.W. Brewer, *MicroRNA-30c-2* limits expression of proadaptive factor XBP1 in the unfolded protein response.* J Cell Biol, 2012. **196**(6): p. 689-98.
26. Upton, J.P., et al., *IRE1alpha cleaves select microRNAs during ER stress to derepress translation of proapoptotic Caspase-2.* Science, 2012. **338**(6108): p. 818-22.
27. Dasuri, K., et al., *Amino acid analog toxicity in primary rat neuronal and astrocyte cultures: implications for protein misfolding and TDP-43 regulation.* J Neurosci Res, 2011. **89**(9): p. 1471-7.
28. Reina, C.P., X. Zhong, and R.N. Pittman, *Proteotoxic stress increases nuclear localization of ataxin-3.* Hum Mol Genet, 2010. **19**(2): p. 235-49.
29. Schiffer, N.W., et al., *Identification of anti-prion compounds as efficient inhibitors of polyglutamine protein aggregation in a zebrafish model.* J Biol Chem, 2007. **282**(12): p. 9195-203.
30. Silva, R.M., et al., *Critical roles for a genetic code alteration in the evolution of the genus Candida.* EMBO J, 2007. **26**(21): p. 4555-65.
31. Geslain, R., et al., *Chimeric tRNAs as tools to induce proteome damage and identify components of stress responses.* Nucleic Acids Res, 2010. **38**(5): p. e30.
32. Paredes, J.A., et al., *Low level genome mistranslations deregulate the transcriptome and translatome and generate proteotoxic stress in yeast.* BMC Biol, 2012. **10**(1): p. 55.
33. Kimmel, C.B., et al., *Stages of embryonic development of the zebrafish.* Dev Dyn, 1995. **203**(3): p. 253-310.
34. Soares, A.R., et al., *Parallel DNA pyrosequencing unveils new zebrafish microRNAs.* BMC Genomics, 2009. **10**: p. 195.
35. Saeed, A.I., et al., *TM4 microarray software suite.* Methods Enzymol, 2006. **411**: p. 134-93.
36. Saeed, A.I., et al., *TM4: a free, open-source system for microarray data management and analysis.* Biotechniques, 2003. **34**(2): p. 374-8.
37. Pfaffl, M.W., *A new mathematical model for relative quantification in real-time RT-PCR.* Nucleic Acids Res, 2001. **29**(9): p. e45.
38. Pfaffl, M.W., G.W. Horgan, and L. Dempfle, *Relative expression software tool (REST) for group-wise comparison and statistical analysis of relative expression results in real-time PCR.* Nucleic Acids Res, 2002. **30**(9): p. e36.
39. Huang da, W., B.T. Sherman, and R.A. Lempicki, *Bioinformatics enrichment tools: paths toward the comprehensive functional analysis of large gene lists.* Nucleic Acids Res, 2009. **37**(1): p. 1-13.
40. Huang da, W., B.T. Sherman, and R.A. Lempicki, *Systematic and integrative analysis of large gene lists using DAVID bioinformatics resources.* Nat Protoc, 2009. **4**(1): p. 44-57.
41. Carmona-Saez, P., et al., *GENECODIS: a web-based tool for finding significant concurrent annotations in gene lists.* Genome Biol, 2007. **8**(1): p. R3.
42. Nogales-Cadenas, R., et al., *GeneCodis: interpreting gene lists through enrichment analysis and integration of diverse biological information.* Nucleic Acids Res, 2009. **37**(Web Server issue): p. W317-22.
43. Holzschuh, J., et al., *Dopamine transporter expression distinguishes dopaminergic neurons from other catecholaminergic neurons in the developing zebrafish embryo.* Mech Dev, 2001. **101**(1-2): p. 237-43.
44. McLean, D.L. and J.R. Fetcho, *Ontogeny and innervation patterns of dopaminergic, noradrenergic, and serotonergic neurons in larval zebrafish.* J Comp Neurol, 2004. **480**(1): p. 38-56.

45. Zhang, J., et al., *MiR-145, a new regulator of the DNA fragmentation factor-45 (DFF45)-mediated apoptotic network.* Mol Cancer, 2010. **9**: p. 211.
46. Kent, O.A., et al., *Repression of the miR-143/145 cluster by oncogenic Ras initiates a tumor-promoting feed-forward pathway.* Genes Dev, 2010. **24**(24): p. 2754-9.
47. Shi, B., et al., *Micro RNA 145 targets the insulin receptor substrate-1 and inhibits the growth of colon cancer cells.* J Biol Chem, 2007. **282**(45): p. 32582-90.
48. Sachdeva, M., et al., *p53 represses c-Myc through induction of the tumor suppressor miR-145.* Proc Natl Acad Sci U S A, 2009. **106**(9): p. 3207-12.
49. Lin, Y.C., et al., *c-Myb is an evolutionary conserved miR-150 target and miR-150/c-Myb interaction is important for embryonic development.* Mol Biol Evol, 2008. **25**(10): p. 2189-98.
50. Urbich, C., et al., *MicroRNA-27a/b controls endothelial cell repulsion and angiogenesis by targeting semaphorin 6A.* Blood, 2012. **119**(6): p. 1607-16.
51. Stahlhut, C., et al., *miR-1 and miR-206 regulate angiogenesis by modulating VegfA expression in zebrafish.* Development, 2012. **139**(23): p. 4356-65.
52. Shimizu, T. and M. Hibi, *Formation and patterning of the forebrain and olfactory system by zinc-finger genes Fezf1 and Fezf2.* Dev Growth Differ, 2009. **51**(3): p. 221-31.
53. DeCarvalho, A.C., S.L. Cappendijk, and J.M. Fadool, *Developmental expression of the POU domain transcription factor Brn-3b (Pou4f2) in the lateral line and visual system of zebrafish.* Dev Dyn, 2004. **229**(4): p. 869-76.
54. Karlstrom, R.O., et al., *Genetic analysis of zebrafish gli1 and gli2 reveals divergent requirements for gli genes in vertebrate development.* Development, 2003. **130**(8): p. 1549-64.
55. Kim, S.H., et al., *Specification of an anterior neuroectoderm patterning by Frizzled8a-mediated Wnt8b signalling during late gastrulation in zebrafish.* Development, 2002. **129**(19): p. 4443-55.
56. Devine, C.A. and B. Key, *Robo-Slit interactions regulate longitudinal axon pathfinding in the embryonic vertebrate brain.* Dev Biol, 2008. **313**(1): p. 371-83.
57. Hartnett, L., et al., *Insulin-like growth factor-2 regulates early neural and cardiovascular system development in zebrafish embryos.* Int J Dev Biol, 2010. **54**(4): p. 573-83.
58. Niikura, Y., et al., *Zebrafish Numb homologue: phylogenetic evolution and involvement in regulation of left-right asymmetry.* Mech Dev, 2006. **123**(5): p. 407-14.
59. Aanstad, P., et al., *The extracellular domain of Smoothened regulates ciliary localization and is required for high-level Hh signaling.* Curr Biol, 2009. **19**(12): p. 1034-9.
60. Walker, M.B., et al., *Zebrafish furin mutants reveal intricacies in regulating Endothelin1 signaling in craniofacial patterning.* Dev Biol, 2006. **295**(1): p. 194-205.
61. Topczewska, J.M., et al., *The winged helix transcription factor Foxc1a is essential for somitogenesis in zebrafish.* Genes Dev, 2001. **15**(18): p. 2483-93.
62. Skarie, J.M. and B.A. Link, *FoxC1 is essential for vascular basement membrane integrity and hyaloid vessel morphogenesis.* Invest Ophthalmol Vis Sci, 2009. **50**(11): p. 5026-34.
63. Leslie, J.D., et al., *Endothelial signalling by the Notch ligand Delta-like 4 restricts angiogenesis.* Development, 2007. **134**(5): p. 839-44.
64. Kaur, S., et al., *Expression pattern for unc5b, an axon guidance gene in embryonic zebrafish development.* Gene Expr, 2007. **13**(6): p. 321-7.
65. Miyashita, T., et al., *PlexinA4 is necessary as a downstream target of Islet2 to mediate Slit signaling for promotion of sensory axon branching.* Development, 2004. **131**(15): p. 3705-15.
66. Sieger, D., D. Tautz, and M. Gajewski, *her11 is involved in the somitogenesis clock in zebrafish.* Dev Genes Evol, 2004. **214**(8): p. 393-406.

67. Phng, L.K., et al., *Nrarp coordinates endothelial Notch and Wnt signaling to control vessel density in angiogenesis.* Dev Cell, 2009. **16**(1): p. 70-82.
68. Waskiewicz, A.J., H.A. Rikhof, and C.B. Moens, *Eliminating zebrafish pbx proteins reveals a hindbrain ground state.* Dev Cell, 2002. **3**(5): p. 723-33.
69. Nornes, S., et al., *Independent and cooperative action of Psen2 with Psen1 in zebrafish embryos.* Exp Cell Res, 2009. **315**(16): p. 2791-801.
70. Mahler, J., A. Filippi, and W. Driever, *DeltaA/DeltaD regulate multiple and temporally distinct phases of notch signaling during dopaminergic neurogenesis in zebrafish.* J Neurosci, 2010. **30**(49): p. 16621-35.
71. White, Y.A., J.T. Kyle, and A.W. Wood, *Targeted gene knockdown in zebrafish reveals distinct intraembryonic functions for insulin-like growth factor II signaling.* Endocrinology, 2009. **150**(9): p. 4366-75.
72. Oates, A.C., C. Mueller, and R.K. Ho, *Cooperative function of deltaC and her7 in anterior segment formation.* Dev Biol, 2005. **280**(1): p. 133-49.
73. Monteiro, R., et al., *Two novel type II receptors mediate BMP signalling and are required to establish left-right asymmetry in zebrafish.* Dev Biol, 2008. **315**(1): p. 55-71.
74. Eimon, P.M., et al., *Delineation of the cell-extrinsic apoptosis pathway in the zebrafish.* Cell Death Differ, 2006. **13**(10): p. 1619-30.
75. Eimon, P.M. and A. Ashkenazi, *The zebrafish as a model organism for the study of apoptosis.* Apoptosis, 2010. **15**(3): p. 331-49.
76. Isayama, F., et al., *TNF alpha-induced Ras activation due to ethanol promotes hepatocyte proliferation independently of liver injury in the mouse.* Hepatology, 2004. **39**(3): p. 721-31.
77. Chipuk, J.E. and D.R. Green, *How do BCL-2 proteins induce mitochondrial outer membrane permeabilization?* Trends Cell Biol, 2008. **18**(4): p. 157-64.
78. Du, C., et al., *Smac, a mitochondrial protein that promotes cytochrome c-dependent caspase activation by eliminating IAP inhibition.* Cell, 2000. **102**(1): p. 33-42.
79. Li, J., B. Lee, and A.S. Lee, *Endoplasmic reticulum stress-induced apoptosis: multiple pathways and activation of p53-up-regulated modulator of apoptosis (PUMA) and NOXA by p53.* J Biol Chem, 2006. **281**(11): p. 7260-70.
80. Reimertz, C., et al., *Gene expression during ER stress-induced apoptosis in neurons: induction of the BH3-only protein Bbc3/PUMA and activation of the mitochondrial apoptosis pathway.* J Cell Biol, 2003. **162**(4): p. 587-97.
81. Pyati, U.J., et al., *p63 mediates an apoptotic response to pharmacological and disease-related ER stress in the developing epidermis.* Dev Cell, 2011. **21**(3): p. 492-505.
82. Arnaud, E., et al., *The zebrafish bcl-2 homologue Nrz controls development during somitogenesis and gastrulation via apoptosis-dependent and -independent mechanisms.* Cell Death Differ, 2006. **13**(7): p. 1128-37.
83. Zeng, L., et al., *The mouse Fused locus encodes Axin, an inhibitor of the Wnt signaling pathway that regulates embryonic axis formation.* Cell, 1997. **90**(1): p. 181-92.
84. Schneider, I., et al., *Zebrafish Nkd1 promotes Dvl degradation and is required for left-right patterning.* Dev Biol, 2010. **348**(1): p. 22-33.
85. Van Raay, T.J., et al., *Naked1 antagonizes Wnt signaling by preventing nuclear accumulation of beta-catenin.* PLoS One, 2011. **6**(4): p. e18650.
86. Kawano, Y. and R. Kypta, *Secreted antagonists of the Wnt signalling pathway.* J Cell Sci, 2003. **116**(Pt 13): p. 2627-34.
87. Sartori da Silva, M.A., et al., *Essential role for the d-Asb11 cul5 Box domain for proper notch signaling and neural cell fate decisions in vivo.* PLoS One, 2010. **5**(11): p. e14023.
88. Diks, S.H., et al., *The novel gene asb11: a regulator of the size of the neural progenitor compartment.* J Cell Biol, 2006. **174**(4): p. 581-92.

89. Hodkinson, P.S., et al., *Mammalian NOTCH-1 activates beta1 integrins via the small GTPase R-Ras.* J Biol Chem, 2007. **282**(39): p. 28991-9001.
90. Baek, D., et al., *The impact of microRNAs on protein output.* Nature, 2008. **455**(7209): p. 64-71.
91. Junge, H.J., et al., *TSPAN12 regulates retinal vascular development by promoting Norrin- but not Wnt-induced FZD4/beta-catenin signaling.* Cell, 2009. **139**(2): p. 299-311.
92. Xu, D., C. Sharma, and M.E. Hemler, *Tetraspanin12 regulates ADAM10-dependent cleavage of amyloid precursor protein.* FASEB J, 2009. **23**(11): p. 3674-81.
93. Fleuriel, C., et al., *HIC1 (Hypermethylated in Cancer 1) epigenetic silencing in tumors.* Int J Biochem Cell Biol, 2009. **41**(1): p. 26-33.
94. Tse, W.K., et al., *Genome-wide loss-of-function analysis of deubiquitylating enzymes for zebrafish development.* BMC Genomics, 2009. **10**: p. 637.
95. Hortopan, G.A. and S.C. Baraban, *Aberrant expression of genes necessary for neuronal development and Notch signaling in an epileptic mind bomb zebrafish.* Dev Dyn, 2011. **240**(8): p. 1964-76.
96. Ramel, M.C. and A.C. Lekven, *Repression of the vertebrate organizer by Wnt8 is mediated by Vent and Vox.* Development, 2004. **131**(16): p. 3991-4000.
97. Shin, D., et al., *Intrinsic and extrinsic modifiers of the regulative capacity of the developing liver.* Mech Dev, 2012. **128**(11-12): p. 525-35.
98. Kratz, E., et al., *Functional characterization of the Bcl-2 gene family in the zebrafish.* Cell Death Differ, 2006. **13**(10): p. 1631-40.
99. Penaloza, C., et al., *Cell death in development: shaping the embryo.* Histochem Cell Biol, 2006. **126**(2): p. 149-58.
100. Logan, C.Y. and R. Nusse, *The Wnt signaling pathway in development and disease.* Annu Rev Cell Dev Biol, 2004. **20**: p. 781-810.
101. Cau, E. and P. Blader, *Notch activity in the nervous system: to switch or not switch?* Neural Dev, 2009. **4**: p. 36.
102. Ingham, P.W. and A.P. McMahon, *Hedgehog signaling in animal development: paradigms and principles.* Genes Dev, 2001. **15**(23): p. 3059-87.
103. Briscoe, J. and B.G. Novitch, *Regulatory pathways linking progenitor patterning, cell fates and neurogenesis in the ventral neural tube.* Philos Trans R Soc Lond B Biol Sci, 2008. **363**(1489): p. 57-70.
104. Kume, T., *Novel insights into the differential functions of Notch ligands in vascular formation.* J Angiogenes Res, 2009. **1**: p. 8.
105. Clevers, H., *Wnt/beta-catenin signaling in development and disease.* Cell, 2006. **127**(3): p. 469-80.
106. Yang, Y., *Wnt signaling in development and disease.* Cell Biosci, 2012. **2**(1): p. 14.
107. Leung, A.K. and P.A. Sharp, *MicroRNA functions in stress responses.* Mol Cell, 2010. **40**(2): p. 205-15.
108. Chen, P.Y., et al., *The developmental miRNA profiles of zebrafish as determined by small RNA cloning.* Genes Dev, 2005. **19**(11): p. 1288-93.

Chapter 4 - Establishing a zebrafish transgenic line to study proteotoxic stress

Marisa Reverendo, Ana Soares, Patrícia Pereira, Manuel Santos

Manuscript in preparation

4. Establishing a zebrafish transgenic line to study proteotoxic stress

4.1. Abstract

Proteotoxic stress in vertebrates is associated withl ageing and conformational diseases. However, it is still unclear how proteome instability and protein aggregation cause human diseases and accelerate ageing processes. To clarify this question we have produced a transgenic zebrafish line that expresses a misreading serine tRNA that destabilizes the proteome, increases protein aggregation and generates proteotoxic stress. The transgenic fish recapitulate the expression pattern of heat shock proteins, accumulation of protein aggregates and mitochondrial network morphology alterations, observed in cells exposed to proteotoxic stress. We have also observed deregulation of miR-145, which is involved in gut development, miR-1 that regulates muscle gene expression and angiogenesis and miR-27c which is present in zebrafish embryo stages. This transgenic line will permit detailed study of the effects of proteotoxic stress in different physiological contexts, during development and in fully differentiated adult tissues.

4.2. Introduction

Accurate protein synthesis and tight control of protein folding and degradation are absolutely essential for cell functioning and homeostasis [1, 2]. However, synthesis errors can lead to protein misfolding, aggregation and degradation. Eukaryotic cells possess a protein surveillance and quality control network composed by molecular chaperones, endoplasmic reticulum (ER) associated degradation pathway (ERAD), autophagy and the ubiquitin proteasome pathway (UPP) that handle aberrant proteins. Molecular chaperones are a fundamental component of the proteostasis network as they participate in several cellular processes, especially in the folding/refolding and assembly steps and also in the deposition and degradation of aggregated and misfolded proteins [3, 4]. These molecules are classified in several sub-classes according to their molecular weight, namely HSP100, HSP90, HSP70, HSP40 and the small heat shock proteins (sHSP), these chaperones recognize and refold misfolded or aggregated proteins [3, 4]. Saturation of this chaperone network, high level of synthesis of aberrant proteins, ageing and environmental insults results in the accumulation of misfolded proteins in cytoplasm and in the ER. These proteins tend to accumulate in aggregated structures which are characteristic of human conformational diseases [5]. The ER is also important in this process as it handles the proteins destined for the secretory pathway and articulates numerous signaling pathways. The ER stress response (UPR) is central in this signaling network as it restores homeostatic control of this organelle and provides downstream signals to other sub-cellular locations. Signaling from the stressed ER shapes cellular proliferation, inflammation, apoptosis and is connected with mitochondrial dynamics and physiology [6]. Indeed, ER stress can initiate apoptosis through the BCL family and high levels of ER oxidative stress or deregulated calcium

signaling trigger mitochondrial alterations. In our previous work (chapter 2), we showed that protein synthesis errors drive mitochondrial dysfunction, suggesting that aberrant protein synthesis is an efficient proteotoxic stress activator.

A mistranslation mouse model has highlighted the biological and biomedical relevance of protein synthesis errors. Mice harboring a mutant alanyl-tRNA synthetase that charges alanine tRNAs with serine accumulate misfolded proteins and display extensive neuronal damage [7]. Moreover, mRNA mistranslation models using misreading tRNAs have been established in yeast [8], human cell lines, chick embryos [9] and in zebrafish embryos (chapter 2). These models demonstrated that mutant tRNAs are an excellent proteotoxic stress generator and that zebrafish is a good model to study the effects of mRNA mistranslation on vertebrates. Indeed, zebrafish embryos have several advantages, namely short generation time, high conservation of zebrafish and human genomes and gene functions, external developmental and optical transparency that greatly facilitate embryo manipulation, and finally availability of techniques that allow for gene overexpression and knockdown that facilitate *in vivo* analysis of gene function [10-12]. Zebrafish embryos also allow for direct observation of embryogenesis and are promising models for ageing and conformational diseases studies since the zebrafish nervous system mirrors the major aspects of the human nervous system and unlike mammals zebrafish have regenerative capabilities in several tissues [13-15]. These characteristics of the zebrafish model prompted us to produce transgenic fish to evaluate the role of mistranslation on proteotoxic stress, ageing and disease. Our system is based on a mutant zebrafish Ser-tRNA that introduces errors at the leucine CTG codon into polypeptides during mRNA translation, thus producing a randomly mutated proteome. Importantly, this model will allow for the evaluation of proteotoxic stress in the whole organism at developmental and adult stages. Our

previous work established a link between proteotoxic stress and miRNA regulation. MicroRNAs are 20-22 nucleotide long small non-coding RNAs that are capable of regulating translation and decay of their target mRNAs [16, 17]. These small RNAs are evolutionary conserved in Eukarya and have the potential to target several different mRNAs. Importantly, miRNAs are known to participate in several developmental and pathological processes [18]. In zebrafish, miRNAs are fundamental for embryo development and exert their functions at various levels, for example driving neurogenesis [19], regulating angiogenesis and vascular integrity [20], and modulating organ and embryo patterning [21, 22]. Interestingly, recent studies have shown that miRNAs are involved in cellular stress response modulation trough the interaction with the ER stress response adaptors XBP1 and IREα.

Our preliminary results show induction of molecular chaperones Hsp70 and Hsp90, accumulation of intracellular protein aggregates and morphological alterations in the mitochondrial network. Furthermore, this transgenic zebrafish model also allows for studying miRNA regulation in response to proteotoxic stress and will be an important tool to study the effects of proteotoxic stress on ageing, neurological degeneration and disease development.

4.3. Material and methods

4.3.1. Zebrafish husbandry and mutant serine tRNA plasmid construct

Zebrafish (AB strain) were maintained at 28ºC on a 14 h-light/10 h-dark cycle. Stages of embryonic development were determined based on the number of hours after fertilization and morphological standards [23]. Zebrafish maintenance followed the Portuguese law for animal experimentation (Regulatory Guideline nº 1005/92, October 23rd, 1992). Endogenous Ser-tRNA genes and flanking regions were amplified from zebrafish genomic DNA and digested with BgLII restriction enzymes. The fragments were cloned into the pT2AL200R150G [24] vector producing the plasmid pT2tRNA^{Ser}. Mutant Ser-tRNA^{Leu} construct was produced using the plasmid pT2tRNA^{Ser} by site directed mutagenesis of nucleotide positions corresponding to the anticodon of the mature Ser-tRNA to leucine CAG anticodon. Mutation was selected according to similarity of amino acid properties, blossom score, codon usage and total codon counts (Chapter 2). The empty and tRNA plasmids (endogenous and Ser-tRNA^{Leu}) were injected into zebrafish embryos at one-cell stage, the injected solution contained 25ng/µl of circular plasmid DNA and 25 ng/µl transposase mRNA. The transposase mRNA was synthesized from PCS-TP [11] as described in [25]. Founder embryos were staged in system water and observed under a stereo-microscope equipped with a GFP fluorescence filter (Nikon). GFP positive fish were selected, maintained and crossed with wild type to obtain heterozygotic F1 transgenic fish. F2 of empty construct, endogenous Ser-tRNA and Ser-tRNA$^{Leu}_{CAG}$ generations were produced by crosses of the F1 populations.

4.3.2. Northern blot analysis

Total RNA of 24hpf embryos were resolved on 15% polycralyamide gels for 18 hours at 500V. The section of gel containing the tRNAs was semi-dry transferred to a nitrocellulose membrane (Hybond N, Amershan) and membranes were cross linked using a UV Stratalinker-1800 from Stratagene. Probes were prepared by 5' phosphorylation of 10pmol of short oligonucleotides with γ-^{32}P-ATP. Membranes were hybridized overnight at the oligos Tm minus 5 degrees with rotation, washed and then exposed to a K-screen and scanned using a Molecular Imager FX (Bio-Rad).

4.3.3. Southern blot analysis

Genomic DNA was isolated from tail clips and 2-4µg of DNA, digested with EcoRI and resolved on a 1% agarose gel. Fractioned DNA was transferred to nylon membrane (Hybond N+, Amersham) by capillary blotting and cross-linked using ultraviolet irradiation. Membranes were probed with γ-^{32}P labeled GFP oligo probe. Membranes were hybridized overnight at 42ºC with rotation, washed and then exposed to a K-screen and scanned using Molecular Imager FX (Bio-Rad).

4.3.4. Western immunoblotting

For western blot analysis 24hpf embryos were dechorionated and deyolked [26]. Whole embryos lysates were extracted using 1x SDS sample buffer at 95ºC for 5 minutes. Approximately 50 µg/lane of protein were loaded on 12% or 15% SDS–PAGE minigels. After electrophoresis the proteins were wet transferred to nitrocellulose membrane and blocked. Blocked membranes were incubated with primary antibodies: anti-GFP (Clontech), anti-β-tubulin (Invitrogen), anti-HSP90 (StressMarq) and anti-HSP70 (StressMarq) diluted in TBS-T with 5% LFM. Detection was performed using a

secondary antibody labeled with an infrared dye (IRDye 800CW, Li-COR) at room temperature in the dark. Membranes were scanned and analyzed using the Odyssey® IR scanner and images were analyzed using Odyssey® imageing software 3.0 with default settings. The results obtained are expressed as the relative percentage normalized for control sample values.

4.3.5. HSPB1 mCherry fusion reporter

The mCherry gene was cloned into BamHI and ClaI sites of the pT2AL200R150G vector [24] replacing the GFP gene. *HSPB1* promoter [27] and coding region (without stop codon) were amplified from zebrafish genomic DNA and cloned sequentially at XhoI, SalI and Sal, BamHI sites of the pT2AL200R150G-mCherry vector. A mixture of the mCherry fusion reporter and mutant tRNA plasmids was injected in phenol red/KCl in one-cell stage embryos and embryos were observed under an epifluorescence microscope (Zeiss) and photographed using GFP and mCherry filters.

4.3.6. Acridine orange staining

Acridine orange (AO) is a cell permeable nucleic acid dye which is sequestered by lysosomes and does not enter the nucleus. However, upon cell death intracellular pH changes and AO is released into the cytoplasm. For cell death staining, 24hpf embryos were washed and dechorionated. Live embryos were stained for apoptotic cells with 5µg/ml AO for 30 min in the dark. After incubation, embryos were washed with system water and photographed using an epifluorescence microscope. Fluorescent images were obtained using an Imager.Z1 (Zeiss), AxioCam HRm camera (Zeiss) and AxioVision software (Zeiss).

4.3.7. Mitochondria staining

Live imageing of mitochondria in zebrafish was carried out using MitoTracker® Red CM-H2XRos (Molecular Probes®). 24hpf embryos were dechorionated and incubated with MitoTracker 500nM for 30 mins in the dark. For imageing, anesthetized zebrafish embryos were embedded in methyl cellulose and overlayed with vectashield. Mito Tracker fluorescence was documented by epifluorescence microscopy. Fluorescence images were obtained using an Imager.Z1 (Zeiss), a Rhod 20 filter, AxioCam HRm camera (Zeiss) and AxioVision software (Zeiss).

4.3.8. Total RNA extraction

Total RNA was extracted using Trizol® according to manufacturer´s instructions. Briefly, 200 24hpf embryos were collected, dechorionated and stored at -80ºC. Frozen embryo pellets were ressuspended in 1mL of TRIZOL and disrupted using precellys 24 (Bertin technologies). The total extracts were incubated at room temperature for 5 minutes and further extracted with chlorophorm and isopropyl alcohol. Total RNA pellets were washed with 75% ethanol and ressuspended in milliQ water. To remove contaminating DNA, samples were treated with DNAseI (Fermentas) following the manufacturer instructions and stored at -80ºC. RNA was quantified using Nanodrop 1000 Spectrophotometer (Thermo Scientific) and quality was verified using the Agilent 2100 Bioanalyzer.

4.3.9. Real-time quantitative PCR

Quantification of miRNA expression was carried out using NCode™ miRNA First-Strand cDNA module and Platinum® SYBR® Green qPCR Super Mix-UDG (Invitrogen). Total RNA was extracted using Trizol® and treated with DNAseI. Total

RNA was polyadenylated and used to produce cDNA. cDNA was prepared from 500ng of total polyadenylated RNA using Superscript III (Invitrogen) according to the manufacturer´s instructions. Real-time Quantitative PCR was carried out using the ABI Prism 7500 Sequence Detector System (Applied Biosystems). The reactions were carried out at 95ºC for 2 min, 95ºC for 15s and 60ºC for 30s with 50 repetitions. The threshold cycle data (CT) and baselines were determined using auto settings. All assays, including no template controls, were performed in triplicate and relative quantification of gene expression was calculated by the $2^{-\Delta\Delta CT}$ method [28], where the control sample was the endogenous serine tRNA and the experimental internal control was U6 small RNA (RNU6B). Probes were U6: 5'-GACACGCAAATTCG TGAAGCGTTCCATA-3', mir-145: 5'-GTCCAGTTT TCCCAGGAATCCC-3', mir-1: 5'-TGGAATGTAAAGAAGTATGTAT-3' and mir-27c: 5'-TTCACAGTGGTTAAG TTCTGC-3'. All the analyses were carried out using REST-MCS tool [29].

4.3.10. MicroRNA target prediction

The miRNA targets were identified with the Eimmo (MirZ) [30], miRBASE Targets [31] and TargetScan Fish [32] databases. The computational targets were considered when they were retrieved from at least two of the algorithms.

4.3.11. Statistical analysis

Data was analyzed using GraphPad Prism. The differences between control and conditioned embryos were assessed by Student's t-test or ANOVA with post test Dunnett's Multiple Comparison Test. In all cases, p values < 0.05 were considered statistically significant.

4.4. Results

4.4.1. Transgenesis system

In this study we used the mutant Ser-tRNA$_{CAG}^{Leu}$ described earlier in this thesis as a generator of proteotoxic stress (Figure 4.1A). We chose this particular mutant tRNA because our previous results showed that it was the most efficient proteotoxic stress generator. For this, an endogenous zebrafish Ser-tRNA was amplified and mutated in the anti-codon region by site directed mutagenesis to yield the mutant Ser-tRNA harbouring the CAG leucine anti codon. This mutant tRNA is charged with Ser because the seryl-tRNA synthetase (SerRS) does not recognize the anticodon arm and mutations in this structural domain do not affect tRNA charging specificity [33, 34]. The transgenic fish were produced using the Tol2 system, a transposon based method of DNA integration into chromosomal DNA that already harbors the eGFP gene, which is useful to follow transgene integration (Figure 4.1B) [25]. Tol2 is a eukaryotic class II transposon, which moves via excision and integration without replication. Upon mobilization the transposase cleaves the DNA through binding to its terminal inverted repeats, cuts and inserts foreign DNA at the target site and finally the host DNA repair mechanisms repair and link the inserted cuts [35]. The non-autonumus Tol2 construct has been optimized so that it cannot transpose by itself. The transposon sequence was also reduced to the minimal Tol2 cis-sequence and minimal subterminal repetitive sequences in order to remove unnecessary part of the vector that might affect the gene cloned in the construct [24].

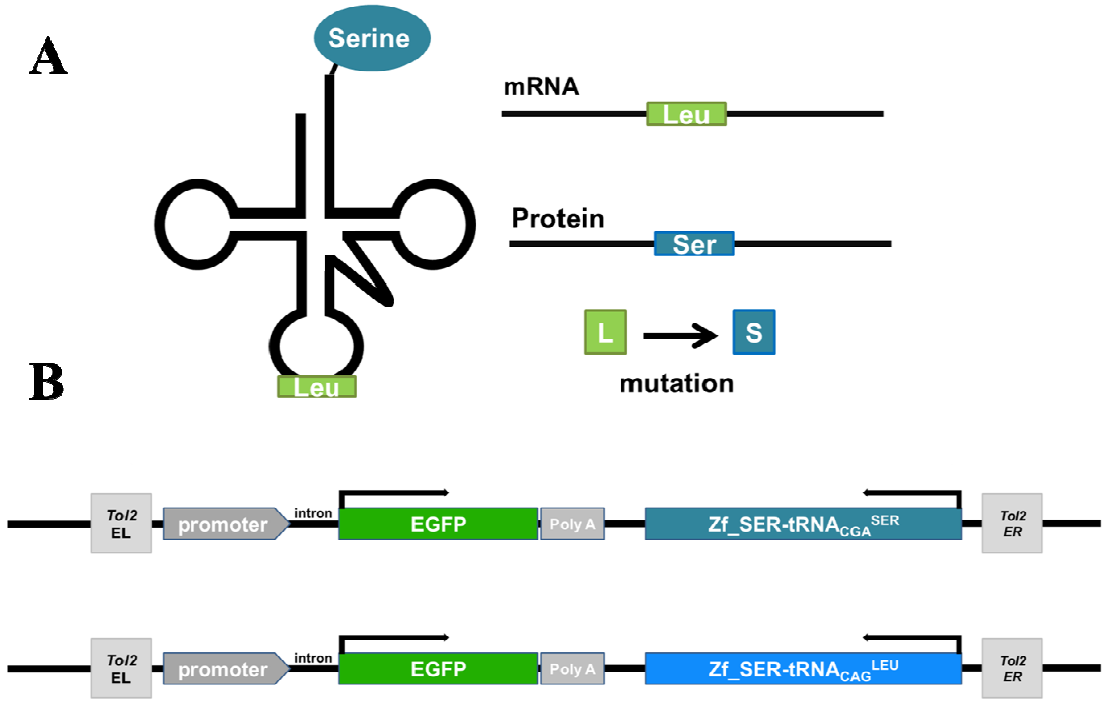

Figure 4.1. Mistranslation model and plasmid construct.
A) The zebrafish endogenous Ser-tRNA$_{CGA}$ gene was altered in the anticodon region by site directed mutagenesis in order to replace the original anticodon with the leucine CAG anticodon. This mutant Ser-tRNA$_{CAG}^{Leu}$ inserts Ser at Leu CUG codons on a global scale, destabilizing the proteome. **B)** The WT and mutant tRNAs were cloned in the vector pT2AL200R150G [1] and co-microinjected with the transposase mRNA into 1 cell stage zebrafish embryos.

For transposition the minimal Tol2 construct requires transposase in trans which is achieved by co-injecting the construct and transposase mRNA into zebrafish embryos. In order to detect the expression and processing of the mutant tRNA and insertions of the construct into zebrafish embryos we performed Northern and Southern blot analysis (Figure 4.2A, Supplementary Figure 1). The results show that the mutant Ser-tRNA$_{CAG}^{Leu}$ was stably expressed in F2 fish and that transgenesis resulted in single insertions for the WT construct and the mutant tRNA genes. Mutant tRNA decoding activity was indirectly assessed by measuring GFP fluorescence levels.

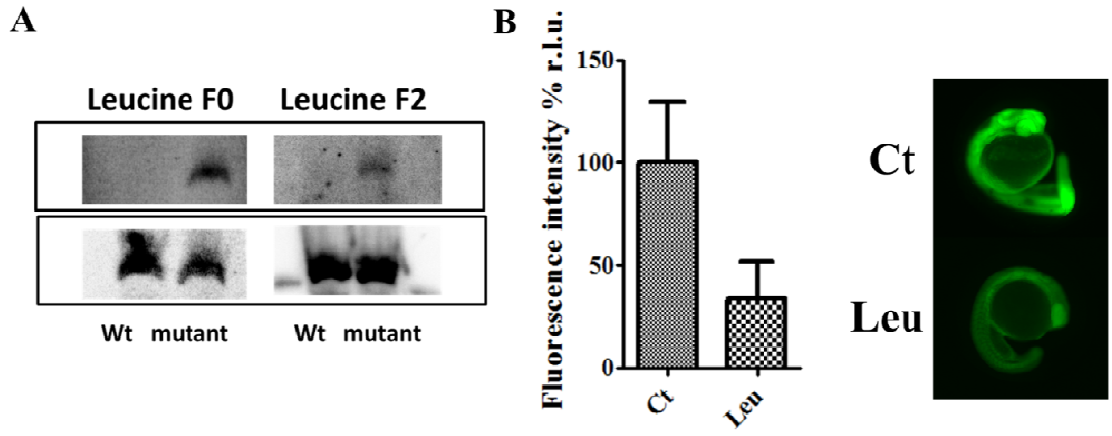

Figure 4.2. tRNA detection and activity.
A) Northern blot analysis showing expression of the mutant serine tRNA. **B**) GFP fluorescence levels were used to monitor the activity of the mutant tRNA. The EGFP gene contains 18 CTG codons and serine misincorporation at these sites, in single or multiple insertions, reduced or shifted GFP fluorescence. Data are presented as the mean ± SD (n =2). Relative fluorescence units are relative to control.

Since the eGFP gene has 18 CTG codons targeted by the mutant Ser-tRNA$_{CAG}^{Leu}$, which are distributed through the entire length of the GFP gene, we were expecting significant decrease in GFP fluorescence due to misincorporation of Ser at the Leu CTG sites. After normalization (by the total amount of GFP detected by western blot) GFP fluorescence levels were significantly lower in the embryos expressing the Ser-tRNA$_{CAG}^{Leu}$, fluorescence levels were reduced up to 34% probably to the cumulative effect of several leucine to serine substitutions (Figure 4.2B), as we have predicted.

4.4.2. Transgenics early development

Transgenic zebrafish expressing the Ser-tRNA$_{CAG}^{Leu}$ were analyzed regarding general phenotypic aspects at 24hpf, 5dpf and 2 months. Ser-tRNA$_{CAG}^{Leu}$ transgenics displayed reduced viability at 24hpf (56% of survival) which decreased to 34% at 5dpf (Figure 4.3A-B). Morphological alterations were observed as a result of the expression of the Ser-tRNA$_{CAG}^{Leu}$. Indeed, at 24hpf 37% of the embryos showed several

malformations, mainly undeveloped head and body regions (Figure 4.4A). At 5dpf 34% of the embryos had malformations, including reduced pigmentation, reduced body size and some maintained heart edema (Figure 4.4B). At 2 months post fertilization the surviving embryos had shorter body length (decreased from approximately 1.17cm to 0.71cm) (Figure 4.4C), thus supporting our previous results presented in chapter 3. In other words, mistranslation of CTG codons by the mutant tRNA affected embryo development, nonetheless the effects observed in transgenic fish were inferior in magnitude relative to those discussed in chapter 3, suggesting that the tRNA levels may be reduced in this system or even that stable integration into the genome may allow the cell to stabilize mutant tRNA expression at low level.

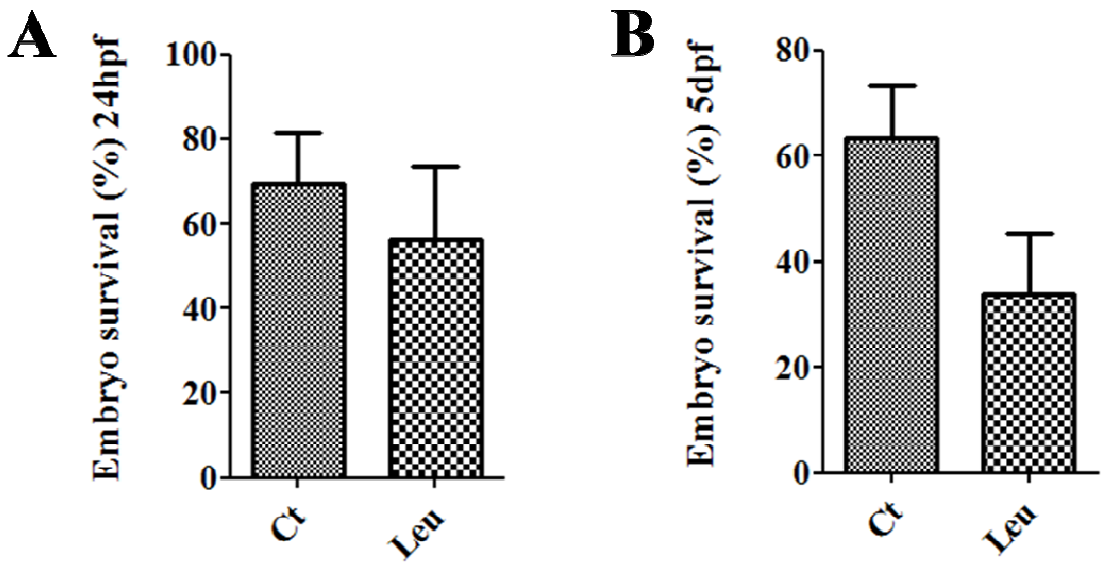

Figure 4.3. Transgenic embryo suvival.
Embryo survival was determined at 24hpf (**A**) and at 5dpf (**B**). Mistranslating embryos had a lower (56% and 37%) survival at 24hpf and 5dpf, relative to control embryos. Control embryos refer to non-mistranslating embryos harboring the endogenous tRNA construct. Data are presented as the mean ± SD (n =3).

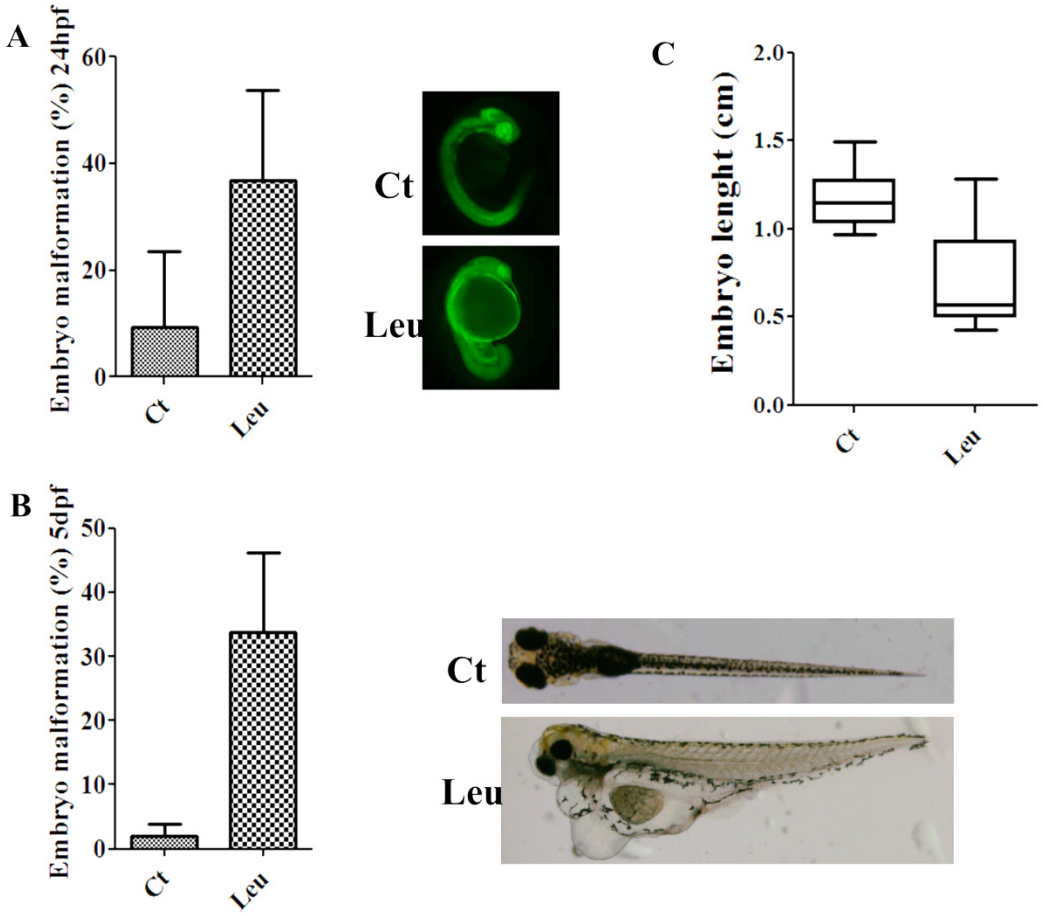

Figure 4.4. Phenotypic analysis of mistranslating transgenic zebrafish.
A) The expression of the mutant serine tRNA produced morphological alterations in zebrafish embryos at 24hpf (A) and at 5dpf (**B**). Data are presented as the mean ± SD (n =3). **C**) Embryo length at 2 months is reduced from 1.17cm to 0.71cm) in mutant tRNA transgenics. Data are presented as the mean ± SD (n =3).

4.4.3. Transgenics recapitulate several proteotoxic stress features

Our previous work on the cellular effects of proteotoxic stress in zebrafish embryos showed that mistranslating tRNAs activate the general stress response and that these embryos are a good model system to tackle the biology of proteotoxic stress and proteome instability. We have monitored the impact of mistranslation in our transgenic fish by quantifying heat shock expression and accumulation of protein aggregates. We have analyzed the induction of Hsp90 and Hsp70 by western blotting and the results showed increased levels of both chaperones in the transgenic mistranslating fish **(**Figure 4.5**).**

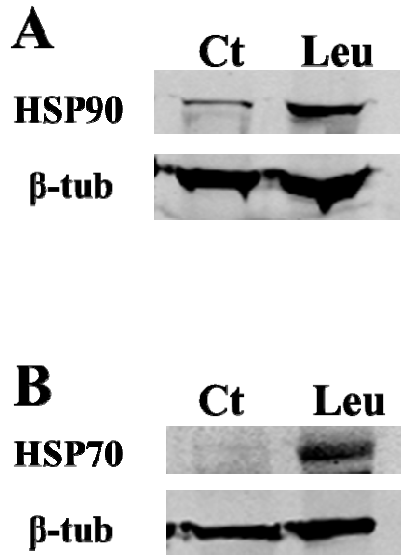

Figure 4.5. Mistranslation up regulates expression of molecular chaperones.
Western blot analysis of control and proteotoxic stress transgenics showing up-regulation of molecular chaperones HSP90 (**A**) and HSP70 (**B**).

Additionally we used the fusion reporter of mCherry-HSP27 described earlier (chapter 2) to monitor protein aggregation (Figure 4.6). There was a clearly visible increase in protein aggregates in response to mRNA mistranslation.

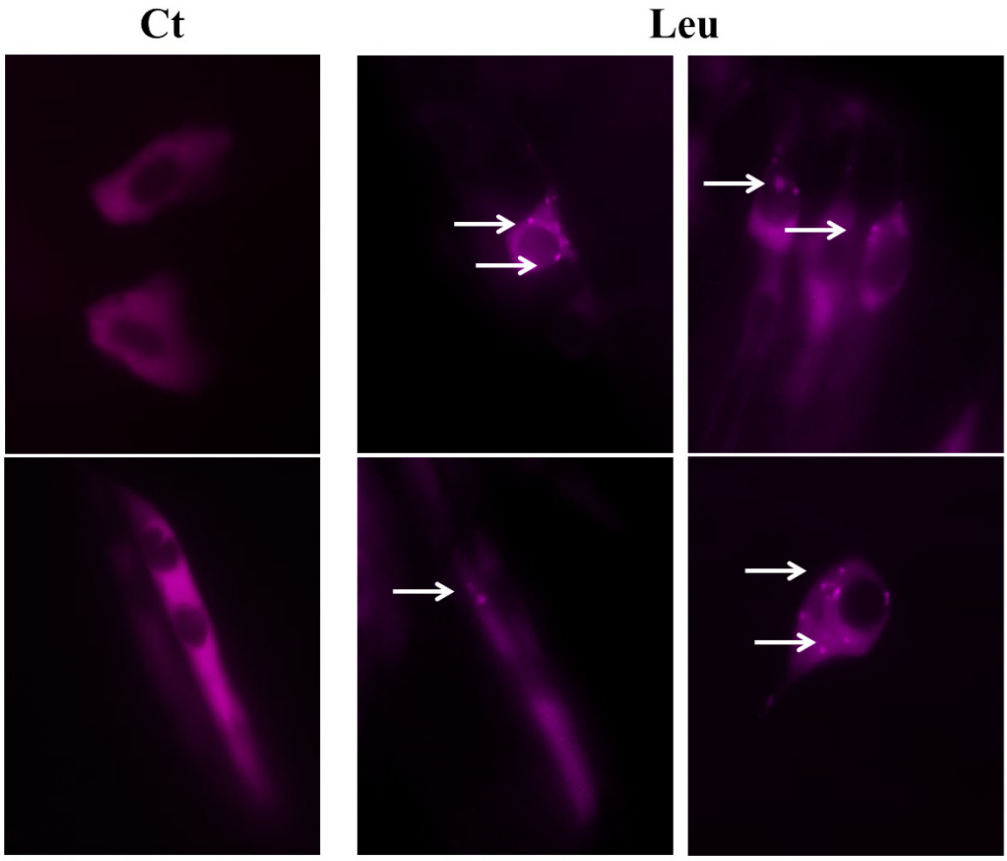

Figure 4.6. Protetoxic stress transgenic zebrafish accumulate intracellular protein aggregates.
The accumulation of protein aggregates was monitored using a HSPB1-mCherry fusion protein by fluorescence microscopy at 24hpf. The molecular chaperone HSPB1 (HSP27) binds to aggregated proteins and can be used to monitor their accumulation in the cell when fused to a fluorescent probe. In the control zebrafish, fluorescence was evenly distributed throughout the cytoplasm, while in the mistranslating zebrafish there was formation of fluorescent foci which is indicative of the presence of protein aggregates.

This prompted us to further investigate if the transgenic fish also displayed the apoptotic phenotype and mitochondrial network alterations associated with proteotoxic stress observed in the embryos described in chapeter 2. Acridine orange labelling showed extensive staining in the transgenics expressing the mutant tRNA (Figure 4.7)

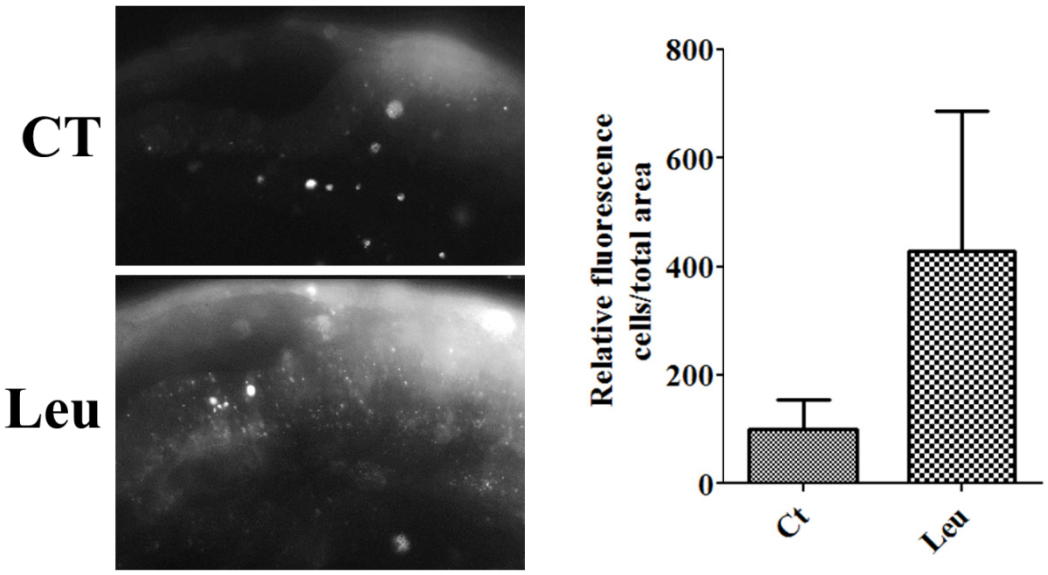

Figure 4.7. Protetoxic stress induced by mistranslations increased apoptosis.
A) Transgenic zebrafish expressing the control and mistranslating tRNAs were stained at 24hpf with acridine orange. Lateral view of the head region of the mistranslating embryos expressing the Ser-$tRNA_{CAG}^{Leu}$. **B**) The mistranslating zebrafish displayed extensive staining, indicating increased levels of apoptosis. Data shown are the mean ± SD (n =3). Units are relative to control sample in percentage

The structure of the mitochondrial network was analyzed by means of staining the embryos with the mitochondrial dye MitoTracker® Red CM-H2XRos (Molecular Probes®). There was significant alteration of the morphology of the mitochondrial network; the mitochondria were mainly small and spherical in contrast with the morphology of the mitochondria of the control embryos which was tubular (Figure 4.8).

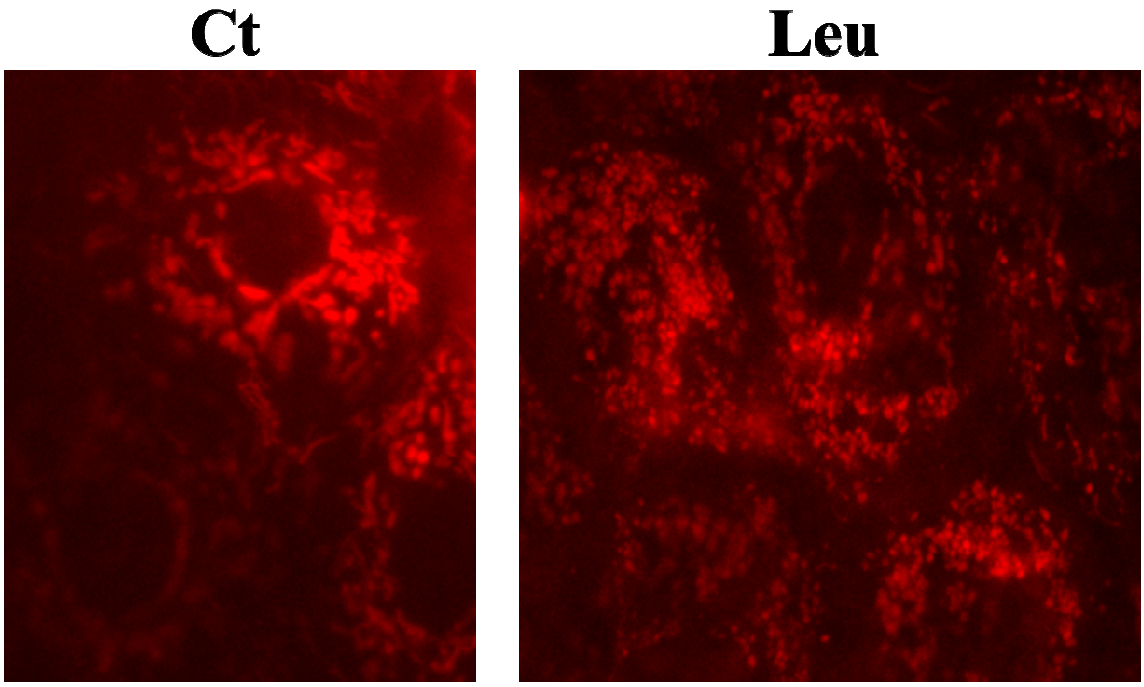

Figure 4.8. Mistranslation has a strong impact on the mitochondrial network.
Control and mistranslation transgenic zebrafish were stained with Mito TrackerRed® at 24hpf and observed with fluorescence microscopy. The structure of the mitochondrial network was disrupted in the mistranslating transgenic fish, in particular there was an increase in fluorescent foci indicating that most mitochondria were spherical and individualized.

4.4.4. MiRNA expression driven by proteotoxic stress

Since proteotoxic stress has a profound effect on gene expression we have investigated whether it would impact miRNA expression. Since miRNAs play a key role in post-transcriptional gene regulation we have determined if the deregulated miRNAs we detected previously (chapter 3) were also deregulated in this transgenic zebrafish model. For this, we have quantified miR-145 and miR-27c that were deregulated in embryos expressing several mutant tRNAs and miR-1 which is important for muscle cell development and was deregulated by the Ser-$tRNA_{CAG}^{Leu}$. Analysis by qPCR confirmed the deregulalated previously observed, and we detected 1.5, -1.5, -2.2 fold deregulation for mir-145, mir-1 and miR-27c respectively. Putative targets of these deregulated miRNAs were predicted using the Eimmo, miRBASE targets and TargetScan Fish algorithms and were considered only when they were identified by at

least two of these databases. The putative targets for these miRNAs (Supplementary Tables 1, 2, 3) have detailed described earlier in chapter 3. We can highlight several targets of miR-145 such as *dll4*, *unc5b*, *plxna4* and *rbpja* which are involved in transcription, cellular and development processes, and angiogenesis [36-39]. Putative targets of miR-1 are mainly related to embryo and cell morphogenesis, development and transcription, examples are the validated targets *arpc4l*, *pfn2l* and *copz1* which participate in the regulation of actin binding and vesicular transport [40]. Finally, predicted targets of miR-27c are related to cell cycle and cellular processes, development and patterning, transcription and apoptosis. Of the targets involved in apoptosis we can highlight the putative targets *apaf1*, *fas*, *bad*, *dffb*, and *bcl2*. Globally, our data show that the response to misreading tRNAs in the transgenic fish is consisted with what we observed in the zebrafish model, supporting the idea that that misreading tRNAs are a good tool to study proteotoxic stress.

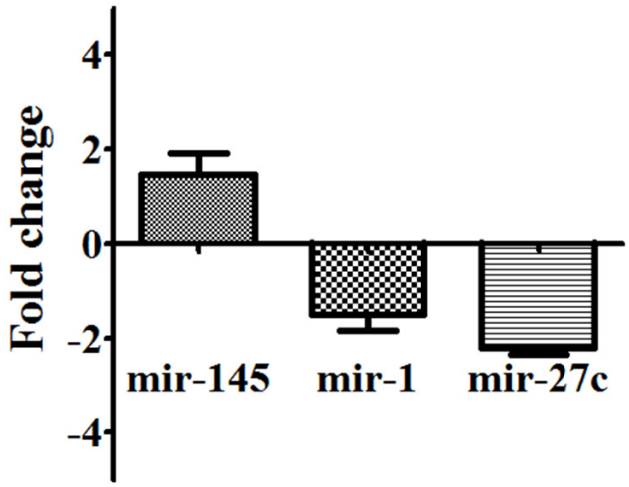

Figure 4.9. Mistranslation deregulated miRNA expression.
Fold change deregulation of miR-145, miR-1 and miR-27c. This group of miRNAs was examined because we detected them in our previous study. Fold variation was determined by qPCR using U6 small RNA as the internal control. qPCR results were normalized and fold changes calculated using REST software.

4.5. Discussion

This work describes the generation of stable transgenic zebrafish expressing a mutant tRNA that incorporates Ser at Leu CTG sites. This is the first transgenic zebrafish for studying proteotoxic stress induced by mRNA mistranslation. This transgenic fish reinforces the notion that proteome imbalance produced by mRNA mistranslation impacts negatively on cellular homeostasis and embryo development. Our previous work described in chapters 2, 3 showed that the Ser-tRNA$_{CAG}^{Leu}$ was a strong stress inducer and a good tRNA for studying the biology of proteotoxic stress in a multicellular organism. The results presented in this chapter are in line with our earlier studies since the transgenic zebrafish expressing the Ser-tRNA$_{CAG}^{Leu}$ showed reduced survival, embryonic morphological alterations and reduction in body length. We further saw that transgenic fish have increased levels of Hsp70 and Hsp90 and accumulated protein aggregates, which are important biomarkers of proteotoxic stress [41]. The transgenic fish also have significant alterations in the morphology of the mitochondrial network highlighting important roles of proteotoxic stress on the dynamics and homeostasis of mitochondria.

In this work we confirmed that the mutant Ser-tRNA$_{CAG}^{Leu}$ can deregulate miRNA expression. Our data confirmed the deregulation of mir-145, mir-1 and mir-27c induced by proteotoxic stress in the transgenic fish (see also chapter 3). The miR-145 regulates the development of the gastrointestinal tract [42, 43], suggesting that development of this particular organ system may be greatly affected by proteotoxic stress conditions. MiR-145 has been described as a tumor suppressor miRNA due to its interaction with anti-apoptotic factors and pro-apoptotic activity [44-46]. The pro-apoptotic ability of this miRNA correlates with the increased levels of apoptosis observed in mistranslating

embryos, suggesting that this miRNA might be a key effector of proteotoxic stress. In a recent work [47], a mutant Ser-tRNA with an anticodon coding for isoleucine has suppressed tumor development in a xenograft mouse model. In this model the proteotoxic stress generated by the Ser-tRNA^{Ile} increased apoptosis levels and reduced tumor cell viability. Our work shows that proteotoxic stress up regulates several tumor suppressor miRNAs, namely miR-145 (chapter 3) and it is tempting to speculate that miRNA induction by proteotoxic stress may be involved in the anti tumoral mechanism mediated by mutant tRNAs [47]. The putative targets of miR-1 and miR-27c are involved is various cellular and physiological processes. From the targets of these three miRNAs we can highlight those involved in embryo patterning, cell cycle and morphogenesis and transcriptional control. Interestingly, several apoptotic factors, namely *traf4b*, *dffb*, *apaf1*, *faz*, *bad* and *bcl2*, are putative targets of miR-27c, suggesting that repression of this miRNA facilitates the apoptotic process. MiR-1 has been identified as a muscular miRNA with important roles in development of muscle tissues, and is involved in heart diseases such as hypertrophy [48-50]. In zebrafish, this miRNA has also been identified as a regulator of muscle cell development and in angiogenesis during muscle development [40, 51]. This miRNA is also required for proper function of the adult heart in mice [52] and it will be interesting to monitor whether adult transgenic fish develop heart failure as they age and how this organ reacts to proteotoxic stress. Additionally, genes involved in developmental signaling pathways, namely *wnt10a*, *dll4*, *zirc2a*, *zgc:114200* and *rbpja* were retrieved as putative targets of miR-145, *dvl2* as a putative target of miR-27c and finally *wnt4b*, *notch1b*, *cacybp* as putative targets of miR-1. We observed severe morphological alterations in embryo development (Figure 4), raising the possibility that the phenotypic aspects of proteotoxic stress may, up to some extent, be driven by miRNA deregulation. This

illustrates the importance of microRNA deregulation because it has the potential to greatly amplify the effects of mRNA mistranslation on gene expression profiles.

In conclusion, our new mistranslating zebrafish transgenic line displays important biomarkers of proteotoxic stress, suggesting that it can be used to dissect the biology of proteotoxic stress in vertebrates. Also, is creates the opportunity to study the physiology of this process during development and adult stages as well. The transgenics will facilitate analysis of preoteotoxic stress features in fully develop tissues and organs, which will be of great relevance to address questions related to ageing and late onset diseases. Our data further suggests that miRNA deregulation may play a role in the response to proteotoxic stress and may mediate developmental defects detected in the mistranslating embryos, and it will be important to further evaluate such deregulation in the transgenic line to get deeper insight into this phenomenon.

4.6. Supplementary data

Supplementary figure 1. Southern blot analysis shows that the integration pattern was the same for the control construct and also for the mutant tRNA construct.

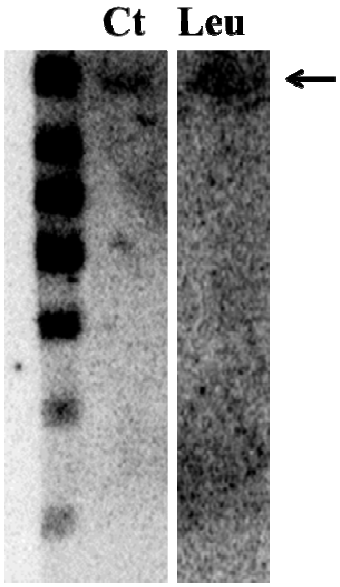

Supplementary table 1. Putative targets or miR-145. miRNA targets were identified with the Eimmo (MirZ), miRBASE Targets and TargetScan Fish databases. The computational targets were considered when they were retrieved from at least two of the algorithms. GO terms were identified using DAVID database and manually curated to remove redundant terms.

miR-145	
Target	**GO Term –Biological Process**
snx14	Cell communication
dll4, unc5b, hspa12b, fli1a, rbpja	Angiogenesis
loc554469	Cell cycle, regulation of transcription
plxna4, sema3aa, tfap2a	Cell morphogenesis, nervous system development
cib2, zgc:158263	Cell surface receptor linked signal transduction
atoh7, sox2, pax6b	Eye development, transcription, multicellular organismal development
hs3st1	Heparan sulfate biosynthesis
tlr3	Immune system process, Toll-like receptor signaling pathway
slc30a7	Ion transport
cd63	Lysosome
zgc:114200	Metabolic process, gene expression, Notch signaling pathway
pgd, cyp1a, mtmr6, lpl, chka, psat1, gys2, st6galnac5, hmgcra	Metabolism
eef2k	Mitotic cell cycle, mitotic spindle organization
clptm1, spata18, skib, fgf24, msxd, dmd	Multicellular organismal development, cell differentiation
pnrc2	Nuclear-transcribed mrna catabolic process, nonsense-mediated decay, transcription,
sod1	Oxygen and reactive oxygen species metabolic process
zic2a	Pattern specification process, nervous system development , Hedgehog signaling pathway
si:dkey-121j17.5, src, grk1a	Phosphorylation, protein modification process
ptk2.1	Protein complex assembly, erbb signaling pathway, VEGF signaling pathway, Regulation of actin cytoskeleton
calrl2	Protein folding, protein metabolic process
ptp4a1, opn1lw2	Protein modification process, dephosphorylation
mbtps1, cul1b, ube4b, pias2	Proteolysis
sppl3	Regulation of apoptosis
carhsp1, irx6a, mta2, pou2f1b, si:dkey-109n11.1, gata6, med25, nr2f1a, sox19a	Transcription, regulation of transcription
mknk2b	Regulation of translation, response to stress, MAPK signaling pathway
apex1	Response to DNA damage stimulus, regulation of apoptosis, Base excision repair
xrn2	RNA degradation
hnrpl, utp15	RNA processing
rhpn2, arrb1	Signal transduction
vcanb	Skeletal system development, ossification, multicellular organismal development,
mrrf	Translation
ergic3, rh50, ttpa, apoeb, chrne	Transport
slc25a14	Transport, mitochondrial transport
aars	Trna metabolic process, Aminoacyl-trna biosynthesis
wnt10a	Wnt receptor signaling pathway, calcium modulating pathway, Hedgehog signaling pathway

Supplementary table 2. Putative targets of mir-1. miRNA targets were identified with the Eimmo (MirZ), miRBASE Targets and TargetScan Fish databases. The computational targets were considered when they were retrieved from at least two of the algorithms. GO terms were identified using DAVID database and manually curated to remove redundant terms.

miR-1	
Target	**GO Term –Biological Process**
hs6st2	Angiogenesis, blood vessel development
notch1b	Blood vessel development, Notch signaling pathway,
calm1b, calm1a, calm2b, calm3a, calm3b	Calcium signaling pathway
nrxn2a	Cell adhesion molecules (cams)
nadl1.1, cxcl12a	Cell morphogenesis
tagln2, pfn2l	Cell morphogenesis, cytoskeleton organization
mtnr1c	Cell surface receptor linked signal transduction
snap25a	Cytokinesis, cell division
arpc4l	Cytoskeleton organization
zgc:165555	DNA packaging, chromatin organization
paics	Eye development, metabolism
copz1	Eye development, protein localization
hs3st3b1b	Glycosaminoglycan degradation, Heparan sulfate biosynthesis
ak2	Immune system development
asb4, arf1l, rabif	Intracellular signaling cascade
slc40a1, slc39a13, kctd10	Ion transport
vtg3	Lipid transport
cd63	Lysosome
rpia, atic, dpyd, ddost, alg8, arg2, azin1b, zgc:136871, entpd1, acat2, hccsa, nudt9, zgc:153896, ass1, bhmt, adh8b	Metabolism
cbr1l, dhrs1, idh1	Oxidation reduction
atp6v1c1a	Oxidative phosphorylation, proton transport
ccng2	P53 signaling pathway
bmpr2a	Pattern specification process
bsk146, dyrk2, prkacab	Protein amino acid phosphorylation, phosphorylation
tuba8l4	Protein complex assembly
fkbp9	Protein folding
ppih	Protein folding, Spliceosome
m6pr	Protein targeting to lysosome
zgc:136971	Proteolysis
fancd2	Regulation of cell death, regulation of apoptosis
eif5a	Regulation of translation
amh	Reproductive developmental process,
igf2b, igf2a, her7	Somitogenesis, pattern specification process
hnrpkl	Spliceosome
tbp, hoxa3a, hoxb2a, nr4a3, meis3, dlx2b, elk4, hsf2, cnot3a, pax2a	Transcription, regulation of transcription
slc25a27	Transmembrane transport
wnt4b, cacybp	Wnt signaling pathway

Supplementary table 3. Putative targets of mir-27c. miRNA targets were identified with the Eimmo (MirZ), miRBASE Targets and TargetScan Fish databases. The computational targets were considered when they were retrieved from at least two of the algorithms. GO terms were identified using DAVID database and manually curated to remove redundant terms.

miR-27c	
Target	**GO Term –Biological Process**
tbx16, ptenb	Angiogenesis
apaf1, faz, bad, dffb, traf4b, bcl2	Apoptosis
tpm1	Cardiac muscle contraction
cdh11, cd36	Cell adhesion
mlh1, sesn2, cth1	Cell cycle
b4galt1	Cell motion
zgc:152951	Cell redox homeostasis
mc4r, gpr98	Cell surface receptor linked signal transduction
setd1ba	Chromatin organization
snap25a	Cytokinesis, cell division
nfia, kbtbd5, dnase1l3l,	DNA metabolic process
disc1	Embryonic morphogenesis
col2a1a, eya1	Embryonic organ development
rdh5, atoh7, ctbp2, prkci	Eye development
cx43	Heart development , embryonic organ development
dvl2	Hindbrain development , Wnt signaling pathway, Notch signaling pathway
il22, zgc:136614, si:ch211-234p6.13	Immune response
arl3l2, arl5a	Intracellular signaling cascade
nup50	Intracellular transport
abcc9, cacng2a, trpc6, slc34a2a, slc25a28	Ion transport
xdh, aanat1, pdss1, amt, psat1, sult1st3, nt5e, pla2g6, c1galt1c1, atic, atp13a	Metabolism
lhb	Neuroactive ligand-receptor interaction, gnrh signaling pathway
acadvl	Oxidation reduction
cygb2	Oxygen transport
sox4b	Pancreas development
bmpr2a, aldh1a2, eng2a, bmpr1aa, bmpr1ab	Pattern specification process
prkcq, stk35, prkg1a, stk33, pdpk1b, axin1, ephb4a	Phosphorylation
fabp2	PPAR signaling pathway
st3gal2l, st3gal5l, gyltl1b	Protein amino acid glycosylation
tuba7l, zgc:153426	Protein complex assembly
cct7, hsp90b1	Protein folding
malt1, usp2a, ubr5	Proteolysis
zgc:63523	Regulation of cell shape
bms1l	Ribosome biogenesis
ddx3	RIG-I-like receptor signaling pathway
qk, rbm39b, dus1l, nxf1	RNA processing
crsp7, vsx1, hoxc13a, pou3f3b, bhlhe40, hoxc11a, nr1i2, rfx2, rybpb, thrap6, nkx6.1, ef1, nkx1.2la, dbx2, foxd1, pknox2, sfmbt2, per3, tbpl2, isl1	Transcription , regulation of transcription
qrsl1, si:ch211-216l23.2, rps15a, mknk2b	Translation
oat	Transmembrane transport

4.7. References

1. Hartl, F.U., A. Bracher, and M. Hayer-Hartl, *Molecular chaperones in protein folding and proteostasis.* Nature, 2011. **475**(7356): p. 324-32.
2. Reynolds, N.M., B.A. Lazazzera, and M. Ibba, *Cellular mechanisms that control mistranslation.* Nat Rev Microbiol, 2010. **8**(12): p. 849-56.
3. Liberek, K., A. Lewandowska, and S. Zietkiewicz, *Chaperones in control of protein disaggregation.* EMBO J, 2008. **27**(2): p. 328-35.
4. Vabulas, R.M., et al., *Protein folding in the cytoplasm and the heat shock response.* Cold Spring Harb Perspect Biol, 2010. **2**(12): p. a004390.
5. Kaganovich, D., R. Kopito, and J. Frydman, *Misfolded proteins partition between two distinct quality control compartments.* Nature, 2008. **454**(7208): p. 1088-95.
6. Malhotra, J.D. and R.J. Kaufman, *The endoplasmic reticulum and the unfolded protein response.* Semin Cell Dev Biol, 2007. **18**(6): p. 716-31.
7. Lee, J.W., et al., *Editing-defective tRNA synthetase causes protein misfolding and neurodegeneration.* Nature, 2006. **443**(7107): p. 50-5.
8. Paredes, J.A., et al., *Low level genome mistranslations deregulate the transcriptome and translatome and generate proteotoxic stress in yeast.* BMC Biol, 2012. **10**(1): p. 55.
9. Geslain, R., et al., *Chimeric tRNAs as tools to induce proteome damage and identify components of stress responses.* Nucleic Acids Res, 2010. **38**(5): p. e30.
10. Kishi, S., et al., *The zebrafish as a vertebrate model of functional aging and very gradual senescence.* Exp Gerontol, 2003. **38**(7): p. 777-86.
11. Kawakami, K., et al., *A transposon-mediated gene trap approach identifies developmentally regulated genes in zebrafish.* Dev Cell, 2004. **7**(1): p. 133-44.
12. Ali, S., et al., *Zebrafish embryos and larvae: a new generation of disease models and drug screens.* Birth Defects Res C Embryo Today, 2011. **93**(2): p. 115-33.
13. Poss, K.D., L.G. Wilson, and M.T. Keating, *Heart regeneration in zebrafish.* Science, 2002. **298**(5601): p. 2188-90.
14. Poss, K.D., M.T. Keating, and A. Nechiporuk, *Tales of regeneration in zebrafish.* Dev Dyn, 2003. **226**(2): p. 202-10.
15. Sager, J.J., Q. Bai, and E.A. Burton, *Transgenic zebrafish models of neurodegenerative diseases.* Brain Struct Funct, 2010. **214**(2-3): p. 285-302.
16. Bartel, D.P., *MicroRNAs: genomics, biogenesis, mechanism, and function.* Cell, 2004. **116**(2): p. 281-97.
17. Carthew, R.W. and E.J. Sontheimer, *Origins and Mechanisms of miRNAs and siRNAs.* Cell, 2009. **136**(4): p. 642-55.
18. Bartel, D.P. and C.Z. Chen, *Micromanagers of gene expression: the potentially widespread influence of metazoan microRNAs.* Nat Rev Genet, 2004. **5**(5): p. 396-400.
19. Giraldez, A.J., et al., *MicroRNAs regulate brain morphogenesis in zebrafish.* Science, 2005. **308**(5723): p. 833-8.
20. Fish, J.E., et al., *miR-126 regulates angiogenic signaling and vascular integrity.* Dev Cell, 2008. **15**(2): p. 272-84.
21. Morton, S.U., et al., *microRNA-138 modulates cardiac patterning during embryonic development.* Proc Natl Acad Sci U S A, 2008. **105**(46): p. 17830-5.
22. Li, N., et al., *Regulation of endoderm formation and left-right asymmetry by miR-92 during early zebrafish development.* Development, 2011. **138**(9): p. 1817-26.
23. Kimmel, C.B., et al., *Stages of embryonic development of the zebrafish.* Dev Dyn, 1995. **203**(3): p. 253-310.

24. Urasaki, A., G. Morvan, and K. Kawakami, *Functional dissection of the Tol2 transposable element identified the minimal cis-sequence and a highly repetitive sequence in the subterminal region essential for transposition.* Genetics, 2006. **174**(2): p. 639-49.
25. Kawakami, K., *Transgenesis and gene trap methods in zebrafish by using the Tol2 transposable element.* Methods Cell Biol, 2004. **77**: p. 201-22.
26. Link, V., A. Shevchenko, and C.P. Heisenberg, *Proteomics of early zebrafish embryos.* BMC Dev Biol, 2006. **6**: p. 1.
27. Wu, Y.L., et al., *Development of a heat shock inducible gfp transgenic zebrafish line by using the zebrafish hsp27 promoter.* Gene, 2008. **408**(1-2): p. 85-94.
28. Pfaffl, M.W., *A new mathematical model for relative quantification in real-time RT-PCR.* Nucleic Acids Res, 2001. **29**(9): p. e45.
29. Pfaffl, M.W., G.W. Horgan, and L. Dempfle, *Relative expression software tool (REST) for group-wise comparison and statistical analysis of relative expression results in real-time PCR.* Nucleic Acids Res, 2002. **30**(9): p. e36.
30. Gaidatzis, D., et al., *Inference of miRNA targets using evolutionary conservation and pathway analysis.* BMC Bioinformatics, 2007. **8**: p. 69.
31. Griffiths-Jones, S., et al., *miRBase: tools for microRNA genomics.* Nucleic Acids Res, 2008. **36**(Database issue): p. D154-8.
32. Ulitsky, I., et al., *Extensive alternative polyadenylation during zebrafish development.* Genome Res, 2012. **22**(10): p. 2054-66.
33. Cusack, S., A. Yaremchuk, and M. Tukalo, *The crystal structure of the ternary complex of T.thermophilus seryl-tRNA synthetase with tRNA(Ser) and a seryl-adenylate analogue reveals a conformational switch in the active site.* EMBO J, 1996. **15**(11): p. 2834-42.
34. Lenhard, B., et al., *tRNA recognition and evolution of determinants in seryl-tRNA synthesis.* Nucleic Acids Res, 1999. **27**(3): p. 721-9.
35. Munoz-Lopez, M. and J.L. Garcia-Perez, *DNA transposons: nature and applications in genomics.* Curr Genomics, 2010. **11**(2): p. 115-28.
36. Leslie, J.D., et al., *Endothelial signalling by the Notch ligand Delta-like 4 restricts angiogenesis.* Development, 2007. **134**(5): p. 839-44.
37. Kaur, S., et al., *Expression pattern for unc5b, an axon guidance gene in embryonic zebrafish development.* Gene Expr, 2007. **13**(6): p. 321-7.
38. Miyashita, T., et al., *PlexinA4 is necessary as a downstream target of Islet2 to mediate Slit signaling for promotion of sensory axon branching.* Development, 2004. **131**(15): p. 3705-15.
39. Sieger, D., D. Tautz, and M. Gajewski, *The role of Suppressor of Hairless in Notch mediated signalling during zebrafish somitogenesis.* Mech Dev, 2003. **120**(9): p. 1083-94.
40. Mishima, Y., et al., *Zebrafish miR-1 and miR-133 shape muscle gene expression and regulate sarcomeric actin organization.* Genes Dev, 2009. **23**(5): p. 619-32.
41. Morimoto, R.I., *Proteotoxic stress and inducible chaperone networks in neurodegenerative disease and aging.* Genes Dev, 2008. **22**(11): p. 1427-38.
42. Zeng, L., A.D. Carter, and S.J. Childs, *miR-145 directs intestinal maturation in zebrafish.* Proc Natl Acad Sci U S A, 2009. **106**(42): p. 17793-8.
43. Zeng, L. and S.J. Childs, *The smooth muscle microRNA miR-145 regulates gut epithelial development via a paracrine mechanism.* Dev Biol, 2012. **367**(2): p. 178-86.
44. Chen, X., et al., *MicroRNA145 targets BNIP3 and suppresses prostate cancer progression.* Cancer Res, 2010. **70**(7): p. 2728-38.
45. Spizzo, R., et al., *miR-145 participates with TP53 in a death-promoting regulatory loop and targets estrogen receptor-alpha in human breast cancer cells.* Cell Death Differ, 2010. **17**(2): p. 246-54.

46. Zhang, J., et al., *MiR-145, a new regulator of the DNA fragmentation factor-45 (DFF45)-mediated apoptotic network.* Mol Cancer, 2010. **9**: p. 211.
47. Zhou, D.H., et al., *Anti-tumor effects of an engineered "killer" transfer RNA.* Biochem Biophys Res Commun, 2012. **427**(1): p. 148-53.
48. Sokol, N.S. and V. Ambros, *Mesodermally expressed Drosophila microRNA-1 is regulated by Twist and is required in muscles during larval growth.* Genes Dev, 2005. **19**(19): p. 2343-54.
49. Chen, J.F., et al., *The role of microRNA-1 and microRNA-133 in skeletal muscle proliferation and differentiation.* Nat Genet, 2006. **38**(2): p. 228-33.
50. Cordes, K.R. and D. Srivastava, *MicroRNA regulation of cardiovascular development.* Circ Res, 2009. **104**(6): p. 724-32.
51. Stahlhut, C., et al., *miR-1 and miR-206 regulate angiogenesis by modulating VegfA expression in zebrafish.* Development, 2012. **139**(23): p. 4356-65.
52. Mishima, Y., C. Stahlhut, and A.J. Giraldez, *miR-1-2 gets to the heart of the matter.* Cell, 2007. **129**(2): p. 247-9.

Chapter 5 – General discussion

5. General Discussion

5.1. The cellular effects of mistranslation on zebrafish proteostasis

The maintenance of a functional proteome is fundamental to life, even though translational errors that occur naturally at a frequency of 10^{-4} are not associated with cell degeneration, small increases in the level of error are detrimental [1]. Loss of proteostasis with concomitant proteome aggregation is associated with neurodegeneration and cellular ageing [2, 3]. In metazoans different cell types have different associated proteomes and the proteostasis network has to fit the functions of each type of cell. Different compositions of the proteostasis network may underlie the differences observed in response to proteotoxic stress among cell types [4]. Additionally, the onset of protein conformational diseases and ageing is associated with the loss of proteostasis and the decline of quality control systems. In *Caenorhabditis elegans*, ageing is accompanied by extensive proteome aggregation due to gradual collapse of proteostasis. Interestingly, the aggregated protein fraction is enriched in proteins that are over-represented in the aggregates of human conformational diseases [5, 6]. These examples illustrate the importance of tight control of proteome homeostasis and implicate proteotoxic stress conditions in ageing and associated diseases. We have shown that ageing in zebrafish is accompanied by accumulation of insoluble protein aggregates in line with the observation made in *C. elegans*, indicating that loss of proteostasis is a conserved feature of ageing in eukaryotes.

The major goal of this thesis was to develop a vertebrate model system to investigate how proteome aggregation causes cell degeneration and disease. And also to understand how cells cope with loss of proteostasis and with protein aggregation. For

this, we have destabilized protein structure on a proteome wide scale by misincorporating serine at various amino acid sites. We targeted protein structure by replacing specific amino acid residues with serine to impact protein stability at different levels according to the chemical properties of the WT residue (namely: alanine, glycine, leucine and valine) and serine. Since errors in protein synthesis in vertebrates are mainly deleterious leading to loss of cellular fitness and disease, the induction of mistranslation events decreased zebrafish embryo viability and increased protein aggregation. The proteotoxic stress generated by mRNA mistranslation deregulated gene expression, in particular genes associated with the stress response, accumulation of protein aggregates, increased ROS production and lead to mitochondrial dysfunction.

Since alterations in protein structure can result in protein misfolding and aggregation it was not surprising to observe accumulation of ubiquitinated protein aggregates in the mistranslating zebrafish. These results correlate with increased expression of molecular chaperones and activation of the UPS. Protein aggregates can be deposited in the JUNQ and IPOD compartments according to their ubiquitination status and salvage potential. Misfolded proteins that maintain solubility accumulate in the JUNQ were they can be refolded by molecular chaperones or degraded by the associated proteasomes. On the other hand, the terminally aberrant and insoluble proteins are concentrated in the IPOD [7]. Our results indicate that protein aggregates produced by mRNA mistranslation accumulated in insoluble fractions, but also in the JUNQ since we detected accumulation of ubiquitinated protein deposits in the perinuclear region and increased proteasome activity.

Our gene expression results showed that the accumulation of protein aggregates is accompanied by up regulation of genes of the proteome quality control systems, which

are commonly upregulated during stress. The transcriptional gene expression response showed up regulation of cytosolic and ER molecular chaperones and oxidative stress defense genes. We have shown that mRNA mistranslation generated by our mutant tRNAs activated Hsp70 and Hsp90, which are involved in different steps of protein folding. Some of the chaperones can promote folding of newly synthetized polypeptides in association with the ribosome; this is the case of Hsp60 and Hsp70, which are particularly relevant to control folding of mistranslated proteins. However, Hsp70s can also facilitate protein degradation, as can Hsp90 and the sHSPs that function downstream of Hsp70 [8]. We also detected activation of the specialized stress response UPR though induction of ER chaperones, namely *hsp90b1*/*grp94*, *hspa5*/*bip* and eIF2α kinases that resulted in translational attenuation. Bip is a sensor protein that recognizes and binds misfolded polypeptides, keeping proteins in a folding competent state until they are properly folded in the ER. It also participates in the translocation and stabilization of newly synthetized proteins across the ER membrane. This molecular chaperone is a crucial element of the UPR that recognizes increased folding loads in the ER lumen and intervenes in protein stabilization or subsequent transport to the cytosol and degradation by the proteasome – ERAD system. The ERAD is activated by sustained ER stress conditions and recognizes accumulated misfolded proteins, redirecting them to the cytosol. Misfolded proteins are labeled with ubiquitin residues and retrotranslocated to the cytosol where they are degraded by the 26S proteasome. We have detected increased protein ubiquitination and proteasomal activity, in our mutant embryos, suggesting that the UPP and UPR contribute to the mistranslation phenotypes. The embryos expressing the mutant tRNAs showed similar responses to different types of mistranslation indicating that the proteome quality control network detects the mistranslated proteins in a similar way. However, misincorporation of serine at alanine

sites was the least toxic of the mistranslation conditions tested while serine misincorporation at leucine induced higher activation levels of the protein quality control components. In other words, the level of proteome instability is correlated with the chemical differences between the misincorporated amino acids. This is relevant to optimize the zebrafish model for future studies of ageing and proteotoxic stress biology.

The activation of the UPR by mistranslation also supports our hypothesis that mistranslation models can be used to study human diseases. Indeed, the UPR coordinates several quality control mechanisms of the secretory pathway, which can either be adaptive or pro apototic and play roles in several pathologies such as cancer, neurodegenerative, metabolic and inflammatory diseases [9]. Furthermore, ER stress signals extend beyond the homeostatic control of the organelle, namely into mitochondrial regulation, ROS production and other pathways such as the JNK and TOR signaling [10, 11]. Understanding the underlying mechanism connecting ER stress management and cellular homeostasis may yet provide important tools to deal with human ER associated diseases. On the other hand, deregulation of the UPP is of particular interest as ubiquination plays several important functions in parallel with the ubiquitin proteasome system. Ubiquitination regulates several cellular events such as cell cycle progression, endocytosis, apoptosis and importantly transcription and DNA repair; in zebrafish it can regulate lens development [12]. In our model system, stress response pathways were activated in a mutant dependent manner that correlates with the nature of the amino acid substitutions. Therefore, our method allows for the generation of different levels of proteotoxic stress that affect cellular homeostasis differently. These results illustrate the activation of the known stress responses to the production of aberrant and aggregation prone proteins; indicating that these misreading tRNAs are introducing mutations widely through the proteome.

5.2. Implication of mRNA mistranslation for ROS production and mitochondrial dysfunction

A link between the UPR and the production of ROS in the ER, or subsequent Ca^{2+} release from the ER targeting the mitochondria and increasing mitochondrial ROS production has been addressed in several systems [10, 13-15]. The ER oxidative disulfide folding is the main source of ER ROS, as molecular oxygen is the terminal electron acceptor and this can produce reactive oxygen species and oxidized glutathione [15, 16]. The increased folding demand on the ER lumen produces ROS as a consequence of repeated cycles of protein folding and decrease the pool of the antioxidant glutathione [13, 17]. ROS accumulation in the cell may expand the damages introduced into the proteome by mistranslation, as oxidative damage to proteins also affects their function and stability, promoting protein aggregation. Proteome oxidative damages are associated with conformational disorders, including Parkinson's disease, Alzheimer's disease, and cancer [18, 19]. Our mutant mistranslating tRNAs increase the accumulation of insoluble protein deposits, activating the UPR while impacting the ER folding ability, thus activating of the unfolded protein response. This prompted us to determine if oxidative stress was being generated as a result of the expression of our mutant mistranslating tRNAs. We have observed increased ROS production in the mistranslating embryos, which leads to high apoptotic levels and elevated embryo mortality. In our model, the generation of ROS probably precedes apoptotic signaling. Indeed, survival of the mistranslating embryos recovered in the presence of ROS scavengers. The increased production of ROS was also accompanied by up-regulation of *cat*, the anti-oxidant genes *glrx*, *mgst1*, *gstp1* and the peroxissomal *pex13*, *lonp2*,

zgc:114079 and *pmp34* genes. This suggests that peroxisome proliferation is induced at the transcriptional level by the oxidative stress associated with mRNA mistranslation.

ROS are physiologically relevant since they are mediators in various signaling pathways, however high levels of ROS lead to oxidative stress that can cause oxidative damage to lipids, proteins and nucleic acids. ROS can have diverse origins, namely the mitochondria, the peroxisome, the cytoplasm, the ER and the cell membrane; nonetheless the mitochondria are likely the most important source of oxidative stress [20]. Mitochondrial DNA is very susceptible to oxidative damage due to the high ROS content of the mitochondria and also the lack of histones in the mitochondrial genome [21-23]. Interestingly our proteotoxic stress conditions lead to the accumulation of oxidative damages in the mitochondrial genome, specifically in response to Ser-$tRNA_{CGC}^{Ala}$ (0.39 lesions/10Kb), Ser-$tRNA_{UCC}^{Gly}$ (0.82 lesions/10Kb), Ser-$tRNA_{CAC}^{Val}$ (0.77 lesions/10Kb) and Ser-$tRNA_{CAG}^{Leu}$ (1.62 lesions/10Kb), disrupted the mitochondrial network and reduced mitochondrial membrane potential. The mRNA profiling showed that the gene expression deregulation pattern was in line with the alterations we observed in the mitochondrial network. Important genes to mitochondrial homeostasis and maintenance were deregulated, namely *park2*/*parkin* that promotes degradation of damaged mitochondria and *park7*/*dj-1* which is proteoctive against elevated levels of ROS. A group of genes involved in mitochondrial network dynamics was also deregulated, in particular *rhot2*, *zgc:63910*/*mtfp1* and *mff*. And the mitochondrial fusion and fission balance are of crucial importance for diverse biological processes such as apoptosis, embryonic developmental and human diseases [24-26]. The ER and mitochondria are interconnected at the molecular level, enabling Ca^{2+} and ATP shuttling. This connection increases under stress conditions and potentiates apoptosis activation [27, 28]. Also, association of ER and mitochondrial membranes plays a role

in the dynamics of mitochondrial attachment to the cytoskeleton [28]. Our work indicates that mRNA mistranslation causes ER stress, which has the potential to deregulate the mitochondria ER association equilibrium. The observed mitochondrial dysfunction alongside with increased oxidative state resume the parameters characteristic of several human diseases [29]. Our data suggests that mRNA mistranslation disrupts mitochondrial structure through increased fission processes associated with elevated cellular ROS levels. Mistranslation can also affect organelle stability as a result of errors during cytosolic translation of proteins that integrate the organelle structure, a good example are the components of the electron transport chain of the mitochondria that are encoded by the nuclear DNA. Our results also suggest that the ROS accumulated during mistranslation can be produced both in the ER and in the mitochondria, as we observed the induction of the UPR and disruption of the mitochondrial network with loss of mitochondrial membrane potential. The folding environment of the ER strongly relies on the redox potential of its lumen and stress conditions may increase ROS production. The mitochondria are another oxidative stress generator since by-products of the mitochondrial respiratory chain and also transmission of ER stress to the mitochondria by calcium signalling can increase the cellular ROS levels. The increased folding demand of the stressed ER by increased protein misfolding and the maintenance of Ca^{2+} gradients deplete the ER of ATP. As a consequence there is an increased demand for ATP production at the mitochondrial respiratory chain resulting in increased production of ROS in the mitochondria. Further work will be necessary to address the relative contribution of the ER and of other subcellular compartments to ROS production during proteotoxic stress generated by mRNA mistranslation, nevertheless the ER and mitochondria are likely important players in the oxidative stress phenotype of mRNA mistranslation.

5.3. Gene expression changes in mistranslating zebrafish embryos

The study of the response to proteotoxic stress generated on our mutant tRNAS showed significant changes in gene expression. The Ser-$tRNA_{CAG}^{Leu}$ mutant tRNA was the one with the highest effect on gene deregulation, with a marked trend toward gene upregulation. Gene Ontology enrichment (Biological Pathway) showed enrichment of several GO-terms related to cellular and developmental processes. Several cellular processes were deregulated, namely regulation of transcription and oxidation-reduction processes, proteolysis, apoptotic processes, dorsal/ventral pattern formation, phosphorylation, response to stress, anterior/posterior pattern specification and somitogenesis.

Mistranslating embryos had reduced viability with associated developmental malformations and increased apoptotic levels. Deregulation of apoptotic and developmental signaling pathways such as Hedgehog, Wnt and Notch was highlighted in our transcriptome analysis. Apoptosis is central to vertebrate embryonic development as it allows for establishment of tissue identity and also for overall developmental progress [30, 31]. The apoptotic stimuli are integrated in intrinsic and extrinsic signaling pathways and contribute to tissue homeostasis; so their interactions with other cell homeostasis mechanisms pose a very interesting study subject. We have observed deregulated levels of several factors that participate in apoptotic activation pathways, in particular elements of the extrinsic pathway *tnfrsfa*, *tnfsf10l*, *fas* and *casp8*, and several elements of the intrinsic pathway, namely BCL2L family factors *bcl2l*, *bbc3*, *bad*, *baxa*, *bnip3l*, *bmf1*, *boka* and other apoptosis related genes, such as *xiap*, *bag3*, *tp53*, *tp63*, *zgc*:158776/*diablo*, *perp*, *mdm2*. The activation of apoptosis at the gene expression level is further supported by the increased apoptotic states of mistranslating embryos.

Staining of apoptotic cells revealed a sharp increase in cell death for the Ser-$tRNA_{UCC}^{Gly}$, Ser-$tRNA_{CAC}^{Val}$ and Ser-$tRNA_{CAG}^{Leu}$. The pattern of apoptotic activation correlates with the results previously described in assays to determine the UPR and UPP states. Additionally, caspase activation assays (caspases 8, 9, and 3-7) show increased activity in responde to mRNA mistranslation. We determined that both the intrinsic and extrinsic apoptotic pathways are activated since the misreading tRNAs induced death receptors, the Bcl-2 family and effector caspases. This indicates that apoptosis is compensating for the effects of aberrant polypeptides being produced due to the mutant tRNAs decoding activity. Since apoptosis plays a pivotal role during embryo development, our results suggest that proteotoxic stress interferes with developmental progression by exacerbating cell death responses.

Signaling pathways involved in embryo development were highly affected at the gene expression level by mRNA mistranslation, as we observed wide deregulation of various central signaling pathways in vertebrate embryo development, namely Hedgehog signaling, Wnt signaling and Notch signaling. Several negative regulators of the Wnt pathway were induced suggesting that this pathway is being repressed by mRNA mistranslation. In the case of the Notch pathway we have observed induction of a group of factors that function as positive activators. The wide expression deregulation of genes involved in the signaling pathways mentioned above (described in detail in chapter 3) highlights the fact that mRNA mistranslation strongly disrupts zebrafish embryo development.

The activation of extrinsic cell death pathway is of particular interest considering embryonic development, since its mediators in zebrafish are present in several tissues including the developing central nervous system [32], and we observed extensive deregulation of developmental pathways at the gene expression level as well as

compromised developmental progression of zebrafish embryos. Furthermore, we also detected activation of apoptosis though the Bcl-2 family unveiling a potential activation of mitochondrial deregulation directly dependent cell ER stress, and possibly mediation by Bbc3/Puma, a known ER stress signal adaptor of mitochondrial apoptosis [33].

Further work is necessary to understand how mRNA mistranslation deregulates developmental signaling and more importantly if increased apoptosis does indeed interfere in embryo early development. An underlying link between proteotoxic stress and developmental deregulation that can be explored is the distribution of the Heat Shock Factor (HSF) during mRNA mistranslation. HSFs are transcription factors induced by stress conditions that regulate transcription of molecular chaperones. They protect cells against proteotoxic stress but are also involved in developmental regulation. Recent evidences show that HSF1 and HSF2 knockouts have consequences for development of *Droshophila melanogaster* and mice [34]. We can speculate that sequestration of HSFs at chaperone sites may deplete them from their parallel transcription activities that are necessary for eukaryotic development.

5.4. MicroRNA misexpression in mistranslating zebrafish embryos

MicroRNAs are a class of small non coding RNA molecules involved in the regulation of translation and mRNA decay. They control various cellular processes such as cell survival and cell death [35] and can also intervene in embryo development and in diseases. Interestingly these regulatory RNAs are a large class of regulatory molecules far larger in number than other important regulator, such as kinases and phosphatases [36]. They have also been associated to cellular stress responses such as the ER – UPR,

indicating that they play an important role in the UPR. Indeed, they function at the levels of the UPR factors XBP1 and IREα [37-40]. We tried to identity a miRNA signature of proteotoxic stress in zebrafish embryos and our miRNA profiling data showed that mRNA mistranslation up regulates miR-145, miR-2195, miR-190b and miR-365 and down regulates miR-17a*, miR-27c, miR-732, miR-1, miR-16c and let-7g. This set of miRNAs and their target genes are poorly described in zebrafish; however miR-145 is important for zebrafish gut development and miR-1 is involved in angiogenesis and muscle cell development [41-43]. We consider of increased relevance the deregulation of miR-2195, miR-145 and miR-27c since they were deregulated in several mistranslation conditions. In order to have a general overview of the potential gene regulation executed by our proteotoxic stress responsive miRNAs we performed target prediction using the Eimmo, Miranda and TargetScan Fish algorithms. This revealed that the deregulated miRNAs have several putative targets that are important factors in embryo development, apoptosis, cell cycle and cell morphogenesis and several of these targets were also deregulated at the gene expression level. For example targets of miR-145, in particular *plxna4* and which regulate axon branching and patterning [44, 45], *pnrc2*, which is involved in nonsense mediated decay [46], and Notch factor *otud7b* were silenced by proteotoxic stress. We have also analyzed putative targets of miR-27c and several of them were deregulated at the gene expression level, namely Notch signaling components *axin1*, apoptosis related factors *bad* and *fas*, endoplasmic reticulum chaperone *hsp90b1*/*grp98* and transcription factors, such as *hoxc11a*, *rfx2*, *foxd1* and *ef1* were upregulated. This suggests that miRNA deregulation might be a relevant hallmark of proteotoxic stress and a fundamental contributor to the embryonic phenotypic aspects that we observed for the mistranslating embryos. It will

be very important to test the regulation of putative targets by de deregulated miRNAs to widen our knowledge of the impact of protoeotoxic stress on miRNA regulation.

5.5. Proteotoxic stress transgenics

The molecular processes of proteotoxic stress have become increasingly relevant to understand ageing and ageing associated diseases. Therefore, the establishment of a proteotoxic stress zebrafish transgenic line is an important tool to tackle the biology of protetoxic stress in a fully developed vertebrate organism. Our transgenic model recapitulates the phenotypic aspects that we observed in mistranslating zebrafish embryos. We have observed the activation of molecular chaperones and accumulation of protein aggregates which are important hallmarks of proteotoxic stress. We have also observed disruption of the mitochondrial network, a fundamental aspect of proteotoxic stress, that may be related to the increased production of ROS that is associated with mistranslation. Additionally, we observed deregulation of miR-145, miR-27c and miR-1 in this transgenic model which is in agreement with the miRNA deregulation in the embryos. Additionally, the miRNAs that we tested so far in the transgenic model are also expressed in adult tissues and we anticipate that the effects of miRNA deregulation to be present in fully differentiated tissues as well. Vertebrate models of proteotoxic stress have been produced in chick embryos and human cell lines, and of particular importance and relevance we can highlight the sticky mouse. This mouse model of mistranslation is based on editing defective alanyl tRNA synthetase [3] and presents extensive degeneration of purkinje cells, and increased protein aggregation. It will be interesting to compare the mouse and our transgenic zebrafish models and determine the effects on senescence and ageing. Our data show that the zebrafish is an excellent model

to study the biology of protoeotoxic stress, but exposure of zebrafish embryos to mRNA mistranslation has a deep impact on early development and this might complicate dissection of the pathways directly affected by proteotoxic stress. Conversely, the transgenic model will allow for the study of proteotoxic stress in a fully developed organism and in ageing animals without the complicated gene expression programs intrinsic to embryo development. The transgenic model will also be a powerful tool to dissect developmental aspects and responses to stress, and proteotoxic stress in particular given the impact that we observed in this processes.

5.6. Conclusions and future perspectives

Our data show that tRNA mediated mistranslation induces proteome aggregation and activation of the stress response pathways. Therefore, our method is useful to study the cellular responses to protein aggregation and proteotoxic stress. Moreover, our method generates mitochondrial dysfunction, that together with protein aggregation mimic major endpoints of neurodegenerative diseases [29]. Characterization of the protein aggregates should provide valuable insight into their composition and it will be very interesting to determine which specific proteins are being deposited in these aggregates. The mitochondrial deregulation that we have observed should be further analyzed to clarify how proteotoxic stress interferes with mitochondrial function.

Another important aspect of our work is the observed deregulation of miRNA expression. There is little information on the role of proteotoxic stress on miRNA deregulation and our zebrafish model system creates an opportunity to clarify this issue. The targets of the deregulated miRNAs should be experimentally validated in order to understand how theses regulators contribute to the mistranslation phenotype. Finally, our work shows that it is possible to produce transgenic zebrafish that mistranslate the genetic code, using mutant tRNAs. We believe that these fish will provide unique opportunities to unravel the biology of proteotoxic stress and clarify how protein aggregation cause disease and accelerates ageing. Our data supports a model where errors in protein biosynthesis saturate the cell quality control mechanism in the cytoplasm and ER, but it will be interesting to clarify whether saturation of protein quality control systems is the main trigger of cell degeneration or whether protein aggregates are toxic and the main cause of cellular senescence. This work raises several important questions (Figure 5.1):

-what is the nature and specific localization of protein aggregates;

-do protein aggregates accumulate in organelles;

-what is the nature of the mitochondrial dysfunction in response to proteotoxic stress;

-how is embryo development affected;

-how does proteotoxic stress deregulate miRNA expression.

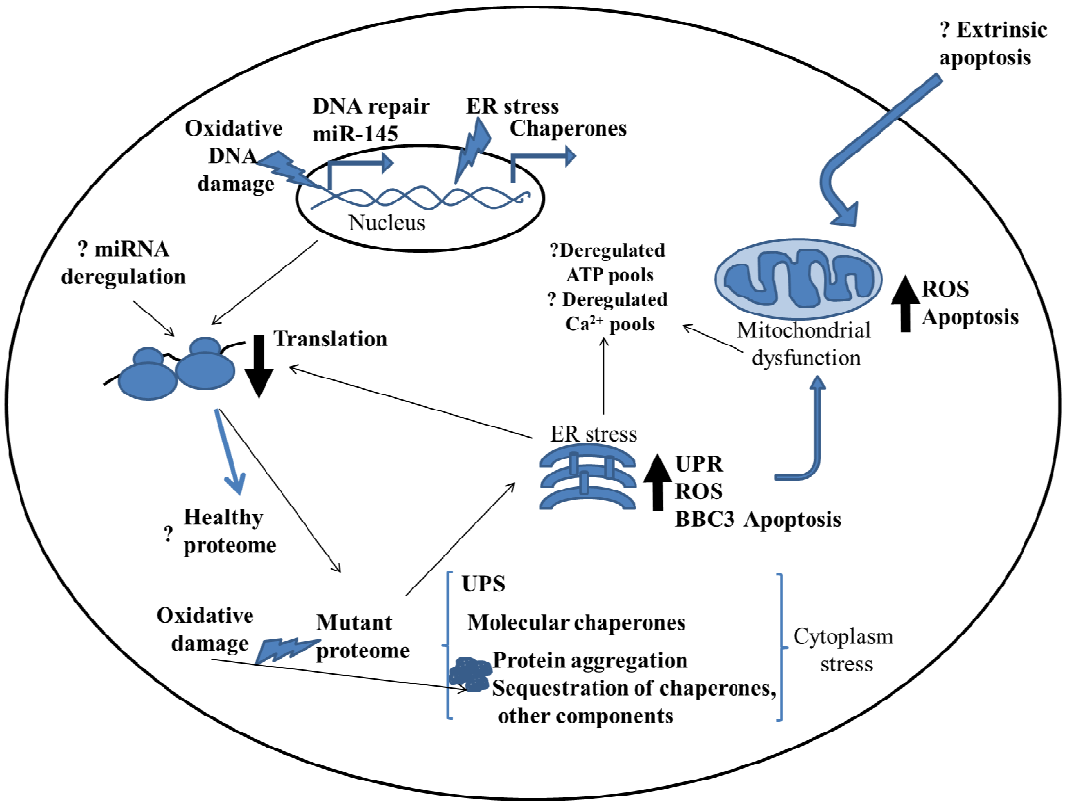

Figure 5.1 General overview of the effects of mistranslation on cellular deregulation. Misincorporation of amino acids during translation leads to the production of aberrant proteins. These proteins aggregate with subsequent chaperone and accessory factors sequestration. Aberrant proteins also cause ER stress and UPR activation. ER stress and subsequent mitochondrial dysfunction are believed to produce increased levels of ROS that damage nucleic acids, proteins and lipids. Several questions remain elusive, in particular how are the apoptotic pathways activated, and what is the role of mistranslation in miRNA expression deregulation. And, how is the native proteome affected and maintained in such stress conditions.

5.7. References

1. Drummond, D.A. and C.O. Wilke, *The evolutionary consequences of erroneous protein synthesis.* Nat Rev Genet, 2009. **10**(10): p. 715-24.
2. Morimoto, R.I., *Proteotoxic stress and inducible chaperone networks in neurodegenerative disease and aging.* Genes Dev, 2008. **22**(11): p. 1427-38.
3. Lee, J.W., et al., *Editing-defective tRNA synthetase causes protein misfolding and neurodegeneration.* Nature, 2006. **443**(7107): p. 50-5.
4. Gidalevitz, T., V. Prahlad, and R.I. Morimoto, *The stress of protein misfolding: from single cells to multicellular organisms.* Cold Spring Harb Perspect Biol, 2011. **3**(6).
5. Ben-Zvi, A., E.A. Miller, and R.I. Morimoto, *Collapse of proteostasis represents an early molecular event in Caenorhabditis elegans aging.* Proc Natl Acad Sci U S A, 2009. **106**(35): p. 14914-9.
6. David, D.C., et al., *Widespread protein aggregation as an inherent part of aging in C. elegans.* PLoS Biol, 2010. **8**(8): p. e1000450.
7. Kaganovich, D., R. Kopito, and J. Frydman, *Misfolded proteins partition between two distinct quality control compartments.* Nature, 2008. **454**(7208): p. 1088-95.
8. Chen, B., et al., *Cellular strategies of protein quality control.* Cold Spring Harb Perspect Biol, 2011. **3**(8): p. a004374.
9. Wang, S. and R.J. Kaufman, *The impact of the unfolded protein response on human disease.* J Cell Biol, 2012. **197**(7): p. 857-67.
10. Malhotra, J.D. and R.J. Kaufman, *The endoplasmic reticulum and the unfolded protein response.* Semin Cell Dev Biol, 2007. **18**(6): p. 716-31.
11. Ron, D. and P. Walter, *Signal integration in the endoplasmic reticulum unfolded protein response.* Nat Rev Mol Cell Biol, 2007. **8**(7): p. 519-29.
12. Berke, S.J. and H.L. Paulson, *Protein aggregation and the ubiquitin proteasome pathway: gaining the UPPer hand on neurodegeneration.* Curr Opin Genet Dev, 2003. **13**(3): p. 253-61.
13. Malhotra, J.D., et al., *Antioxidants reduce endoplasmic reticulum stress and improve protein secretion.* Proc Natl Acad Sci U S A, 2008. **105**(47): p. 18525-30.
14. Harding, H.P., et al., *An integrated stress response regulates amino acid metabolism and resistance to oxidative stress.* Mol Cell, 2003. **11**(3): p. 619-33.
15. Haynes, C.M., E.A. Titus, and A.A. Cooper, *Degradation of misfolded proteins prevents ER-derived oxidative stress and cell death.* Mol Cell, 2004. **15**(5): p. 767-76.
16. Tu, B.P. and J.S. Weissman, *Oxidative protein folding in eukaryotes: mechanisms and consequences.* J Cell Biol, 2004. **164**(3): p. 341-6.
17. Malhotra, J.D. and R.J. Kaufman, *Endoplasmic reticulum stress and oxidative stress: a vicious cycle or a double-edged sword?* Antioxid Redox Signal, 2007. **9**(12): p. 2277-93.
18. Nystrom, T., *Role of oxidative carbonylation in protein quality control and senescence.* EMBO J, 2005. **24**(7): p. 1311-7.
19. Grune, T., et al., *Decreased proteolysis caused by protein aggregates, inclusion bodies, plaques, lipofuscin, ceroid, and 'aggresomes' during oxidative stress, aging, and disease.* Int J Biochem Cell Biol, 2004. **36**(12): p. 2519-30.
20. Brown, G.C. and V. Borutaite, *There is no evidence that mitochondria are the main source of reactive oxygen species in mammalian cells.* Mitochondrion, 2012. **12**(1): p. 1-4.
21. Mandavilli, B.S., J.H. Santos, and B. Van Houten, *Mitochondrial DNA repair and aging.* Mutat Res, 2002. **509**(1-2): p. 127-51.
22. Santos, J.H., B.S. Mandavilli, and B. Van Houten, *Measuring oxidative mtDNA damage and repair using quantitative PCR.* Methods Mol Biol, 2002. **197**: p. 159-76.

23. Van Houten, B., V. Woshner, and J.H. Santos, *Role of mitochondrial DNA in toxic responses to oxidative stress.* DNA Repair (Amst), 2006. **5**(2): p. 145-52.
24. Chen, H., et al., *Mitofusins Mfn1 and Mfn2 coordinately regulate mitochondrial fusion and are essential for embryonic development.* J Cell Biol, 2003. **160**(2): p. 189-200.
25. Suen, D.F., K.L. Norris, and R.J. Youle, *Mitochondrial dynamics and apoptosis.* Genes Dev, 2008. **22**(12): p. 1577-90.
26. Detmer, S.A. and D.C. Chan, *Functions and dysfunctions of mitochondrial dynamics.* Nat Rev Mol Cell Biol, 2007. **8**(11): p. 870-9.
27. Bravo, R., et al., *Increased ER-mitochondrial coupling promotes mitochondrial respiration and bioenergetics during early phases of ER stress.* J Cell Sci, 2011. **124**(Pt 13): p. 2143-52.
28. Raturi, A. and T. Simmen, *Where the endoplasmic reticulum and the mitochondrion tie the knot: The mitochondria-associated membrane (MAM).* Biochim Biophys Acta, 2012.
29. Federico, A., et al., *Mitochondria, oxidative stress and neurodegeneration.* J Neurol Sci, 2012.
30. Fuchs, Y. and H. Steller, *Programmed cell death in animal development and disease.* Cell, 2011. **147**(4): p. 742-58.
31. Penaloza, C., et al., *Cell death in development: shaping the embryo.* Histochem Cell Biol, 2006. **126**(2): p. 149-58.
32. Eimon, P.M. and A. Ashkenazi, *The zebrafish as a model organism for the study of apoptosis.* Apoptosis, 2010. **15**(3): p. 331-49.
33. Li, J., B. Lee, and A.S. Lee, *Endoplasmic reticulum stress-induced apoptosis: multiple pathways and activation of p53-up-regulated modulator of apoptosis (PUMA) and NOXA by p53.* J Biol Chem, 2006. **281**(11): p. 7260-70.
34. Akerfelt, M., R.I. Morimoto, and L. Sistonen, *Heat shock factors: integrators of cell stress, development and lifespan.* Nat Rev Mol Cell Biol, 2010. **11**(8): p. 545-55.
35. Bartel, D.P., *MicroRNAs: genomics, biogenesis, mechanism, and function.* Cell, 2004. **116**(2): p. 281-97.
36. Leung, A.K. and P.A. Sharp, *MicroRNA functions in stress responses.* Mol Cell, 2010. **40**(2): p. 205-15.
37. Bartoszewski, R., et al., *The unfolded protein response (UPR)-activated transcription factor X-box-binding protein 1 (XBP1) induces microRNA-346 expression that targets the human antigen peptide transporter 1 (TAP1) mRNA and governs immune regulatory genes.* J Biol Chem, 2011. **286**(48): p. 41862-70.
38. Behrman, S., D. Acosta-Alvear, and P. Walter, *A CHOP-regulated microRNA controls rhodopsin expression.* J Cell Biol, 2011. **192**(6): p. 919-27.
39. Byrd, A.E., I.V. Aragon, and J.W. Brewer, *MicroRNA-30c-2* limits expression of proadaptive factor XBP1 in the unfolded protein response.* J Cell Biol, 2012. **196**(6): p. 689-98.
40. Upton, J.P., et al., *IRE1alpha cleaves select microRNAs during ER stress to derepress translation of proapoptotic Caspase-2.* Science, 2012. **338**(6108): p. 818-22.
41. Zeng, L., A.D. Carter, and S.J. Childs, *miR-145 directs intestinal maturation in zebrafish.* Proc Natl Acad Sci U S A, 2009. **106**(42): p. 17793-8.
42. Stahlhut, C., et al., *miR-1 and miR-206 regulate angiogenesis by modulating VegfA expression in zebrafish.* Development, 2012. **139**(23): p. 4356-65.
43. Mishima, Y., et al., *Zebrafish miR-1 and miR-133 shape muscle gene expression and regulate sarcomeric actin organization.* Genes Dev, 2009. **23**(5): p. 619-32.
44. Miyashita, T., et al., *PlexinA4 is necessary as a downstream target of Islet2 to mediate Slit signaling for promotion of sensory axon branching.* Development, 2004. **131**(15): p. 3705-15.

45. Love, C.E. and V.E. Prince, *Expression and retinoic acid regulation of the zebrafish nr2f orphan nuclear receptor genes.* Dev Dyn, 2012. **241**(10): p. 1603-15.
46. Cho, H., K.M. Kim, and Y.K. Kim, *Human proline-rich nuclear receptor coregulatory protein 2 mediates an interaction between mRNA surveillance machinery and decapping complex.* Mol Cell, 2009. **33**(1): p. 75-86.